UNIVERSITEIT VAN PRETORIA
UNIVERSITY OF PRETORIA
YUNIBESITHI YA PRETORIA

CONSTRUCTAL DESIGN AND OPTIMISATION OF COMBINED MICROCHANNELS AND MICRO PIN FINS FOR MICROELECTRONIC COOLING

by

Olayinka Omowunmi ADEWUMI

Submitted in partial fulfilment of the requirements for the degree

Doctor of Philosophy in Mechanical Engineering

in the

Faculty of Engineering, Built Environment and Information Technology

University of Pretoria

Under the supervision of

Prof T Bello-Ochende

Prof JP Meyer

2016

UNIVERSITEIT VAN PRETORIA
UNIVERSITY OF PRETORIA
YUNIBESITHI YA PRETORIA

ABSTRACT

Title: Constructal design and optimisation of combined microchannels and micro-pin fins for microelectronic cooling

Author: Olayinka Omowunmi Adewumi

Supervisors: Prof. Tunde Bello-Ochende and Prof. Josua P. Meyer

Department: Mechanical and Aeronautical Engineering

University: University of Pretoria

Degree: Doctor of Philosophy (Mechanical Engineering)

Microchannels and micro pin fins have been employed for almost four decades in the cooling of microelectronic devices and research is still being done in this field to improve the thermal performance of these micro heat sinks. In this research, the constructal design and computational fluid dynamics code was used with a goal-driven optimisation tool to numerically investigate the thermal performance of a novel design of combining microchannels and micro pin fins for microelectronic cooling applications. Existing designs of microchannels were first optimised and thereafter, three to seven rows of micro pin fins were inserted into the microchannels to investigate whether there was further improvement in thermal performance. The microchannels and micro pin fins were both embedded in a highly conductive solid substrate.

UNIVERSITEIT VAN PRETORIA
UNIVERSITY OF PRETORIA
YUNIBESITHI YA PRETORIA

Abstract

The three-dimensional geometric structure of the combined micro heat sink was optimised to achieve the objective of maximised thermal conductance, which is also minimised thermal resistance under various design conditions. The micro heat sinks investigated in the study were the single microchannel, two-layered microchannels with parallel and counter flow configurations, three-layered microchannels with parallel and counter flow configurations, the single microchannel with circular-, square- and hexagonal-shaped micro pin-fin inserts and the two-layered microchannels with circular-shaped micro pin-fin inserts. A numerical computational fluid dynamics (CFD) package with a goal-driven optimisation tool, which employs the finite-volume method, was used to analyse the fluid flow and heat transfer in the micro heat sinks investigated in this work. The thermal performances of all the micro heat sinks were compared for different application scenarios.

Furthermore, the temperature variation on the heated base of the solid substrate was studied for the different micro heat sinks to investigate which of the heat sink designs minimised the temperature rise on the heated base best. This is very important in microelectronic cooling applications because temperature rise affects the reliability of the device. The heat sink design that best maximised thermal conductance and minimised temperature rise on the heated base was chosen as the best for microelectronic cooling. For all the cases considered, fixed volume constraints and manufacturing constraints were applied to ensure real-life applicability. It was concluded that optimal heat sink design for different application scenarios could be obtained speedily when a CFD package which had an optimisation tool was used.

UNIVERSITEIT VAN PRETORIA
UNIVERSITY OF PRETORIA
YUNIBESITHI YA PRETORIA

Keywords: *Microchannels, micro pin fins, computational fluid dynamics, goal-driven optimisation, heat transfer, fluid flow, constraints, optimal heat sink, thermal conductance, thermal resistance, constructal theory, temperature variation*

UNIVERSITEIT VAN PRETORIA
UNIVERSITY OF PRETORIA
YUNIBESITHI YA PRETORIA

DEDICATION

This thesis is dedicated to:

The Almighty God, the God of all knowledge

and

My husband, Olusegun Johnson Adewumi

UNIVERSITEIT VAN PRETORIA
UNIVERSITY OF PRETORIA
YUNIBESITHI YA PRETORIA

ACKNOWLEDGEMENTS

I want to thank, first of all, the Almighty God – the One who gave me the life, strength, wisdom, knowledge and understanding to carry out this research work.

I wish to express my sincere gratitude to my supervisor, Prof. Tunde Bello-Ochende, for his technical guidance and support throughout the research work. Thank you for your great help, which allowed me to finish my study successfully.

My deepest thanks go to my co-supervisor and head of the department, Prof. Josua P. Meyer, who facilitated my coming to South Africa to study. Your technical and financial support, which allowed the successful completion of this study, is greatly appreciated.

Special thanks to all the staff and postgraduate students in the Thermofluids Research Group. You all made this work enjoyable and very fulfilling.

I also wish to thank our departmental administrative officers, Tersia Evans, Elizabe Pieterse and Ntsindy Mnyamana, for your guidance and support.

Profs. A. Bejan and S. Lorente, I want to thank you for your encouragement to continue in my chosen area of research in constructal theory and design. It was a great honour meeting you at one of the constructal law conferences for the first time.

UNIVERSITEIT VAN PRETORIA
UNIVERSITY OF PRETORIA
YUNIBESITHI YA PRETORIA

I want to express my profound gratitude to the Dean, Faculty of Engineering, University of Lagos, Prof. O.A. Fakinlede. I appreciate your encouragement and support before and throughout the period of my study in South Africa. To all my colleagues in the Department of Mechanical Engineering, University of Lagos, I say a very big thank you. I also want to thank my employer, the University of Lagos, Nigeria, for granting me study leave in order to pursue a higher degree.

My friends, Olabode Olakoyejo, Lanre Obayopo, Francis Okafor, Saheed Adio, Daniel Evim, Ade Onitiri, Sunday Oyekeye, Sunday Adelaja, Noah Olanrewaju, I thank you all for your consistent encouragement, as well as for your generous social and emotional support.

To my spiritual family in South Africa, all the pastors and members of The Redeemed Christian Church of God Jesus House for All Nations Pretoria and our sister church in Mamelodi, you are all wonderful people. Thank you for being there for me. I want to also acknowledge the support of all the pastors and members of The Redeemed Christian Church of God, Kingdom Palace Area. Thank you all for your prayers.

To my parents, Mr and Mrs Obademi and Mr and Mrs Adewumi, I thank you very much for all the emotional, spiritual and financial support. I also want to say a big thank you to all my brothers and sisters, Mr and Mrs Oguntuase, Mr and Dr (Mrs) Ewete, Kola, Yemi, Mr Wale Adewumi, Mr and Mrs Femi Bosede, Mr and Mrs

UNIVERSITEIT VAN PRETORIA
UNIVERSITY OF PRETORIA
YUNIBESITHI YA PRETORIA

Kunle Sanya, and my dearest sister, Taye Adewumi. Being a part of this great family has been a great blessing to me.

To my loving husband, Olusegun Johnson Adewumi, your prayer, love and support gave me the needed courage to be away from the family for a while to pursue my study in South Africa. Words are not enough to express my gratitude for your support all the way. To my lovely children, Sharon, Deborah and Samuel, thank you so much for your love and understanding even though it was difficult being away from you for a while.

I would like to acknowledge and duly appreciate the financial support from DST/the National Research Foundation (NRF), the Tertiary Education Support Programme (TESP), University of Pretoria, the South African National Energy Research Institute (SANERI)/South African National Energy Development Institute (SANEDI), the Council of Scientific and Industrial Research (CSIR), the Energy Efficiency and Demand Side Management (EEDSM) Hub and NAC.

UNIVERSITEIT VAN PRETORIA
UNIVERSITY OF PRETORIA
YUNIBESITHI YA PRETORIA

TABLE OF CONTENTS

UNIVERSITEIT VAN PRETORIA
UNIVERSITY OF PRETORIA
YUNIBESITHI YA PRETORIA

LIST OF FIGURES

UNIVERSITEIT VAN PRETORIA
UNIVERSITY OF PRETORIA
YUNIBESITHI YA PRETORIA

UNIVERSITEIT VAN PRETORIA
UNIVERSITY OF PRETORIA
YUNIBESITHI YA PRETORIA

UNIVERSITEIT VAN PRETORIA
UNIVERSITY OF PRETORIA
YUNIBESITHI YA PRETORIA

UNIVERSITEIT VAN PRETORIA
UNIVERSITY OF PRETORIA
YUNIBESITHI YA PRETORIA

UNIVERSITEIT VAN PRETORIA
UNIVERSITY OF PRETORIA
YUNIBESITHI YA PRETORIA

UNIVERSITEIT VAN PRETORIA
UNIVERSITY OF PRETORIA
YUNIBESITHI YA PRETORIA

LIST OF TABLES

UNIVERSITEIT VAN PRETORIA
UNIVERSITY OF PRETORIA
YUNIBESITHI YA PRETORIA

NOMENCLATURE

A	area, m^2
AR_c	channel aspect ratio
AR_s	aspect ratio of solid substrate
Be	Bejan number
C	global thermal conductance
$CF1$	counterflow1
$CF2$	counterflow2
C_p	heat capacity, J/K
D_f	micro pin-fin diameter, m
D_h	channel hydraulic diameter, m
H_c	channel height of single microchannel, m
$H_{c1,c2,c3}$	channel height of different layers, m
H_f	micro pin-fin height, m
k_f	thermal conductivity of fluid, W/mK
k_s	thermal conductivity of solid wall, W/mK
L_f	length of sides of square and hexagonal micro pin fins, m
M	total height of computational volume, m
$M_{1,2,3}$	height of different layers, m
N	number of rows of micro pin fins
N	axial length of computational volume, m

UNIVERSITEIT VAN PRETORIA
UNIVERSITY OF PRETORIA
YUNIBESITHI YA PRETORIA

P	pressure, Pa
PF	parallel flow
PP	pumping power, W
Re	Reynolds number
Q	heat transfer rate, W
R_{th}	thermal resistance, ˚C/W
q''	surface heat flux, W/m^2
$S_{1\text{-}n}$	micro pin-fin spacing
T	temperature, ˚C
$t_{1,6,8}$	half-width thickness of vertical solid, m
t_2	channel base thickness, m
$t_{3,5,7}$	channel base to height distance, m
u,v,w	velocities in the x-, y- and z-directions, m/s
V	volume of computational domain, m^3
W	width of computational domain, m
W_c	channel width of single microchannel, m
$W_{c1,c2,c3}$	channel width of different layers, m
W_t	total width of solid substrate, m
x, y, z	Cartesian coordinates, m

Greek symbols

α	thermal diffusivity, m^2/s

UNIVERSITEIT VAN PRETORIA
UNIVERSITY OF PRETORIA
YUNIBESITHI YA PRETORIA

μ	dynamic viscosity, kg/m.s
ν	kinematic viscosity, m^2/s
ρ	density, kg/m^3
∂	differential or derivative
ϕ	volume fraction
Δ	Difference
Ω	interface between solid and fluid

Subscripts

Atm	Atmosphere
Base	heated solid base
f	Fluid
In	Inlet
Max	maximum
Min	minimum
opt	optimum
out	outlet
Solid	Solid
1-n	number of layers
T	Total

UNIVERSITEIT VAN PRETORIA
UNIVERSITY OF PRETORIA
YUNIBESITHI YA PRETORIA

PUBLICATIONS IN JOURNALS, BOOKS AND CONFERENCE PROCEEDINGS

The following articles and conference papers have been produced during this research:

1. **O.O. Adewumi**, T. Bello-Ochende and J.P. Meyer, "Constructal design of combined microchannel and micro pin fins for electronic cooling", *International Journal of Heat and Mass Transfer*, Vol. 66, pp. 315-323, 2013.

2. **O.O. Adewumi**, T. Bello-Ochende and J.P. Meyer; "Analysis of the thermal performance of single and multi-layered microchannels with fixed volume constraint", *ASME Journal of Heat Transfer*, submitted on February 2, 2015.

3. **O.O. Adewumi**, T. Bello-Ochende and J.P. Meyer; "Numerical investigation into the thermal performance of single microchannels with varying axial length and different shapes of micro pin-fin inserts", *Heat Transfer Engineering*, accepted on April 25, 2016**.**

4. **O.O. Adewumi,** T. Bello-Ochende and J.P. Meyer; "Constructal design of single microchannel heat sink with varying axial length and temperature-dependent fluid properties", *International Journal of Heat and Technology*, Vol. 34, No 1; pp 167-172, 2016.

UNIVERSITEIT VAN PRETORIA
UNIVERSITY OF PRETORIA
YUNIBESITHI YA PRETORIA

5. T. Bello-Ochende, **O.O. Adewumi**, J.P. Meyer; "Increased heat load effects on the thermal performance of single- and two-layered microchannels with varying axial length and micro pin-fin inserts", *International Journal of Fluid Mechanics Research*, Vol. 43, pp 441-455, 2016.

6. **O.O. Adewumi**, T. Bello-Ochende and J.P. Meyer, "Geometric optimisation of rectangular microchannel heat sink inserted with micro pin fins", *Proceedings of Constructal Law Conference*, Nanjing, China, pp. 221-232, 14-15 October 2013. **(Presented)**

7. **O.O. Adewumi**, T. Bello-Ochende and J.P. Meyer, "Temperature variation on the heated base of a solid substrate cooled with different type of heat sinks", *10th International Conference on Heat Transfer, Fluid Mechanics and Thermodynamics*, Orlando, Florida, 14-16 July 2014. **(Presented)**

8. **O.O. Adewumi**, T. Bello-Ochende and J.P. Meyer, "Geometric optimisation of multi-layered microchannel heat sink with different flow arrangements", *Proceedings of the 15th International Heat Transfer Conference*, Kyoto, Japan, 10-15 August 2014. **(Presented)**

UNIVERSITEIT VAN PRETORIA
UNIVERSITY OF PRETORIA
YUNIBESITHI YA PRETORIA

9. **O.O. Adewumi**, T. Bello-Ochende and J.P. Meyer, "Comparison between the thermal performance of single and two-layer microchannels inserted with micro pin fins", *Proceedings of the 15th International Heat Transfer Conference*, Kyoto, Japan, 10-15 August 2014. **(Presented)**

10. **O.O. Adewumi**, T. Bello-Ochende and J.P. Meyer, "Constructal design of single microchannel with varying axial length and temperature-dependent fluid properties", *Proceedings of Constructal Law Conference 2015*, Parma, Italy. (**Presented**)

11. **O.O. Adewumi**, T. Bello-Ochende and J.P. Meyer, "Numerical investigation into two-layered microchannel with varying axial length and temperature-dependent fluid properties", *Proceedings of ASME International Mechanical Engineering Congress and Exposition 2015*, Houston, Texas. (**Presented**)

UNIVERSITEIT VAN PRETORIA
UNIVERSITY OF PRETORIA
YUNIBESITHI YA PRETORIA

CHAPTER 1: INTRODUCTION

1.1. BACKGROUND

Micro devices are characterised by reduced dimensions and increasing power generation, which require the need to transfer high heat fluxes in somewhat small surfaces and volumes [1]. A microelectronic device is an example of the application of such a micro device. One of the major challenges faced in the design of microelectronic devices, where many electronic chips are packed into a fixed volume, is their thermal management [2-8]. For over five decades, it has been observed that increased circuit power dissipation and increased packaging density have led to a significant rise in chip and module heat fluxes especially in high-end computers [9]. It has also been well accepted that over 50% of electronic failures are thermally related [10]. As a result, the thermal design goal of microelectronic devices is to ensure that temperature limits, which could cause system failure, are not exceeded. This is to guarantee reliability of the device. Reliability, which is defined as the reciprocal of the mean time between failures (MTBF), has been described as the statistical probability that a device will operate without failure for a stated period of time [10].

Heat sinks, which are heat exchangers that conduct heat from a heat-generating base to a fluid or its surrounding by convection, have been known to be one of the best, most common and cost-effective hardware employed for thermal management of microelectronic equipment because of its capacity to remove high heat fluxes from

UNIVERSITEIT VAN PRETORIA
UNIVERSITY OF PRETORIA
YUNIBESITHI YA PRETORIA

surfaces [11-16]. Microelectronics needs to be designed in such a way that heat transfer density is maximised by maintaining a thermal pathway with minimum resistance from the device heat source to the eventual heat sink. This allows the overall global thermal resistance of the device to be minimised giving rise to a maximised thermal conductance, which is a way of measuring the thermal performance of cooling devices. It has been observed that the thermal resistance in heat sinks arise

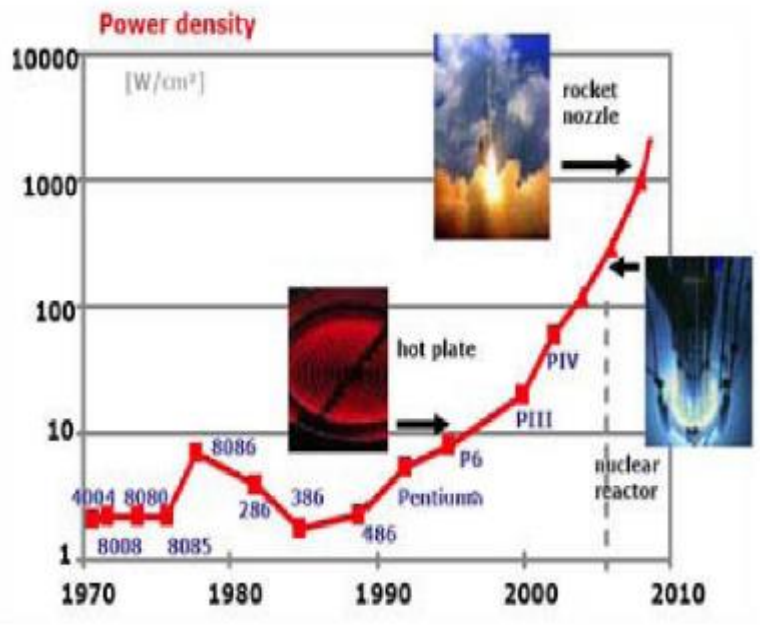

Figure 1.1: Increasing power density (Source: Intel) [5]

UNIVERSITEIT VAN PRETORIA
UNIVERSITY OF PRETORIA
YUNIBESITHI YA PRETORIA

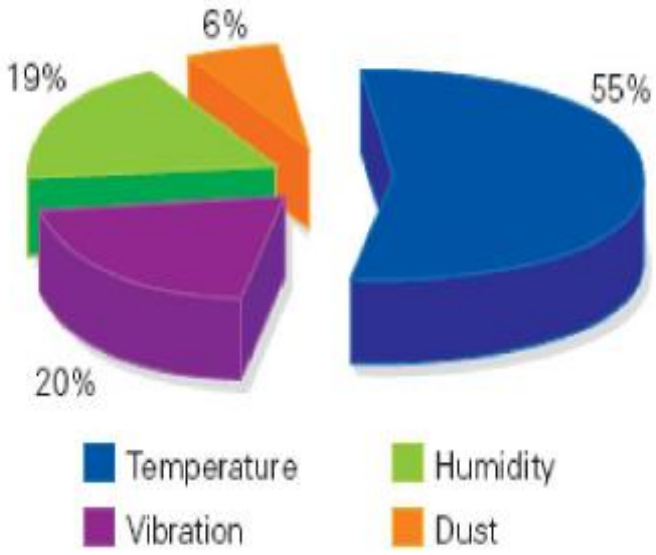

Figure 1.2: Causes of defects in defence-related electronics [5]

from three major sources [12], namely conduction resistance in the heat sink, convection resistance between the microchannel surfaces and the coolant and resistance due to the temperature rise of the cooling fluid in the heat exchanger. The thermal resistance, R, which is a way of measuring the thermal performance as stated above, can be expressed as Equation (1.1):

$$R = \frac{T_b - T_\infty}{Q} \tag{1.1}$$

UNIVERSITEIT VAN PRETORIA
UNIVERSITY OF PRETORIA
YUNIBESITHI YA PRETORIA

$$R_{cond} = \frac{1}{kA} \tag{1.2}$$

$$R_{conv} = \frac{1}{hA} \tag{1.3}$$

where Equations (1.2) and (1.3) are the conductive and convective resistances respectively and h and k are the convective heat transfer coefficient and thermal conductivity respectively [17].

The constructal law, which is an evolutionary principle of increase of flow access in time [18, 19], has been used by many researchers to determine the geometric configuration of heat sinks that best maximises heat transfer from heated surfaces or volumes to the cooling fluid [20-29]. The law holds that shape and structure are meant to aid flow and as a result, optimisation of the geometric parameters of micro heat sinks, which are mostly interdependent, must be considered for optimum thermal performance.

The introduction of computational fluid dynamics (CFD) simulations with the arrival of supercomputers has made multi-parameter optimisation possible in a lesser time frame. Also, because experiments are mostly expensive and time consuming, the use of commercial CFD codes has increased dramatically. Some advantages of numerical studies over experimental studies that have made CFD simulations popular are as follows: many design variables can be varied simultaneously to arrive at optimal

UNIVERSITEIT VAN PRETORIA
UNIVERSITY OF PRETORIA
YUNIBESITHI YA PRETORIA

designs that meet the desired objectives and provide quantitative insight into the flow and heat transfer process at micro-scale level.

1.2. MOTIVATION

Constructal design, which is the use of constructal law for better engineering design, is the greatest motivation for this work [18, 19, 30, 31]. It involves the generation of configurations taking into consideration the global objectives and global constraints. With the use of constructal law in the design and geometric optimisation of microelectronic structures, a configuration is not assumed but allowed freedom to morph until optimum dimensions are obtained.

1.3. AIM OF THE RESEARCH

The aim of the current research is to carry out numerical investigations on conjugate heat transfer in different types of micro heat sinks based on constructal theory and design. Also, a new heat sink will be modelled to improve the thermal performance of existing micro heat sinks. The geometric optimisation of the heat sinks will be achieved by using a computational fluid dynamics code, which has a goal-driven optimisation algorithm. The design parameters chosen become design variables and a search for the optimal geometry based on these design variables and the objective

UNIVERSITEIT VAN PRETORIA
UNIVERSITY OF PRETORIA
YUNIBESITHI YA PRETORIA

function will be carried out using the optimisation algorithm of the computational fluid dynamics software.

1.4. OBJECTIVES OF THE RESEARCH

The objectives of the study are as follows:

- to geometrically optimise the micro heat sinks (single and stacked microchannels) in such a way that the global thermal conductance is maximised or peak temperature of the solid substrate being cooled is minimised for fixed and varied axial lengths;
- to geometrically optimise a new design of micro heat sink, which combines microchannels and micro pin fins for fixed and varied axial lengths and compare the thermal performance of this new design with the conventional microchannel heat sinks;
- to investigate the performance of different micro heat sinks based on the temperature non-uniformity of the solid substrate that is cooled and propose a best choice of micro heat sink based on both maximum thermal conductance and temperature non-uniformity.

UNIVERSITEIT VAN PRETORIA
UNIVERSITY OF PRETORIA
YUNIBESITHI YA PRETORIA

1.5. SCOPE OF THE STUDY

In this thesis, the constructal design approach is employed to efficiently optimise the geometries of different micro heat sinks with forced convective heat transfer and steady, laminar and incompressible fluid flow using CFD and numerical optimisation. The micro heat sinks considered are the single, two- and three-layered microchannels, the combination of the single microchannel and three different shapes of micro pin fins, and the combination of the two-layered microchannel and the circular-shaped micro pin fins. A fixed total volume of these heat sinks is investigated for fixed and varying axial lengths. Different boundary conditions of velocity, pressure, heat flux and heat load are also considered. The thermal performance of the different heat sinks is based on both the maximised thermal conductance study and the temperature variation of the heated base of the solid substrate that employed the use of the micro heat sinks listed above. Water is used throughout this research as the cooling fluid with constant and temperature-dependent properties.

With microelectronic devices becoming smaller and smaller, a fixed volume constraint is applied to both the single and multi-layered microchannels. Also, the thermal performance of all the micro heat sinks considered, based on the minimisation of peak temperature, resulting in the maximising of the thermal conductance, is compared.

UNIVERSITEIT VAN PRETORIA
UNIVERSITY OF PRETORIA
YUNIBESITHI YA PRETORIA

1.6. RESEARCH METHODOLOGY

Numerical analysis is used to achieve the objectives of this research. Computational fluid dynamics software (ANSYS 14.0), which has a goal-driven optimisation algorithm, is used to model the geometry of the computational domain, generate the grid, solve the necessary equations that govern the fluid flow and heat transfer and also search for the optimal design variables that meet the global objective to be achieved.

1.7. MATERIAL SELECTION

Silicon is selected as the material of choice for the solid substrate being cooled by the micro heat sink because of its relatively high thermal conductivity and low cost. Diamond, copper and aluminium are other materials that could have been chosen but diamond substrate has high cost and poor manufacturability, while copper and aluminium are still very hard when one considers manufacturing micro-scale heat sinks.

UNIVERSITEIT VAN PRETORIA
UNIVERSITY OF PRETORIA
YUNIBESITHI YA PRETORIA

1.8. ORGANISATION OF THE THESIS

The thesis consists of seven chapters that provide details into the study carried out and each chapter is divided into sections and subsections for better organisation, ease of reading and referencing. Each chapter is outlined below:

- Chapter 1 gives an introduction to the study, presents the objectives of the research and the methodology used to carry out the research.

- Chapter 2 provides a detailed discussion of the relevant published works on single microchannels, stacked microchannels, micro pin fins, constructal design and heat sinks. Relevant literature on the application of response surface optimisation to heat sink design is also discussed.

- Chapter 3 contains a review of the numerical modelling and optimisation technique employed for the analysis. The mass, momentum and energy conservation equations governing the transport of mass and heat are discussed and the underlying principles and equations governing the optimisation algorithm are explained.

UNIVERSITEIT VAN PRETORIA
UNIVERSITY OF PRETORIA
YUNIBESITHI YA PRETORIA

- Chapter 4 applies the numerical and optimisation methodology in Chapter 3 to the constructal design and optimisation of single and stacked microchannel heat sinks. Detailed results of the optimal geometry were also presented.

- Chapter 5 presents and develops a new design of micro heat sink, which combines microchannels and micro pin fins. The numerical and optimisation methodologies stated in Chapter 3 are employed to numerically optimise the single microchannels and two-layered microchannel with parallel and counter flow configurations inserted with micro pin fins. A comparison between the combined designs is also made.

- Chapter 6 investigates the temperature variation on the heated base of a solid substrate cooled with different types of heat sinks. The heat sinks chosen for the investigation are the single microchannel, the combined design of the single microchannel with circular-shaped micro pin fins, the two-layered microchannel with parallel flow configuration, the two-layered microchannel with counter flow configuration and the combined design of the two-layered microchannel with the different configurations inserted with circular-shaped micro pin fins. The thermal performances of these micro heat sinks are also compared.

UNIVERSITEIT VAN PRETORIA
UNIVERSITY OF PRETORIA
YUNIBESITHI YA PRETORIA

- Chapter 7 provides a general summary of the findings of the study, conclusions, as well as recommendations for future work.

UNIVERSITEIT VAN PRETORIA
UNIVERSITY OF PRETORIA
YUNIBESITHI YA PRETORIA

CHAPTER 2: LITERATURE REVIEW

2.1. INTRODUCTION

This chapter gives a summary of relevant literature that gives insight into the analytical, numerical and experimental investigations of heat transfer and fluid flow in microchannels and micro pin fins and the optimisation of these heat sinks.

2.2. SINGLE MICROCHANNEL HEAT SINKS

Flow in microchannels has been studied broadly for decades, mainly because new and efficient methods are being sought for cooling electronic devices [1]. The approach of utilising forced fluid flow through microchannel heat sinks to remove high heat fluxes in microelectromechanical systems (MEMS) was first presented by Tuckerman and Pease [12-15, 32-34]. Since then, many analytical, experimental and numerical investigations have been carried out with the aim of improving the thermal performance of single microchannels. The geometric aspects of microchannels were also considered to obtain optimal channel dimensions that give the best thermal performance depending on the operating conditions. To obtain this optimal

UNIVERSITEIT VAN PRETORIA
UNIVERSITY OF PRETORIA
YUNIBESITHI YA PRETORIA

configuration, geometric optimisation was carried out using different optimisation techniques. Some of these works are mentioned below.

R.W. Knight *et al.* [35] present an analytical scheme to solve the governing equations of fluid dynamics and combined conduction and convection heat transfer for both laminar and turbulent flow in a heat sink with applications to microchannels. The scheme used could obtain the dimensions of the heat sink that gave the minimum thermal resistance between the portion of the heat sink with maximum temperature and the cooling fluid. Their results showed 10 to 35% improvement in the thermal resistance over the results presented by Tuckerman and Pease [32] and by Goldberg [36].

C. Perret *et al.* [37] used analytical tools to obtain an overall evaluation of all thermal resistances associated with a novel cooling device fully built in silicon technology. The cooling device presented involved micromachining the bottom side of a circuit wafer so that microchannel heat sinks could be embedded directly into the silicon material. Pascosma software, a home-developed software, with adequate analytical models was used to obtain the optimum dimensions of the silicon micro heat sink. Prototypes were also tested and there were good agreements between the experimental and calculated values.

UNIVERSITEIT VAN PRETORIA
UNIVERSITY OF PRETORIA
YUNIBESITHI YA PRETORIA

Murakami and Mikic [38] carried out an analytical optimisation study of circular multichannel heat sinks with application to electronic devices. The analytical method used obtained the optimum values of geometric parameters of the multichannel heat sink for minimum pumping power or minimum pressure drop for both laminar and turbulent regimes.

Upadhye and Kandlikar [39] analysed the heat transfer and pressure drop characteristics of single-phase flow of water through an electronic chip with a direct cooling area of 25 mm by 25 mm. Considering the effect of the channel dimensions on the pressure drop, the temperature of the cooling fluid at the outlet and the rate of heat transfer, results obtained indicated that a narrow and deep channel was better than a wide and shallow channel.

An entropy generation minimisation (EGM) procedure was used by Khan *et al.* [40] to optimise the overall performance of microchannel heat sinks. The overall thermal performance was measured by minimised pumping power and thermal resistance and the optimisation was done simultaneously. A parametric study was carried out and the design variables considered were the channel aspect ratio, fin spacing ratio, heat sink material, Knudsen numbers and accommodation coefficients. The study was carried out to investigate how the different design variables affected the thermal and hydraulic performance of the microchannel.

Turkakar and Okutucu-Ozyurt [41] improved on existing analytical optimisation models by considering entrance effects and property variations in their search for

UNIVERSITEIT VAN PRETORIA
UNIVERSITY OF PRETORIA
YUNIBESITHI YA PRETORIA

optimal dimensions of water-cooled rectangular silicon microchannel heat sinks. In addition, they introduced a new optimisation model that accounted for multiple heat sources. Their objective was the minimising of the thermal resistance at constant pumping power and the Intel Core i7-900 Desktop Processor, which is known to dissipate 130 W of heat flux, was chosen as their reference processor. From the optimisation carried out, a maximum substrate temperature of 41˚C was reached for heat sink channel width of 149µm, fin thickness of 18µm, channel height of 300µm and pumping power of 0.088W.

Pence [42] used an analytical technique to compare the maximum channel wall temperature along and total pressure drop across a microchannel heat sink, which had a fractal-like branching channel network and straight channel arrangement. The fractal-like channel network was found to have yielded a 60% reduction in pressure drop for the same total flow rate and identical total convective surface areas as that of the straight channel. A 30 ˚C lower wall temperature was also achieved with the fractal-like channel network under identical pumping power conditions.

Ryu *et al.* [43] developed a three-dimensional numerical analysis procedure to investigate the thermal performance of a microchannel heat sink. The objective of this work was the minimisation of thermal resistance of the microchannel heat sink subject to specified pumping power. The optimal fin-channel shape that minimised the thermal resistance was obtained using the random search technique. It was discovered

UNIVERSITEIT VAN PRETORIA
UNIVERSITY OF PRETORIA
YUNIBESITHI YA PRETORIA

that among various design variables, the channel width appeared to be the most crucial quantity in dictating the performance of a microchannel heat sink.

In another numerical study carried out by Ryu *et al.* [44], a three-dimensional analysis procedure was also developed and coupled with the steepest descent algorithm to investigate the thermal performance of a manifold microchannel heat sink and to obtain its optimal geometric dimensions. It was observed that the manifold microchannel heat sink had a lower thermal resistance of more than 50% when compared with the traditional microchannel. Their results also showed that the channel width and depth were the most critical design variables in dictating heat sink performance.

Muller and Frechette [45] numerically optimised forced convection in microchannel heat sinks for minimum pump power at high heat fluxes for air and water in single-phase flow with no transition. The optimum values of the chosen design parameters were found numerically by Newton method. From their investigations, it was observed that large aspect ratios for the flow channels were good for high heat fluxes. It was also observed that each design had an optimum fin height and ratio of fin thickness to channel width.

Gawali and Kamble [46] carried out a numerical analysis of rectangular micro-channel under forced convection heat transfer with hydraulic diameters ranging from 476 to 550 micrometres, height of 400 to 600 micrometres and spacing range of 250

UNIVERSITEIT VAN PRETORIA
UNIVERSITY OF PRETORIA
YUNIBESITHI YA PRETORIA

to 400 micrometres. The material of the microchannel was copper. From their analysis, it was observed that the hydraulic diameter of the microchannel was dependent on the flow rate of water.

Patel and Modi [47] numerically investigated forced convection of water in silicon-based single rectangular microchannel heat sink for electronic chips cooling using a commercial computational fluid dynamics (CFD) software FLUENT taking into consideration three different pressure drops. From their analysis, it was observed that the forced convection water-cooled microchannel heat sink had a better capability for use in thermal management of the electronic devices.

A detailed numerical simulation of heat transfer in silicon-based microchannel heat sink was conducted by Li and Peterson [13] using a simplified three-dimensional conjugate heat transfer model consisting of a two-dimensional fluid flow and three-dimensional heat transfer. This investigation was conducted to optimise the geometric structure of the microchannel heat sink. From their investigations, it was observed that the design and optimisation of microchannel heat sinks depended on important parameters, which were the physical geometry of the microchannel and the thermo physical properties of the substrate. From another numerical investigation carried out using a three-dimensional conjugate heat transfer model [34], the thermal resistance of optimised silicon-based, parallel microchannel heat sink was obtained for different pumping powers and results were compared with those obtained previously by

UNIVERSITEIT VAN PRETORIA
UNIVERSITY OF PRETORIA
YUNIBESITHI YA PRETORIA

Tuckerman and Pease [32]. Their results showed that using optimised geometric dimensions enhanced the overall cooling capacity of the heat sink.

Liu and Garimella [48] compared five different approximate analytical models that gave closed-form solutions for single-phase convective heat transfer in microchannels and then set up a general computational fluid dynamics (CFD) model to obtain the "exact" solution. The optimisation computations were carried out using the commercial solver MATLAB and it was observed that the minimum thermal resistance was always attained at the largest allowable aspect ratio. The results obtained demonstrated that the models developed were accurate enough to make predictions for practical designs.

A numerical study of the three-dimensional fluid flow and heat transfer in a rectangular microchannel heat sink with water as cooling fluid was carried out by Qu and Mudawar [49]. They developed a numerical code based on the finite difference method and the SIMPLE algorithm to solve the governing equations. It was observed that the highest temperature occurred at the heated base surface of the heat sink immediately above the channel outlet and that increasing the thermal conductivity of the solid substrate reduced the temperature at the heated base surface of the heat sink especially near the channel outlet. Experimental investigations were also carried out to investigate the pressure drop and heat transfer characteristics of a single-phase microchannel heat sink employing deionised water as cooling fluid and results compared with those obtained numerically [50]. The pressure drop and temperature

UNIVERSITEIT VAN PRETORIA
UNIVERSITY OF PRETORIA
YUNIBESITHI YA PRETORIA

distribution results were in good agreement with the numerical predictions showing that conventional Navier-Stokes and energy equations could effectively predict the fluid flow and heat transfer of microchannel heat sinks.

Chen *et al.* [51] developed a three-dimensional model in non-circular microchannel heat sinks (triangular, rectangular and trapezoidal) in order to numerically analyse the heat transfer and fluid flow through them. The comparison of thermal efficiencies of the different geometries was conducted and it was observed that the triangular micro-channel had the highest thermal efficiency.

Kou *et al.* [52] developed a three-dimensional numerical model to study the effects of heat transfer characteristics in a microchannel. This numerical investigation was conducted to search for the optimum channel width of the microchannel that gave minimum thermal resistance. The results of their study showed that a larger flow area, larger flow power and shorter substrate thickness could obtain lower thermal resistance. Also, when the pumping power was fixed at 0.01W and 0.1W, the effect of the decrease in channel height on the optimal channel width was not significant. At lower pumping power of 0.001 W and 0.0001 W, it was discovered that the optimum channel strongly depended on the channel height.

Husain and Kim [53] carried out a multi-objective optimisation of silicon microchannel heat sink using surrogate analysis and hybrid multi-objective evolutionary approach in combination with three-dimensional Navier-Stokes analysis.

UNIVERSITEIT VAN PRETORIA
UNIVERSITY OF PRETORIA
YUNIBESITHI YA PRETORIA

The objective functions were the thermal resistance and pumping power, while two design variables related to the microchannel depth, namely width and fin-width, were chosen for the optimisation. The cooling fluid was water with temperature-dependent properties. Results showed the existing trade-off between thermal resistance and pumping power over the selected design space in which the microchannel heat sink was optimised.

In another numerical investigation carried out, Husain and Kim [54] geometrically optimised a rectangular microchannel heat sink using three different surrogate models. In this numerical study, thermal resistance was the single objective function while pumping power was the constraint. Results showed that the different surrogate models yielded different optimum microchannel geometries but predicted almost the same value of thermal resistance.

Toh *et al.* [55] numerically investigated the three-dimensional fluid flow and heat transfer phenomena in heated microchannels. Results showed that at lower Reynolds numbers, the temperature of water increased, which caused a decrease in viscosity and as a result, smaller frictional losses. The numerical procedure used in their study also correctly predicted the location of the maximum thermal resistance and the drop in thermal resistance as one approached the trailing edge of the heater.

Fedorov and Viskanta [56] carried out a theoretical and numerical analysis to investigate the flow and conjugate heat transfer in the microchannel-based heat sink

UNIVERSITEIT VAN PRETORIA
UNIVERSITY OF PRETORIA
YUNIBESITHI YA PRETORIA

for electronic packaging applications. Their results showed that the three-dimensional mathematical model developed was able to predict correctly fluid flow and heat transfer in microchannels. Their analysis also strongly showed that forced convection water-cooled microchannel heat sink had a superior potential for application in thermal management of electronic packages.

A numerical investigation into heat transfer in a silicon substrate containing rectangular microchannels was carried out by Ambatipudi and Rahman [57]. The channel depth, channel width, number of channels and flow rates through the channel were varied to investigate the effects of channel aspect ratio, Reynolds number and the number of channels on the thermal performance of the device. Results showed that when the Reynolds number and channel width were constant, the pressure drop was inversely proportional to the depth of the channel. Also increasing the number of channels was found to increase the local Nusselt number along the entire length of the channel.

Xia *et al.* [58] numerically investigated the effect of different geometric structures, which included inlet/outlet locations (I-, C- and Z-type), header shapes (triangular, trapezoidal and rectangular) and microchannel cross-sectional shapes (conventional microchannel, microchannel with off-set fan-shaped re-entrant cavities and microchannel with triangular re-entrant cavities), on the performance of the heat sink. It was discovered that the microchannel with off-set fan-shaped and triangular re-entrant cavities enhanced the heat transfer more than the conventional rectangular

UNIVERSITEIT VAN PRETORIA
UNIVERSITY OF PRETORIA
YUNIBESITHI YA PRETORIA

microchannel heat sink. Also, the C-type inlet/outlet heat sink had better heat transfer characteristics for a volume flow rate of 150 ml/min. From their investigations, it was concluded that this type of inlet/outlet arrangement was able to prolong the life of microelectronic devices.

Numerical investigations into constrained fluid flow and conjugate heat transfer in microchannel heat sinks (MCHS) with converging channels were carried out by Dehghan *et al.* [59]. Their results showed that the required pumping power of the optimum width-tapered configuration was 0.25% of that required for the straight channel with the same heat removal capacity and maximum pressure drop of 3 kPa. It was also discovered that an MCHS with moderate width-tapered ratio removed the same amount of heat flux as the MCHS with straight flow channels but with a substantial reduction in the required pumping power.

Xie *et al.* [60] carried out a numerical investigation using CFD on three-dimensional laminar flow and convective heat transfer in bifurcated MCHS with multiple length bifurcation plates. The effect of the velocity at the inlet and number of bifurcation plates on the pressure drop, flow structures and temperature distributions was comprehensively studied to estimate the cooling performance of the bifurcating MCHS. Results obtained in this study showed that the thermal performance of the bifurcated MCHS was better than its smooth MCHS counterpart with an enhancement factor of up to 2.0. It was concluded that an accurate design of the multiple length bifurcation could be used to improve the overall performance of the MCHS.

UNIVERSITEIT VAN PRETORIA
UNIVERSITY OF PRETORIA
YUNIBESITHI YA PRETORIA

Qu *et al.* [61] experimentally investigated heat transfer characteristics of water flowing through trapezoidal silicon microchannels with hydraulic diameter ranging from 62 to 169 micrometres. Their results were compared with numerical predictions and it was found that an experimentally determined Nusselt number was much lower than that of the numerical analysis. As a result, a modified relation which accounted for roughness-viscosity effects was proposed to interpret the experimental results.

Experimental investigations were also carried out by Lee *et al.* [62] to see if classical correlations based on conventional-sized channels could accurately predict the thermal behaviour of single-phase flow through rectangular microchannels. Based on their numerical predictions and experimental data, it was confirmed that the conventional analysis approach could be used to predict heat transfer behaviour in microchannels based on the dimensions they considered.

A bibliographical review of experimental works carried out on the convective heat transfer through microchannels by Morini [63] revealed that while some authors found the predictions of conventional theory to agree with experimental results, some others discovered the opposite for the same range of hydraulic diameter. As a result of these variations, it was suggested that further systematic studies on convective heat transfer in microchannels were necessary to obtain sufficient information on transport mechanisms in microchannels.

UNIVERSITEIT VAN PRETORIA
UNIVERSITY OF PRETORIA
YUNIBESITHI YA PRETORIA

Naphon and Khonseur [64] experimentally investigated the heat transfer characteristics and pressure drop in microchannel heat sinks with various geometric configurations under constant heat flux. Their results revealed that the shape and the size of roughness irregularities of the microchannel surface had a great effect on improving heat transfer performance and the pressure drop variations.

An experimental facility was designed by Garimella and Singhal [65] to carry out experimental investigations into fluid flow and heat transfer in microchannels with hydraulic diameter ranging from 250 to 1 000 micrometres. Fluid flow and heat transfer behaviour were carefully analysed to verify the Reynolds number for transition from laminar to turbulent flow and also to assess the validity of the conventional correlations used in predicting these characteristics. Their results showed that experimental results matched well with the predictions. Pumping requirements of microchannel heat sinks were also analysed and the microchannel dimensions were optimised to minimise the pumping power requirements for a given heat removal rate.

A liquid-cooled aluminium microchannel heat sink was designed and fabricated by Zhang *et al.* [66] to study single-phase liquid-cooled microchannel heat sinks for electronic packages. An analytical method which accounted for simultaneous developing flow in microchannel heat sink was also developed to predict the pressure drop and thermal resistance. The analytical prediction and results from the experiments were in good agreement. The analytical results showed that the thermal

UNIVERSITEIT VAN PRETORIA
UNIVERSITY OF PRETORIA
YUNIBESITHI YA PRETORIA

resistances based on the liquid cooling apparatus used could be greatly reduced when advanced thermal interface materials were employed.

From the experimental investigations carried out by Peng and Peterson [67], it was observed that transition and laminar heat transfer in microchannels were not the same as those for liquid flowing through conventional-sized channels. Rather, they were more complex. They also presented evidence to show that there existed an optimal channel size of rectangular microchannel with single-phase liquid flow and forced convective heat transfer.

Hetsroni *et al.* [68] compared experimental results obtained by different investigators with theoretical and numerical results obtained for single-phase heat transfer in microchannels. The analysis of data of heat transfer in four different shapes of microchannels with hydraulic diameters ranging from 60 μm to 2000 μm was carried out. One of the observations made was that the experimental study of heat transfer in microchannels was a complex problem because of the small sizes of the channels. Comparison of measured data based on several models of heat transfer could be used to estimate how applicable conventional theory was. It could also be used to estimate the correctness of the many hypotheses related to the heat transfer process.

Rezania *et al.* [69] carried out an experimental investigation into the application of plate-fin microchannel heat sink in thermoelectric power generators (TEG) in order to create a light and compact system. Their results showed that there was a slow increase

UNIVERSITEIT VAN PRETORIA
UNIVERSITY OF PRETORIA
YUNIBESITHI YA PRETORIA

in the temperature difference of the hot and cold sides of the TEG with flow rate at the imposed constant heat flux. It was also seen that at each temperature difference, there existed a unique flow rate that resulted in maximum net power in the system.

Adham *et al.* [16] reviewed broadly available literature on non-circular microchannel heat sinks especially on rectangular microchannels. According to their review, earlier studies (from 1981 to 1999) mostly used experimental or analytical methods to carry out their investigations, while more current studies (from 2000 to the end of 2012) depended more on numerical simulations and evolutionary algorithms to carry out their investigations. Liquid cooling was also preferred to gaseous cooling and there was more emphasis on laminar flow as the prevailing flow condition.

2.3. STACKED MICROCHANNEL HEAT SINKS

Development of stacked microchannel heat sinks was also necessary to provide efficient cooling of microelectronic devices. The two major advantages this type of microchannel heat sink offers are heat transfer and fluid flow at low pressure drops while maintaining temperature uniformity of the chips [70].

Wei and Joshi [71] observed with smaller velocity at flow inlet, that a stack of microchannel needed less pumping power to remove a certain heat rate when compared with a single-layered microchannel because of the larger heat transfer area

UNIVERSITEIT VAN PRETORIA
UNIVERSITY OF PRETORIA
YUNIBESITHI YA PRETORIA

provided. In their analytical study, a single objective minimisation of overall thermal resistance was carried out with aspect ratio, fin thickness, ratio of channel width to fin thickness as variables using genetic algorithms on a simple thermal resistance network they developed. The constraints used in their optimisation study were a maximum pressure drop of 4 bars and maximum volumetric flow rate of 1 000 ml/min. They also investigated the effect of the number of layers in the stack, pumping power per unit area and channel length on the total thermal resistance. Their results showed that for a constant pumping power of 0.01W, the optimal number of layers was three.

Numerical investigations were also carried out by Wei and Joshi [72] on a multi-layered stack of liquid cooled microchannels and their results showed that for a given heat removal capability for the heat sink, the required pumping power or pressure for the stacked microchannels with more than two layers was significantly lower when compared with a single microchannel.

Wei *et al.* [73] carried out numerical and experimental investigations of the thermal performance of stacked microchannel heat sinks involving studies on the effect of coolant flow direction, flow rate allocation among layers and non-uniform heating. Their results showed that even though the counter flow arrangement provided better temperature uniformity, the parallel flow configuration had the best performance in reducing peak temperature. This was also observed by Patterson *et al.* [74], who carried out a conjugate numerical study of heat transfer inside stacked microchannels

UNIVERSITEIT VAN PRETORIA
UNIVERSITY OF PRETORIA
YUNIBESITHI YA PRETORIA

with parallel, counter flow and serial flow arrangements. Their results showed that at low flow rates, the parallel-flow configuration performed better but at very high flows, the heat sink with counter flow of fluid outperformed the one with parallel flow.

Jeevan *et al.* [75] carried out a numerical optimisation of stacked microchannel heat sink to minimise the thermal resistance using one- and two-dimensional finite element models (FEM) with genetic algorithms. Their results were compared with results obtained by Wei and Joshi [71], who used the thermal resistance network model. Their one-dimensional FEM approach was in very good agreement with Wei and Joshi's results but the two-dimensional (2D) FEM approach gave better results. They also used the two-dimensional FEM approach to obtain the optimal number of stack layers for minimum thermal resistance and fixed pumping power per unit area of 0.01 W/cm^2 as three.

Jeevan *et al.* [76] also carried out numerical optimisation of a double-layered counter flow (DLCF) microchannel heat sink with rectangular channels using FEM with genetic algorithms and box optimisation method to determine the minimal thermal resistance when a fixed pumping power constraint was applied. When compared with a single-layer counter flow (SLCF) and single-layer parallel-flow (SLPF) microchannel heat sink, their results showed that based on the minimisation of thermal resistance, the DLCF microchannel performed better than the SLCF and SLPF microchannel heat sinks.

UNIVERSITEIT VAN PRETORIA
UNIVERSITY OF PRETORIA
YUNIBESITHI YA PRETORIA

Cheng [77] conducted a numerical investigation on a two-layer stacked microchannel heat sink with multiple MEMS easy processing passive microstructures. The aim of their investigation was to discover how the ratio of embedded structure height to microchannel height and the fluid property affected the thermal performance of their design. Their results showed that in terms of reduction of thermal resistance, the stacked microchannel with the passive microstructure performed better than the popular smooth microchannels.

Chong *et al.* [78] analytically modelled an SLCF and DLCF microchannel heat sink with rectangular channels using the thermal resistance network and available correlations. Their results were numerically verified using a three-dimensional computational fluid dynamics (CFD) conjugate heat transfer model, which showed good agreements. The aim of their study was to calculate the thermal performance of the heat sinks. Their thermal resistance model was linked with complex multivariable constrained direct search optimisation algorithm to optimise the SLCF and DLCF heat sinks under given constraints. From their results, it was observed that the laminar flow heat sinks performed better than their turbulent counterparts for both heat transfer and hydrodynamic analysis.

Hegde and Seetharamu [79] used the FEM approach to numerically investigate the effects of non-uniform base heating on the performance of parallel-flow and counter flow stacked microchannel heat sinks and compared their results with the case of

UNIVERSITEIT VAN PRETORIA
UNIVERSITY OF PRETORIA
YUNIBESITHI YA PRETORIA

uniform heating. From their study, it was observed that when uniform heating was compared with non-uniform heating for the counter flow arrangement, uniform heating gave a more uniform base temperature distribution when peak temperature was lowest.

Three-dimensional numerical investigations into the conjugate heat transfer performance of trapezoidal-shaped double-layered microchannel heat sink with parallel-flow and counter flow arrangements were carried out by Sharma *et al.* [80] and their results were compared with that of the rectangular double-layered heat sink of the same flow area. When all the configurations were compared, their results showed that the trapezoidal double-layered heat sink performed much better than its rectangular counterpart in terms of minimum thermal resistance and minimum temperature variations but in their study, the trapezoidal shape was not optimised to obtain optimal performance.

Vafai and Zhu [81] proposed a new concept of cooling of electronic components using a counter-current flow of fluid through a two-layered microchannel heat sink. The focus of their study was temperature distribution, thermal resistance and optimisation of the geometry design parameters. Their results showed that the two-layered microchannel had a substantial improved performance over the conventional one-layered design for the range of parameters used in the study.

UNIVERSITEIT VAN PRETORIA
UNIVERSITY OF PRETORIA
YUNIBESITHI YA PRETORIA

A numerical analysis was carried out by Hung *et al.* [82] to study the effects of substrate materials, different coolants, different geometric parameters and pumping power on the temperature distribution, pressure drop and thermal resistance for a double-layered microchannel heat sink. One of the observations made in their study was that the thermal resistance of the microchannel heat sink could be minimised by optimising the geometric parameters. Their results showed that for the same dimensions of heat sink, there was a 6.3% improvement in the thermal performance of the double-layered microchannel over that of the single-layered one.

Lin *et al.* [83] used a three-dimensional solid-fluid conjugated model coupled with a simplified conjugate-gradient method to optimise the flow and heat transfer of a double-layered microchannel heat sink made of silicon and cooled with water. In their study, six design variables were considered in their search for a minimum global thermal resistance at fixed pumping powers, coolant volumetric rates and pressure drops through the heat sink. Results obtained confirmed that the optimal design depended strongly on the constraint conditions.

Hung *et al.* [84] used a simplified conjugate-gradient method and a three-dimensional fluid flow and heat transfer model to investigate numerically the optimal geometric parameters of a double-layered microchannel heat sink. The design variables considered for optimisation were the number of channels, channel width ratio, lower-channel aspect ratio and the upper-channel aspect ratio, while the overall thermal resistance was the objective function. Their results showed that optimal thermal

UNIVERSITEIT VAN PRETORIA
UNIVERSITY OF PRETORIA
YUNIBESITHI YA PRETORIA

resistance decreased with increase in pumping power and thereafter, tended to approach a constant value. It was also mentioned that increasing pumping power was not always cost-effective for practical heat sink design.

Leng *et al.* [85] developed a multi-parameter optimisation algorithm, which included a three-dimensional heat sink model and a simplified conjugate-gradient method to optimise a novel double-layered microchannel heat sink with truncated top channels [86]. It was observed from their study that the design directions of the search variables strongly depended on the constraint condition. As the pumping power was increased, the optimal design required a larger number of channels and smaller channel width, channel height and smaller dimensionless truncation length.

Wu *et al.* [87] numerically investigated the effects of channel number (width ratio), aspect ratio and velocity ratio on the overall thermal performance of a double-layered microchannel heat sink (DL-MCHS). When the condition of identical inlet velocity in the upper and lower channels was compared with adjusting the inlet velocity of the upper channel to be smaller, it was discovered that the latter case had the potential to improve the overall performance of the DL-MCHS at a given pumping power.

Other recent studies on optimisation of double-layered microchannel heat sinks were also carried out by Leng *et al.* [88] and Xie *et al.* [89].

UNIVERSITEIT VAN PRETORIA
UNIVERSITY OF PRETORIA
YUNIBESITHI YA PRETORIA

2.4. MICRO PIN-FIN HEAT SINKS

One of the cooling methods that have also been proposed for electronic equipment is the pin-fin heat sink because of its capability of dissipating high heat fluxes, which is a very important consideration in the thermal management in microelectronic devices [90, 91]. Other advantages of the pin-fin heat sink are the large surface area for dissipation of heat that it provides, its effective reduction of thermal resistance of the package, the less space it takes and its low contribution to weight and cost above other options [92]. Many analytical, numerical and experimental investigations have been carried out to investigate heat transfer and fluid flow in this type of heat sink, some of which are outlined below.

Kim *et al.* [90] carried out investigations on fluid flow and forced convective heat transfer through fully shrouded pin-fin heat sinks. A novel compact modelling method based on volume-averaging technique was used for the analysis of the heat and fluid flow and results obtained were validated experimentally using 20 aluminium pin-fin heat sinks of conventional sizes. Optimisation of the pin-fin heat sink was carried out based on minimised thermal resistance and their results showed that the thermal performance of the optimised pin-fin heat sink was improved by about 50% over the optimised straight fin heat sinks subject to the same constraints.

UNIVERSITEIT VAN PRETORIA
UNIVERSITY OF PRETORIA
YUNIBESITHI YA PRETORIA

Khan *et al.* [91] developed analytical models to determine heat transfer from pin-fin heat sinks used in electronic packaging applications. The predictions of their models validated previous numerical and experimental results. One of the observations made in their study was that the pin-fin heat sink with in-line arrangement gave higher heat sink resistance and lower pressure drop than the staggered arrangement. In another analytical study carried out, mathematical models were developed for predicting thermal and hydraulic resistances for both in-line and staggered arrangement of a cylindrical pin-fin heat sink in laminar forced convection [92].

Khan *et al.* also applied the entropy generation minimisation technique to study the thermodynamic losses caused by heat transfer and pressure drop in cylindrical pin-fin heat sinks for both in-line and staggered arrangements [93]. All relevant design parameters for pin-fin heat sinks were optimised simultaneously by minimising the entropy generation rate subject to manufacturing and design constraints. Their results showed that three and four parameter optimisation for in-line arrangement of pin fins gave lower entropy generation rate. It was also observed that for a given size and heat load, the global performance of a pin-fin heat sink depended on dimensions of the pin fins, pin density, longitudinal and transverse spacing, interface material, location and size of heat sources, method of manufacturing and type of heat sink material, approach velocity and arrangement of the pins.

An analytical study was carried out by Yeh [94] to determine the dimensions of cylindrical pin fins and rectangular fins with fixed volumes that maximised heat transfer. Observations made from their study showed that fins with insulated tip had

UNIVERSITEIT VAN PRETORIA
UNIVERSITY OF PRETORIA
YUNIBESITHI YA PRETORIA

an optimum aspect ratio, which decreased with increased fin volume or heat transfer coefficient at the fin base.

An analytical study of the thermal performance of micro pin fins of variable diameter and rough surface was conducted by Diez *et al.* [95]. The influence of a random, isotropic surface roughness on truncated micro pin fins of variable diameter for hyperbolic, trapezoidal and concave parabolic geometries was reported. It was observed that the approximate method based on truncated power series accurately predicted the temperature distributions, efficiency and effectiveness of smooth pin fins, which were practically the same for rough micro pin fins.

Park *et al.* [96] numerically optimised a seven by seven square pin-fin heat sink made of aluminium. The objective was to minimise the thermal resistance at the junction of the chip and heat sink and the overall pressure drop in the heat sink simultaneously. The chosen design variables were the fin height and width and fan-to-heat sink distance. The parametric studies carried out in this study showed that the fin width had a strong influence on the objective functions, while the effect of the fan-to-heat sink distance was relatively small compared with the other two design variables.

The overall performance of square-shaped and circular micro pin-fin heat sinks with single-phase liquid flow operating under similar conditions was numerically investigated by John *et al.* [97]. The effect of thermal resistance and pressure drop subject to axial and transverse pitch distance, aspect ratio and hydraulic diameter of

UNIVERSITEIT VAN PRETORIA
UNIVERSITY OF PRETORIA
YUNIBESITHI YA PRETORIA

pin fin, and the liquid flow rate through the device was studied. It was observed that at low Reynolds numbers (below 300), the circular pin-fin heat sinks performed better than its square counterpart but the reverse was the case at high Reynolds numbers (above 300).

Yang and Peng [98] carried out a numerical investigation of the thermal performance of heat sinks with impingement cooling with the aim of examining how the fin shape of the heat sink affected its thermal performance. Their results showed that the effect of fin dimensions on Nusselt number was more obvious at high Reynolds numbers than at low Reynolds numbers. The potential of optimising the un-uniform fin width design was also demonstrated.

Sahiti *et al.* [99] carried out an optimisation procedure that yielded a heat exchanger performance plot that allowed performance of pin fins to be compared based on two operating parameters, which were the heat transfer rate per unit base surface area and the power input for the same area. Their results showed that elliptical cross-sections of pin fins offered the best performance when compared with all other investigated cross-sections of pin fins. The design parameters considered in the optimisation were the transverse and stream-wise pin spacing, the inlet fluid velocity and the elliptical axis ratio.

A finite element model was developed by Galvis *et al.* [100] to predict both the Nusselt number and friction factor for heat transfer and turbulent fluid flow in a micro

UNIVERSITEIT VAN PRETORIA
UNIVERSITY OF PRETORIA
YUNIBESITHI YA PRETORIA

heat exchanger using different turbulent models. The micro heat exchanger consisted of a narrow planar flow passage between flat parallel plates with small staggered cylindrical pin fins spanning the walls. The renormalised group (RNG) model was found to be the best model to predict Nusselt number and friction factor in micro heat exchangers. Their predicted results were compared with experimental results in open literature and it was observed that the finite element model developed tended to over-predict the friction factor at high Reynolds numbers by about 31%. It was concluded that better turbulence modelling is required for better prediction of flow field in micro heat exchangers.

Rubio-Jimenez *et al.* [101] proposed and numerically analysed a novel design of different shapes of micro pin fins with variable density (which allowed the gradual increase of heat transfer area as coolant passes through the system) to generate a more uniform temperature for integrated circuit (IC) chip junctions. The fin shapes considered were circle, square, elliptical and flat with two redounded sides. Their results showed that fin shape was an important design parameter when considering pressure drop rather than heat dissipation. The heat transfer area to fluid volume ratio mainly affected the heat dissipation.

Tahat *et al.* [102] experimentally investigated steady-state heat transfer from a horizontal base plate with cylindrical pin fins protruding vertically upwards for both staggered and in-line arrangements of the pin fins. The pin fins were orthogonal to mean air flow. Their results showed that for the staggered and in-line arrangements,

UNIVERSITEIT VAN PRETORIA
UNIVERSITY OF PRETORIA
YUNIBESITHI YA PRETORIA

heat loss rose as the Reynolds number was increased but decreased as the pin-fin spacing was increased for both stream-wise and span-wise directions. Correlations that showed the dependence of Nusselt number on Reynolds number and pin-fin pitch were also developed.

A comprehensive analytical and experimental heat transfer analysis over a bank of micro pin fins was carried out by Peles *et al.* [103]. Their results showed that the thermo-hydraulic performance of flow across a micro-scale cylindrical pin-fin array was superior to that of the plain microchannel-based cooling. It was also observed that forced convection over shrouded micro pin-fin heat sinks was a very effective heat transfer mode and they advised that to suppress the convective thermal resistance, dense pin-fin configurations should be used at high Reynolds numbers, while sparse arrangements were preferable at low Reynolds numbers.

Kosar *et al.* [104] experimentally investigated pressure drops and friction factors due to the flow of de-ionised water over staggered and in-line circular and diamond-shaped micro pin-fin bundles to assess whether the conventional scale correlations adequately predicted flow at micro scale. It was shown that the available large-scale correlations did not efficiently predict pressure drop obtained at micro scale and as a result, modified correlations based on their experimental results using micro-scale devices were proposed.

UNIVERSITEIT VAN PRETORIA
UNIVERSITY OF PRETORIA
YUNIBESITHI YA PRETORIA

Kosar and Peles [105] carried out another experimental study on the heat transfer and pressure drop of de-ionised water over a bank of shrouded staggered micro pin fins to obtain average heat transfer coefficients for effective heat fluxes ranging from 3.8 to 167 W/cm^2 and Reynolds numbers from 14 to 112. It was discovered that only a few of the conventional scale correlations provided the correct ground for comparison with micro-scale fins because end-wall effects were significant at low Reynolds number flow over intermediate pin fins.

Experimental results of heat transfer and pressure drop of cross-flow over five micro-scale pin-fin heat sinks were also presented by Kosar and Peles [106] to compare the thermal-hydraulic performance of the heat sinks at fixed mass flow rate, pressure drop and pumping power. The different geometric shapes of the pin fins were circular, hydrofoil-based, cone-shaped and rectangular. It was observed that large spacing between pin fins and in-line arrangement of the fins resulted in lower heat transfer coefficients. Also, micro pin fins with sharp pointed regions generated higher heat transfer coefficients than streamlined ones.

Siu-Ho *et al.* [107, 108] carried out an experimental investigation of the pressure drop and heat transfer characteristics of a single-phase square-shaped micro pin-fin heat sink in staggered arrangement and evaluated average friction factor, local averaged heat transfer coefficient with the measured pressure drop and temperature distribution. It was observed that friction factor decreased with increasing Reynolds number, local

UNIVERSITEIT VAN PRETORIA
UNIVERSITY OF PRETORIA
YUNIBESITHI YA PRETORIA

heat transfer coefficient had a higher value near the heat sink inlet and decreased along the flow direction.

An experimental study of pressure drop in a two-phase heat sink containing an array of staggered square micro pin fins was also done by Qu and Siu-Ho [109]. From their study, it was observed that micro pin fins offered better flow stability than parallel microchannels. They also carried out an experimental study on the thermal and hydraulic characteristics of liquid single-phase flow in an array of staggered square micro pin fins [110]. From their results, they were able to develop two new heat transfer correlations based on the average heat transfer data.

New experimental data and numerical results of heat transfer characteristics of tapered pin-fin heat sink under constant heat flux for laminar and turbulent flow of air were presented by Naphon and Sookkasem [111]. The study was carried out for both in-line and staggered arrangement of 16 and 17 pin fins respectively. It was observed that when the inlet air temperature was kept constant, the outlet air temperature decreased with increasing Reynolds number. Also, the average surface temperature decreased with increasing Reynolds number as a result of the dependence of the heat transfer from the fin on air mass flow rate. Their results showed that at low Reynolds number, the flow characteristics on the second row of fins were affected by the first row but this phenomenon decreased at higher Reynolds number.

UNIVERSITEIT VAN PRETORIA
UNIVERSITY OF PRETORIA
YUNIBESITHI YA PRETORIA

Prasher *et al.* [112] carried out an experimental investigation of pressure drop and thermal resistance of silicon-based, low aspect ratio square and round staggered micro pin-fin cold plates under cross-flow conditions. They observed that correlations available in open literature could not predict the friction factor and Nusselt numbers for the micro pin-fin array and as a result, more studies were needed to understand the thermal and hydraulic performances of these types of heat sinks.

Wang *et al.* [113] proposed the introduction of short pin fins on the surfaces of plate-fin heat sinks to improve the thermal performance of the plate-fin heat sinks. The fabrication of short copper pin fins on copper plates was done using a micro-fabrication approach based on photolithography and electroplating technologies. Their results showed that based on best design parameters, their proposed design improved the thermal performance of the heat sink by 78.3% with only 7.8% increase in the channel pressure drop.

The use of micro pin-fin heat sinks as an effective alternative to microchannel heat sinks for removing high heat fluxes from small areas was investigated by Jasperson *et al.* [114]. The comparison between the two types of heat sinks was based on thermal performance, hydraulic performance and cost of manufacturing. The pin fins investigated were made of copper, square shaped and in staggered arrangement. It was concluded that neither of the heat sinks was better for all applications. An example presented in their study revealed that even though the micro pin fin had better thermal performance, the pressure drop across it was approximately twice as large as that

UNIVERSITEIT VAN PRETORIA
UNIVERSITY OF PRETORIA
YUNIBESITHI YA PRETORIA

across the microchannel heat sink at low rates. Also, because of the extra machining time required, micro pin-fin heat sinks were roughly three times as expensive to make.

Yang and Peng [115] numerically investigated the thermal and hydraulic performance of a compound heat sink made up of a combination of plate-fin heat sink and pin fins. The shapes of the pin fins considered in this study were the circular and square shapes. This investigation was carried out to examine how the configuration of the pin fin affected the thermal resistance and pressure drop of the compound design. Their numerical results revealed that at the same wind velocity, the thermal resistance of the compound heat sink was lower than that of the plate-fin heat sink but the pressure drop of the compound design was much higher. It was also shown that the compound heat sink with circular-shaped pin fins performed better than that with square-shaped ones.

Ndao *et al.* [116] carried out a comprehensive analysis of various electronics cooling technologies (microchannels, circular pin fins and offset strip-fin heat sinks) and this analysis was based on their thermal performances. A multi-objective thermal design optimisation was carried out based on minimising the thermal resistance and pressure drops. Their results showed that the offset strip-fin heat sink performed better than all others, but for relatively low pumping powers, the microchannel heat sink offered the lowest thermal resistances.

UNIVERSITEIT VAN PRETORIA
UNIVERSITY OF PRETORIA
YUNIBESITHI YA PRETORIA

2.5. CONSTRUCTAL DESIGN AND HEAT SINKS

A more recent approach applied to studies carried out to investigate forced convection heat transfer in heat sinks is a geometric optimisation technique involving constraint specification. This approach is based on the constructal theory, which begins with the global objective(s) and the global constraint(s) of the flow system, and the fact that in the beginning, the geometry of the flow is missing [18, 19]. Constructal law states as follows: "For a finite-size flow system to persist in time, its configuration must change in time such that it provides easier access to its currents" [30]. Numerous investigators have applied this law to the geometric optimisation of heat sinks [20-29, 31, 117-122] for better engineering design. In their studies, a search for geometric configuration that minimises thermal resistance (or maximises thermal conductance) was conducted.

Olakoyejo *et al.* [20] studied the numerical and analytical optimisation of geometric structures of square cooling channels of vascularised material with a localised self-cooling property subject to a heat flux on one side with the aim of minimising the peak temperature at every point in the solid body. Their results showed that material property had a significant influence on the performance of the cooling channel. As a result, when designing the cooling structure of a vascularised material, it was noted that the internal and external geometries of the structure, material properties and pump power requirements were identified as major parameters to be considered in

UNIVERSITEIT VAN PRETORIA
UNIVERSITY OF PRETORIA
YUNIBESITHI YA PRETORIA

obtaining efficient and optimal designs for best performance. In another numerical and analytical study carried out by Olakoyejo *et al.* [27], the geometric optimisation of circular and square-shaped cooling channels in forced convection with internal heat generation was investigated. Their numerical results were in good agreement with the analytical method used in the study and it was observed that for the range of parameters used in their study, the square channels performed better than the circular ones.

Bello-Ochende *et al.* [21] studied the geometric optimisation of a silicon-based microchannel heat sink using a combination of numerical optimisation and constructal theory. The objective of their study was to minimise the wall peak temperature subject to various constraints. Observations from results obtained showed that the optimal peak wall temperature decreased exponentially with an increase in pressure. Also, for a given pressure drop, there was a unique optimal geometric configuration that gave a minimised peak wall temperature.

The geometric optimisation of a three-dimensional microchannel heat sink was carried out by Bello-Ochende *et al.* [24, 117] to minimise the peak temperature from the walls to the coolant fluid. The effect of the total solid volume fraction and pressure drop on the aspect ratio, channel hydraulic diameter and peak temperature was investigated numerically. Their results showed that the global thermal conductance for a microchannel heat sink can be maximised by optimising the aspect

UNIVERSITEIT VAN PRETORIA
UNIVERSITY OF PRETORIA
YUNIBESITHI YA PRETORIA

ratio and hydraulic diameter of the microchannel for laminar forced conjugate heat transfer. Their numerical optimisation results also showed that the optimal microchannel shape and the minimised peak temperature are functions of the applied pressure difference and solid volume fraction.

The constructal optimisation method has also been used in the optimisation of pin-fin heat sinks. Almogbel and Bejan [118] used the constructal optimisation method to maximise the global conductance of cylindrical assemblies of pin fins subject to fixed total volume and amount of fin material. In their study, the parameters derived from the optimisation were the external aspect ratio of the volume and the internal ratio between the pin-fin diameters. It was observed that the amount of fin material had a negligible effect on the optimised ratio of the fin diameter.

Bello-Ochende *et al.* [23] also used the constructal technique to determine the geometric configuration of two rows of pin fins that maximised the total heat transfer rate. The parameters of interest were relative diameters, heights and spacing between the fins. From their results, it was concluded that the pin-fin flow structure performed best for non-uniform height and diameter of pin fins.

Muzychka [26] carried out an analytical study of heat transfer and fluid flow in micro-tube heat sinks and heat exchangers using the constructal multi-scale design approach. The results from their study showed that improved performance of heat sink and heat exchanger core structures could be obtained by using multi-scale design techniques

UNIVERSITEIT VAN PRETORIA
UNIVERSITY OF PRETORIA
YUNIBESITHI YA PRETORIA

rather than the conventional design approaches. Another analytical study was carried out by Muzychka [25] on heat transfer from arrays of circular and non-circular ducts subject to finite volume and pressure drop constraints. When the approximate results for optimal duct dimensions in the study were compared with exact results in open literature, there was excellent agreement.

Salimpour *et al.* [122] numerically optimised the geometries of an array of circular, square and isosceles triangle cross-sections of microchannels using the constructal design approach. Some correlations were developed from the results obtained from their study, which helped to predict the optimal hydraulic diameter and dimensionless heat transfer per unit volume. It was discovered that the microchannel with square cross-section had the highest heat transfer per unit volume for the volume considered in their study.

In another numerical investigation carried out by Salimpour *et al.* [123], the geometric optimisation of three-dimensional MCHS with rectangular, elliptic and isosceles triangular cross-sections were studied using the constructal design approach. Results obtained from their investigations showed that the MCHS with rectangular and elliptic cross-sections had similar performances, while the MCHS with isosceles triangular cross-sections had weaker performances for the constraints and geometric parameters considered. Their numerical results were also compared with approximate results obtained from scale analysis and there were good agreements.

UNIVERSITEIT VAN PRETORIA
UNIVERSITY OF PRETORIA
YUNIBESITHI YA PRETORIA

Li *et al.* [124] designed a series of novel rectangular straight MCHS with Y-shaped bifurcations and numerically analysed the heat transfer and pressure drop for all cases considered using CFD. Their results showed that the thermal resistance of the Y-shaped bifurcated MCHS design decreased to about three-fifths of that of the corresponding continuous straight MCHS at maximum inlet velocity of 1.4 m/s. It was also shown that the angle between the two arms of the Y-shaped bifurcation had a great effect on the thermal performance of the heat sink.

2.6. RESPONSE SURFACE OPTIMISATION AND HEAT SINKS

Khuri and Mukhopadhyay [125] provided a detailed survey of the various stages in the development of response surface methodology (RSM) over the years starting from the 1950s. The RSM, introduced by Box and Wilson [126], uses a group of mathematical and statistical techniques to develop an adequate functional relationship between a response of interest and a number of input variables [125]. The RSM has been used in the optimisation of some processes apart from heat sinks [127, 128]. RSM is also applied to computer simulations of physical systems where it is used to build a model of the system (a metamodel) and thereafter, optimisation is carried out on the metamodel where the assumption made is that the metamodel is a good representation of the physical system being modelled [129-134]. Some of the research works carried out on optimisation of heat sinks using RSM are mentioned below.

UNIVERSITEIT VAN PRETORIA
UNIVERSITY OF PRETORIA
YUNIBESITHI YA PRETORIA

Cheng *et al.* [135] showed how a combination of computational fluid dynamics (CFD) simulation and RSM can be used in analysing the thermal performance of a high input/output, seven-chip, indirect liquid-cooled multichip module that was to be applied to a kind of supercomputer. After simulating the heat transfer and fluid flow of the multichip module using CFD, a study on the effect of many factors on the thermal performance of the module was carried out and thereafter, a one-factor-at-a-time (OFAT) experimentation was used to select important factors. The response surface model of the maximum temperature in the module in relation to the selected important factors was then established with the central composite design (CCD) based RSM and the analysis of variance was used to check its validity.

A systematic experimental design based on RSM was used by Chiang [136] to investigate the influence of height and thickness of fin, width of passage between fins, distance between the cooling fan and the tip of fins of a parallel-plain fin (PPF) heat sink with an axial flow cooling fan on thermal resistance and pressure drop. The CCD was the RSM design used in the study. Experimental results confirmed that the proposed model was reasonably accurate for describing the thermal resistance and pressure drops within the limit of factors used in the study.

Chiang and Chang [137] and Chiang *et al.* [138] also used RSM in finding the optimal values of design parameters of a pin-fin-type heat sink which achieved high thermal performance (minimisation of thermal resistance and pressure drop). The design parameters chosen for their study were height and diameter of pin fin and width of pitch between fins and these were explored by experiments performed using CCD.

UNIVERSITEIT VAN PRETORIA
UNIVERSITY OF PRETORIA
YUNIBESITHI YA PRETORIA

The experimental results for the confirmation run showed that their response surface model was reasonable and accurate.

Park and Moon [139] carried out a numerical investigation using CFD coupled with the progressive quadratic response surface method (PQRSM), which is one of the sequential approximate optimisation (SAO) algorithms, to obtain values of design variables which minimised pressure drop and thermal resistance in a plate-fin heat sink. From their results, it was observed that the most dominant design variables were the base-part fin width and the lower-part fin width. Their results were validated with those obtained from the sequential quadratic programming (SQP) method.

Srisomporn and Bureerat [140] demonstrated the superiority of using combined RSM and multi-objective evolutionary optimiser over only using the evolutionary optimiser in the optimisation of plate-fin heat sinks based on the minimisation of heat junction temperature and fan pumping power. Their results showed that the real-code strength Pareto evolutionary algorithm (multi-objective optimiser) combined with the response surface technique outperformed the sole use of the former using the same design conditions and equal number of function evaluations for both.

Li and Kim [141] used multi-objective optimisation methods to design heat transfer surfaces of a three-dimensional channel with elliptic-shaped pin-fin arrays with the aim of finding the optimal geometry size that achieved an acceptable trade-off between augmentation of the turbulent heat transfer and reduction in friction loss. Response surface approximations were used to generate surrogate models and to

UNIVERSITEIT VAN PRETORIA
UNIVERSITY OF PRETORIA
YUNIBESITHI YA PRETORIA

approximate the Pareto optimal front. Their results showed that for the same pin-fin cross-sectional area, a longer pitch and shorter pin-fin height generated better heat transfer performance. They concluded that the multi-objective optimisation, which was based on a combination of a weighted sum strategy and evolutionary methods with local search methods (combining the response surface method and Reynolds-averaged Navier-Stokes (RANS) analysis), was a reliable and economic means of designing a heat transfer channel with extruded pin-fin arrays.

Park *et al.* [142] used the Kriging method (one of the metamodels used in response surface optimisation) associated with CFD to obtain optimal solutions for the plate-fin-type heat sink with an air deflector. The objective of their numerical optimisation was the minimisation of pressure loss subject to maximum temperature and geometric constraints. The Kriging method was used because it reduced computational cost by one-sixth times compared with the sequential quadratic programming (SQP) method.

Husain and Kim [53] also used response surface approximation, Kriging and radial basis neural network methods to construct surrogates for the optimisation of a rectangular microchannel heat sink. Thermal resistance was the single objective function while using pumping power as the constraint. The search of the optimum point was done using SQP.

Yu *et al.* [143] carried out a numerical optimisation of a radial heat sink adapted to a circular light-emitting diode (LED) under natural convection heat transfer. Parametric studies were conducted to compare the effects of number of long fins, long fin length,

UNIVERSITEIT VAN PRETORIA
UNIVERSITY OF PRETORIA
YUNIBESITHI YA PRETORIA

middle fin length and heat flux on the thermal resistance and average heat transfer coefficient for the heat sink array and thereafter, the optimisation of the heat sink geometry was carried out using a CCD and an evolutionary algorithm.

In the investigation carried out by Wang *et al.* [113], a design of experiments (DOE) procedure using the Taguchi method was used to determine the influence of pin-fin height, diameter, spacing and cross-sectional shape on thermal conductance and channel pressure drop.

2.7. CONCLUSION

This chapter outlined various published literature on analytical, numerical and experimental investigations that were carried out for heat transfer and fluid flow in different types of heat sinks (single microchannels, stacked microchannels and micro pin fins) with major emphasis on the different optimisation techniques that were used to obtain optimal dimensions of these heat sinks.

Constructal design has been applied in the optimisation of single microchannels and micro pin fins, but it has not been applied in the optimisation of stacked microchannel with the same total volume of substrate as that of the single microchannel heat sinks. In this research study, the application of constructal design in the optimisation of single and stacked microchannels under a fixed volume constraint was investigated with the aim of improving its thermal performance. A novel design and geometric optimisation of combining single and stacked microchannels with micro pin fins were also explored in this work. The objective of this new design was to enhance the

UNIVERSITEIT VAN PRETORIA
UNIVERSITY OF PRETORIA
YUNIBESITHI YA PRETORIA

thermal performance of the heat sink. Also, the effect of varying the axial length of the solid substrate on the thermal performance of the different microchannels under a fixed volume constraint was extensively investigated.

The computational fluid dynamics code employed to carry out the numerical simulations in this study has a goal-driven optimisation tool, which uses the response surface optimisation procedure. Some of the published works that employed the response surface optimisation method were also outlined in this chapter.

UNIVERSITEIT VAN PRETORIA
UNIVERSITY OF PRETORIA
YUNIBESITHI YA PRETORIA

CHAPTER 3: NUMERICAL MODELLING AND OPTIMISATION

3.1. INTRODUCTION

Computational fluid dynamics (CFD) involves the numerical analysis of fluid flow and heat transfer in systems by means of a computer and the codes used make use of numerical algorithms that can tackle fluid flow problems [144]. The commercial CFD software used in the numerical analysis in this research study is ANSYS 14.0 [145], which employs a finite volume method [146]. The processes involved in using this CFD software to define the geometry, discretise the computational domain, solve the governing equations and carry out the optimisation of the geometric configuration will be discussed extensively in the subsequent sections.

3.2. NUMERICAL MODELLING PROCEDURE

The CFD codes used in carrying out numerical modelling of fluid flow and heat transfer problems consist of three main elements, as follows:

UNIVERSITEIT VAN PRETORIA
UNIVERSITY OF PRETORIA
YUNIBESITHI YA PRETORIA

Pre-processing: This is the first stage of any numerical modelling procedure. It involves the defining of the geometry, that is, the computational domain, the subdivision of this domain into sub-domains, which is called the grid generation, the selection of the physical and chemical phenomena that need to be modelled, the defining of all fluid properties and specifications of boundary conditions.

Solver execution: The integration and solving of all the equations that govern the flow and heat transfer over the computational domain are carried out during this next stage.

Post-processing: Results obtained from numerical simulations are analysed here and many CFD commercial packages are also equipped with versatile data visualisation tools that aid extensive analysis of numerical results.

3.3. GEOMETRY AND GRID GENERATION

A numerical procedure cannot be carried out without first defining a geometry, which is the computational domain, and thereafter, this domain is divided into a finite number of discretised control volumes on which the governing equations can be solved. Using ANSYS 14.0, the computational domain and the grid are generated [145].

The governing non-linear partial differential equations for fluid flow and heat transfer through the computational domain are also solved using this CFD tool. The equations solved are the conservation of mass (continuity), conservation of momentum and conservation of energy equations.

UNIVERSITEIT VAN PRETORIA
UNIVERSITY OF PRETORIA
YUNIBESITHI YA PRETORIA

3.4. CONSERVATION OF MASS

In the Eulerian reference frame, the most general form for the continuity equation for fluids is given by [147]:

$$\frac{D\rho}{Dt} + \rho div\mathbf{V} = 0 \tag{3.1}$$

where ρ is the density of the fluid, t is time and $\boldsymbol{V}$ is the velocity vector of the fluid. For incompressible flow, that is, constant density, Equation (3.1) becomes:

$$div\mathbf{V} = 0 \tag{3.2}$$

3.5. CONSERVATION OF MOMENTUM

The conservation of momentum equation, which is derived from Newton's second law, relates the applied force to the resulting acceleration of a particle with mass. For Newtonian viscous fluids, Navier and Stokes fundamentally derived the following equation using indicial notation:

$$\rho\frac{D\mathbf{V}}{Dt} = \rho\mathbf{g} - \nabla P + \frac{\partial}{\partial x_j}\left[\mu\left(\frac{\partial v_i}{\partial x_j} + \frac{\partial v_j}{\partial x_i}\right)\right] + \delta_{ij}\lambda div\mathbf{V} \tag{3.3}$$

where $\boldsymbol{g}$ is the vector acceleration of gravity, P is pressure, x is the spatial coordinate, μ is the coefficient of viscosity, v is the velocity component, δ_{ij} is the Kronecker delta

UNIVERSITEIT VAN PRETORIA
UNIVERSITY OF PRETORIA
YUNIBESITHI YA PRETORIA

function and λ is the vexing coefficient associated with volume expansion [110]. Using Stokes' hypothesis, $\lambda = -\frac{2}{3}\mu$.

For incompressible flow, the vexing coefficient λ and div $\boldsymbol{V}$ vanish (due to the continuity relationship) and this simplifies Equation (3.3) to:

$$\rho \frac{D\mathbf{V}}{Dt} = \rho\mathbf{g} - \nabla P + \mu\nabla^2\mathbf{V} \tag{3.4}$$

3.6. CONSERVATION OF ENERGY

The conservation of energy equation is derived from the first law of thermodynamics, which states that increase in energy in a system results from work and heat added to the system. If one neglects the effects of radiation, the standard form of the energy equation is:

$$\rho \frac{Dh}{Dt} = \frac{DP}{Dt} + div(k\nabla T) + \Phi \tag{3.5}$$

where h is the enthalpy of the fluid, k is the thermal conductivity, T is the temperature of the fluid and Φ represents the dissipation function expressed as:

$$\Phi = \mu\left[2\left(\frac{\partial u}{\partial x}\right)^2 + 2\left(\frac{\partial v}{\partial y}\right)^2 + 2\left(\frac{\partial w}{\partial z}\right)^2 + \left(\frac{\partial v}{\partial x} + \frac{\partial u}{\partial y}\right)^2 + \left(\frac{\partial w}{\partial y} + \frac{\partial v}{\partial z}\right)^2 + \left(\frac{\partial u}{\partial z} + \frac{\partial w}{\partial x}\right)^2\right] + \lambda\left(\frac{\partial u}{\partial x} + \frac{\partial v}{\partial y} + \frac{\partial w}{\partial z}\right)^2 \tag{3.6}$$

For incompressible flow with constant thermal conductivity and low velocities, the viscous dissipation becomes negligible. As a result, Equation 3.5 is simplified to:

UNIVERSITEIT VAN PRETORIA
UNIVERSITY OF PRETORIA
YUNIBESITHI YA PRETORIA

$$\rho C_p \frac{DT}{Dt} = k\nabla^2 T \tag{3.7}$$

For steady conjugate heat transfer applications, Equation 3.7 becomes:

$$\rho C_p (V.\nabla T) = k_f \nabla^2 T \tag{3.8}$$

$$k_{solid} \nabla^2 T = 0 \tag{3.9}$$

where Equation (3.8) is for the fluid medium, while Equation (3.9) is for the solid medium with k_f and k_s the thermal conductivities for the fluid and solid respectively.

3.7. BOUNDARY CONDITIONS

After the geometric representation of domain of interest is created in the ANSYS 14.0 workbench [145], the mesh is generated and all the appropriate boundaries for various surfaces are named before their specified values are applied (based on the physics of the problem) the FLUENT solver used to run the simulations.

3.8. NUMERICAL SOLUTION PROCEDURE

The conservation of mass, momentum and energy equations along with the boundary conditions are solved numerically using the three-dimensional ANSYS 14.0 commercial CFD package [145], which employs a finite volume method. The detail of this method is explained in open literature [146].

The computational domain is first meshed and thereafter, the second-order upwind scheme is used to discretise the combined convection and diffusion terms in the

UNIVERSITEIT VAN PRETORIA
UNIVERSITY OF PRETORIA
YUNIBESITHI YA PRETORIA

momentum and energy equations. The SIMPLE algorithm is employed to solve the coupled pressure-velocity fields in the equations. The solution is assumed to converge when set values of the normalised residuals of the continuity, momentum and energy equations are attained.

3.9. NUMERICAL OPTIMISATION

The goal-driven optimisation (GDO) tool is one of the tools under the ANSYS Design Exploration in ANSYS Workbench [145], of which the main aim is to identify the relationship between the performance of a product and the design variables. It uses the response surface methodology (RSM) for its optimisation process. The RSM uses a group of mathematical and statistical techniques to develop an adequate functional relationship between a response of interest and a number of input variables, which are explained further in literature with equations [125] and [129].

If the response variable of interest is represented by y and the set of input variables by $x_1, x_2, x_3, \ldots\ldots\ldots\ldots, x_k$, then one could write a functional relationship between the response variable of interest and input variables using two models. If the nature of the relationship between them is exactly known based on underlying principles, then the experimenter could write a functional relationship often called a mechanistic model as shown below:

$$y = g\left(x_1, x_2, x_3, \ldots\ldots\ldots\ldots, x_k\right) + \varepsilon \tag{3.10}$$

UNIVERSITEIT VAN PRETORIA
UNIVERSITY OF PRETORIA
YUNIBESITHI YA PRETORIA

where ε is the error in the system.

But if the underlying principle is not fully understood, the unknown function g must be approximated with an appropriate empirical model and the relationship can be written as:

$$y = f\left(x_1, x_2, x_3, \ldots\ldots\ldots, x_k\right) + \varepsilon \tag{3.11}$$

where the function f is usually a first- or second-order polynomial and the empirical model is called a response surface model.

3.9.1. Response surface methodology and computer experiments

When the response surface methodology is applied to computer simulation experiments, it is used to build a model of the system being investigated. This model is called a metamodel. It is on this metamodel that optimisation is carried out. If the metamodel is a good representation of the real system, then the optimisation results will be an adequate representation of the optimum conditions of the real system. A metamodel is a mathematical model surrogate of system performance to approximate the relationship between system performance and the design parameters [148].

There are generally two types of simulation models, namely the stochastic simulation model in which the output responses are random variables and the deterministic simulation model in which the output responses are determined by mathematical models on which the computer model is based. Also in the deterministic computer experiment, the usual statistical techniques do not directly apply because there is no random error component, instead the only error in the model is the bias error.

UNIVERSITEIT VAN PRETORIA
UNIVERSITY OF PRETORIA
YUNIBESITHI YA PRETORIA

In the ANSYS 14.0 design exploration, which has the response surface optimisation tool [145], once a model is created and parameters defined, a response surface is created. Based on the number of input parameters, a given number of solutions (design points) is required to build this response surface (an approximation of the response of the system). After inserting a response surface, the design space is defined by giving the minimum and maximum values to be considered for each input variable. The design of experiments (DOE) part of the response surface system creates the design space sampling and when updated, a response surface is created for each output parameter.

The GDO is an optimisation technique that finds design candidates from the response surfaces. The objective is set in the GDO and then the optimisation problem is solved. The accuracy of the response surface for the design candidates is checked by converting it to a design point, and thereafter, a full simulation is performed for that point to check the validity of the output parameters [145]. Any DOE approach is better than the ad hoc trial and error approach to engineering design [149].

In this research study, the deterministic simulation model called the optimal space-filling design is employed for the design of experiments (DOE). This design is better suited to complex models. Its objective is to fill the design space efficiently with minimal number of points while keeping the discrepancy very low. This is a more efficient DOE scheme than the central composite design (CCD). Thereafter, the non-parametric regression (NPR) modelling algorithm is employed to create a response surface. The NPR technique relaxes the assumption of linearity in the regression parameters and as a result, it is used to predict high non-linear behaviour of outputs

UNIVERSITEIT VAN PRETORIA
UNIVERSITY OF PRETORIA
YUNIBESITHI YA PRETORIA

with respect to inputs. For example, if the input sample generated from the DOE is X, where X is defined by

$$X = \{x_1, x_2, x_3, ..., x_M\} \tag{3.12}$$

x_i is a N-dimensional vector, which represents the input variable, the objective is to determine an equation of the form,

$$Y = \sum_{i=1}^{N} \left(A_i - A_i^*\right) K\left(\overrightarrow{X_i}, X\right) + b \tag{3.13}$$

where $K\left(\overrightarrow{X_i}, X\right)$ is the kernel map and the quantities A_i and A_i^* are Lagrange multipliers.

After the response surface is created, the screening method, which is a non-iterative direct sampling method, is used for the design optimisation. It uses a quasi-random generator based on the Hammersley algorithm and it has a low discrepancy sequence. The Hammersley algorithm generates a set of N Hammersley points using the radix-R notation of an integer [145, 149]. For example, an integer *n* can be represented as a sequence of digits as:

$$n = n_m, n_{m-1}, ..., n_2, n_1, n_0 \tag{3.14}$$

The integer n can be represented in radix-R notation as:

$$n = n_0 + n_1 R + n_2 R^2 + ... + n_m R^m \tag{3.15}$$

where $m = \lceil \log_R n \rceil = \left\lceil \frac{\ln n}{\ln R} \right\rceil$ (3.16)

The square brackets represent the integer portion of the number inside the brackets.

UNIVERSITEIT VAN PRETORIA
UNIVERSITY OF PRETORIA
YUNIBESITHI YA PRETORIA

The inverse radix number function given by Equation 3.17 below is now constructed from Equation 3.16. It is a function that constructs a unique number on the interval [0, 1] by reversing the order of the digits of *n* around the decimal point.

$$\phi_R(n) = .n_0 n_1 n_2 \ldots\ldots\ldots n_m = n_0 R^{-1} + n_1 R^{-2} + \ldots\ldots + n_m R^{-m-1} \tag{3.17}$$

Finally, the Hammersley sequence for k-dimensional points are given by

$$H_k(i) = \left[\frac{i}{N}, \varphi_{R_1}(i), \varphi_{R_2}(i), \ldots\ldots \varphi_{R_{k-1}}(i) \right] \tag{3.18}$$

where i = 0,……..,N indicates the sample points and the values of $R_1, R_2, \ldots\ldots, R_{k-1}$ are the first *k-1* prime numbers.

3.10. CONCLUSION

This chapter focused on the processes involved in solving fluid flow and heat transfer problems using the ANSYS 14.0 three-dimensional commercial CFD package. The non-linear partial differential equations that govern the mass and heat transport were discussed and the numerical optimisation procedure was also examined.

UNIVERSITEIT VAN PRETORIA
UNIVERSITY OF PRETORIA
YUNIBESITHI YA PRETORIA

CHAPTER 4: CONSTRUCTAL DESIGN AND OPTIMISATION OF SINGLE AND STACKED MICROCHANNEL HEAT SINKS

4.1. INTRODUCTION

This chapter discusses the use of the constructal design technique in the geometric optimisation of single, two-layered and three-layered microchannel heat sinks with the same fixed total volume. The optimisation of the heat sinks will be based on minimising the peak temperature of the highly conductive silicon substrate, which results in maximising the thermal conductance. The thermal performance of these three types of heat sinks will also be compared.

4.2. SINGLE MICROCHANNEL HEAT SINK

This section presents the use of a different optimisation algorithm from the one used by Bello-Ochende *et al.* [21] in the geometric optimisation of single microchannels. The advantage of the numerical optimisation tool used in this study is that the creation of the geometry, grid generation, simulation and optimisation is carried out in the ANSYS

UNIVERSITEIT VAN PRETORIA
UNIVERSITY OF PRETORIA
YUNIBESITHI YA PRETORIA

workbench unlike the method previously used [21], where they had to first create the geometry and generate the grid in the Geometry and Mesh Building Intelligent Toolkit (GAMBIT) before exporting this to FLUENT solver and thereafter, couple the mathematical optimisation algorithm to the solver to obtain the optimisation results.

4.2.1. Physical model

Figure 4.1 shows the physical model of the single microchannel heat sink and Figure 4.2 shows the computational domain, which is an elemental volume. A uniform heat flux is supplied to the bottom of a highly conductive silicon substrate. Forced convection cooling is achieved by liquid fluid flow through the microchannels embedded in the solid substrate, which makes the heat transfer a conjugate problem.

UNIVERSITEIT VAN PRETORIA
UNIVERSITY OF PRETORIA
YUNIBESITHI YA PRETORIA

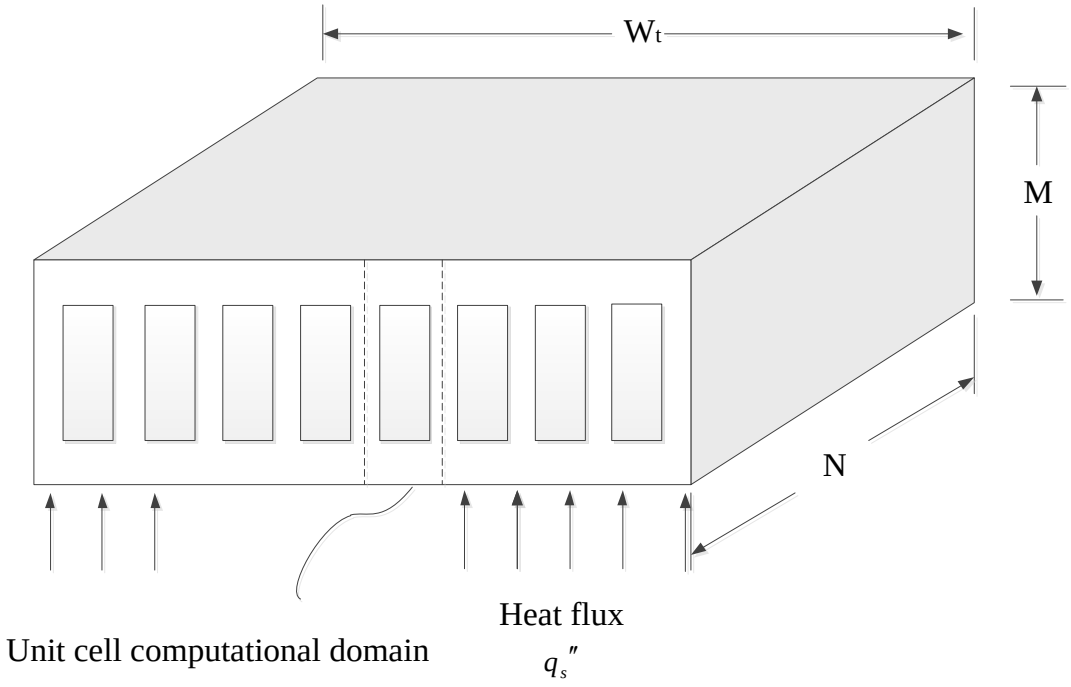

Figure 4.1: Physical model of single microchannel heat sink

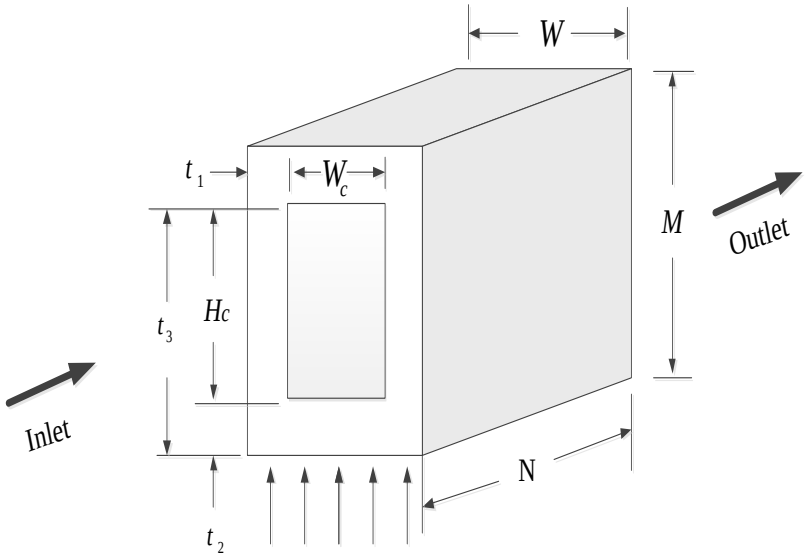

Figure 4.2: Three-dimensional computational domain

UNIVERSITEIT VAN PRETORIA
UNIVERSITY OF PRETORIA
YUNIBESITHI YA PRETORIA

The computational model and the grid are generated using ANSYS 14.0 [145]. Fluid flow through the microchannel is assumed to be steady and laminar. The cooling fluid, which is water, is also assumed to be single-phase, incompressible and homogeneous with constant thermo-physical properties. The temperature of water at inlet is 20 ˚C and a uniform heat flux of 1 MW/m^2 is applied to the bottom wall. A specified pressure difference ΔP is applied to the flow across the axial length of the computational domain and symmetry boundary conditions are specified at the left and right side of the domain. Radiation and natural convection are assumed to be negligible.

4.2.1.1. Grid analysis and CFD code validation

A grid refinement test is carried out until a mesh size with negligible changes in temperature difference ΔT is obtained. The solution is assumed to converge when the normalised residuals of the continuity and momentum equation fall below 10^{-5} while that of the energy equation falls below 10^{-7}. The convergence criterion for the temperature difference as the quantity monitored is:

$$\gamma = \left| \frac{(\Delta T)_i - (\Delta T)_{i-1}}{(\Delta T)_i} \right| \leq 0.01 \qquad (4.1)$$

where i is the mesh iteration index.

The mesh is more refined as *i* increases and *i-1* mesh is selected as the convergence criterion once Equation 4.1 is satisfied.

UNIVERSITEIT VAN PRETORIA
UNIVERSITY OF PRETORIA
YUNIBESITHI YA PRETORIA

Table 4.1 shows the dimensions of the geometry used to carry out the grid refinement test, as shown in Table 4.2 for a Bejan number, Be = 1.9 x 10^8. The Bejan number, Be, is the dimensionless pressure drop parameter [150, 151] expressed as:

$$Be = \frac{\Delta P V^{2/3}}{\alpha \mu} \tag{4.2}$$

Table 4.1: Dimensions of microchannel heat sink for grid refinement tests

t_1 (mm)	M-t_3 (mm)	t_3 (mm)	W_c (mm)	H_c (mm)	W (mm)	M (mm)	N (mm)
0.02	0.21	0.69	0.06	0.48	0.1	0.9	10

Table 4.2: Grid refinement test results

Number of cells	$\Delta T(K)$	$\left\|\frac{(\Delta T)_i - (\Delta T)_{i-1}}{(\Delta T)_i}\right\|$
18 458	14.3420	-
29 777	15.0306	0.0458
47 607	15.4470	0.0270
75 082	15.6063	0.0102
109 599	15.6545	0.0031

The validation of the CFD code used is carried out by comparing the numerical results obtained using this code with the analytical results obtained from the investigation carried out by Khan *et al.*, who analysed the performance of a cylindrical pin-fin heat sink in

UNIVERSITEIT VAN PRETORIA
UNIVERSITY OF PRETORIA
YUNIBESITHI YA PRETORIA

laminar forced convection [92]. The solution trends are in good agreement with a maximum deviation of less than 7%, as shown in Figure 4.3 and 16% in Figure 4.4. This gives confidence in the numerical code adopted.

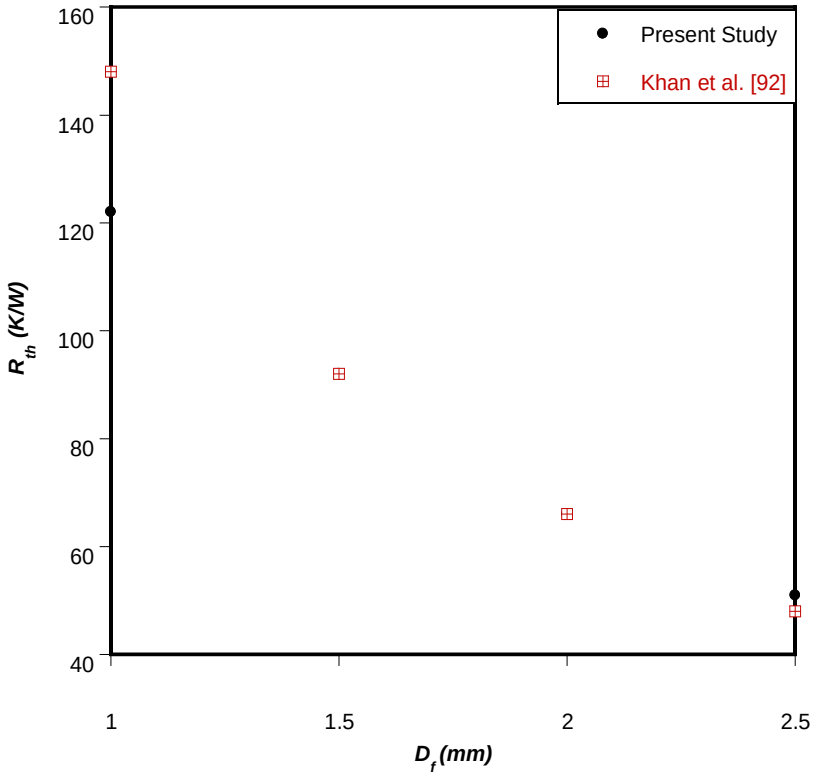

Figure 4.3: Validation of code for thermal resistance versus pin diameter

UNIVERSITEIT VAN PRETORIA
UNIVERSITY OF PRETORIA
YUNIBESITHI YA PRETORIA

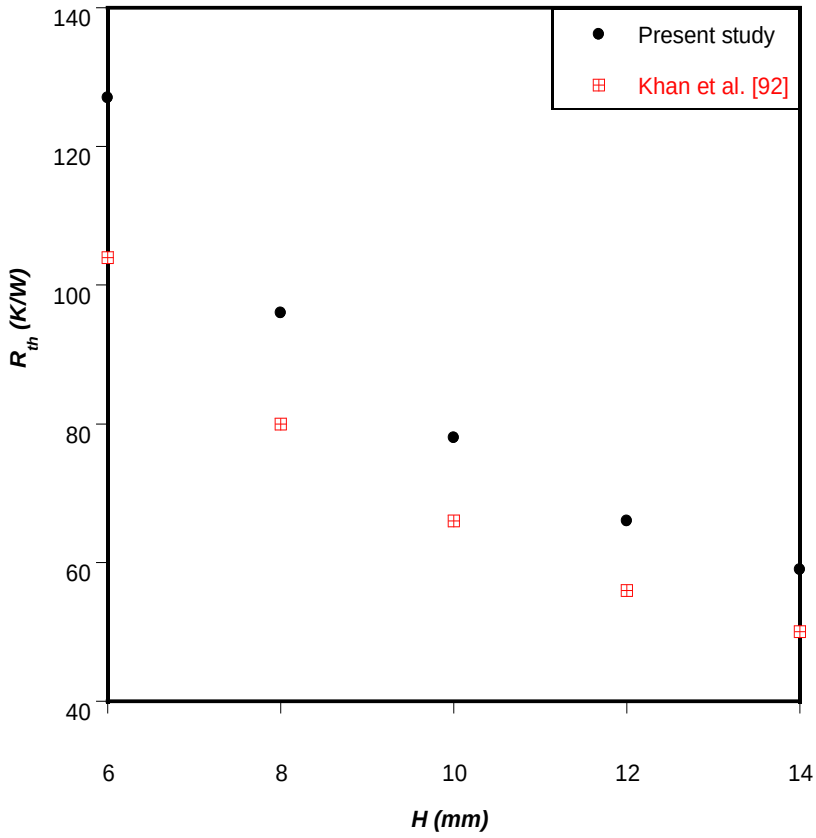

Figure 4.4: Validation of code for thermal resistance versus pin height

4.2.1.2. Design variables and optimisation technique

The length N, height M and width W of the solid are fixed, which makes the volume V fixed, while t_1, t_2, t_3, H_c and W_c are varied but also subject to manufacturing constraints. This geometric configuration has five degrees of freedom. The solid volume fraction or porosity ϕ is defined as the ratio of the solid volume to the total volume of the heat sink, which is only dependent on the cross-sectional area of the heat sink, as shown in Equation (4.3).

UNIVERSITEIT VAN PRETORIA
UNIVERSITY OF PRETORIA
YUNIBESITHI YA PRETORIA

$$\phi = \frac{V_{solid}}{V} = \frac{A_{solid}N}{AN} = \frac{A_{solid}}{A} = \frac{MW - H_c W_c}{MW} \tag{4.3}$$

The fixed global volume is defined as:

$$V = MWN = const \tag{4.4}$$

The manufacturing constraints based on the DRIE (deep reactive ion etching) technique used in manufacturing heat sinks [152, 153] are:

$$\frac{H_c}{W_c} \leq 20 \tag{4.5}$$

$$t_2 \geq 50\mu m \tag{4.6}$$

$$M - t_3 \geq 50\mu m \tag{4.7}$$

Numerical simulations and optimisation are carried out for a fixed total volume V of 0.7, 0.8 and 0.9 mm^3 with fixed length N of 10 mm. The design space for the response surface is defined as $54 \leq W_c \leq 66$ μm, $19 \leq t_1 \leq 29$ μm, $50 \leq M - t_3 \leq 60$ μm and $500 \leq H_c \leq 790$ μm. The optimised design point chosen is required to meet the manufacturing constraints. The range of Bejan numbers used throughout the simulations is between 6.5×10^7 and 3.9×10^8 corresponding to a pressure drop of between 10 to 60kPa. The range of solid volume fractions used in the present simulations based on the set design space is

UNIVERSITEIT VAN PRETORIA
UNIVERSITY OF PRETORIA
YUNIBESITHI YA PRETORIA

$0.42 < \phi < 0.70$. In the GDO, the objective function is to minimise the peak temperature based on the design space.

The measure of performance is the dimensionless global thermal conductance, which can be expressed in dimensionless form as:

$$C = \frac{q^{''} N}{k_f \Delta T} \tag{4.8}$$

where the excess temperature ΔT is

$$\Delta T = T_{max} - T_{min} \tag{4.9}$$

4.2.2. Case Study 1: Optimisation results for fixed axial length and uniform surface heat flux

Table 4.3 shows a comparison between the results obtained by Bello-Ochende *et al.* [21] and the results of the present study for different total volumes at a constant Bejan number. For a total volume of 0.9 mm^3, Figure 4.5 shows a comparison between the numerical investigation of Bello-Ochende *et al.* [21] and this present work for the optimal peak wall temperature difference for different Bejan numbers. The figure shows that the values obtained in the present study are in good agreement with those of the previous work done with an average deviation of about 5.8%.

In Figure 4.6, the influence of the dimensionless pressure drop on the maximised thermal conductance (C_{max}) is reported. It is observed that the global thermal conductance increases with an increase in the dimensionless pressure drop, which is similar to what is

UNIVERSITEIT VAN PRETORIA
UNIVERSITY OF PRETORIA
YUNIBESITHI YA PRETORIA

reported in literature [21, 24, 117]. It can also be observed that as the fixed total volume is reduced, C_{max} also reduces. From Figure 4.7, it can be observed that the minimised peak temperature is inversely proportional to the maximum global thermal conductance C_{max}. This shows that minimising the peak temperature maximises the global thermal conductance. Also, as the fixed total volume is reduced, the minimised peak temperature increases.

Table 4.3: Optimal design results for *Be* = 3.2 x 10^8

	Volume (mm^3)	Minimised Peak Temperature (^{0}C)	Optimised Aspect Ratio $\left(\frac{H_c}{W_c}\right)_{opt}$	Optimised Volume Fraction ϕ_{opt}	Optimised Channel Hydraulic Diameter $(D_h)_{opt}$
Bello-Ochende *et al.* [21]	0.9	29.53	11.752	0.425	0.122
Present study	0.9	29.52	12.228	0.475	0.115
Bello-Ochende *et al.* [21]	0.8	29.79	10.069	0.425	0.123
Present study	0.8	29.63	10.786	0.537	0.114
Bello-Ochende *et al.* [21]	0.7	30.12	10.359	0.386	0.118
Present study	0.7	29.75	8.887	0.573	0.118

UNIVERSITEIT VAN PRETORIA
UNIVERSITY OF PRETORIA
YUNIBESITHI YA PRETORIA

Figure 4.8 shows that the optimal channel aspect ratio $\left(\frac{H_c}{W_c}\right)_{opt}$ is a constant value of 12.228, the solid volume fraction ϕ_{opt} is 0.475 and the channel hydraulic diameter $(D_h)_{opt} = \left(\frac{2H_cW_c}{H_c+W_c}\right)_{opt}$ is 0.115 mm for different Bejan numbers for fixed total volume V of 0.9 mm^3 when the microchannel heat sink is optimised.

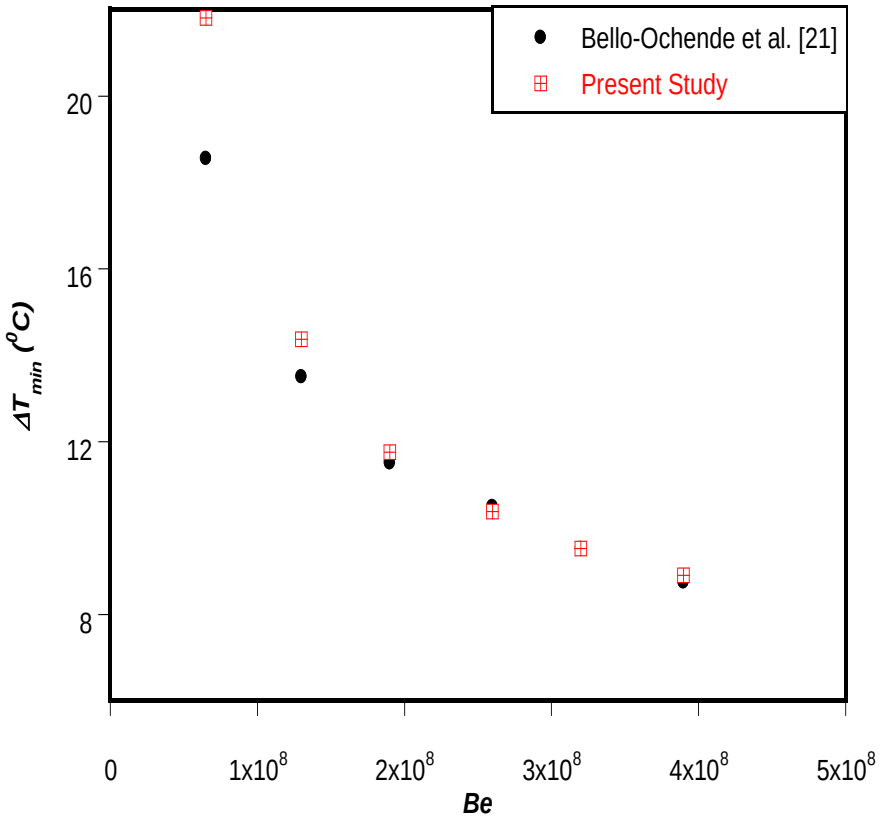

Figure 4.5: Influence of dimensionless pressure drop on optimal peak wall temperature difference for total heat sink volume of 0.9 mm^3

UNIVERSITEIT VAN PRETORIA
UNIVERSITY OF PRETORIA
YUNIBESITHI YA PRETORIA

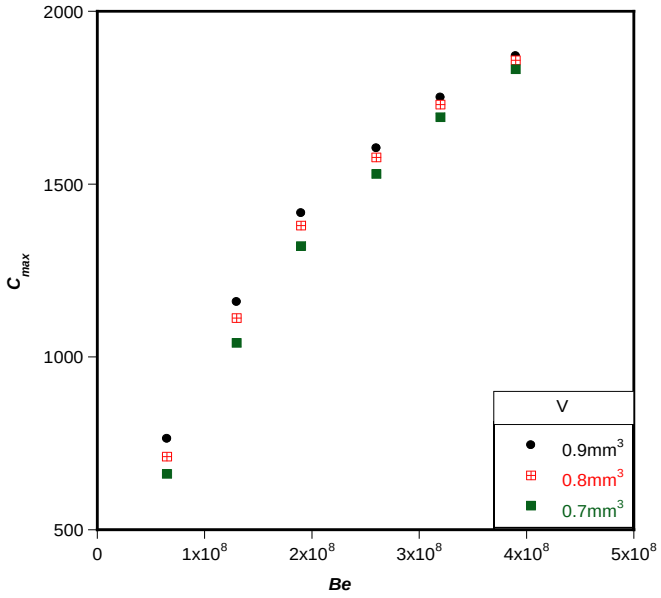

Figure 4.6: Influence of dimensionless pressure drop on the maximised thermal conductance

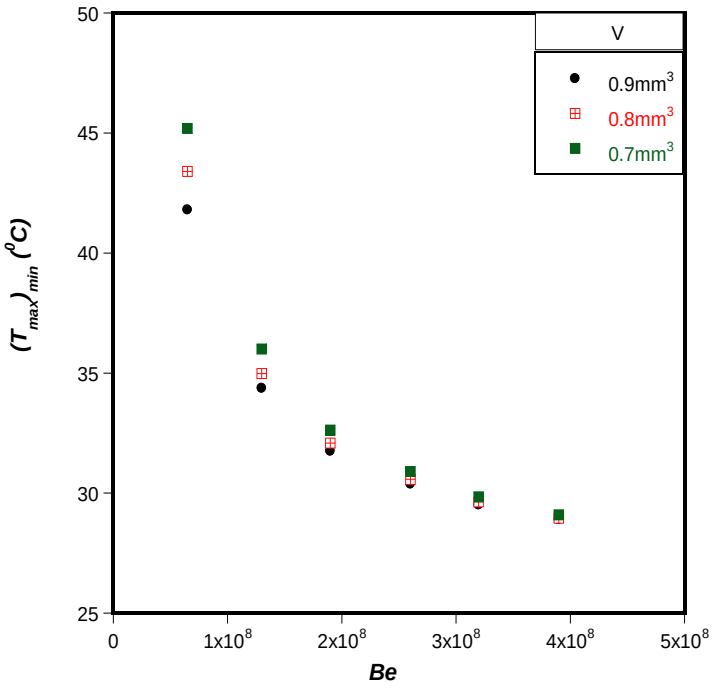

Figure 4.7: Influence of dimensionless pressure drop on minimised peak wall temperature

UNIVERSITEIT VAN PRETORIA
UNIVERSITY OF PRETORIA
YUNIBESITHI YA PRETORIA

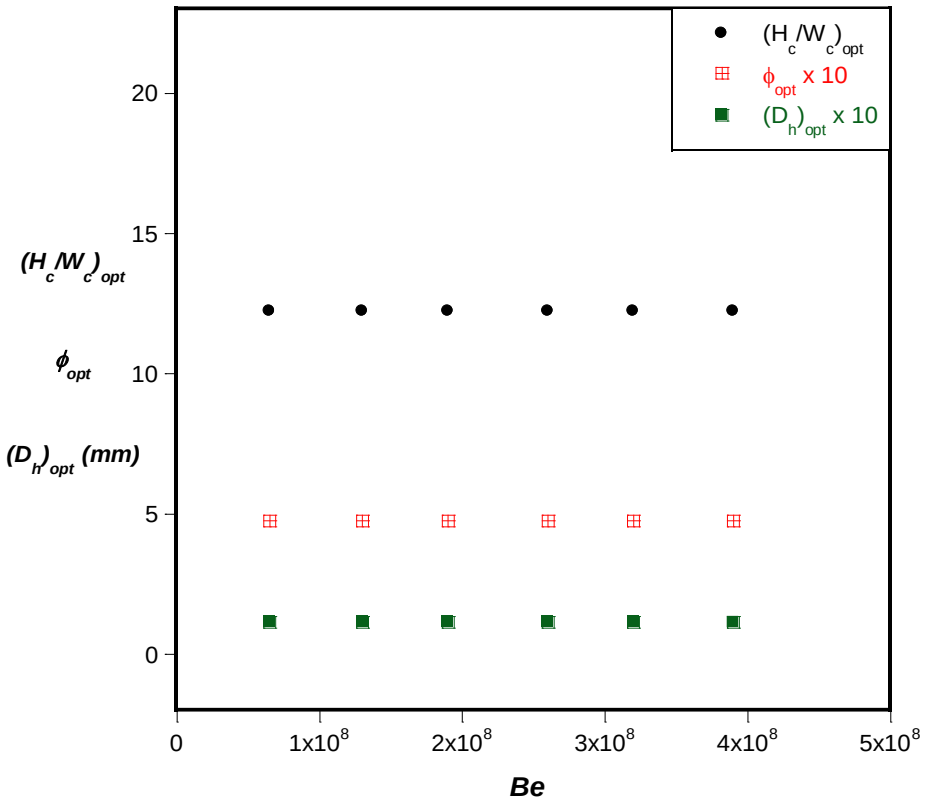

Figure 4.8: Effect of the change in *Be* on optimal channel aspect ratio, solid volume fraction and hydraulic diameter

4.2.3. Case Study 2: Optimisation results for varying axial length and uniform surface heat flux

Figures 4.9 and 4.10 show a comparison between results obtained for the minimised peak temperature and maximised thermal conductance for the fixed and variable length for a fixed total volume V of 0.9 mm^3, uniform surface heat flux q'' of 1MW/m^2 and constant thermophysical properties of water. The geometric configuration has six degrees of freedom. These results show that for the lowest *Be* of 6.5x10^7 (pressure drop of 10kPa),

UNIVERSITEIT VAN PRETORIA
UNIVERSITY OF PRETORIA
YUNIBESITHI YA PRETORIA

the peak temperature is further minimised by 39.8%, which results in over 100% improvement in the maximum thermal conductance.

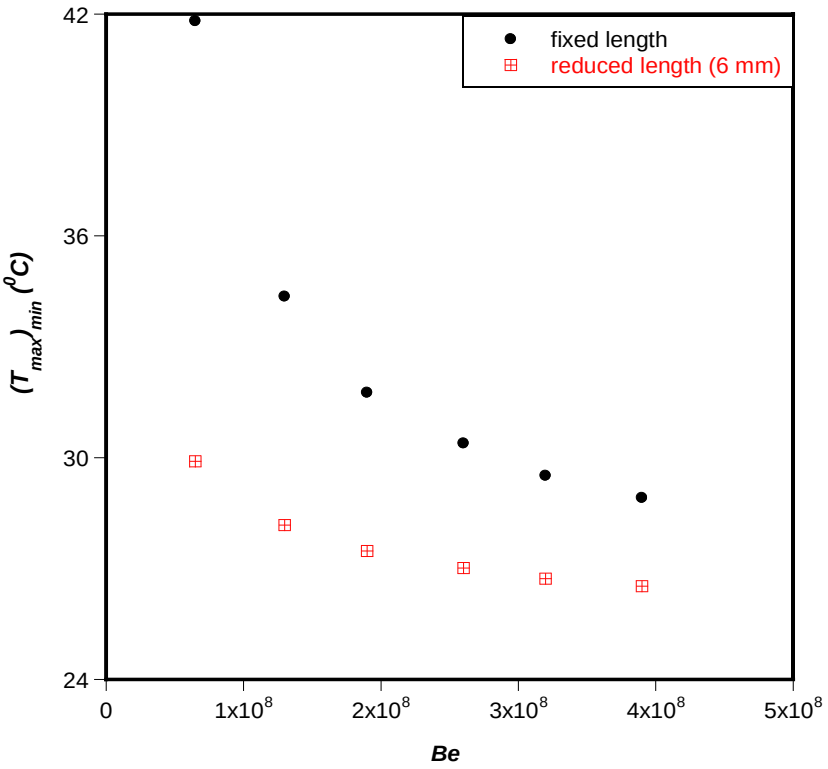

Figure 4.9: Comparison between results of minimised peak temperature for fixed and reduced lengths

UNIVERSITEIT VAN PRETORIA
UNIVERSITY OF PRETORIA
YUNIBESITHI YA PRETORIA

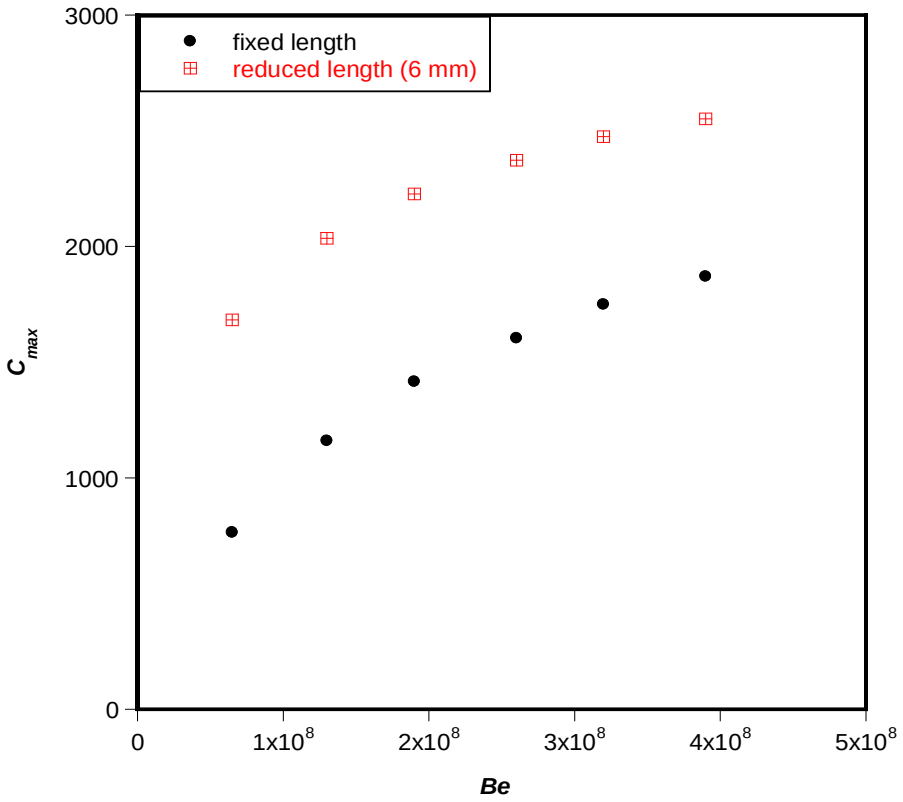

Figure 4.10: Comparison between results of maximised thermal conductance for fixed and reduced length

It can be observed that as the axial length is increased, the minimised peak temperature increases, as shown in Figure 4.11. Figure 4.12 shows that the optimal length for the range of *Be* used in this study is 6 mm. Figure 4.13 shows that the optimal solid substrate aspect ratio $\left(\frac{M}{W}\right)_{opt}$ is 6.667, optimal channel aspect ratio $\left(\frac{H_c}{W_c}\right)_{opt}$ is 9.202, solid volume fraction ϕ_{opt} is 0.440 and channel hydraulic diameter $(D_h)_{opt}$ is 0.172 mm for different Bejan numbers and optimal axial length.

UNIVERSITEIT VAN PRETORIA
UNIVERSITY OF PRETORIA
YUNIBESITHI YA PRETORIA

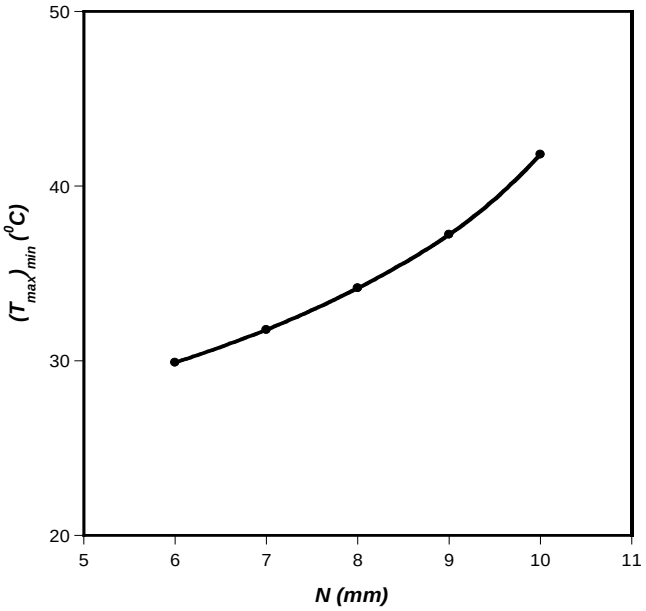

Figure 4.11: Effect of varying axial length on minimised peak temperature for a constant *Be*

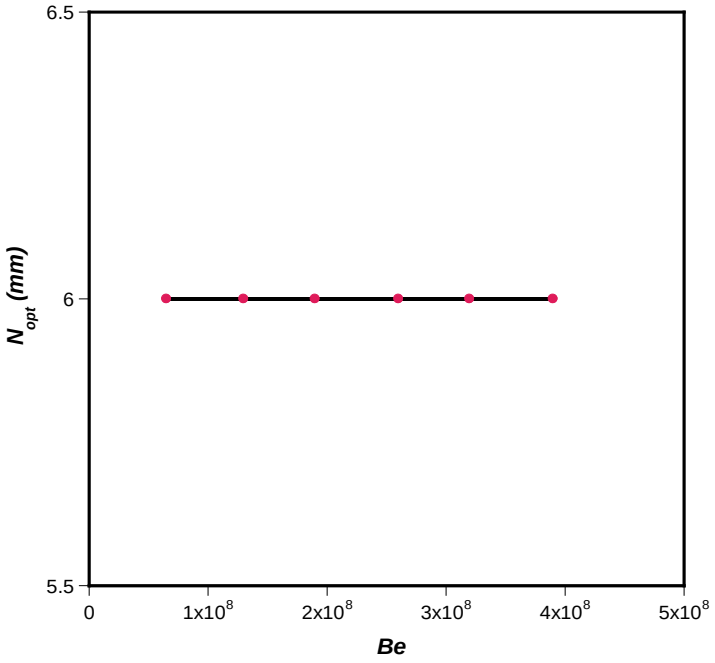

Figure 4.12: Optimal axial length for each Bejan number

UNIVERSITEIT VAN PRETORIA
UNIVERSITY OF PRETORIA
YUNIBESITHI YA PRETORIA

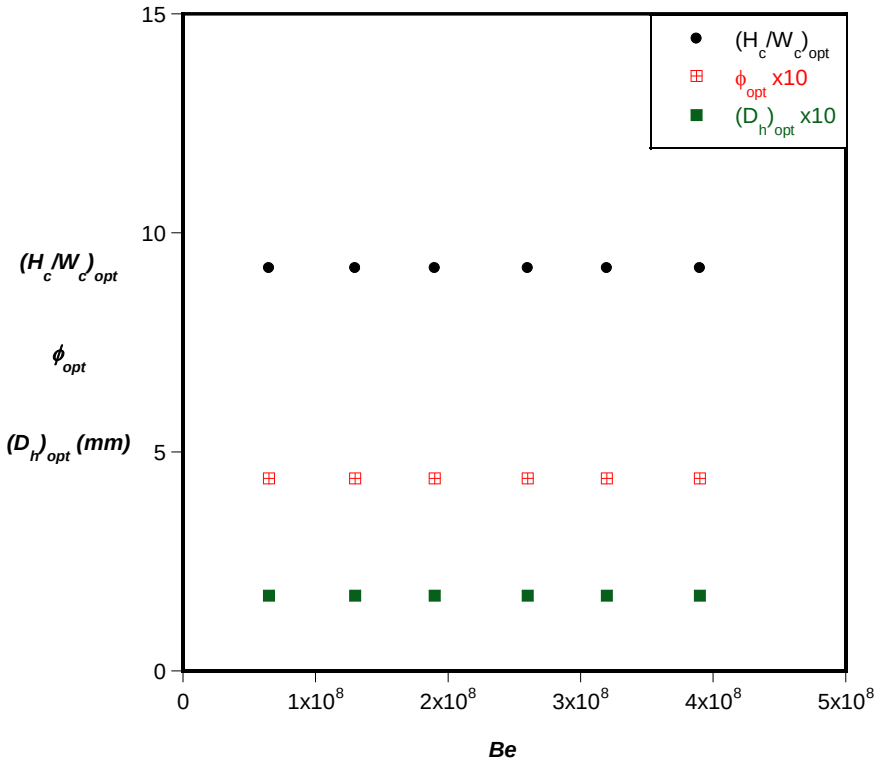

Figure 4.13: Effect of the change in *Be* on optimal channel aspect ratio, solid volume fraction and hydraulic diameter for reduced axial length

4.2.4. Case Study 3: Optimisation results for varying axial length and uniform heat load

Microelectronic chips release heat load Q on the surface of the solid substrate on which they are mounted and the surface area of this solid substrate is used to calculate the surface heat flux q″. This means that if the axial length and width of the solid substrate are free to morph, the surface heat flux q'' will vary. This variation in surface heat flux is taken into consideration in this section with the objective of searching for the optimal geometric configuration of both the solid substrate and microchannel heat sink that

UNIVERSITEIT VAN PRETORIA
UNIVERSITY OF PRETORIA
YUNIBESITHI YA PRETORIA

minimises the peak temperature on the heated surface when the total volume is fixed but axial length is varied. The configuration has eight degrees of freedom.

Numerical simulations and optimisation were carried out for a fixed total volume V of 0.9 mm^3 with varied axial length N of 1 to10 mm. The temperature of water pumped across the microchannel is 20 $^{\circ}C$ at the inlet and total heat load applied to the bottom wall is 100W and defined as:

$$Q = cq^{''}NW \tag{4.10}$$

where NW is the elemental surface area that is heated and the number of microchannels c is assumed to be 100.

The design space for the response surface for the fixed total volume is defined as $50 \leq W_c \leq 80$ μm, $50 \leq M - t_3 \leq 60$ μm, and $500 < H_c < 3000$ μm. Temperature-dependent thermophysical properties of water are defined using the piecewise linear function of temperature as shown in Equation 4.11 below [145]. Radiation and natural convection are assumed to be negligible.

$$\eta(T) = \eta_a + \frac{\eta_{a+1} - \eta_a}{T_{a+1} - T_a}(T - T_a) \tag{4.11}$$

Figure 4.14 shows that at the lowest *Be* used in the study, the result of minimised peak temperature when constant fluid properties assumptions are made is 5% more than when temperature-dependent properties of fluid are used for the numerical simulation. This variation reduces as the *Be* is increased and for the Be of 3.9×10^8, the difference between the two results is less than 1%. From the result shown in Figure 4.14, it can be concluded that it is more accurate to use temperature-dependent fluid properties for water at low pressure drops.

UNIVERSITEIT VAN PRETORIA
UNIVERSITY OF PRETORIA
YUNIBESITHI YA PRETORIA

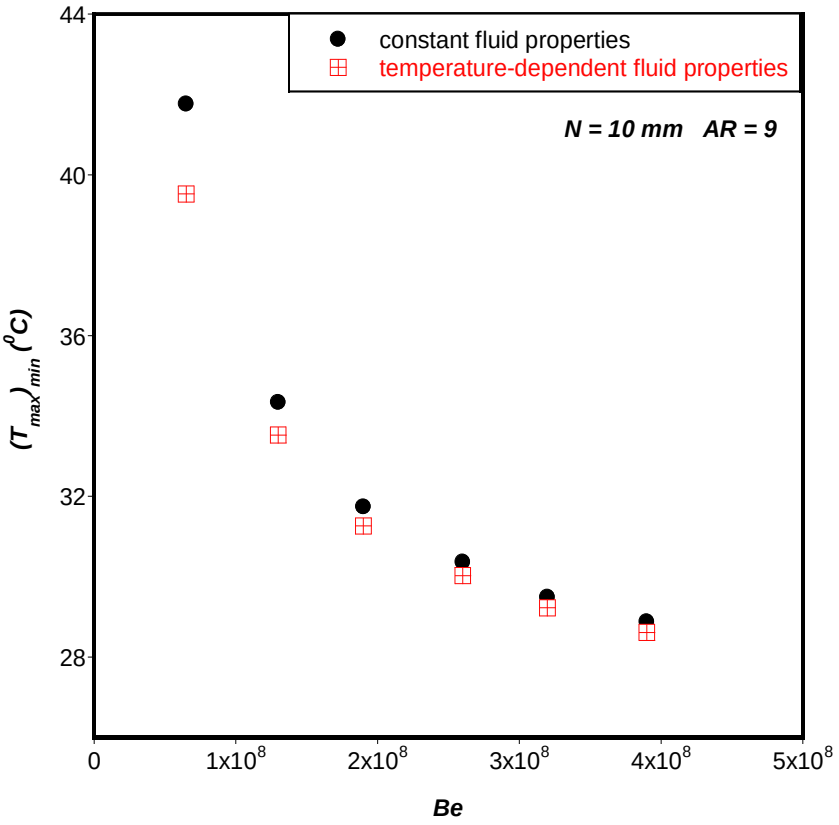

Figure 4.14: Effect of dimensionless pressure drop on minimised peak temperature

Figure 4.15 shows how varying the axial length of the solid substrate affects the surface heat flux q'' on the heated wall for the constant heat load Q of 100W and fixed total volume of 0.9 mm^3. It can be observed that as the length is increased from 1 to 10 mm, q'' reduces. The results also show decreasing surface heat flux as the solid substrate aspect ratio is decreased for all the axial lengths investigated.

UNIVERSITEIT VAN PRETORIA
UNIVERSITY OF PRETORIA
YUNIBESITHI YA PRETORIA

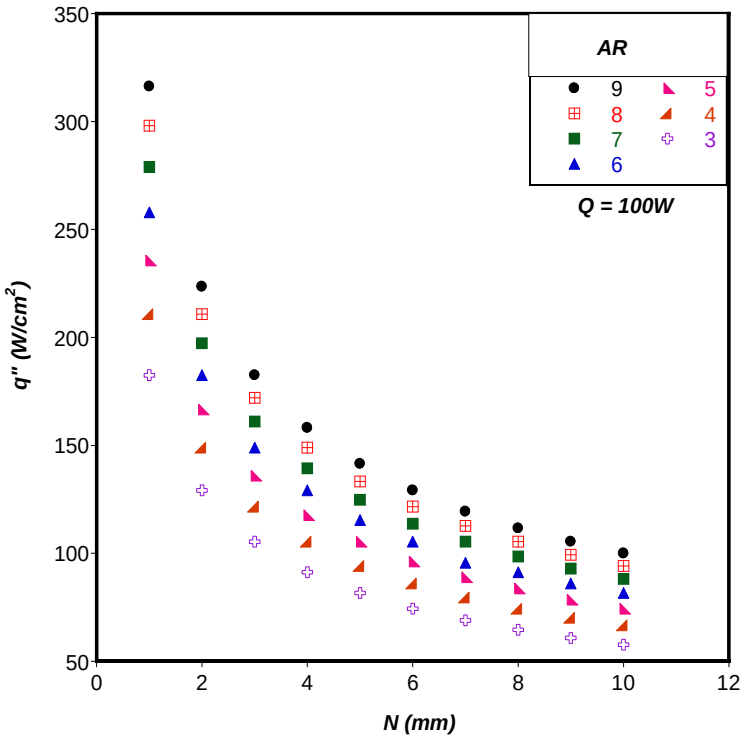

Figure 4.15: Effect of varying axial length on surface heat flux

The effect of varying the axial length of the solid substrate on the minimised peak temperature is shown in Figure 4.16. The results show that at fixed *AR* of 3, the optimal axial length N_{opt} is 3 mm when *Be* is fixed at 6.5 x 10^7, but as Be increases, N_{opt} is discovered to be 5 mm. Increasing the axial length above 5 mm does not further improve the thermal performance of the microchannel, rather the minimised peak temperature increases. Figure 4.17 shows results of the effect of varying *AR* on the minimised peak temperature at a fixed Bejan number *Be* of 1.3 x 10^8. It can be observed that the optimal AR_{opt} is 3 for axial length below 5 mm but AR_{opt} becomes greater than 3 as *N* increases. Results in Figures 4.16 and 4.17 show that global AR_{opt}, which minimises the peak temperature, is 3.

UNIVERSITEIT VAN PRETORIA
UNIVERSITY OF PRETORIA
YUNIBESITHI YA PRETORIA

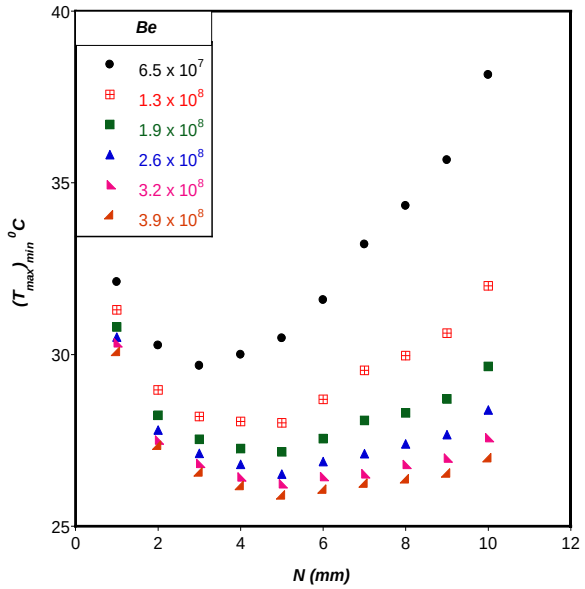

Figure 4.16: Effect of varying axial length on minimised peak temperature for AR = 3

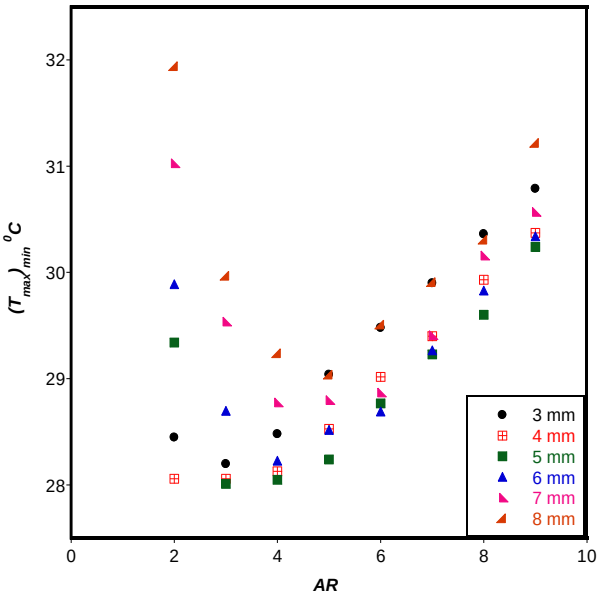

Figure 4.17: Effect of varying substrate aspect ratio AR on minimised peak temperature for Be = 1.3 x 10^8

UNIVERSITEIT VAN PRETORIA
UNIVERSITY OF PRETORIA
YUNIBESITHI YA PRETORIA

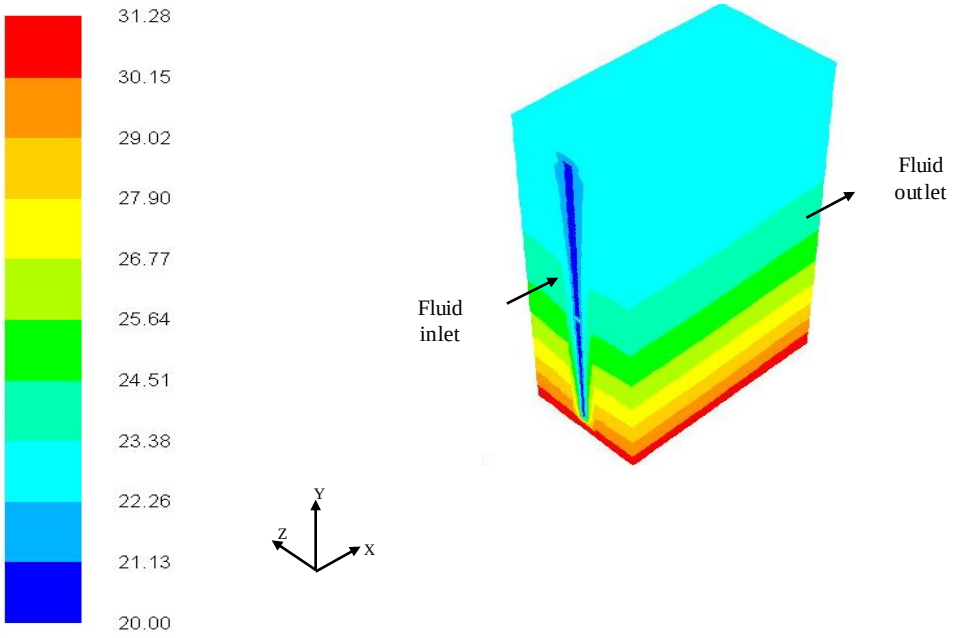

Figure 4.18a

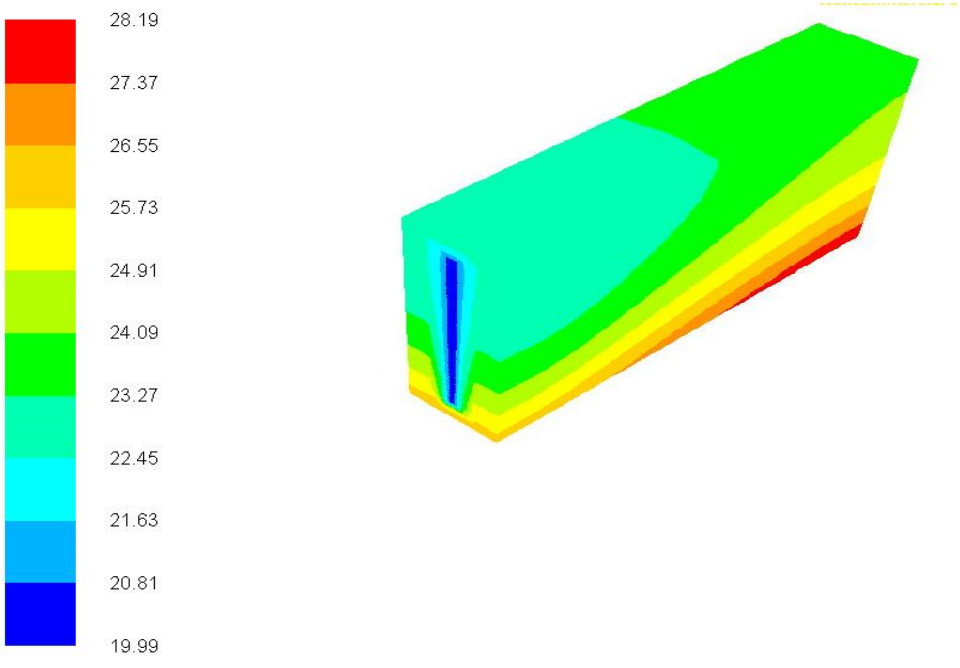

Figure 4.18b

UNIVERSITEIT VAN PRETORIA
UNIVERSITY OF PRETORIA
YUNIBESITHI YA PRETORIA

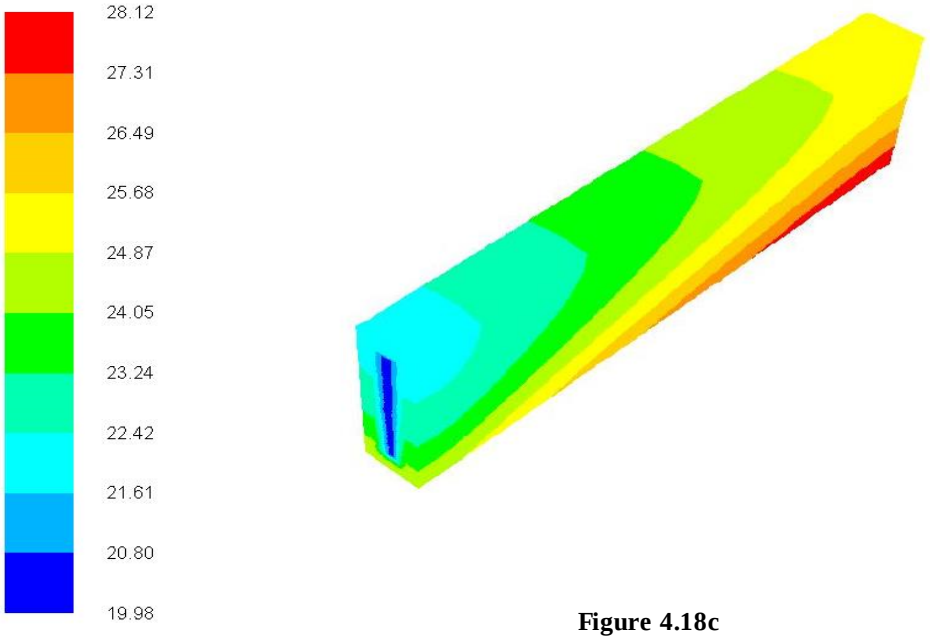

Figure 4.18c

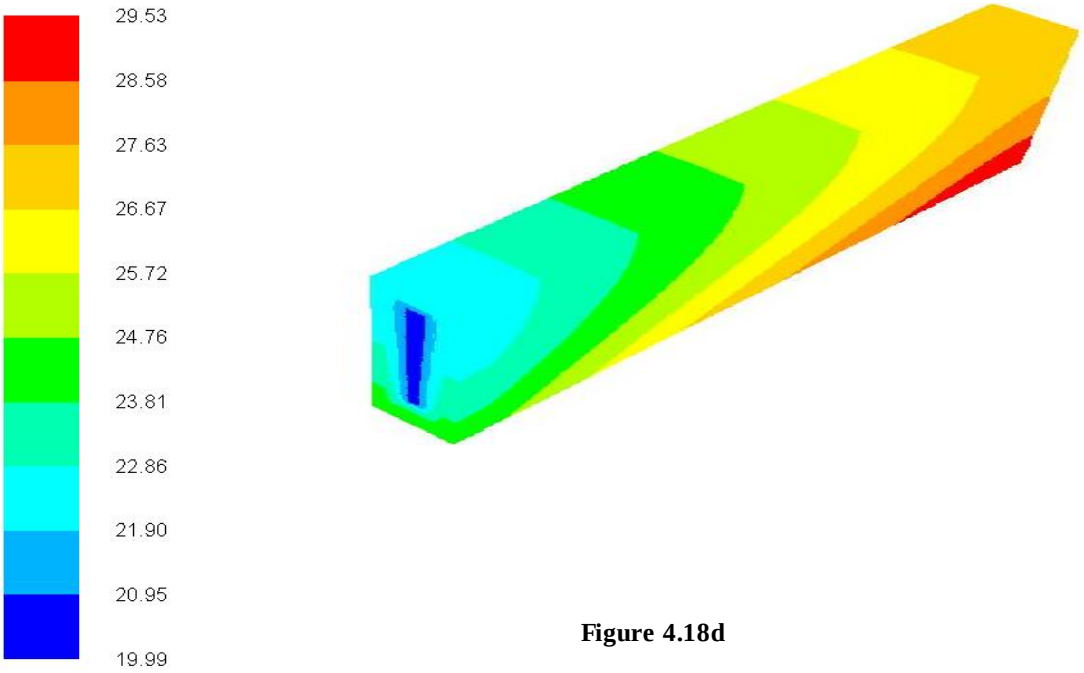

Figure 4.18d

Figure 4.18: Effect of varying axial length on temperature distribution within the solid substrate with AR = 3 (a) 1 mm (b) 3 mm (c) 5 mm (d) 7 mm

UNIVERSITEIT VAN PRETORIA
UNIVERSITY OF PRETORIA
YUNIBESITHI YA PRETORIA

Varying the axial length of the solid substrate and microchannel heat sink affects the temperature distribution within the solid substrate, as observed in Figure 4.18. When the axial length N is 1 mm with solid substrate aspect ratio AR of 3 and ΔP of 20 kPa, there is poor heat transfer from the heated wall to the working fluid. The peak temperature for this configuration is 31.28 ˚C, as shown in Figure 4.18a. As the axial length is further increased to 3 mm while keeping AR fixed as 3, there is an improvement in heat transfer from the heated wall to the working fluid giving 10% reduction in peak temperature, as observed from the temperature contours shown in Figure 4.18b. Further increase in the axial length to 5 mm, as shown in Figure 4.18c, makes the geometric configuration more slender and does not improve the thermal conductance significantly. The peak temperature is 28.12 ˚C, which is just 0.2% reduction in peak temperature when compared with the 3 mm axial length geometry. As the geometry becomes more slender (with increased axial length and reduced solid substrate width), there is an increase in the peak temperature. This is observed in Figure 4.18d for the axial length of 7 mm with peak temperature of 29.53 ˚C, which is an increase of about 5% when compared with the axial length of 5 mm. These changes in peak temperature as the length varies are a result of changes in the volume flow rates and channel aspect ratios, as shown in Figure 4.19.

Figure 4.19 shows how varying the axial length of the solid substrate affects the volume flow rate of the fluid, peak temperature and the channel aspect ratio for AR = 3 and ΔP = 20 kPa. In Figure 4.19a, the volume flow rate decreases with increase in the axial length and as the volume flow rate decreases, the peak temperature decreases but begins to increase when the axial length is greater than 5mm. Figure 4.19b shows that the

UNIVERSITEIT VAN PRETORIA
UNIVERSITY OF PRETORIA
YUNIBESITHI YA PRETORIA

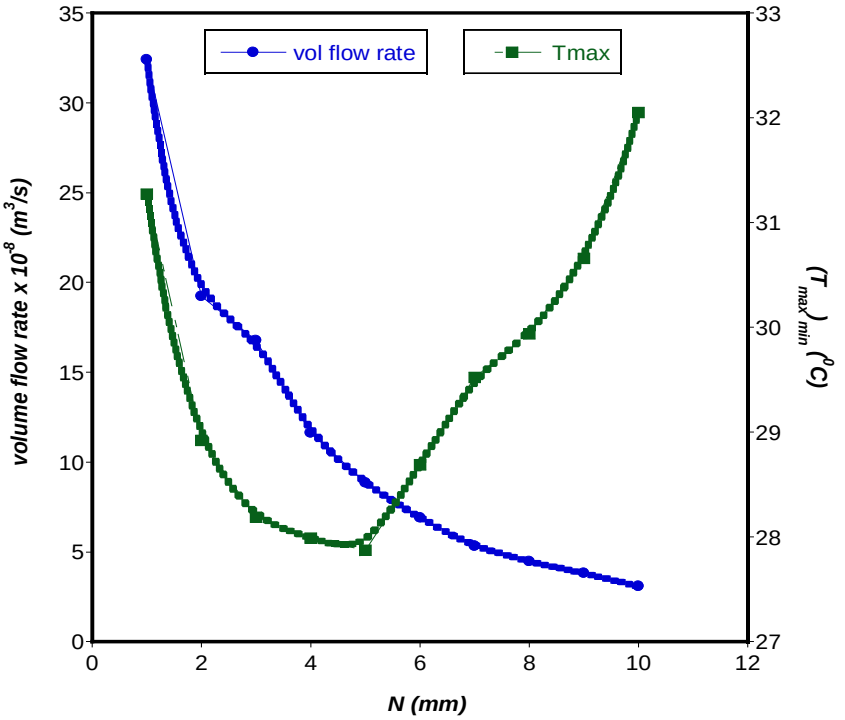

Figure 4.19a

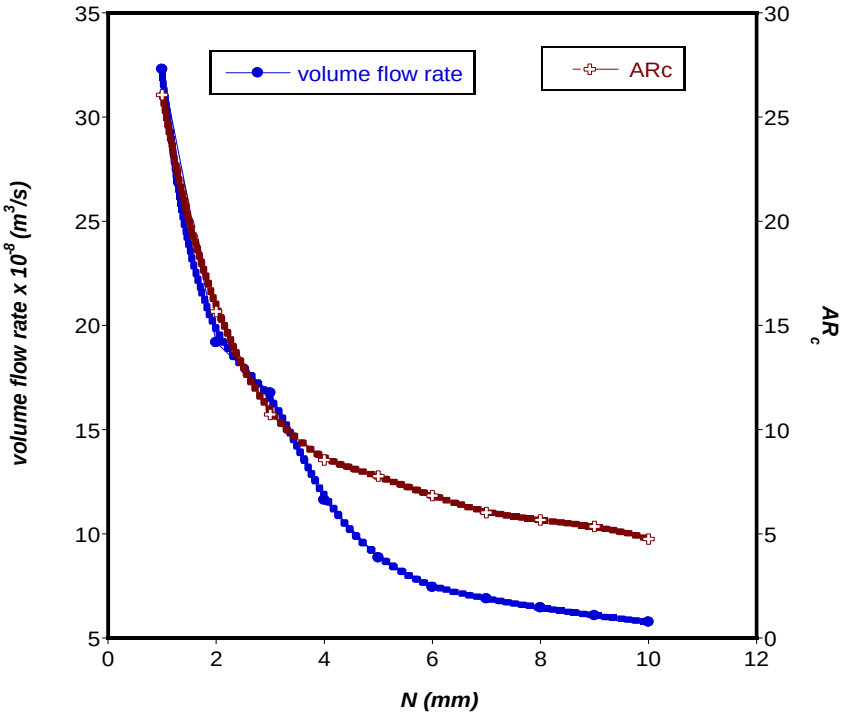

Figure 4.19b

Figure 4.19: Effect of varying axial length on volume flow rate of the cooling fluid and (a) minimised peak temperature (b) channel aspect ratio (AR =3, ΔP =20 kPa)

UNIVERSITEIT VAN PRETORIA
UNIVERSITY OF PRETORIA
YUNIBESITHI YA PRETORIA

decreasing volume flow rate as the axial length increases is due to decreasing channel aspect ratio. The geometric configuration with axial length of 10 mm has the highest peak temperature, lowest volume flow rate and lowest channel aspect ratio. The results in Figures 4.18 and 4.19 show that as the length is increased, there is improvement in heat transfer until a point where an optimum is reached and thereafter, there is poor heat transfer from the heated base to the working fluid due to further decrease in flow rates and channel aspect ratio. This confirms that geometry configuration is very critical in achieving maximum thermal performance in heat sinks. When the aspect ratio of the channel is very large or very small, heat transfer from the heated base to the fluid is very poor.

The results of optimal channel aspect ratio, solid volume fraction, channel hydraulic diameter, solid substrate aspect ratio and axial length for different pressure drops considered are shown in Figure 4.20. For the lowest ΔP of 10kPa, $\left(AR_c\right)_{opt} \approx 11$, $\phi_{opt} \approx 0.8$ and $N_{opt} = 3mm$ but when ΔP is increased from 20 to 60kPa, the optimal channel aspect ratio and solid volume fraction are approximately 8 and 0.7 respectively, while $N_{opt} = 5mm$. The optimal channel hydraulic diameter $\left(D_h\right)_{opt} \approx 140\mu m$ and the solid substrate aspect ratio $\left(AR\right)_{opt} = 3$ for all pressure drops considered in this study. The results presented in Figure 10 show that at higher pressure drops (above 40 kPa), the optimal microchannel and solid substrate dimensions do not vary with changes in the pressure drop.

UNIVERSITEIT VAN PRETORIA
UNIVERSITY OF PRETORIA
YUNIBESITHI YA PRETORIA

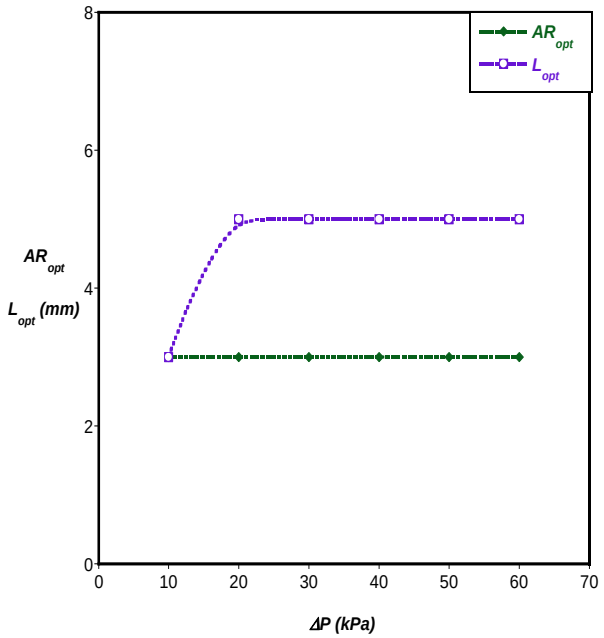

Figure 4.20a

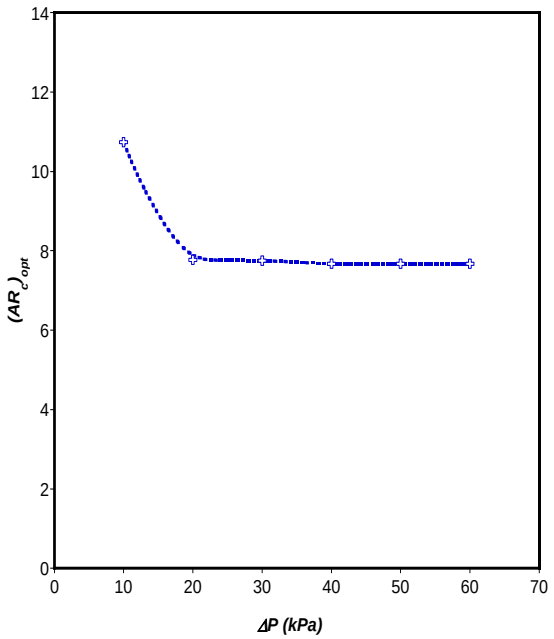

Figure 4.20b

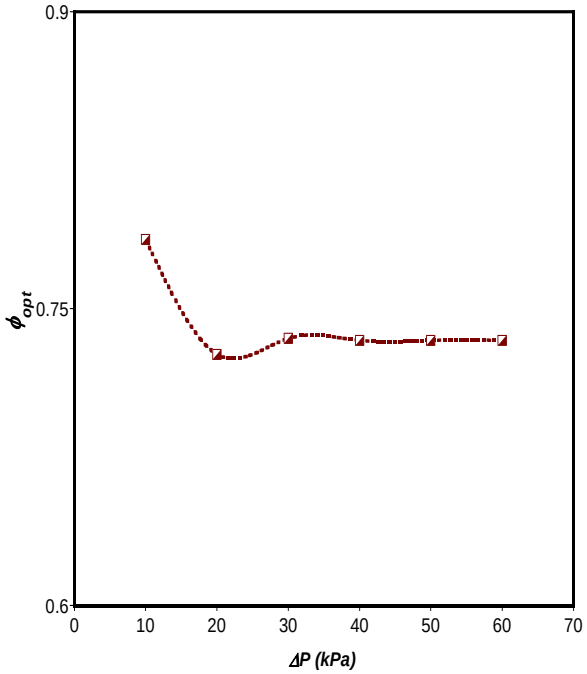

Figure 4.20c

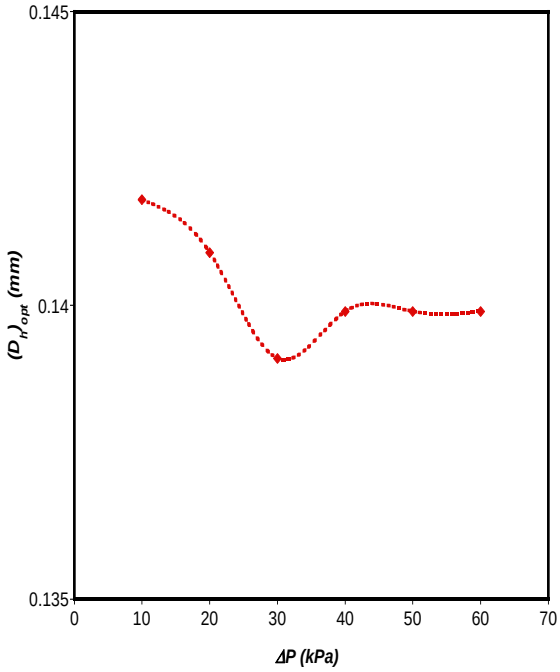

Figure 4.20d

Figure 4.20: Optimal solid substrate dimensions
(a) solid substrate aspect ratio and length (b) channel aspect ratio (c) solid volume fraction (d) hydraulic diameter

UNIVERSITEIT VAN PRETORIA
UNIVERSITY OF PRETORIA
YUNIBESITHI YA PRETORIA

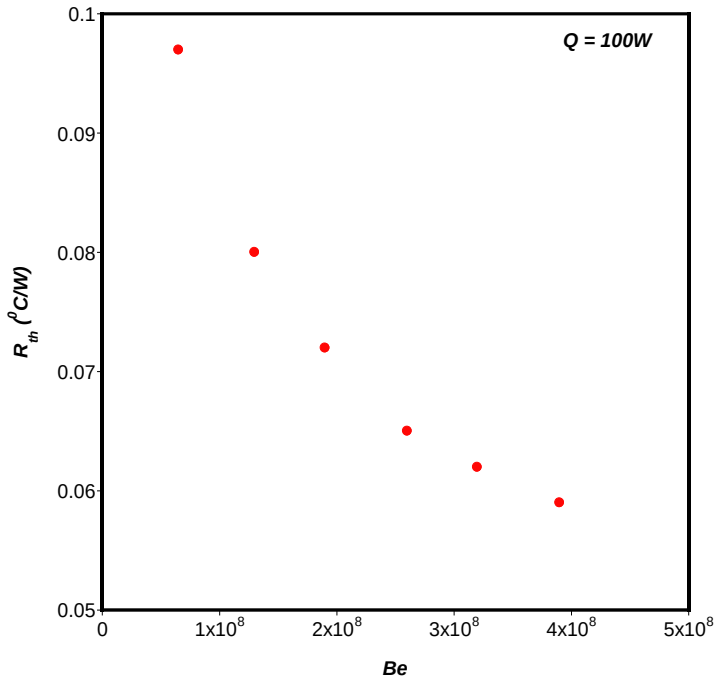

Figure 4.21a

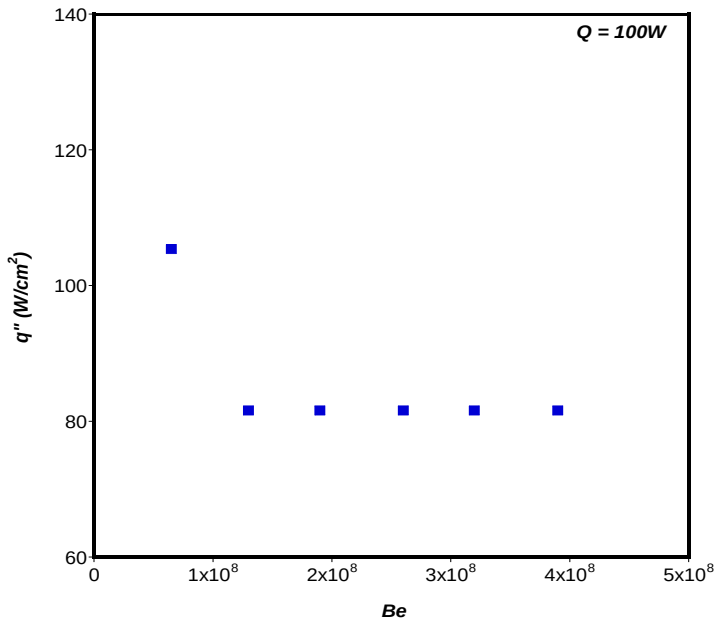

Figure 4.21b

Figure 4.21: Effect of dimensionless pressure drop on the (a) minimised thermal resistance and (b) surface heat flux

UNIVERSITEIT VAN PRETORIA
UNIVERSITY OF PRETORIA
YUNIBESITHI YA PRETORIA

The results of global thermal resistance and corresponding surface heat flux for the optimal microchannel and solid substrate dimensions are shown in Figure 4.21. The thermal resistance, which is the inverse of thermal conductance, is defined as:

$$R_{th} = \frac{\Delta T}{Q} \tag{4.12}$$

As the *Be* decreases, R_{th} decreases from 0.097 to 0.059 ˚C/W, while the surface heat flux q'' decreases from 105.41W/cm^2 for fixed *Be* of 6.5 x 10^7 to a constant value of 81.65W/cm^2 as the *Be* increases from 1.3 x 10^8 to 3.9 x 10^8.

4.3. STACKED MICROCHANNEL HEAT SINKS

This section presents the use of the constructal design technique to optimise the geometry of the two- and three-layered microchannel heat sinks. The thermal performances of these multi-layered heat sinks are also compared with the single microchannel discussed in the previous section.

4.3.1. Brief introduction

In previous investigations carried out on fluid flow and heat transfer in stacked microchannels, as outlined in the literature study [70-78, 80-82], two or more single microchannels of the same dimensions were stacked and as a result, the flow area of the

UNIVERSITEIT VAN PRETORIA
UNIVERSITY OF PRETORIA
YUNIBESITHI YA PRETORIA

fluid was increased because a global constraint was not specified on the total volume of the stacked microchannel geometry. In this study, a fixed total volume constraint is applied to obtain global optima with respect to the channel aspect ratio, solid volume fraction, channel hydraulic diameter and pressure drop.

4.3.2. Physical model

A physical model of a two-layered stacked microchannel is shown in Figure 4.22. Figures 4.23 and 4.24 show the elemental volume used as the computational domain for the two- and three-layered microchannels respectively. Figures 4.25 and 4.26 show the different flow arrangements for the two- and three-layered microchannel heat sinks, namely the two-layered parallel-flow (two-layered PF), two-layered counterflow (two-layered CF), three-layered parallel-flow (three-layered PF), three-layered counterflow1 (three-layered CF1) and three-layered counterflow2 (three-layered CF2) orientations. The length N, height M and width W of the heat sink are fixed, which makes the total volume V fixed while t_1, t_2, t_3, t_5, t_6, t_7, t_8, H_c, H_{c1}, H_{c2}, H_{c3}, W_c, W_{c1}, W_{c2} and W_{c3} are varied but also subject to manufacturing constraints. The two-layered configuration has nine degrees of freedom while the three-layered configuration has twelve degrees of freedom.

UNIVERSITEIT VAN PRETORIA
UNIVERSITY OF PRETORIA
YUNIBESITHI YA PRETORIA

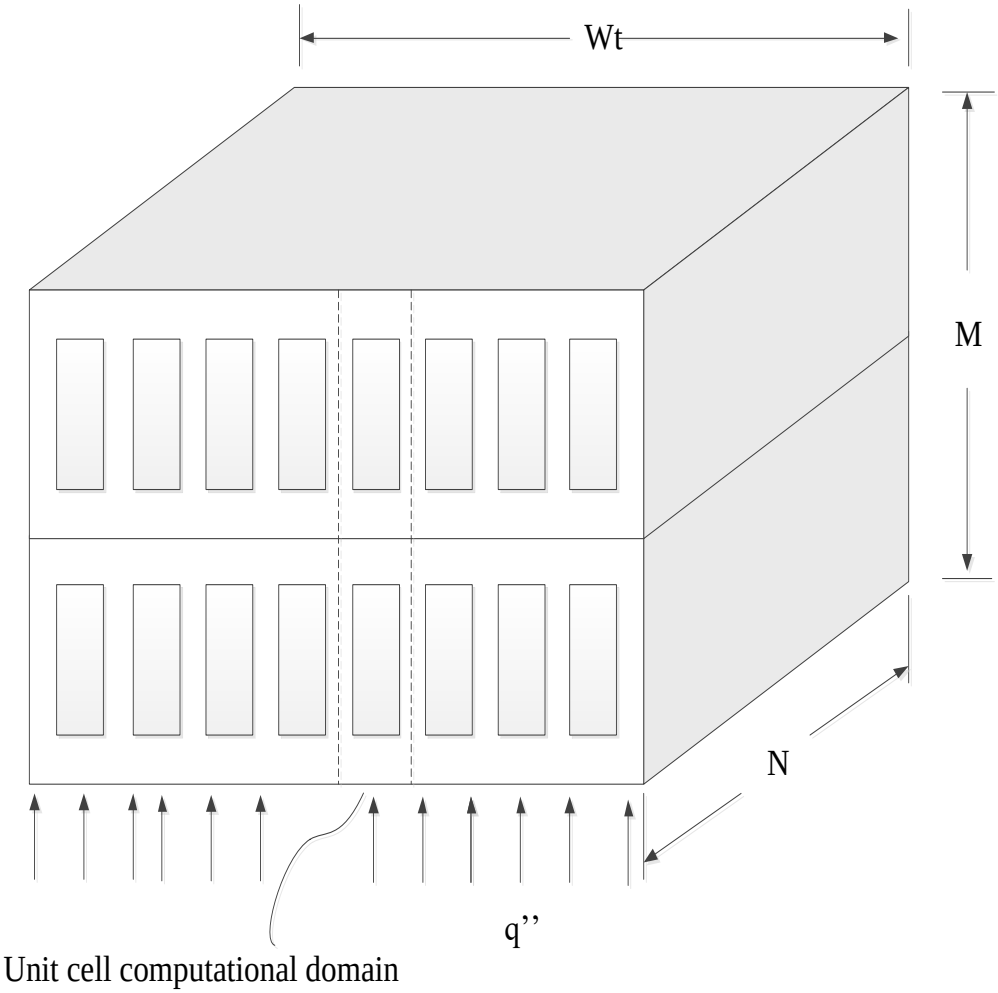

Figure 4.22: Physical model of a two-layered microchannel heat sink

UNIVERSITEIT VAN PRETORIA
UNIVERSITY OF PRETORIA
YUNIBESITHI YA PRETORIA

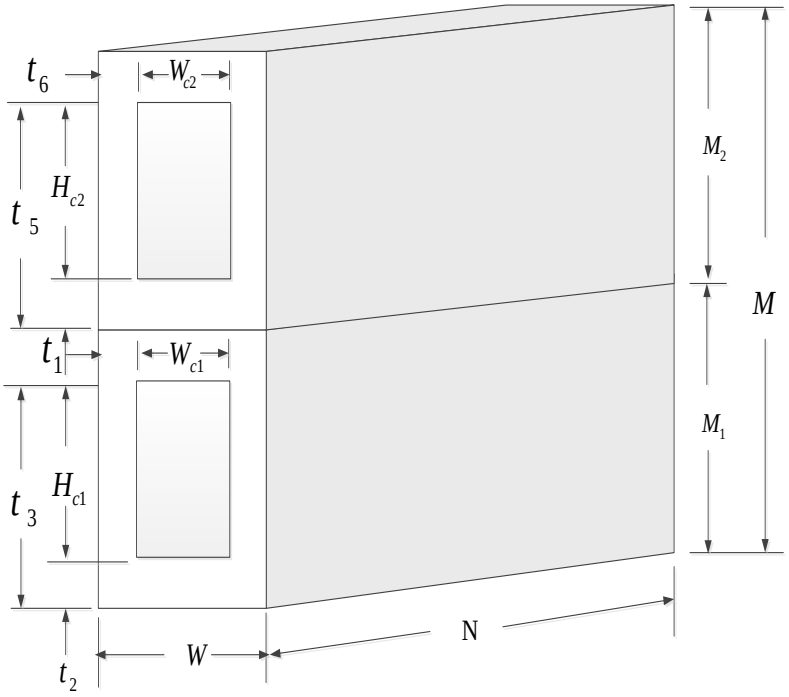

Figure 4.23: Computational domain of the two-layered microchannel

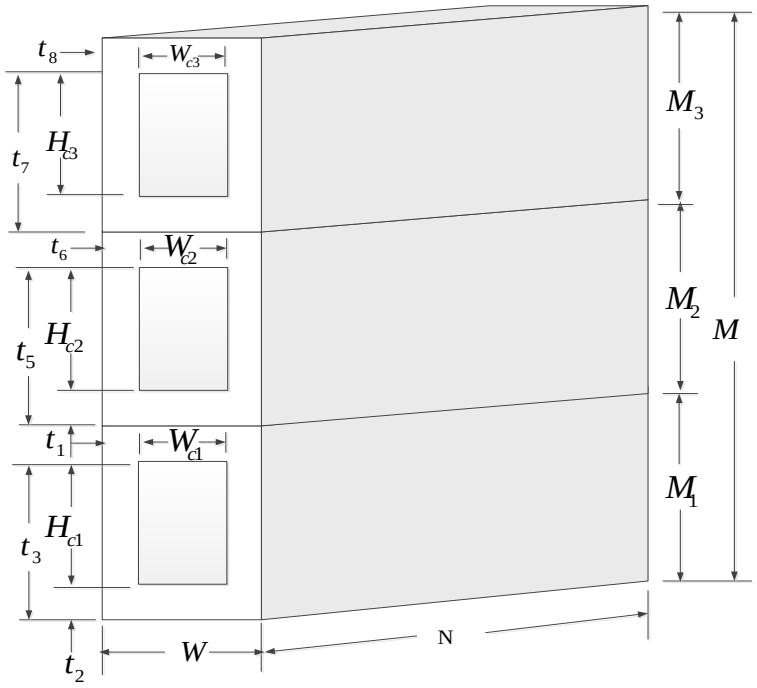

Figure 4.24: Computational domain of the three-layered microchannel

UNIVERSITEIT VAN PRETORIA
UNIVERSITY OF PRETORIA
YUNIBESITHI YA PRETORIA

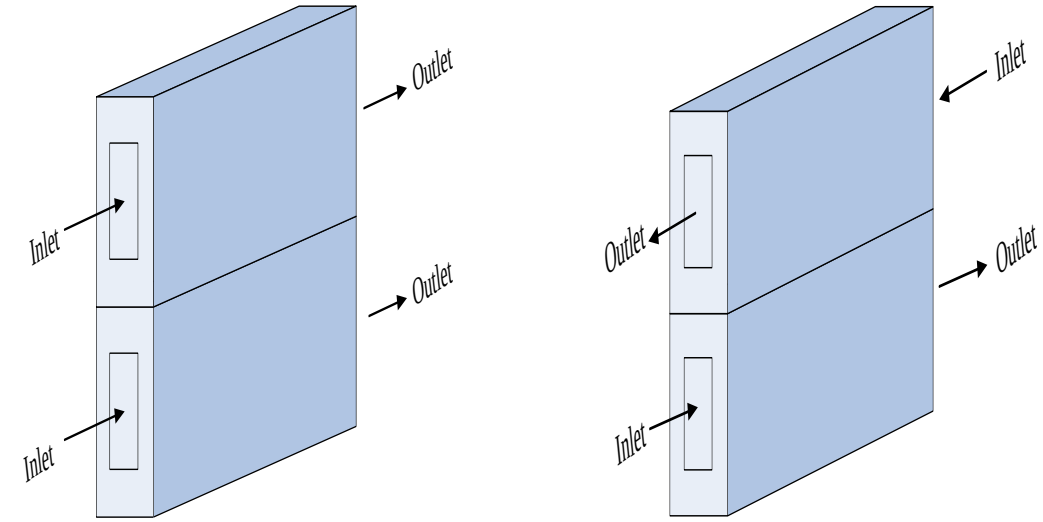

Figure 4.25: Flow arrangement for the two-layered microchannel (a) parallel flow (PF) (b) counterflow (CF)

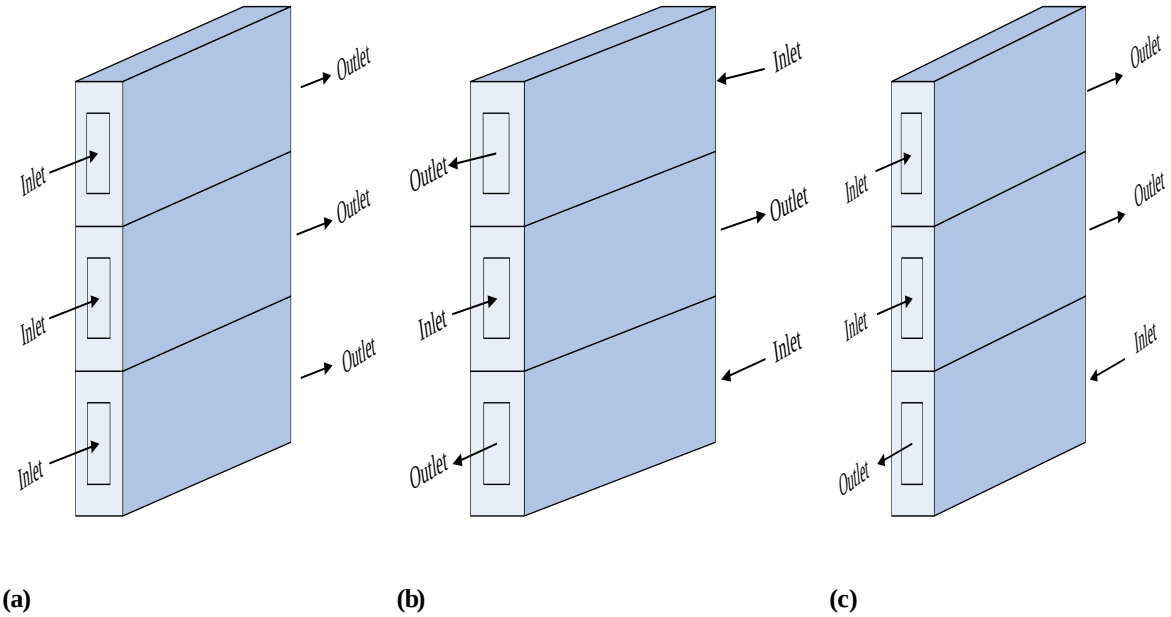

Figure 4.26: Flow arrangement for the three-layered microchannel (a) parallel flow (PF) (b) counterflow1 (CF1) (c) counterflow2 (CF2)

UNIVERSITEIT VAN PRETORIA
UNIVERSITY OF PRETORIA
YUNIBESITHI YA PRETORIA

4.3.2.1. Grid analysis and code validation

Grid refinement tests are also carried out for the two- and three-layered microchannel heat sinks for pressure drop of 30 kPa. Table 4.5 shows the dimensions of the two-layered microchannel used for the grid refinement tests, while Table 4.6 shows the grid refinement test results. Tables 4.7 and 4.8 show the dimensions of the three-layered microchannel used for the grid refinement tests and the grid refinement test results respectively. The convergence criterion is stated in Equation (4.1).

Table 4.4: Dimensions of the two-layered microchannel heat sink for grid refinement test

H_{c1}, H_{c2} (mm)	W_{c1}, W_{c2} (mm)	t_1, t_6 (mm)	M_1-t_3, M_2-t_5 (mm)	M_1, M_2 (mm)	W (mm)
0.250	0.06	0.02	0.10	0.45	0.10

Table 4.5: Grid refinement test results

Number of cells	$\Delta T(K)$	$\left\|\frac{(\Delta T)_i - (\Delta T)_{i-1}}{(\Delta T)_i}\right\|$
24 673	14.0978	-
39 969	14.2467	0.0105
59 374	14.1398	0.0076
83 866	14.2201	0.0056

UNIVERSITEIT VAN PRETORIA
UNIVERSITY OF PRETORIA
YUNIBESITHI YA PRETORIA

Table 4.6: **Dimensions of the three-layered microchannel heat sink for grid refinement test**

H_{c1}, H_{c2}, H_{c3} (mm)	W_{c1}, W_{c2}, W_{c3} (mm)	t_1, t_6, t_8 (mm)	M_1-t_3, M_2-t_5, M_3-t_7 (mm)	M_1, M_2, M_3 (mm)	W (mm)
0.20	0.06	0.02	0.10	0.30	0.10

Table 4.7: Grid refinement test results

Number of cells	$\Delta T(K)$	$\left\|\frac{(\Delta T)_i - (\Delta T)_{i-1}}{(\Delta T)_i}\right\|$
69 939	15.1643	-
103 219	15.3264	0.0106
170 527	15.2010	0.0082
228 707	15.3150	0.0074

The computational fluid dynamics (CFD) code used is validated by comparing the numerical results obtained using this code with the experimental results obtained from the investigation on stacked microchannels carried out by Wei *et al.* [73]. The results of temperature distribution of the heated base along the axial length of the microchannel show very good agreement with an average deviation of 2.4%, as shown in Figure 4.27a, and 2.7%, as shown in Figure 4.27b. The numerical results obtained in this study are also compared with the numerical results obtained for the temperature difference on the heated base of the two-layered microchannel geometry used by Patterson *et al.* [74]. Trends are also in very good agreement with an average deviation of 2.3%, as shown in Figure 4.28.

UNIVERSITEIT VAN PRETORIA
UNIVERSITY OF PRETORIA
YUNIBESITHI YA PRETORIA

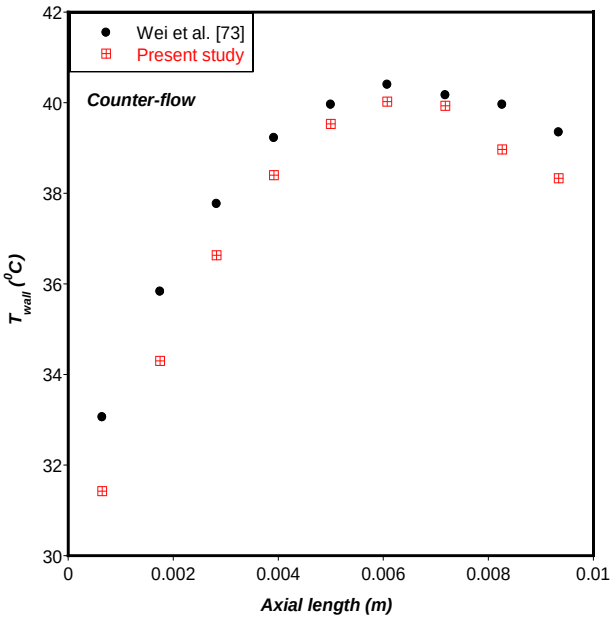

(a)

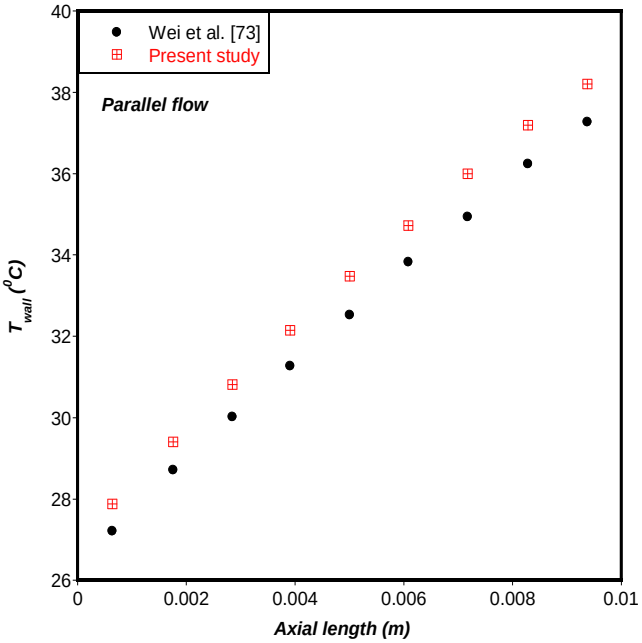

(b)

Figure 4.27: Wall temperatures along the length of a two-layered microchannel (a) counterflow (b) parallel flow

UNIVERSITEIT VAN PRETORIA
UNIVERSITY OF PRETORIA
YUNIBESITHI YA PRETORIA

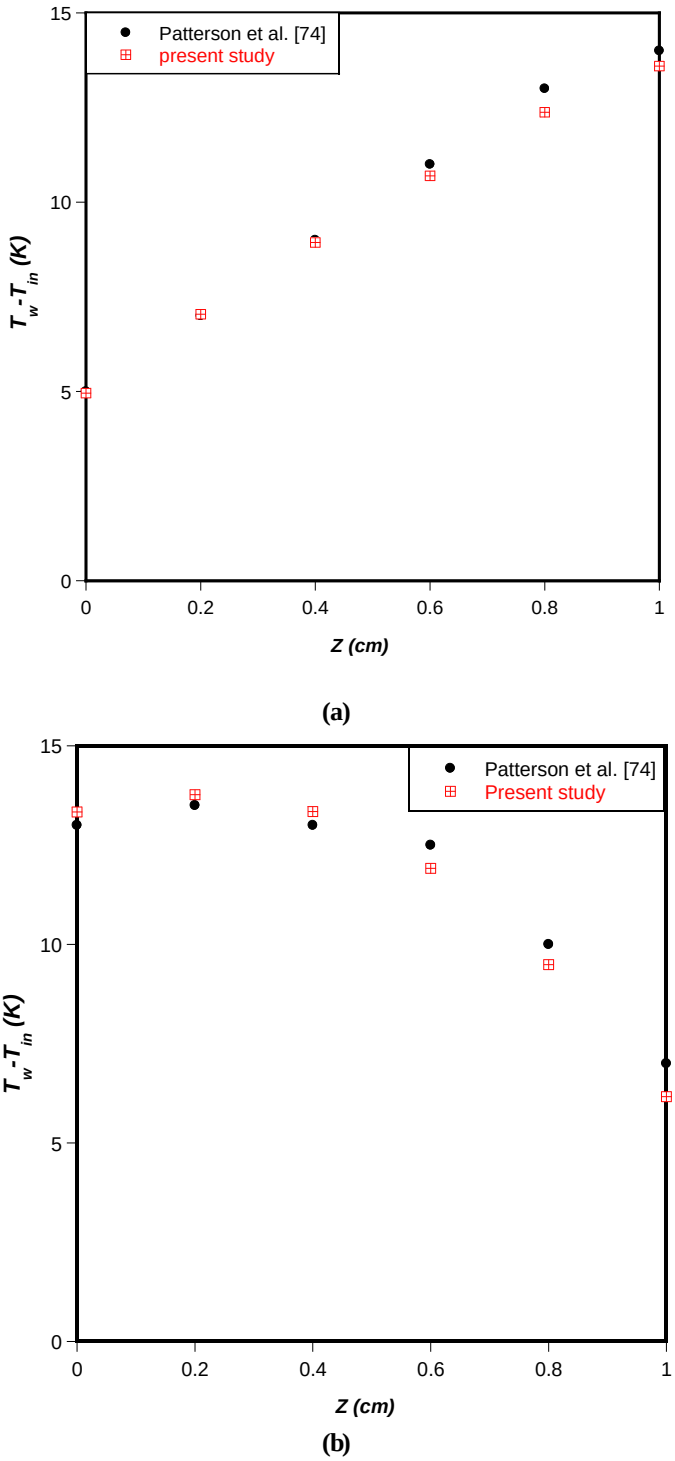

Figure 4.28: Peak wall temperature difference along the axial length of a two-layered microchannel (a) parallel flow (b) counterflow

UNIVERSITEIT VAN PRETORIA
UNIVERSITY OF PRETORIA
YUNIBESITHI YA PRETORIA

4.3.2.2. Design variables and optimisation technique

The solid volume fraction and fixed total volume are the same as stated in Equations (4.3) and (4.4). The manufacturing constraints are:

$$\frac{H_{c1-c3}}{W_{c1-c3}} \leq 20 \tag{4.13}$$

$$t_2 \geq 50\mu m \tag{4.14}$$

$$M_2 - t_5 \geq 50\mu m \quad \text{(Two-layer)} \tag{4.15}$$

$$M_3 - t_7 \geq 50\mu m \quad \text{(Three-layer)} \tag{4.16}$$

where $M_1 + M_2 + ... + M_n = M$ (4.17)

The hydraulic diameter D_h is defined as:

$$\frac{2H_c}{(AR+1)} \tag{4.18}$$

where AR is the channel aspect ratio defined as $\frac{H_c}{W_c}$.

Numerical simulations and optimisation are carried out for a fixed total volume V of 0.9 mm^3, fixed axial length N of 10 mm. The design space for the response surface for a fixed total volume V of 0.9 mm^3 is defined as $54 \leq W_{c1}, W_{c2}, W_{c3} \leq 66$ µm, $19 \leq t_1, t_6, t_8 \leq 29$ µm, $50 \leq M_2 - t_5 \leq 60$ µm (two-layered), $50 \leq M_3 - t_7 \leq 60$ µm (three-layered), $25 \leq M_1 - t_3$, $M_2 - t_5 \leq 30$ (three-layered) and $240 \leq H_{c1}, H_{c2}, H_{c3} \leq 375$ µm. The optimised design point chosen is required to meet the manufacturing constraints.

UNIVERSITEIT VAN PRETORIA
UNIVERSITY OF PRETORIA
YUNIBESITHI YA PRETORIA

4.3.3. Case Study 1: Comparison between the results of single and multi-layered microchannels with fixed axial length and uniform heat flux

The corresponding inlet fluid velocity for the single microchannel presented in Section 4.2.4 is between 0.329 m/s to 1.865 m/s for the range of pressure drop 10 to 60 kPa. The range of Reynolds number (Re_{Dh}) for these velocities is $36 < Re_{Dh} < 210$, where $\mathrm{Re}_{Dh} = \dfrac{\rho_f u_{in} D_h}{\mu_f}$. Therefore, in this section, the inlet velocity of fluid flow into each channel of the two- and three-layered microchannels considered is exactly the same as that of the single microchannel.

4.3.3.1. Maximised thermal conductance

Figure 4.29 shows the comparison between the maximised thermal conductance of the single and multi-layered microchannels with different flow arrangements. Results show that when fluid velocity is 0.329 m/s, the thermal performance of the single microchannel is 0.7% better than that of the two-layered PF and 12% better than that of the two-layered CF. As the inlet velocity is increased, the thermal performance of the two-layered PF increased by 1 to 6%, while the two-layered CF gives 0.9 to 8% increase in thermal performance when compared with that of the single microchannel. These results show that when maximised thermal conductance is considered at the lowest velocity, the two-layered CF performs poorly. When the maximised thermal conductance of the single

UNIVERSITEIT VAN PRETORIA
UNIVERSITY OF PRETORIA
YUNIBESITHI YA PRETORIA

microchannel is compared with that of the three-layered microchannels, the single microchannel has the best performance for low inlet velocities of 0.329 m/s and 0.648 m/s. As the inlet velocity is increased from 0.960 m/s to 1.865 m/s, the three-layered CF2 has the best thermal performance of 4 to 10% increase in maximised thermal conductance when compared with that of the single microchannel.

In summary, these results show that for the same total volume of solid substrate, increasing the microchannel layers to three improves the thermal performance of the microchannel for inlet velocities greater than 0.648 m/s.

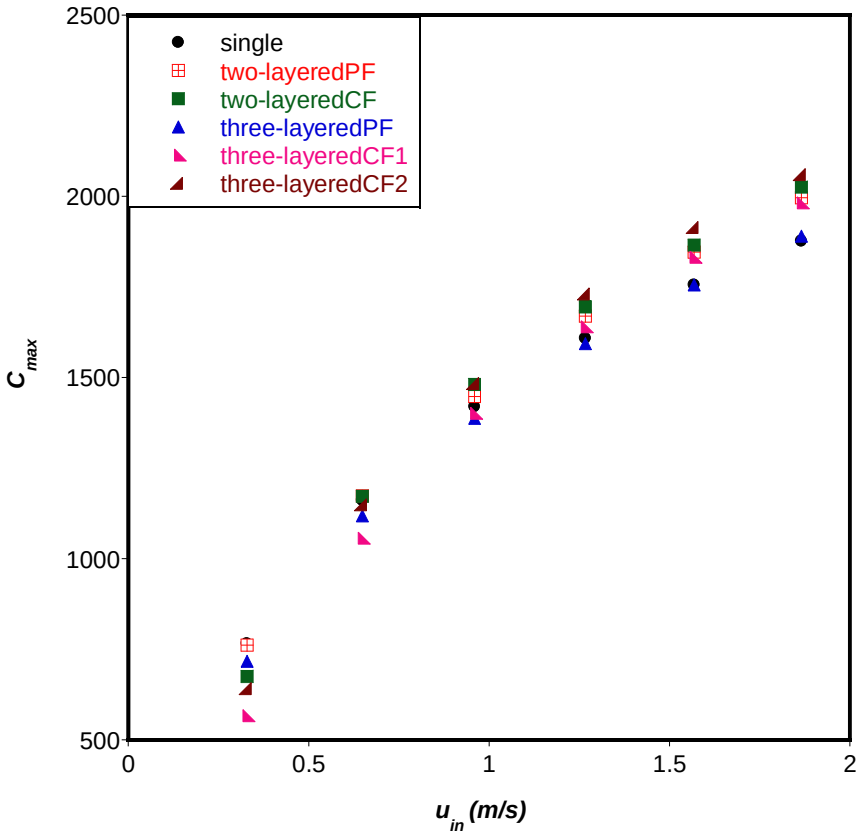

Figure 4.29: Comparison between maximised thermal conductance of the single, two- and three-layered microchannels at different fluid inlet velocities

UNIVERSITEIT VAN PRETORIA
UNIVERSITY OF PRETORIA
YUNIBESITHI YA PRETORIA

4.3.3.2. Optimal dimensions of the two- and three-layered microchannel with different flow arrangements

Figure 4.30 shows the optimal channel aspect ratio, solid volume fraction and hydraulic diameters for the two-layered microchannels with different flow arrangements. Figure 4.30a shows that the optimal channel aspect ratio, solid volume fraction and hydraulic diameter for the bottom layer of the two-layered PF are 6.242, 0.751 and 103 µm respectively. For the top layer, the optimal dimensions are 5.739, 0.734 and 110 µm for fluid inlet velocities of 0.329 m/s to 0.960 m/s. When the fluid velocity is increased above 0.960 m/s, the optimal dimensions for the two-layered PF become 6.644, 0.770 and 97 µm for the bottom layer and 6.335, 0.755 and 101 µm for the top layer. For the two-layered CF, the optimal channel dimensions, as shown in Figure 4.30b, are 5.574, 0.732 and 112 µm for the bottom layer and 5.60, 0.734 and 111 µm for the top layer when the fluid velocity is 0.329 m/s. When the velocity of the fluid is increased to between 0.648 m/s and 1.865 m/s, the optimal dimensions of the two-layered CF are the same as those outlined above for the two-layered PF.

UNIVERSITEIT VAN PRETORIA
UNIVERSITY OF PRETORIA
YUNIBESITHI YA PRETORIA

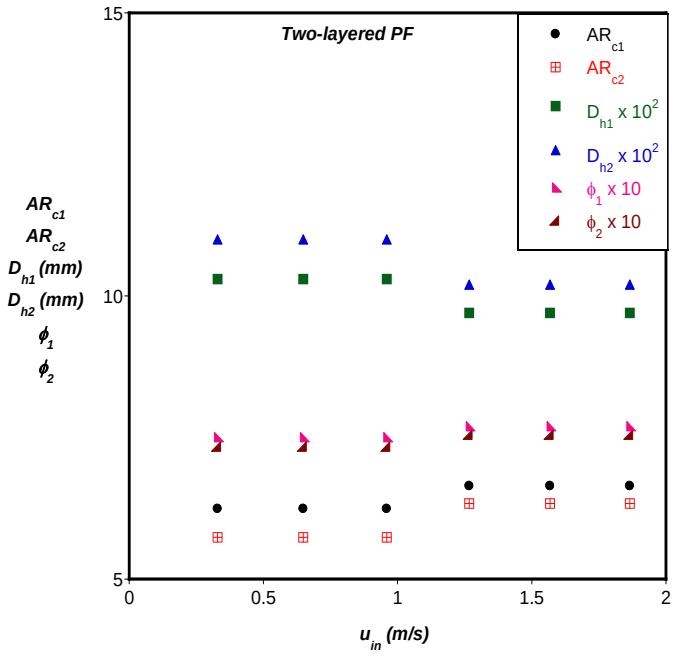

(a)

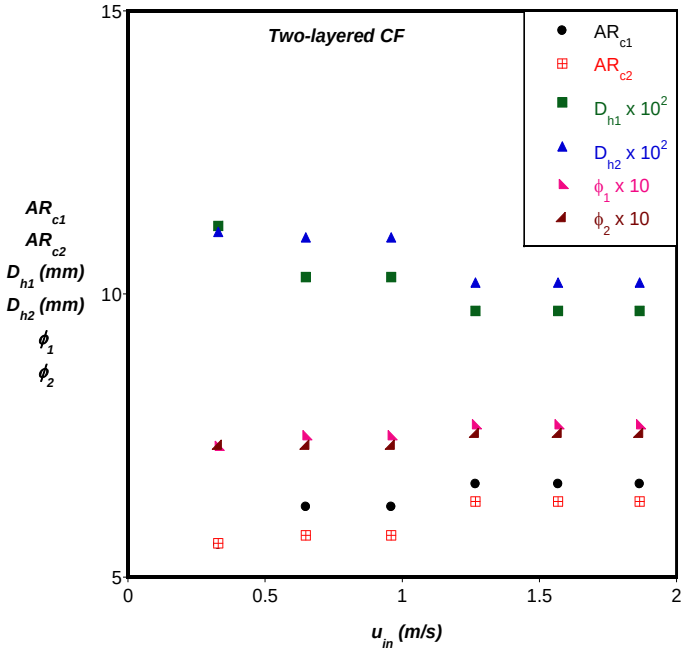

(b)

Figure 4.30: Optimal channel aspect ratio, solid volume fraction and channel hydraulic diameter for (a) two-layered PF (b) two-layered CF

UNIVERSITEIT VAN PRETORIA
UNIVERSITY OF PRETORIA
YUNIBESITHI YA PRETORIA

Figure 4.31 shows the optimal channel aspect ratio, solid volume fraction and hydraulic diameter for the three-layered microchannel with different flow arrangements. For the three-layered PF, the optimal dimensions of the first layer are 3.549, 0.847 and 97 μm for the channel aspect ratio, solid volume fraction and hydraulic diameter respectively when the inlet velocity is 0.329 m/s. For an inlet fluid velocity of 0.648 m/s, the optimal dimensions are 3.872, 0.858 and 91 μm respectively. When the inlet velocity is increased from 0.960 m/s to 1.865 m/s, the optimal dimensions are 3.707, 0.859 and 92 μm respectively. For the second and third layers of the three-layered PF, the optimal dimensions are 3.706, 0.822 and 103 μm for the second layer and 3.509, 0.849 and 97 μm for the third layer when the inlet velocity is 0.329 m/s. For an inlet velocity of 0.648 m/s, the optimal dimensions are 3.905, 0.823 and 102 μm for the second layer and 3.433, 0.849 and 98 μm for the third layer. Further increase in the inlet velocity from 0.960 m/s to 1.865 m/s gives the optimal dimensions for the second layer as 4.377, 0.823 and 93 μm, while the optimal dimensions are 3.574, 0.844 and 98 μm for the third layer. These results are shown graphically in Figure 4.31a.

In summary, the results outlined above show that the optimal dimension of each layer depends on velocity and the position of the layer (whether first, second or third layer). These trends are also observed for the three-layered CF1 and CF2, as shown in Figures 4.31b and 4.31c. It can also be observed that, when a total volume constraint is applied to the multi-layered microchannels, the optimal channel aspect ratios and hydraulic diameters are smaller when compared with those of the single microchannel while the solid volume fraction of the multi-layered microchannels is larger.

UNIVERSITEIT VAN PRETORIA
UNIVERSITY OF PRETORIA
YUNIBESITHI YA PRETORIA

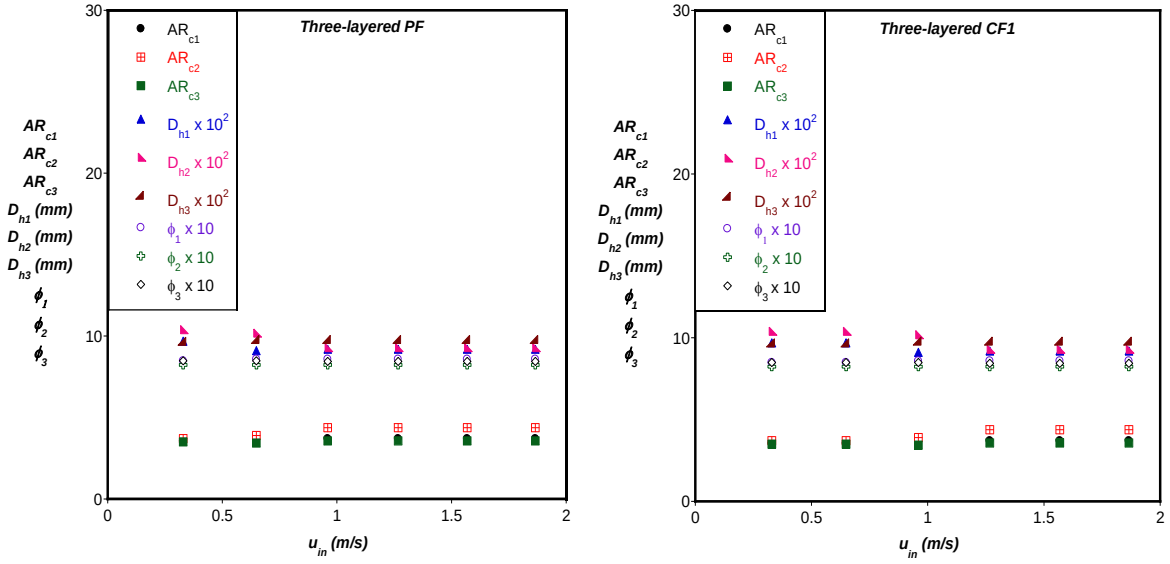

(a)

(b)

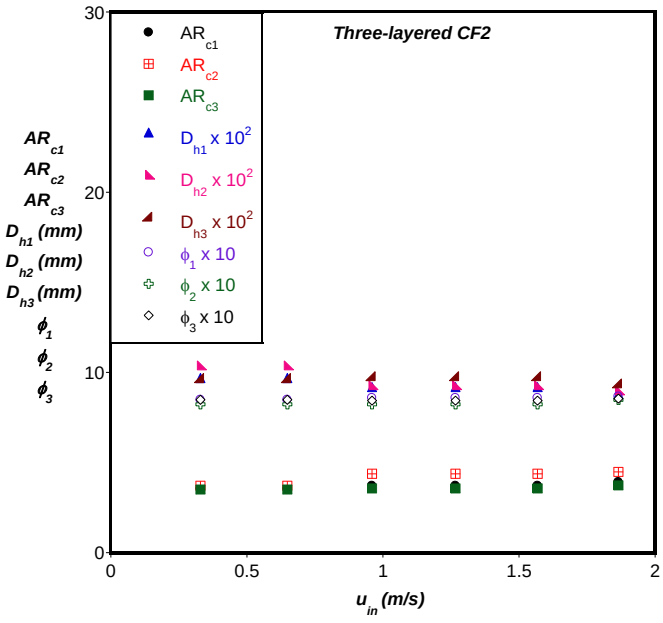

(c)

Figure 4.31: Optimal channel aspect ratio, solid volume fraction and channel hydraulic diameter (a) three-layered PF (b) three-layered CF1 (c) three-layered CF2

UNIVERSITEIT VAN PRETORIA
UNIVERSITY OF PRETORIA
YUNIBESITHI YA PRETORIA

4.3.3.3. Reynolds number, pumping power and pressure drop in single and two-layered microchannel

Figure 4.32 shows the variation in the Reynolds number for increasing fluid inlet velocity in the single- and two-layered microchannels. It can be observed that as the velocity of the fluid increases, the Reynolds number increases, which is the expected trend. The results presented in Figure 4.32a show that for the same inlet velocity, Re_{Dh} for the two-layered PF is reduced by 2% to 10% when the first (bottom) layer is compared with the single microchannel. When the second (top) layer of the two-layered PF is compared with the single microchannel, the Re_{Dh} decreases with about 9% to 15%. A similar trend is also observed when the Re_{Dh} of the two-layered CF is compared with that of the single microchannel. There is a 1% to 10% decrease in Re_{Dh} in the first layer and a 0% to 15% decrease in the second layer, as shown in Figure 4.32b. This variation in Re_{Dh} is caused by the different optimal values of hydraulic diameters for the different types of microchannels. The optimal hydraulic diameter of the top and bottom layer of the two-layered microchannel is smaller than the one for the single microchannel. The Reynolds number range for the two-layered PF and CF considered in this study is $33 < Re_{Dh} < 190$.

Figure 4.33 shows the comparison between the pumping power requirements for the different fluid inlet velocities in the single and two-layered microchannels. Pumping power (PP) used to drive the fluid through the microchannel for an elemental volume is given by:

$$PP = u_{in}.A_c.\Delta P \tag{4.19}$$

UNIVERSITEIT VAN PRETORIA
UNIVERSITY OF PRETORIA
YUNIBESITHI YA PRETORIA

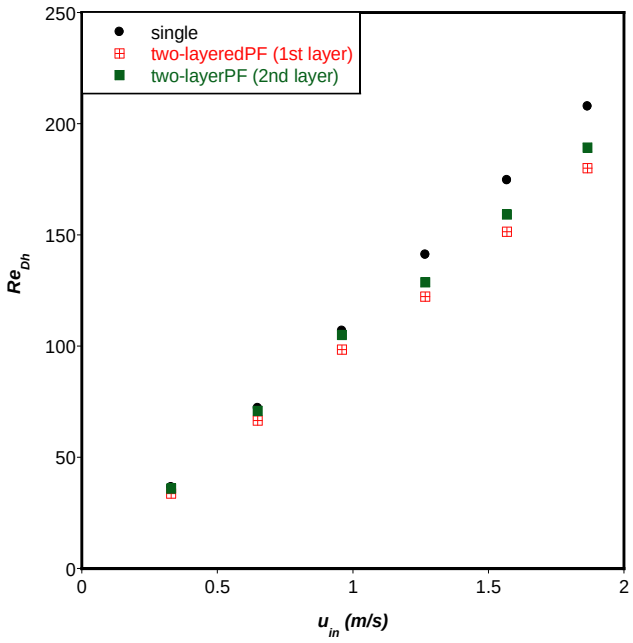

(a)

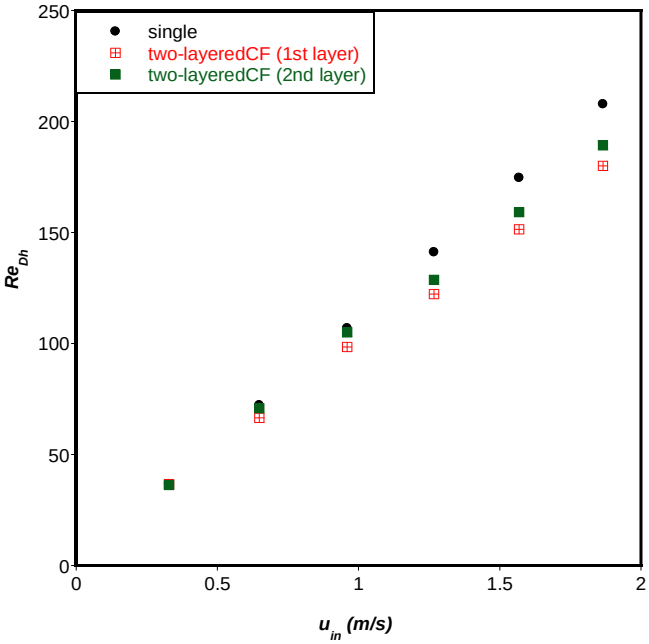

(b)

Figure 4.32: Comparison between Reynolds number for fluid flow in single and two-layered microchannel (a) parallel flow (b) counterflow

UNIVERSITEIT VAN PRETORIA
UNIVERSITY OF PRETORIA
YUNIBESITHI YA PRETORIA

It can be observed that as the velocity of the fluid increases, the required pumping power increases, which is the expected trend. However, the results presented in Figure 4.33a show that the pumping power required for fluid flow into the top and bottom channels is not identical for the same inlet velocity. The bottom channel requires 40% to 50% more pumping power for fluid flow than the top channel. This is because the bottom channel is in direct contact with the heated base. Consequently, more cooling is needed at the bottom layer than at the top layer. This trend can be observed for both the parallel and counterflow orientations (two-layered PF and two-layered CF). Figure 4.33b shows that the total pumping power required for the two-layered microchannel is reduced by about 10% for both the parallel and counterflow arrangement when compared with the single microchannel. These results show that reduced pumping power can be achieved without increasing the total volume of the two-layered microchannel.

Figure 4.34 shows how pressure drop in the single and two-layered microchannels varies with increasing fluid velocity. It can be observed from results presented in Figure 4.34a for the two-layered PF that the average pressure drop in the bottom channel (first layer) is about 60% more than in the top channel (second layer). When the average of the total pressure drop in the two-layered PF is compared with the single microchannel, an average reduction of about 1.4% in the two-layered PF is observed. Figure 4.34b shows the pressure drop comparison between the single and the two-layered CF. It can be observed that the pressure drop in the bottom channel exceeds that in the top channel by about 40% to 60% as the fluid velocity increases. The average total pressure drop in the two-layered CF is also about 1.8% less than that of the single microchannel. This shows that even

UNIVERSITEIT VAN PRETORIA
UNIVERSITY OF PRETORIA
YUNIBESITHI YA PRETORIA

though the fluid velocities in the top and bottom layers are the same, the pressure drops in the different layers are not the same.

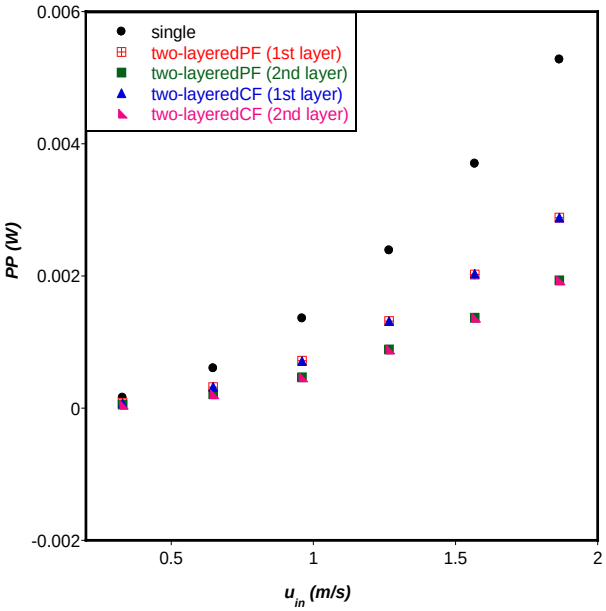

(a)

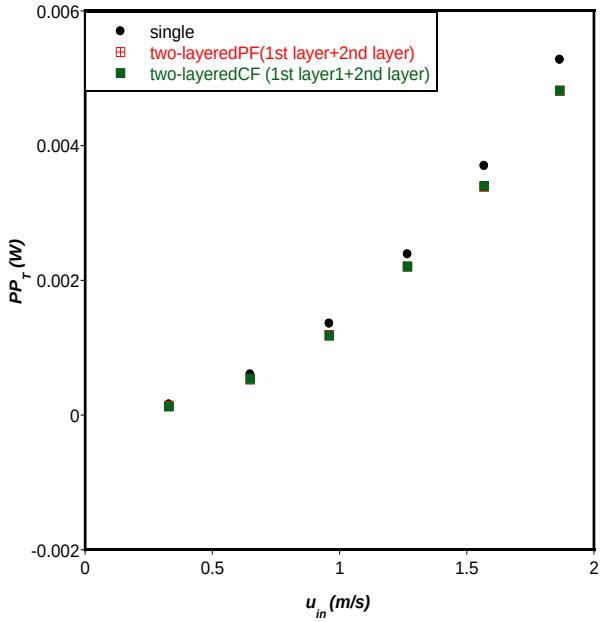

(b)

Figure 4.33: Comparison between pumping power requirements for single and two-layered microchannels (a) each layer (b) total number of layers

UNIVERSITEIT VAN PRETORIA
UNIVERSITY OF PRETORIA
YUNIBESITHI YA PRETORIA

From these results, it is evident that, without increasing the total volume of solid substrate, the average pressure drop in the two-layered microchannel can be reduced.

From Equation 4.17, it is evident that pumping power is a function of the channel cross-section area and pressure drop. The results in this section show that with the two-layered PF and CF, a reduced cross-sectional area and average pressure drop result in reduced pumping power when compared with the single microchannel.

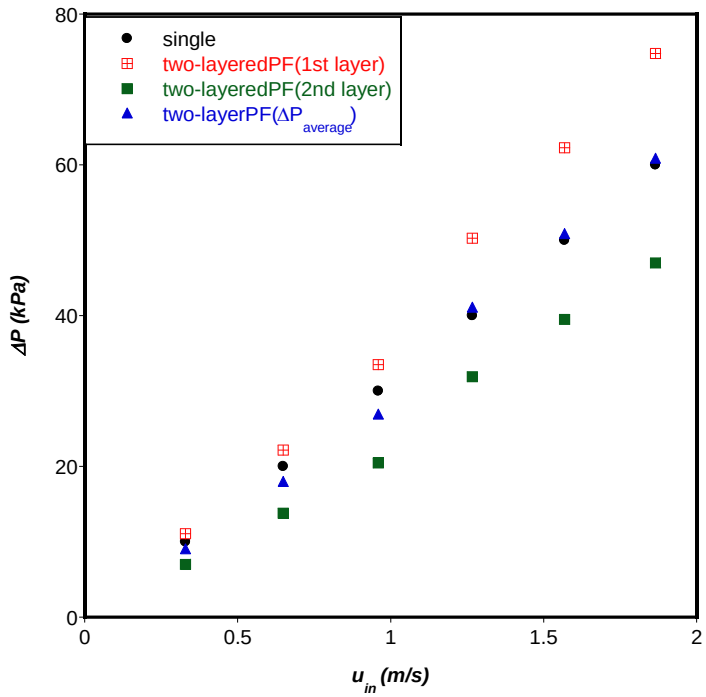

Figure 4.34 (a)

UNIVERSITEIT VAN PRETORIA
UNIVERSITY OF PRETORIA
YUNIBESITHI YA PRETORIA

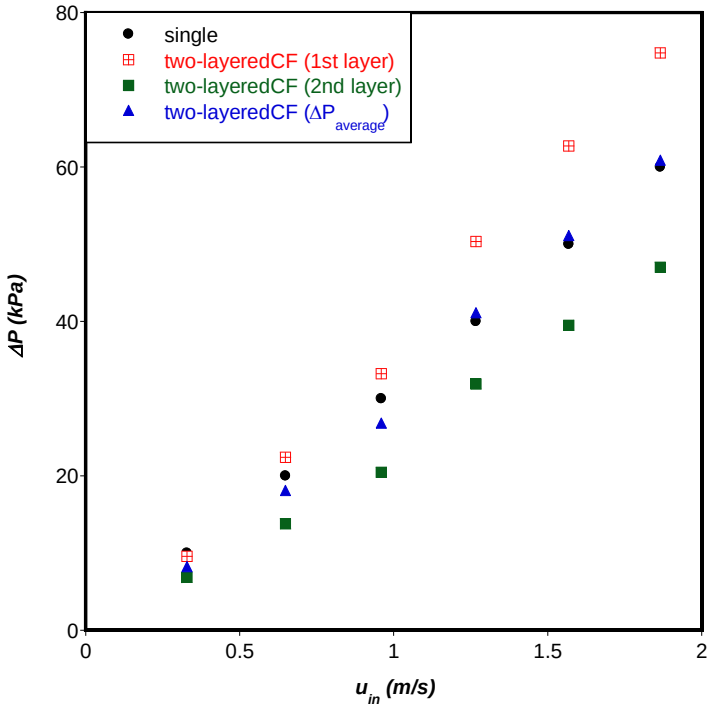

Figure 4.34 (b)

Figure 4.34: Comparison between the pressure drop in single and two-layered microchannels (a) parallel flow (b) counterflow

4.3.3.4. Reynolds number, pumping power and pressure drop in single and three-layered microchannel

A comparison between the variations in the Reynolds number with increasing inlet fluid velocity in the single- and three-layered microchannels with different flow arrangements is presented in Figure 4.35. From the results shown, the single microchannel has the highest Reynolds number for all the inlet velocities considered when compared with the three-layered microchannels PF, CF1 and CF2. An average increase in the Reynolds

UNIVERSITEIT VAN PRETORIA
UNIVERSITY OF PRETORIA
YUNIBESITHI YA PRETORIA

number of over 20% can be observed when the single microchannel is compared with the three-layered PF and an average increase of over 10% can be observed when it is compared with the three-layered CF1 and CF2. The range of Re_{Dh} for the three-layered microchannel with different flow arrangements is $31 < Re_{Dh} < 182$.

Results in Figure 4.35a show that the third layer has the highest Re_{Dh} for inlet velocities from 0.960 to 1.865 m/s for the three-layered PF, while the second layer has the highest Reynolds number at the lower velocities. This same trend can also be observed for the three-layered CF2, as shown in Figure 4.35c. For the three-layered CF1, the third layer has the highest Reynolds number for inlet velocities of 1.267 to 1.865 m/s, while the second layer has the highest values of Re_{Dh} at the lower inlet velocities. This is shown in Figure 4.35b. These variations in the Reynolds number occur because of the optimal hydraulic diameter of each layer in the three-layered microchannel with the different flow arrangements.

UNIVERSITEIT VAN PRETORIA
UNIVERSITY OF PRETORIA
YUNIBESITHI YA PRETORIA

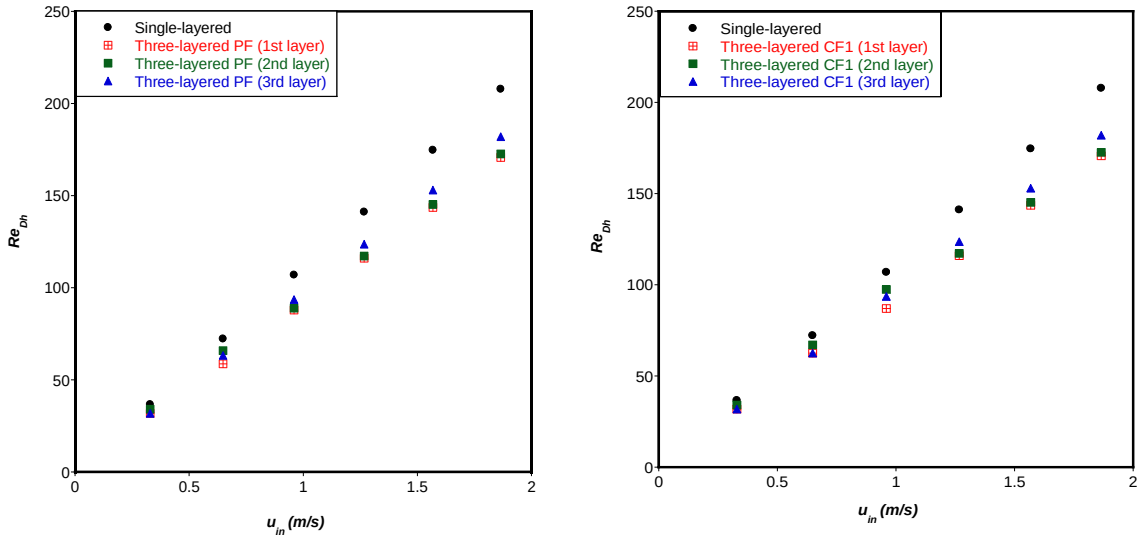

(a) **(b)**

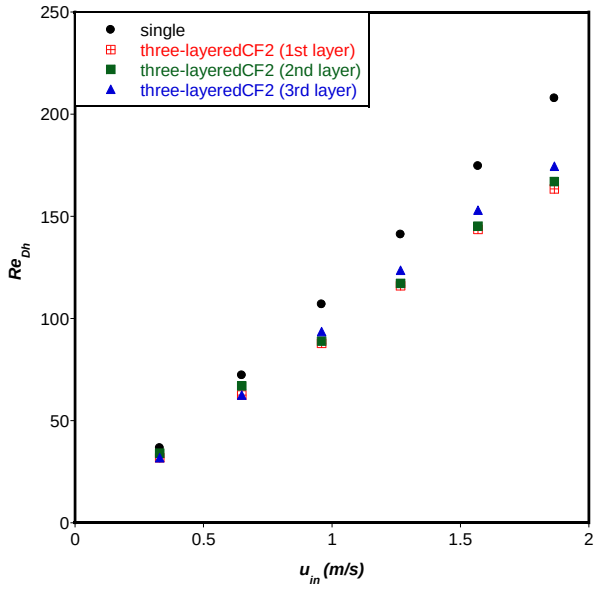

(c)

Figure 4.35: Comparison between the Reynolds number for fluid flow in single and three-layered microchannels (a) parallel flow (b) counterflow1 (c) counterflow2

UNIVERSITEIT VAN PRETORIA
UNIVERSITY OF PRETORIA
YUNIBESITHI YA PRETORIA

Figure 4.36 shows a comparison between the pumping power required for fluid flow through the single and three-layered microchannels with the three different flow arrangements. In Figure 4.35a, it can be observed that the average pumping power required for the single microchannels is 150% more than that required for each layer of the three-layered microchannels PF, CF1 and CF2. It is also shown that for the three-layered PF, CF1 and CF2, the second layer requires up to about 13% more pumping power than that of the first layer and about 15% more than that of the third layer. In Figure 4.36b, the results show that when the total pumping power required for the three-layered microchannel is compared with the requirement for the single microchannel, the three-layered PF, CF1, and CF2 requirements exceed the requirement of the single microchannel by an average of about 12%.

These results show that even though less pumping power is required in the two-layered microchannel, when the layers are increased to three with the same total volume, the total pumping power requirement for the same inlet fluid velocity range increases.

UNIVERSITEIT VAN PRETORIA
UNIVERSITY OF PRETORIA
YUNIBESITHI YA PRETORIA

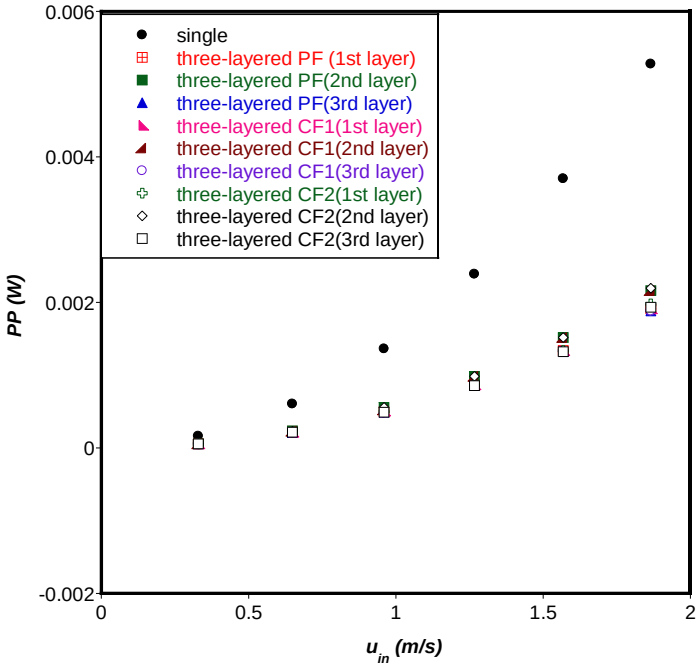

Figure 4.36 (a)

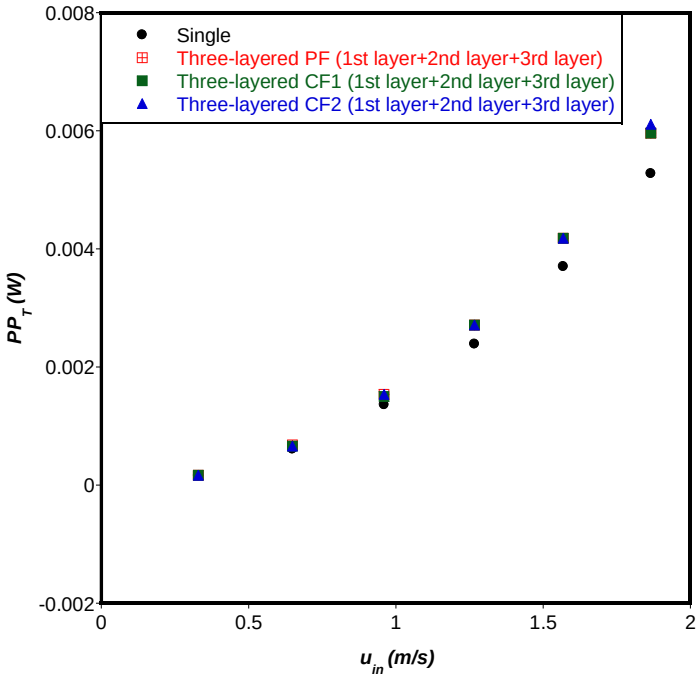

Figure 4.36 (b)

Figure 4.36: Comparison between pumping power requirement for single and three-layered microchannel (a) each layer (b) total number of layers

UNIVERSITEIT VAN PRETORIA
UNIVERSITY OF PRETORIA
YUNIBESITHI YA PRETORIA

Figure 4.37 shows how pressure drop varies with increasing fluid inlet velocity in the single and three-layered microchannels. Figure 4.37a shows the comparison between the single microchannel and each layer of the three-layered PF. From the results, it can be observed that there is increased pressure drop in the different layers of the three-layered PF over that of the single-layered microchannel by an average of 27%. It can also be observed that the first layer has the largest pressure drop in the three-layered PF for inlet velocities of 0.329 and 0.648 m/s, but as the inlet velocity increases, the second layer has the largest pressure drop.

For the three-layered CF1, there is an average increase in pressure drop of about 25% when compared with the single-layered microchannels. For this type of flow orientation, the first layer has the largest pressure drop for all the inlet velocities considered in this study. This is shown graphically in Figure 4.37b. The results of the three-layered CF2 in Figure 4.37c also show an increase in average pressure drop of 28% over the single-layered microchannel. For this flow orientation, the first layer has the largest pressure drop for inlet velocities of 0.329 and 0.648 m/s but as the velocity is increased, the second layer has the largest pressure drop up to the inlet velocity of 1.568 m/s. Thereafter, the first layer again has the largest pressure drop for inlet velocity of 1.865 m/s. From the results, it can be observed that the trend of pressure drop increase depends on the type of configuration. It can also be observed that the pressure drop increases when the number of layers increases to three. This is a result of a further reduction in cross-sectional area of the channel in each layer, resulting in a smaller hydraulic diameter as the number of layers increases to three.

UNIVERSITEIT VAN PRETORIA
UNIVERSITY OF PRETORIA
YUNIBESITHI YA PRETORIA

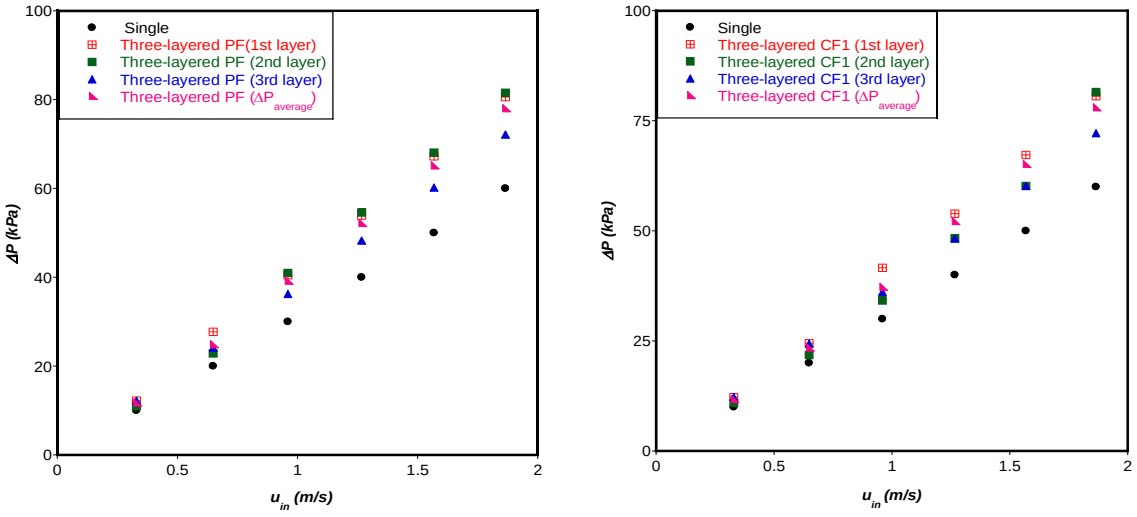

(a) **(b)**

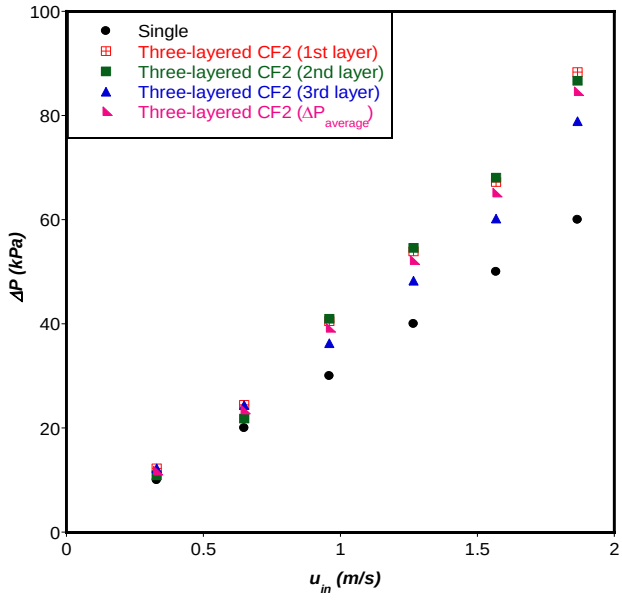

(c)

Figure 4.37: Comparison between the pressure drop in single and three-layered microchannels (a) parallel flow (b) counterflow1 (c) counterflow2

UNIVERSITEIT VAN PRETORIA
UNIVERSITY OF PRETORIA
YUNIBESITHI YA PRETORIA

4.3.4. Case Study 2: Comparison between the thermal performances of single and two-layered microchannel with varying axial length, fixed pressure drop and uniform heat load

In this study, all the lengths of the geometric configuration are free to morph at a fixed volume. Figure 4.38 shows the effect of varying axial length on minimised peak temperature for a two-layered microchannel with fixed solid substrate aspect ratio AR of 4. As the pressure drop ΔP is increased from 10 kPa to 60 kPa, the minimised peak temperature decreases, which is the expected trend. It can also be observed that as the axial length is increased from 1 mm to 10 mm, the minimised peak temperature decreases up to a certain length and thereafter begins to increase. When pressure drop is fixed at 10 kPa, the optimal axial length N_{opt} is discovered to be 3 mm. As ΔP is increased from 20 kPa to 30 kPa, N_{opt} becomes 4 mm and a further increase in pressure drop from 40 kPa to 60 kPa gives a constant value of 5 mm as N_{opt}.

Results presented in Figure 4.39 show how varying AR affects the minimised peak temperature as the axial length is varied. It is observed that there is a decrease in minimised peak temperature as the axial length is increased from 2 mm to 4 mm but as the axial length increases from 5 mm, the minimised peak temperature begins to increase. The optimal axial length and solid substrate ratio is 5 mm and 4 respectively for a fixed pressure drop of 30 kPa.

The results presented in Figures 4.38 and 4.39 show that the optimal axial length in terms of minimised peak temperature depends on the pressure drop. The optimal dimensions of

UNIVERSITEIT VAN PRETORIA
UNIVERSITY OF PRETORIA
YUNIBESITHI YA PRETORIA

the two-layered microchannel and silicon substrate with the corresponding surface heat flux when a heat load of 100 W is applied to the bottom wall are presented in Table 4.8. Results presented in Table 4.8 show that the optimal aspect ratio of the bottom layer of the two-layered microchannel is smaller than that of the top layer for the entire pressure drop investigated. As a result, the optimal channel hydraulic diameter of the bottom layer is greater than that of the top layer. The optimal dimensions show that the highest heat flux 121.72 W/cm^2 is obtained for axial length of 3 mm and pressure drop of 10 kPa, while the lowest is found to be 94.28 W/cm^2 when axial length is 5 mm and pressure drop is 40 kPa to 60 kPa.

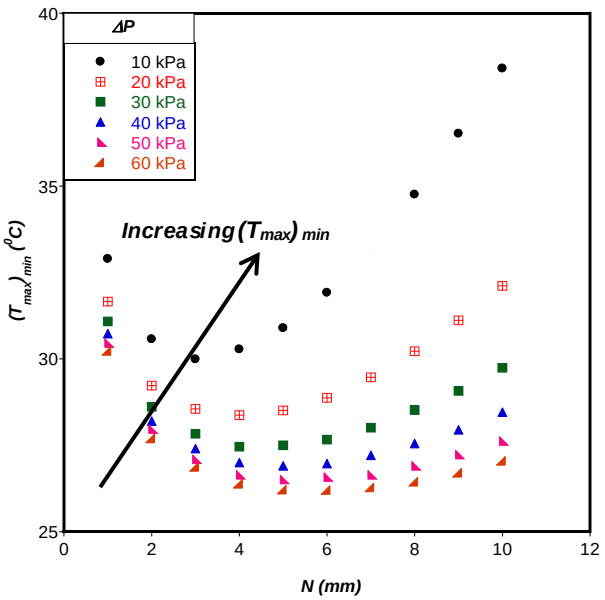

Figure 4.38: Effect of varying axial length on minimised peak temperature for AR = 4

UNIVERSITEIT VAN PRETORIA
UNIVERSITY OF PRETORIA
YUNIBESITHI YA PRETORIA

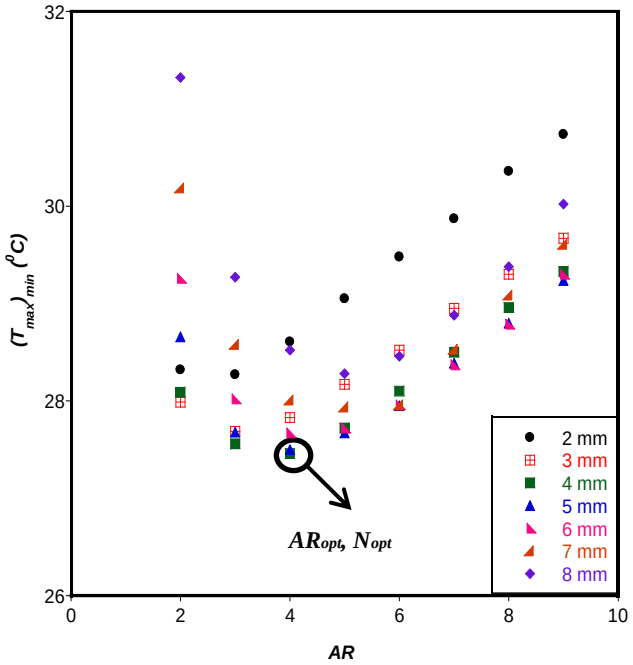

Figure 4.39: Effect of varying solid substrate aspect ratio on minimised peak temperature for ΔP = 30 kPa

Table 4.8: Optimal solid substrate and two-layered microchannel dimensions

ΔP (kPa)	AR_{opt}	N_{opt} (mm)	AR_{c1}	AR_{c2}	D_{h1} (mm)	D_{h2} (mm)	q'' (W/cm^2)
10	4	3	5.91	6.39	0.136	0.127	121.72
20	4	4	4.97	5.53	0.133	0.121	105.41
30	4	4	4.97	5.53	0.133	0.121	105.41
40	4	5	4.34	4.83	0.130	0.119	94.28
50	4	5	4.34	4.83	0.130	0.119	94.28
60	4	5	4.34	4.83	0.130	0.119	94.28

UNIVERSITEIT VAN PRETORIA
UNIVERSITY OF PRETORIA
YUNIBESITHI YA PRETORIA

The optimal *AR*, *ARc* and D_h for each axial length for a fixed pressure drop of 30kPa are shown in Figure 4.40. As axial length increases from 1 mm to 9 mm, *AR* also increases from 2 to 5. The hydraulic diameter (D_h) is defined as $\frac{2H_c}{(AR_c+1)}$, which shows why the D_h of each channel is inversely proportional to AR_c, as shown in Figure 4.40.

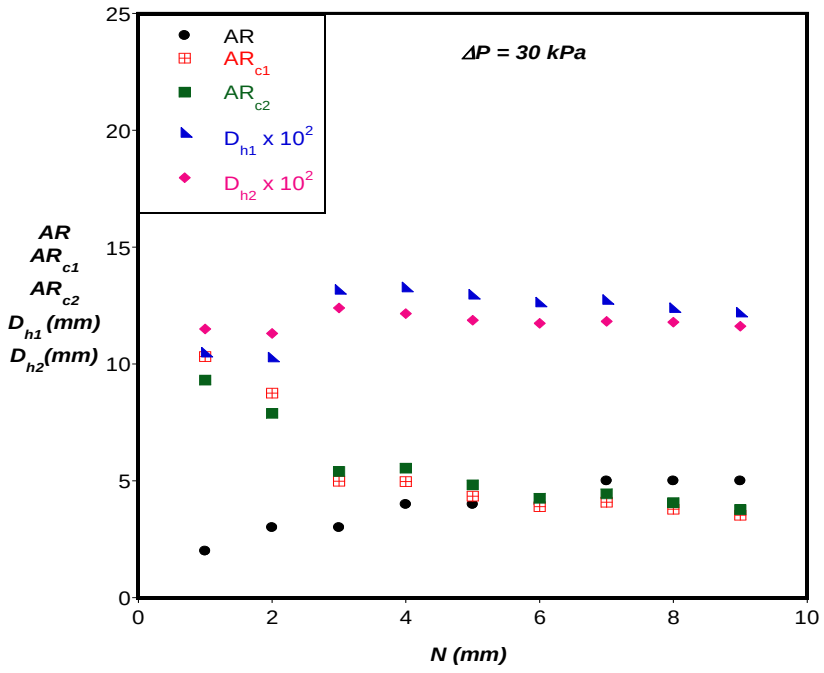

Figure 4.40: Optimal microchannel and solid substrate dimensions for two-layered microchannels with varying axial length

Figure 4.41 shows results of Reynolds number (Re_{Dh}) and volume flow rates for the optimal configuration of each axial length. The volumetric flow rate (Ω) is defined as a product of the cross-sectional area of the optimised channel and the velocity of the fluid,

UNIVERSITEIT VAN PRETORIA
UNIVERSITY OF PRETORIA
YUNIBESITHI YA PRETORIA

while $\mathrm{Re}_{Dh} = \dfrac{\Omega D_h}{\nu A_c}$. The range of Reynolds number and volumetric flow rate at fixed pressure drop of 30 kPa, as shown in Figure 5, at fixed pressure drop of 30 kPa, is $20 < \mathrm{Re}_{Dh} < 120$ and $3.0 \times 10^{-8} < \Omega < 14.9 \times 10^{-8}$ (m^3/s) respectively.

Figure 4.41a shows that for the optimised geometry, the Re_{Dh} of the top layer is greater than that of the bottom layer for all the axial lengths. Also, as the axial length is increased, the Reynolds number and the minimised temperature decrease, but further increase beyond 4 mm leads to an increase in the minimised peak temperature. These results show that there exists an optimum value of Re_{Dh} at which heat transfer from the heated base is most effective. In this study, the optimum Re_{Dh} value is 50 for the bottom layer and 68 for the top layer.

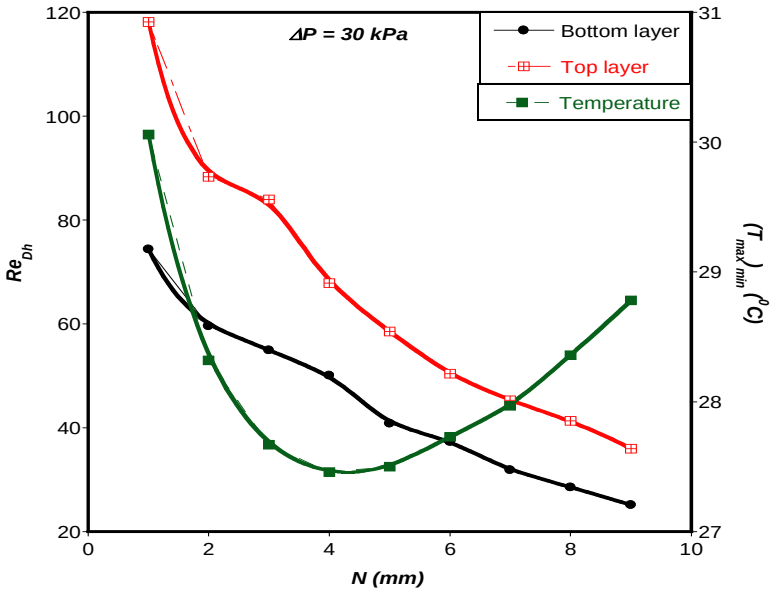

Figure 4.41a

UNIVERSITEIT VAN PRETORIA
UNIVERSITY OF PRETORIA
YUNIBESITHI YA PRETORIA

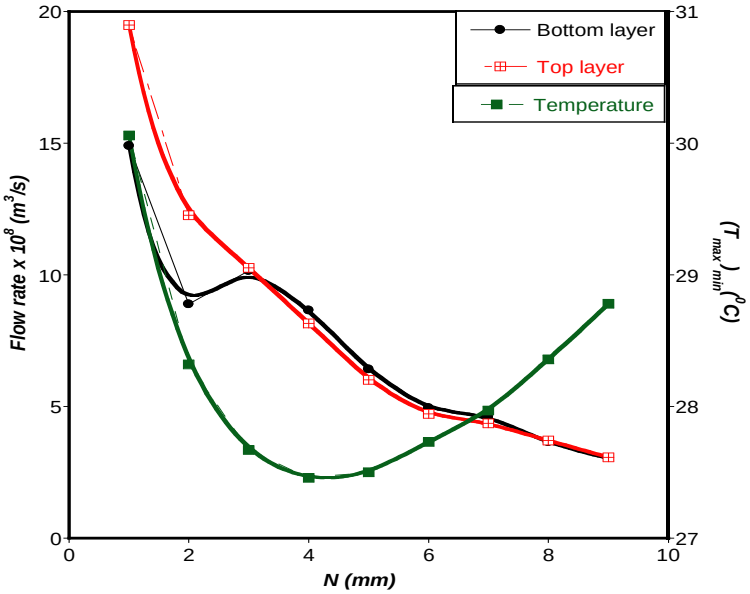

Figure 4.41b

Figure 4.41: Effect of optimal configuration on (a) Reynolds number and (b) flow rates for ΔP = 30 kPa

Figure 4.41b shows the results of volumetric flow rate in the top and bottom layers of the microchannel for each axial length. The volumetric flow rates of the fluid in the top layer of the microchannel are greater than those of the bottom layer for axial lengths of 1 mm to 3 mm. When the axial length is further increased, the volumetric flow rates of the fluid in the bottom layer become greater than those of the top layer by an average of about 4%. Figure 4.42 shows the comparison of the minimised peak temperature with surface heat for the optimised configurations and fixed pressure drop of 30 kPa as axial length is increased. From the results, as *N* increases, q″ decreases. A decrease in the surface heat flux seems to allow an increase in viscous forces, which results in the reduced Reynolds number observed in Figure 4.41a.

UNIVERSITEIT VAN PRETORIA
UNIVERSITY OF PRETORIA
YUNIBESITHI YA PRETORIA

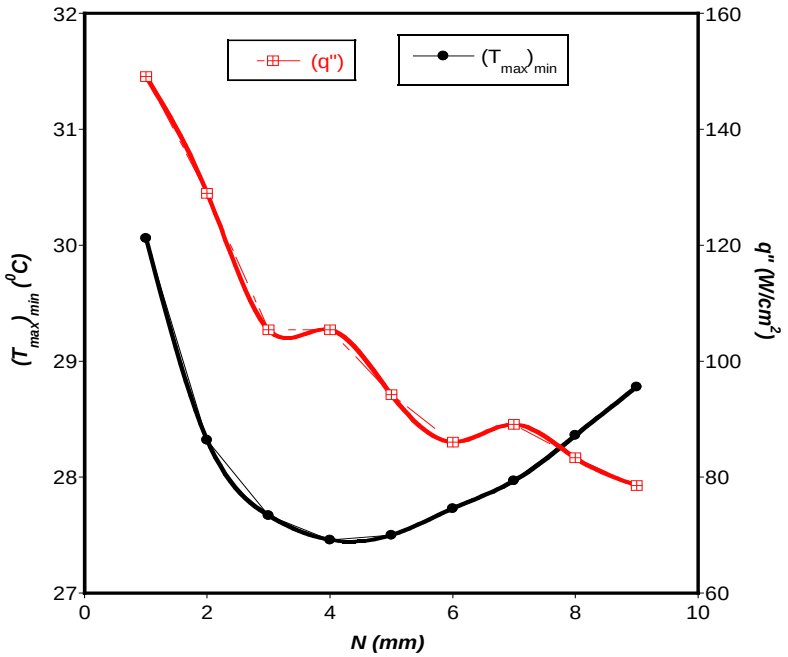

Figure 4.42: Comparison between minimised peak temperature and surface heat flux for each axial length at fixed pressure drop

The thermal performances of the single and two-layered microchannel with the different configuration are compared and results obtained are shown graphically. The minimised thermal resistance $(R_{th})_{min}$ decreases as the pressure drop is increased, which is the expected trend. It can be observed that there is an average reduction of 4.8% in minimised thermal resistance for the two-layered CF when compared with the two-layered PF and 0.7% when compared with the single microchannel, as shown in Figure 4.43. For a pressure drop of 10 kPa, the minimised thermal resistance for the two-layered CF is 0.0966˚C/W, which is the lowest. There is no significant difference between the minimised thermal resistances of the single and two-layered CF microchannels.

Pumping power required for the single- and different configurations of the two-layered microchannels is also investigated and results obtained are shown in Figures 4.44 and

UNIVERSITEIT VAN PRETORIA
UNIVERSITY OF PRETORIA
YUNIBESITHI YA PRETORIA

4.45. For the two-layered microchannel, the average pumping power requirement of the first layer exceeds that of the second layer by about 5%. This is the case for both the two-layered PF and two-layered CF, as shown in Figure 4.44. This trend could be the result of greater cooling effect required in the bottom layer because it is in direct contact with the heated surface. The difference between the total pumping powers required for the different configurations is about 0.2%, which is not significant.

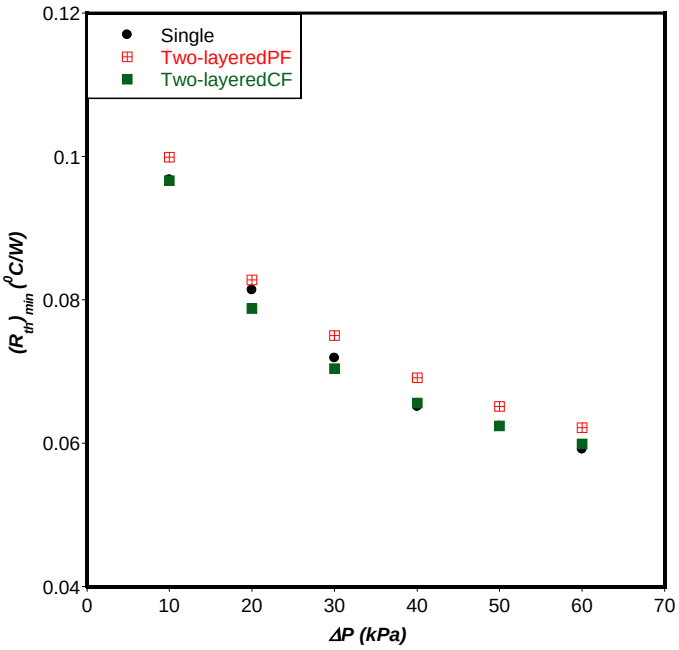

Figure 4.43: Comparison between minimised peak temperature for single and two-layered microchannels with different flow configurations

UNIVERSITEIT VAN PRETORIA
UNIVERSITY OF PRETORIA
YUNIBESITHI YA PRETORIA

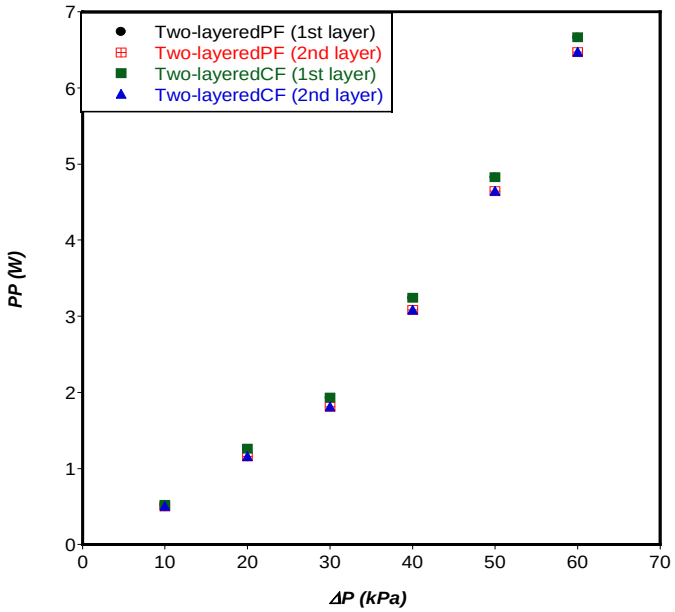

Figure 4.44: Pumping power requirement at different pressure drops for each layer of the two-layered microchannel

Figure 4.45 presents results of total pumping power requirement for the single and two-layered microchannels. The two-layered PF and two-layered CF have an average increase of 5.1% and 5.3% in total pumping power when compared with the single microchannel. These results show that for a shorter axial length with fixed total volume, the single microchannel has the best thermal performance when minimised thermal resistance and pumping power are considered.

UNIVERSITEIT VAN PRETORIA
UNIVERSITY OF PRETORIA
YUNIBESITHI YA PRETORIA

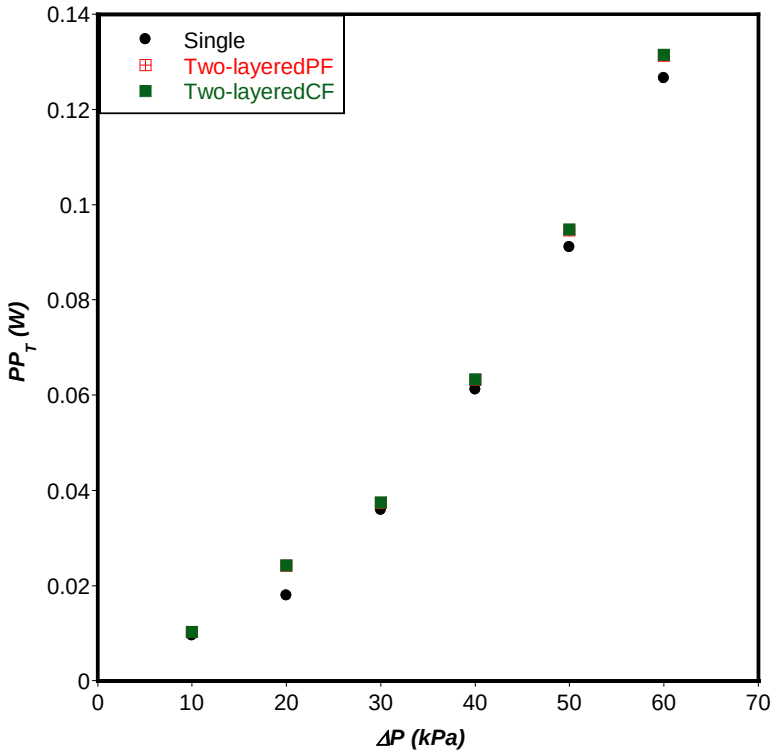

Figure 4.45: Comparison between total pumping power of the different microchannels

4.3.5. Effect of increasing heat load on the thermal performance of single and two-layered microchannels with varying axial length

In this section, the heat load Q on the heated wall of the solid substrate with varying axial length is increased from 100 W to 1 000 W at a fixed pressure drop of 10 kPa and the thermal performance of the single and two-layered microchannels with different flow arrangements are compared to investigate which has the best thermal performance. The

UNIVERSITEIT VAN PRETORIA
UNIVERSITY OF PRETORIA
YUNIBESITHI YA PRETORIA

optimal dimensions obtained for pressure drop of 10 kPa obtained in section 4.2.4 and 4.3.4 was used in this section. These dimensions are shown in the Table 4.9.

Table 4.9: Optimal channel dimensions for uniform heat load of 100 W and pressure drop of 10 kPa

	Single-microchannel	**Two-layered microchannel**	
N (mm)	AR_c	AR_{c1}	AR_{c2}
2	15.67	6.76	7.38
4	10.73	5.01	5.45
6	8.13	4.48	4.88
8	7.90	4.34	4.44
10	7.41	2.84	3.03

Figure 4.46 shows the results of minimised peak temperature for the single microchannel as the heat load on the bottom wall of the solid substrate is increased. As the axial length N increases from 1 mm to 10 mm, the minimised peak temperature decreases but after N exceeds 4 mm, it begins to increase again. It can also be observed that the heat sink has the best thermal performance when axial length N is 3 mm and at lower Q values of 100 and 250 W. When Q is increased from 500 W to 1000 W, the best thermal performance is obtained at axial length N of 4 mm. For heat load Q of 1000 W and N of 4 mm, the minimised peak temperature obtained is 104.8 ˚C. The single microchannel with axial length N of 10 mm has the worst thermal performance for the different heat loads considered.

UNIVERSITEIT VAN PRETORIA
UNIVERSITY OF PRETORIA
YUNIBESITHI YA PRETORIA

Results of the effect of increasing heat load on the minimised peak temperature of the two-layered microchannel with parallel-flow and counterflow configurations are presented in Figure 4.47. For the two-layered PF, as the axial length N is increased from 1 mm to 10 mm, the minimised peak temperature decreases but begins to increase when N exceeds 4 mm. The two-layered PF heat sink has the best thermal performance when axial length N is 3 mm and at Q values of 100 W, 250 W and 500 W but when Q values are 750 W and 1 000 W, the best thermal performance is obtained at axial length N of 4 mm, as shown in Figure 4.47a. For heat load Q of 1 000 W and N of 4 mm, the minimised peak temperature obtained is 107.83 ˚C. The two-layered PF microchannel with axial length N of 10 mm also has the worst thermal performance for the different heat loads considered. Figure 4.47b shows results of the minimised peak temperature for the two-layered CF. The best thermal performance for this heat sink is obtained when axial length is 4 mm for the different Q considered. The worst thermal performance is at N = 10 mm, which is also the trend observed for the single and two-layered PF microchannels. The minimised peak temperature for N = 4 mm and Q = 1000 W is 102.84 ˚C.

UNIVERSITEIT VAN PRETORIA
UNIVERSITY OF PRETORIA
YUNIBESITHI YA PRETORIA

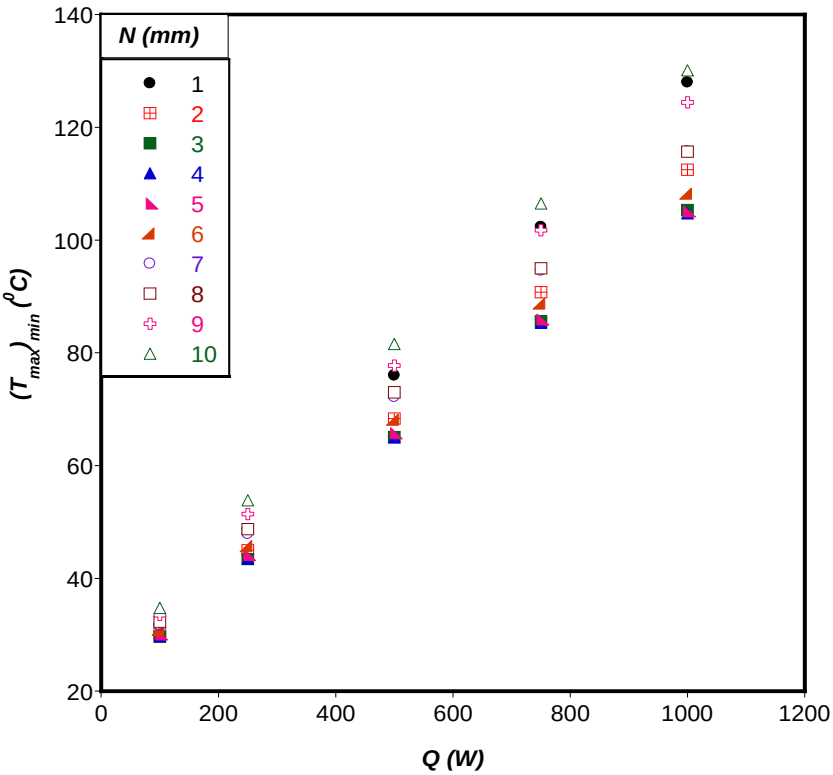

Figure 4.46: Effect of increasing heat load on the thermal performance of single-layered microchannel

UNIVERSITEIT VAN PRETORIA
UNIVERSITY OF PRETORIA
YUNIBESITHI YA PRETORIA

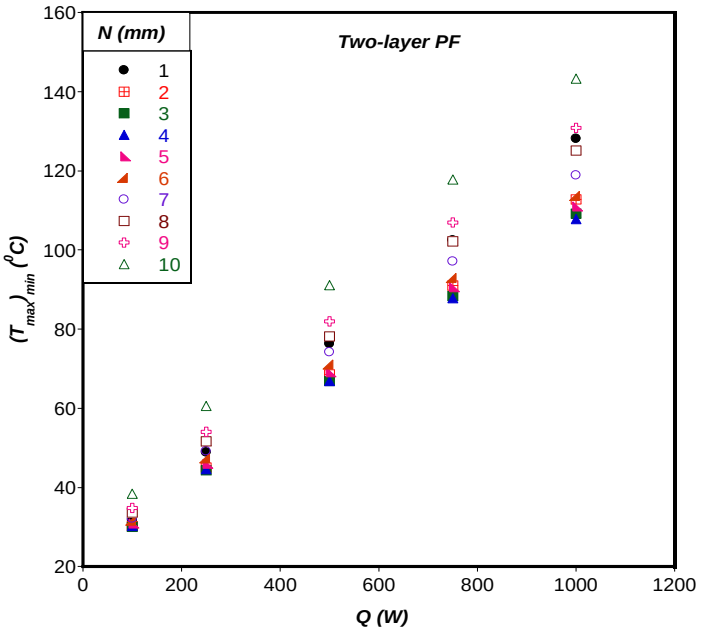

(a)

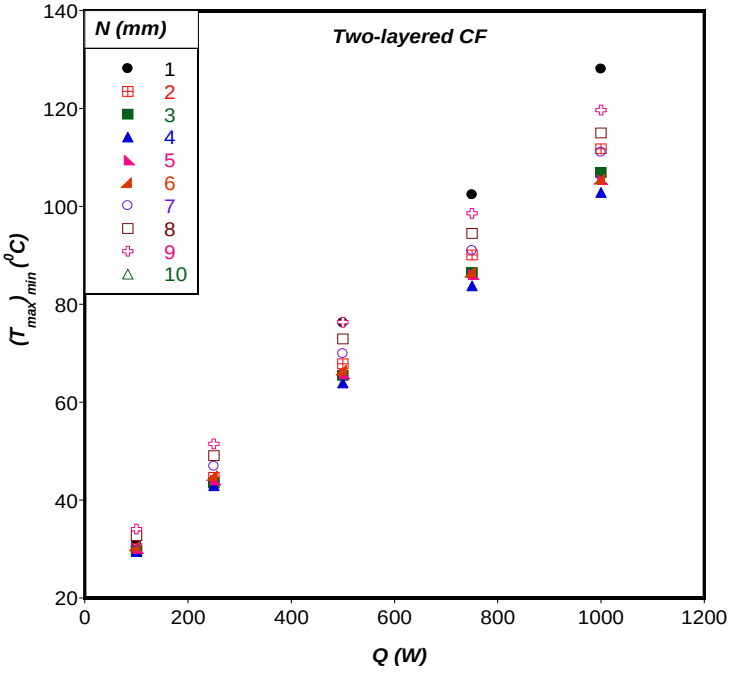

(b)

Figure 4.47: Effect of increasing heat load on the thermal performance of two-layered microchannel (a) two-layered PF (b) two-layered CF

UNIVERSITEIT VAN PRETORIA
UNIVERSITY OF PRETORIA
YUNIBESITHI YA PRETORIA

In Figure 4.48, a comparison between the minimised peak temperature obtained for the single and two-layered microchannel with different flow arrangements, fixed total volume of 0.9 mm^3 and varying axial length when Q is 1 000 W is presented graphically. The two-layered microchannel with counterflow of fluid has the best thermal performance in minimising peak temperature with AR_{c1} of 5.01 and AR_{c2} of 5.45. A reduction of about 2% in minimised peak temperature is obtained when the two-layered CF is compared with the single microchannel, while a reduction of 5% is obtained when compared with the two-layered PF with optimal axial length N_{opt} of 4 mm.

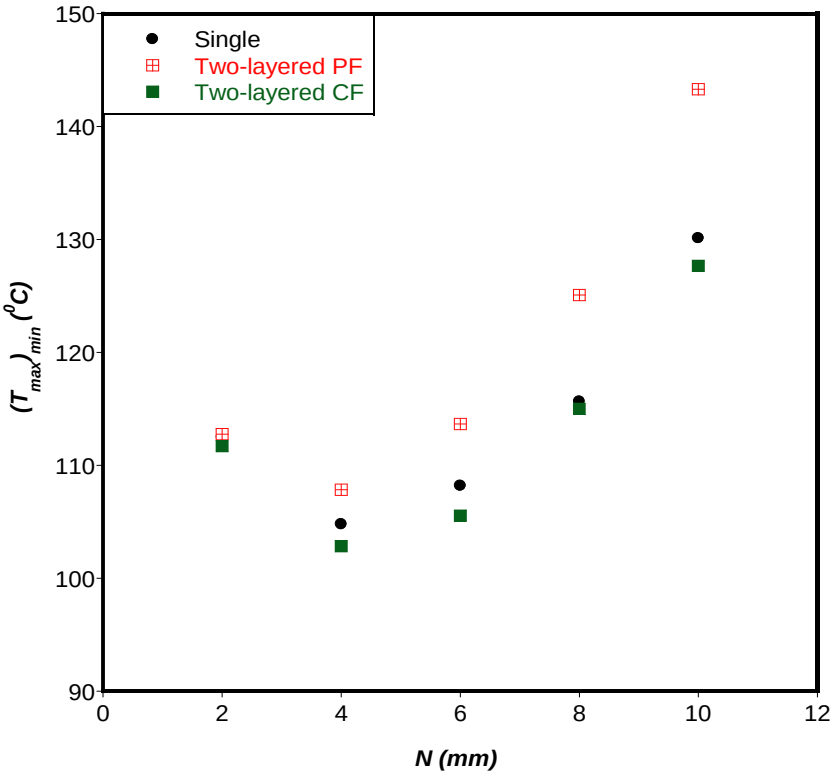

Figure 4.48: Comparison between the minimised peak temperature in single and two-layered microchannels when Q = 1 000 W

UNIVERSITEIT VAN PRETORIA
UNIVERSITY OF PRETORIA
YUNIBESITHI YA PRETORIA

4.4. CONCLUSION

In this chapter, the three-dimensional numerical investigations carried out to optimise the geometric parameters of single, two- and three-layered microchannel heat sinks with different flow arrangements using the constructal law technique for a fixed total volume were presented. Results from the stacked design were compared with those obtained for single microchannels for both fixed and varying axial lengths.

Results of the thermal performance of the single microchannel with varying axial length and uniform surface heat flux showed that at reduced axial length of 6 mm, there was over 100% improvement in the maximised thermal conductance of the heat sink.

The condition of uniform heat load and varying solid substrate aspect ratio was also considered for varying axial length. It was observed that as the axial length N increased from 1 mm to 10 mm, the surface heat flux on the heated base decreased. Also, as the solid substrate aspect ratio AR was increased from 1 to 9, the surface heat flux increased for all the axial lengths considered. The global optima for AR was discovered to be 3 for a pressure drop range of 10 kPa to 60 kPa, while the optimal axial length was 3 mm when pressure drop was fixed at 10 kPa and 5 mm for pressure drop of 20 kPa to 60 kPa.

When the thermal performance of a single microchannel was compared with that of the multi-layered microchannel with different flow arrangements for fixed axial length N of 10 mm, fixed fluid inlet velocity and uniform surface heat flux on the heated base, the

UNIVERSITEIT VAN PRETORIA
UNIVERSITY OF PRETORIA
YUNIBESITHI YA PRETORIA

multi-layered microchannel performed better than the single microchannel in maximising thermal conductance for inlet velocities greater than 0.648 m/s. Results of pumping power requirements and pressure drop presented showed that the two-layered microchannel had lowest total pumping power requirement and lowest pressure drop.

The thermal performance of the single microchannel was also compared with that of the two-layered microchannel with parallel-flow and counterflow arrangement for varying axial length, varying solid substrate aspect ratio, fixed pressure drop and uniform heat load. Results obtained showed that even though the two-layered microchannel with counterflow arrangement had the best performance in minimising thermal resistance, there was over 5% increase in pumping power when compared with the single microchannel.

For the two-layered microchannel with varying axial length and uniform heat load on the heated surface, the optimal solid substrate aspect ratio was discovered to be 4 for the range of pressure drop considered but the optimal axial length N_{opt} depended on pressure drop. At fixed pressure drop of 10 kPa, N_{opt} was 3 mm. When pressure drop was increased, N_{opt} also increased.

When the heat load on the bottom wall of the solid substrate of fixed total volume and varying axial length was increased from 100 W to 1 000 W, it was discovered that the two-layered microchannel with counterflow of fluid and axial length of 4 mm performed best in minimising peak temperature for the range of heat load investigated.

UNIVERSITEIT VAN PRETORIA
UNIVERSITY OF PRETORIA
YUNIBESITHI YA PRETORIA

UNIVERSITEIT VAN PRETORIA
UNIVERSITY OF PRETORIA
YUNIBESITHI YA PRETORIA

CHAPTER 5: COMBINED MICROCHANNEL AND MICRO PIN-FIN HEAT SINK

5.1. INTRODUCTION

This chapter presents a new design of heat sink, which combines a microchannel with rows of micro pin fins. The thermal performance of this combined heat sink design will be compared with that of the microchannel heat sink without the pin-fin inserts. This performance will be based on minimised peak temperature and maximised thermal conductance.

5.2. COMBINED SINGLE MICROCHANNEL AND MICRO PIN FINS

Circular-shaped micro pin fins are inserted into the optimised single microchannel heat sink dimensions obtained in the previous chapter. The geometric optimisation of the combined microchannel and micro pin fin is carried out using ANSYS 14.0 [145], computational fluid dynamics (CFD) code with a goal-driven optimisation tool, subject to global constraints.

UNIVERSITEIT VAN PRETORIA
UNIVERSITY OF PRETORIA
YUNIBESITHI YA PRETORIA

5.2.1. Physical model and design variables

Figure 5.1 shows the elemental volume of the microchannel heat sink inserted with micro pin fins used as the computational domain in this study. The length *N*, height *M* and width *W* of the solid are fixed, which makes the volume *V* fixed while t_1, t_2, t_3, H_c and W_c are varied but also subject to manufacturing constraints. The combined heat sink has seven degrees of freedom. The solid volume and the manufacturing constraints are as stated in Equations 4.3 to 4.7. The micro pin fins inserted into the optimised microchannel are also subject to the manufacturing constraints in Equations (5.1) and (5.2):

$$0.5 \leq \frac{H_f}{D_f} \leq 4.0 \tag{5.1}$$

$$s \geq 50\mu m \tag{5.2}$$

A total fin volume constraint is applied to the micro pin fins where the volume of the cylindrical fins is constant, as shown in Equation (5.3):

$$V_f = V_{f1} + V_{f2} + ... + V_{fn} = constant \tag{5.3}$$

Where the ratio of the total fin volume V_f to the volume of the solid substrate *V* is 2.6 x 10^{-4}.

UNIVERSITEIT VAN PRETORIA
UNIVERSITY OF PRETORIA
YUNIBESITHI YA PRETORIA

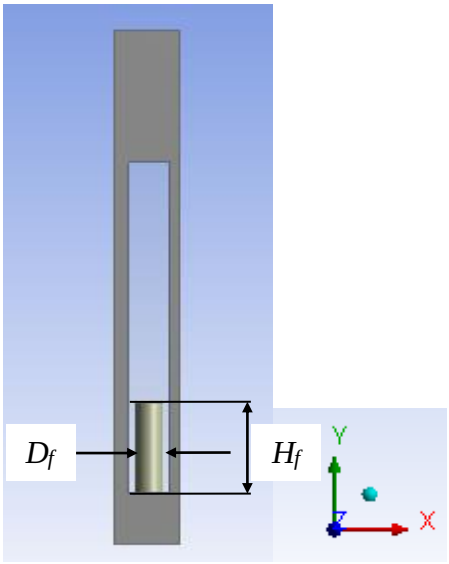

(a) Two-dimensional cross-section

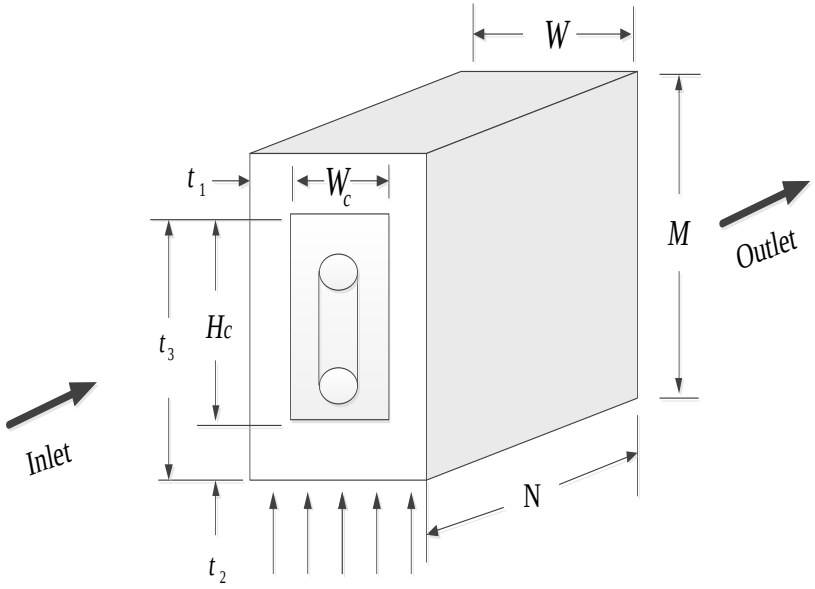

(b) Three-dimensional computational domain

Figure 5.1: Combined single microchannel and micro pin fin

UNIVERSITEIT VAN PRETORIA
UNIVERSITY OF PRETORIA
YUNIBESITHI YA PRETORIA

For the micro pin fins, the design space for the response surface (while taking into consideration the manufacturing constraints) is defined as $30 \leq H_f \leq 160$ µm and $40 \leq D_f \leq 60$ µm. The fin spacing *s* is fixed at 62.5µm with the micro pin fins modelled as arranged at the centre of the microchannel for both fixed and reduced axial lengths. For the variable axial length, the range of length used is $6 \leq N \leq 10$mm, while the design space for the micro pin fins is defined as $70 \leq D_f \leq 95$µm for the pin-fin diameter and $41 \leq H_f \leq 280$µm for the pin-fin height. The thermophysical properties of water flowing through the combined heat sink are assumed to be constant.

5.2.1.1. Grid refinement tests

A grid refinement test is also carried out for the single microchannel with circular-shaped micro pin fins for $Be = 1.9\text{x}10^8$. The convergence criterion is stated in Equation (4.1). The geometric dimensions of the combined design used for the grid refinement test are shown in Table 5.1, while the results are shown in Table 5.2.

Table 5.1: Dimensions of the microchannel and circular-shaped micro pin-fin heat sink for grid refinement test

H_c (mm)	W_c(mm)	t_1 (mm)	H-t_3 (mm)	H_{f1} to H_{f6} (mm)	D_{f1} to D_{f6} (mm)
0.48	0.06	0.02	0.21	0.16	0.04

UNIVERSITEIT VAN PRETORIA
UNIVERSITY OF PRETORIA
YUNIBESITHI YA PRETORIA

Table 5.2: Grid refinement test results

Number of cells	$\Delta T(K)$	$\left\|\frac{(\Delta T)_i - (\Delta T)_{i-1}}{(\Delta T)_i}\right\|$
270 180	14.8490	-
341 594	15.1358	0.0189
432 154	15.5244	0.0250
582 686	15.6441	0.0077

5.2.2. Case Study 1: Optimisation results for fixed axial length and uniform heat flux

Figure 5.2 shows results for the microchannel and combined design with a fixed axial length of 10 mm for a total volume V of 0.9 mm^3. It can be observed that the peak temperature in the optimised microchannel is further minimised when three, four, five and six rows of micro pin fins are inserted into the optimised single microchannel. The integrated design (ID) with three rows of micro pin-fin inserts gives the best result in minimising the peak temperature for all the ranges of Be used in the study, which results in a 4% increase in the maximised thermal conductance for the lowest Bejan number. Figure 5.3 shows a comparison between the maximum global thermal conductance for the optimised microchannel and the integrated design carried out in the study for a total volume V of 0.9 mm^3. It can be observed that there is an increase

UNIVERSITEIT VAN PRETORIA
UNIVERSITY OF PRETORIA
YUNIBESITHI YA PRETORIA

in C_{max} when the micro pin fins are inserted into the microchannel, but when the number of rows of pin fin becomes greater than three, the effect of inserting pin fins into the microchannel becomes insignificant.

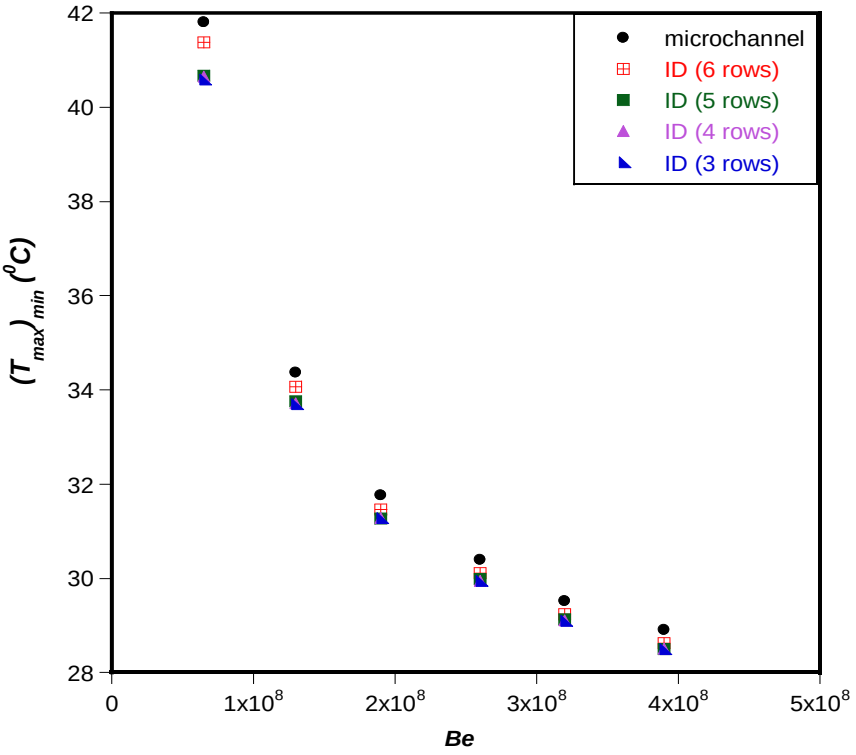

Figure 5.2: Minimised peak temperature for microchannel and the integrated design at fixed total volume *V* of 0.9 mm^3

The optimal micro pin-fin aspect ratio $\left(\frac{H_f}{D_f}\right)_{opt}$ for six rows of micro pin-fin inserts for a solid volume V of 0.9mm^3 is 0.751. When the volume constraint is applied with fixed fin heights, the optimal micro pin-fin aspect ratio for three, four and five rows of micro pin-fin inserts has a constant value of 0.531, 0.614 and 0.686 respectively for

UNIVERSITEIT VAN PRETORIA
UNIVERSITY OF PRETORIA
YUNIBESITHI YA PRETORIA

the whole range of Bejan numbers used in the study. The pin-fin aspect ratio for two rows of micro pin fins is 0.434, which does not meet the manufacturing constraint in Equation 5.1. Therefore, numerical simulations for this are not reported.

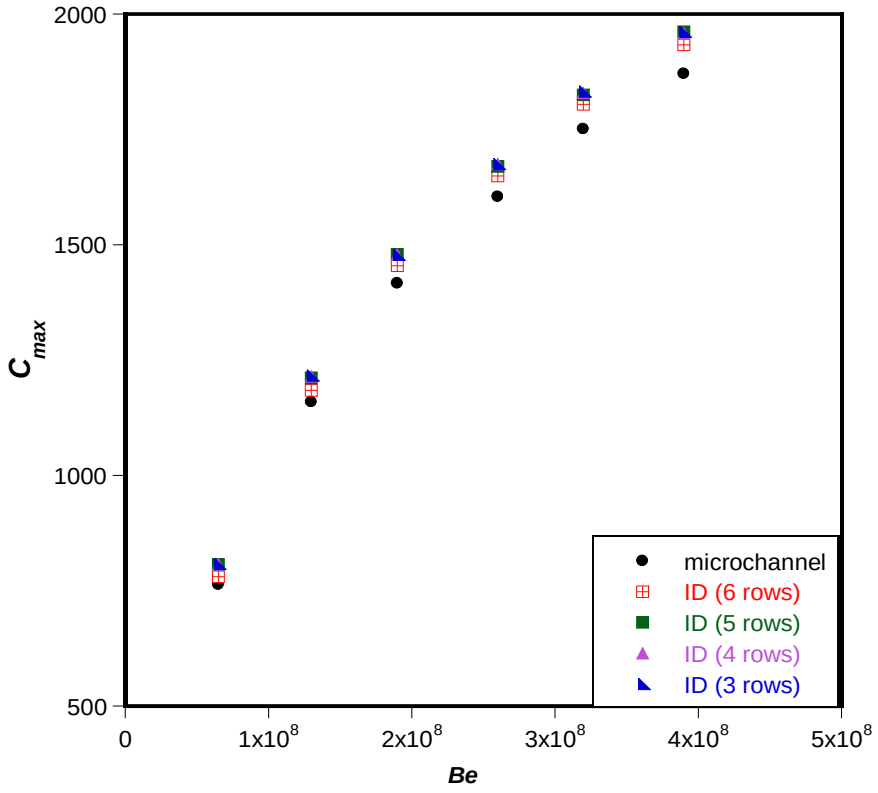

Figure 5.3: Maximised thermal conductance for microchannel and the integrated design at fixed total volume V of 0.9 mm^3

5.2.3. Case Study 2: Optimisation results for reduced axial length and uniform surface heat flux

UNIVERSITEIT VAN PRETORIA
UNIVERSITY OF PRETORIA
YUNIBESITHI YA PRETORIA

Figures 5.4 and 5.5 show the results for the integrated design with four to seven rows of micro pin-fin inserts for minimised peak temperature and maximised thermal conductance for V of 0.9 mm^{3}and N of 6 mm. From these results, it can be observed that six rows of micro pin-fin inserts give the best results with an optimal pin-fin aspect ratio $\left(\frac{H_f}{D_f}\right)_{opt}$ of 0.68, which results in about 5% increase in the maximised thermal conductance for the lowest Bejan number. When the volume constraint is applied, the optimal micro pin-fin aspect ratio for four, five and seven rows of micro pin fins has a constant value of 0.555, 0.621 and 0.735 respectively for the whole range of Bejan numbers used in the study. The pin-fin aspect ratio for the integrated design with three rows is 0.480, which does not meet the manufacturing constraint as stated in Equation 5.1. As a result, numerical simulation results for this are not reported for the reduced axial length.

UNIVERSITEIT VAN PRETORIA
UNIVERSITY OF PRETORIA
YUNIBESITHI YA PRETORIA

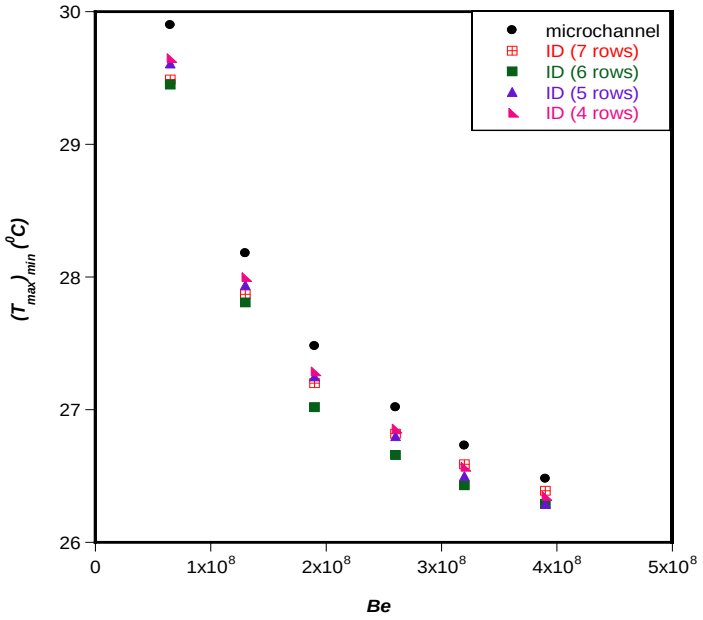

Figure 5.4: Minimised peak temperatures for microchannel and integrated design at fixed total volume V of 0.9mm^3 when length is reduced

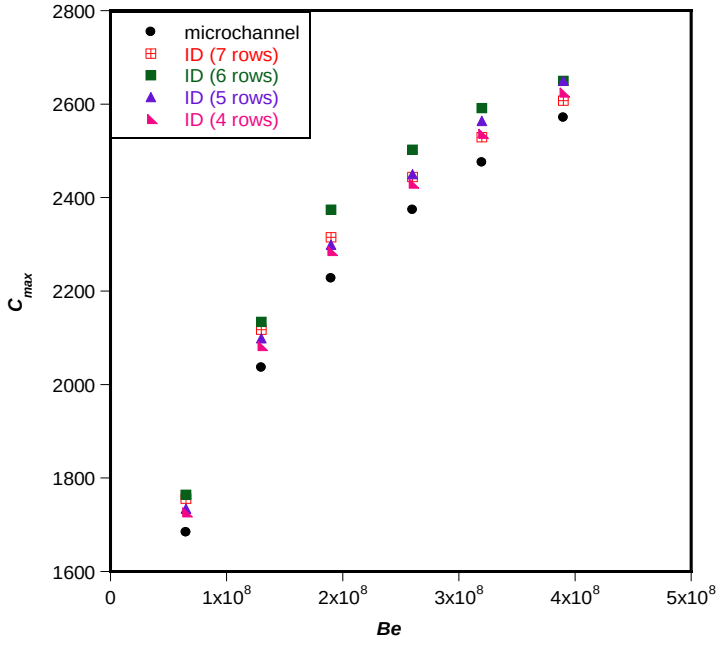

Figure 5.5: Maximised thermal conductance for microchannel and integrated design at fixed total volume V of 0.9mm^3 when length is reduced

UNIVERSITEIT VAN PRETORIA
UNIVERSITY OF PRETORIA
YUNIBESITHI YA PRETORIA

5.2.4. Case Study 3: Optimisation results for varying axial length and constant heat load

Three to seven rows of circular-shaped micro pin fins are inserted into the optimised single microchannel in Section 4.2.4 to investigate whether the thermal performance of the heat sink will be further improved. The thermophysical properties of water flowing through the combined heat sink are assumed to be temperature dependent modelled using Equation 4.11 and the constant heat load applied to the bottom of the solid substrate is 100 W defined by Equation 4.10. The results of minimised peak temperature for fixed total volume V of 0.9 mm^3 are reported. The aspect ratios $\left(\frac{H_f}{D_f}\right)$ of the circular-shaped micro pin fins which meet the manufacturing constraints are 0.53, 0.61, 0.69, 0.75 and 0.81 for three to seven rows of micro pin fins respectively. Results show that combining the single microchannel with circular-shaped micro pin fins reduces the minimised peak temperature further by 2 to 3% for pressure drops of between 10 to 60kPa, as shown in Figure 5.6a. In Figure 5.6b, it can be observed that this reduction in minimised peak temperature gives a corresponding increase in the maximised thermal conductance of about 8 to 10%. The optimal number of rows of micro pin fins for the combined microchannel heat sink with circular-shaped pin-fin inserts that minimises the peak temperature is six, as shown in Figure 5.6.

UNIVERSITEIT VAN PRETORIA
UNIVERSITY OF PRETORIA
YUNIBESITHI YA PRETORIA

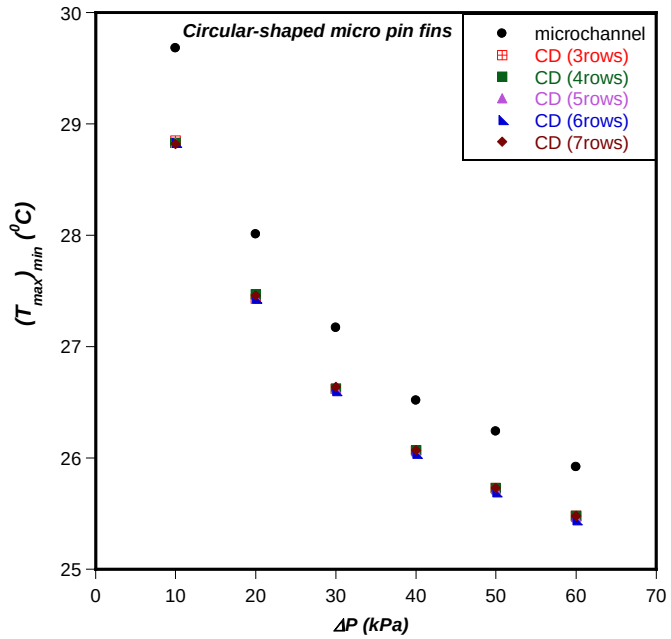

(a)

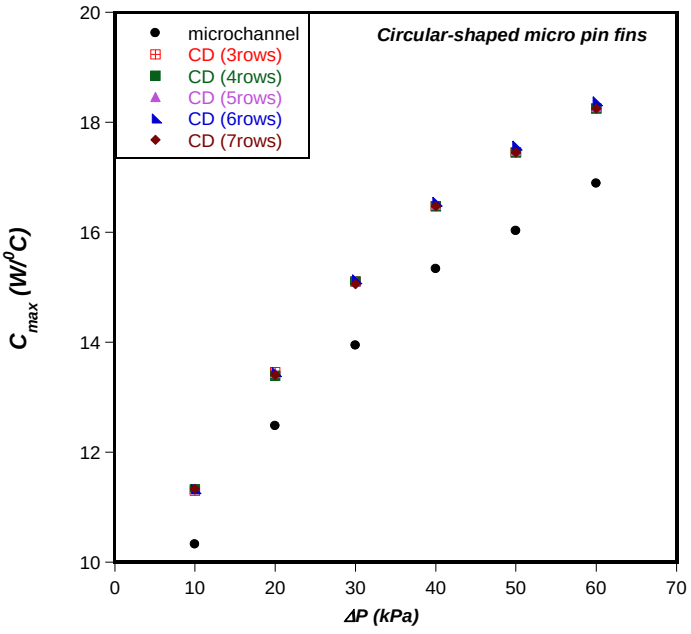

(b)

Figure 5.6: Comparison between the thermal performance of the single-layered microchannel and combined heat sink at different pressure drops (a) minimised peak temperature (b) maximised thermal conductance

UNIVERSITEIT VAN PRETORIA
UNIVERSITY OF PRETORIA
YUNIBESITHI YA PRETORIA

Figure 5.7 shows the results of maximised thermal conductance for the combined microchannel and three to seven rows of micro pin fins when pressure drop is 60 kPa. The combined heat sink with six rows of micro pin fins has the best thermal performance.

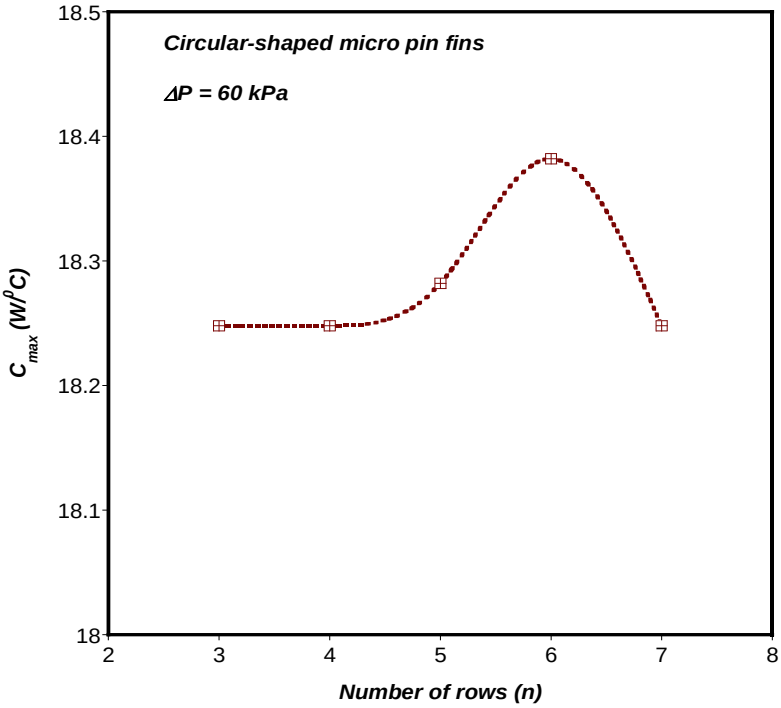

Figure 5.7: Effect of number of rows of circular-shaped micro pin fins on maximised thermal conductance of combined heat sink

UNIVERSITEIT VAN PRETORIA
UNIVERSITY OF PRETORIA
YUNIBESITHI YA PRETORIA

5.3. COMBINED TWO-LAYERED MICROCHANNEL AND MICRO PIN FINS

The previous section showed that combining single microchannel and micro pin fins improved the thermal conductance of the heat sink. As a result of this observation, this section focuses on the thermal performance of a two-layer microchannel with micro pin-fin inserts and its comparison with the results obtained for that of the combined design for single microchannel. The microchannel has a fixed total volume, while the total volume of the cylindrical micro pin fins is also fixed. The cooling fluid is water assumed to be incompressible with homogeneous and constant thermophysical properties. The objective is the maximisation of the thermal conductance, which is achieved by minimising the peak temperature of the solid substrate.

5.3.1. Physical model and design variables

Figure 5.8 shows the elemental fixed volume V used as the computational domain for the two-layered microchannel with the micro pin-fin inserts and the cross-sectional view of the combined design of microchannel with the micro pin-fin inserts for the two-layered design. The geometric configuration has ten degrees of freedom.

The solid volume and manufacturing constraints are stated in Equations (4.3)-(4.4) and (4.13)-(4.15), where the height of the two-layered microchannel M is defined as:

UNIVERSITEIT VAN PRETORIA
UNIVERSITY OF PRETORIA
YUNIBESITHI YA PRETORIA

$$M_1 + M_2 = M$$

(5.4)

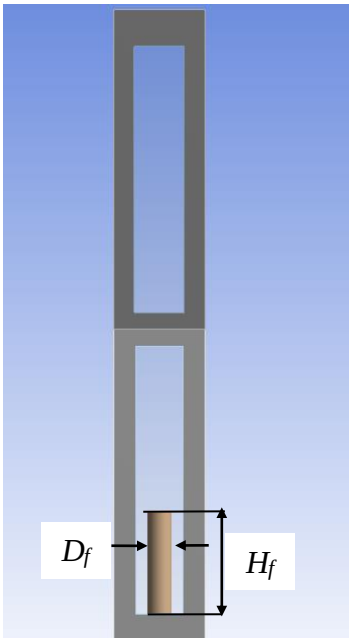

(a) Two-dimensional cross-section

UNIVERSITEIT VAN PRETORIA
UNIVERSITY OF PRETORIA
YUNIBESITHI YA PRETORIA

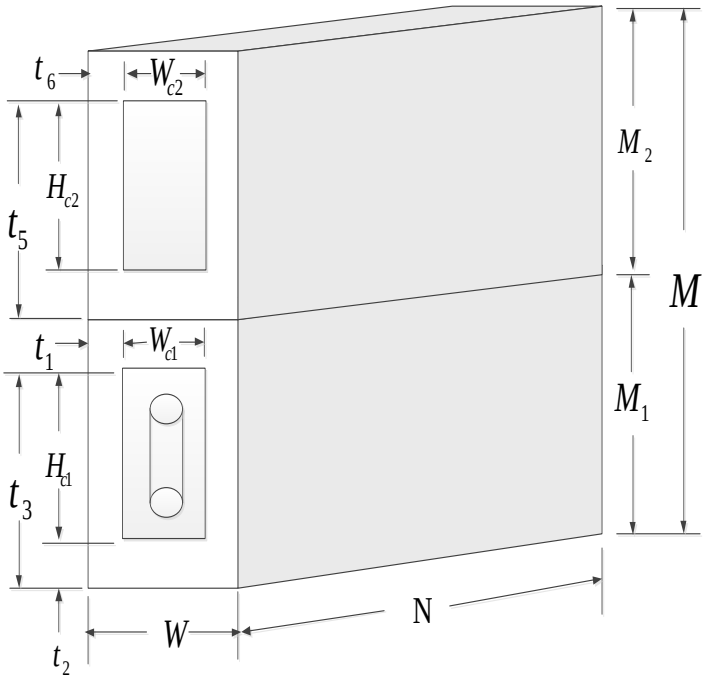

(b) Three-dimensional computational domain

Figure 5.8: Combined two-layered microchannel and micro pin fin

The volume and manufacturing constraints of the micro pin fin are stated in Equations 5.1-5.3.

The design space for the micro pin fins is defined as $30 \leq H_f \leq 160$ µm and $40 \leq D_f \leq 60$ µm for both the fixed and reduced axial length, while the pin-fin spacing *s* is fixed at 62.5µm with the micro pin fins centrally placed in the microchannel.

5.3.2. Case Study 1: Optimisation results for fixed axial length with uniform surface heat flux

UNIVERSITEIT VAN PRETORIA
UNIVERSITY OF PRETORIA
YUNIBESITHI YA PRETORIA

The thermal performance of the two-layered microchannel with parallel-flow and counterflow configuration with fixed axial length of 10 mm does not improve when micro pin fins are inserted. This is shown graphically in Figure 5.9. Micro pin fins are also inserted into the bottom layer of the two-layered microchannel to investigate the effect of the combined design on the thermal performance of the heat sink.

Figure 5.9a shows that even though the minimised peak temperature decreases when the micro pin fins are inserted into the two-layered microchannel with parallel flow of fluid, it is not a significant decrease. When the number of rows of micro pin fins exceeds three, there is no improvement in the results of minimised peak temperature. Figure 5.9b shows that inserting three rows of micro pin fins into the two-layer microchannel with parallel flow of fluid increases the maximised thermal conductance by less than 1% at the lowest *Be* and about 1.5% at the highest *Be*.

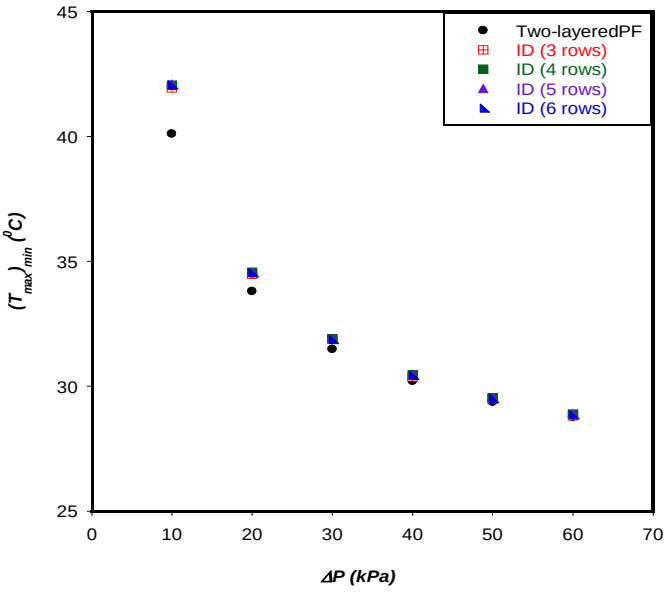

(a) Parallel flow (PF)

UNIVERSITEIT VAN PRETORIA
UNIVERSITY OF PRETORIA
YUNIBESITHI YA PRETORIA

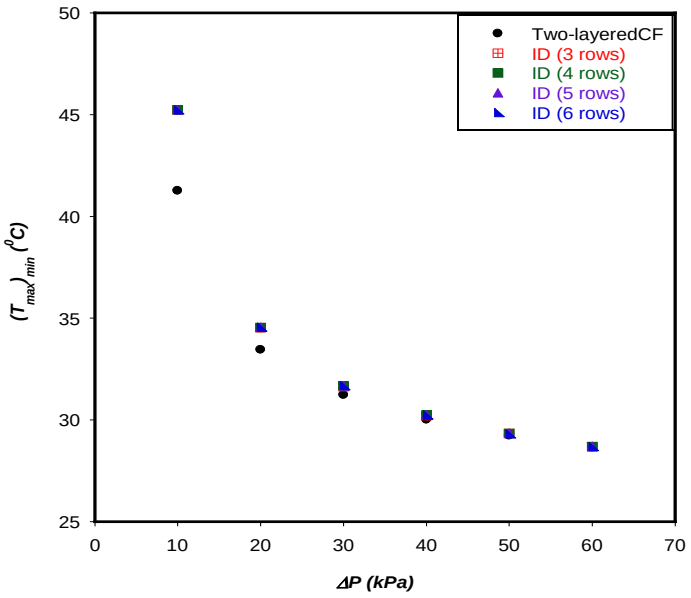

(b) Counterflow (CF)

Figure 5.9: Effect of pressure drop on minimised peak temperature for fixed axial length of combined two-layered microchannel and micro pin fins

5.3.2.1. Comparison between the combined single and two-layered microchannel heat sinks with circular-shaped micro pin fins

Comparison between the thermal performance of single and two-layered microchannels with different flow arrangements inserted with circular-shaped micro pin fins is reported for a fixed axial length when uniform surface heat flux of 100 W/cm^2 is applied to the bottom of the solid substrate. Figure 5.10 shows results of the minimised peak temperature for the combined single and two-layered microchannels with three rows of micro pin-fin inserts for fixed total volume V and V_f and fixed axial

UNIVERSITEIT VAN PRETORIA
UNIVERSITY OF PRETORIA
YUNIBESITHI YA PRETORIA

length N of 10 mm, while Figure 5.11 shows results of maximised thermal conductance of the combined heat sink design. The combined single microchannel and micro pin fins have the best thermal performance for all pressure drops considered in the study. When pressure drop is 10kPa, the combined single heat sink design has an improved maximised thermal conductance of 6.6% over the combined two-layered PF design and 22.6% over the combined two-layered CF design. For the highest pressure drop of 60 kPa considered in the study, the single microchannel with three rows of micro pin-fin inserts is 3.8% better in thermal performance than the combined two-layered PF design and 2.2% than the two-layered CF design.

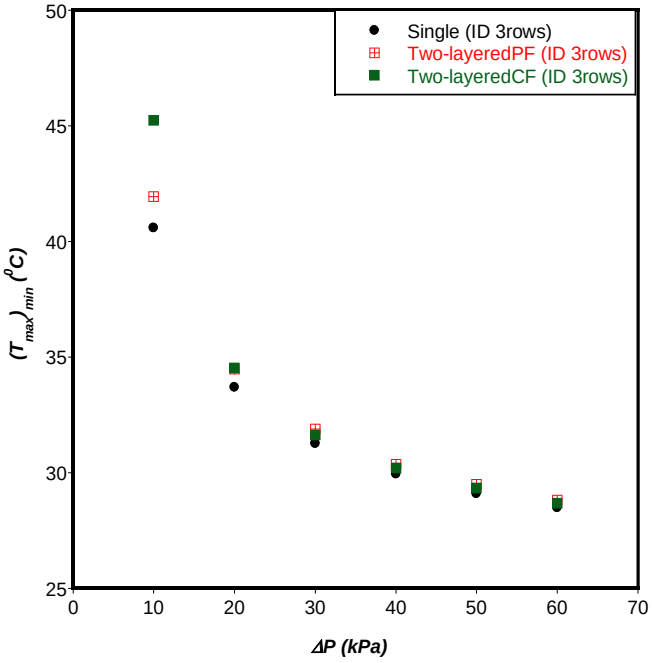

Figure 5.10: Comparison between minimised peak temperature for combined single and two-layered microchannel with micro pin fins (fixed length)

UNIVERSITEIT VAN PRETORIA
UNIVERSITY OF PRETORIA
YUNIBESITHI YA PRETORIA

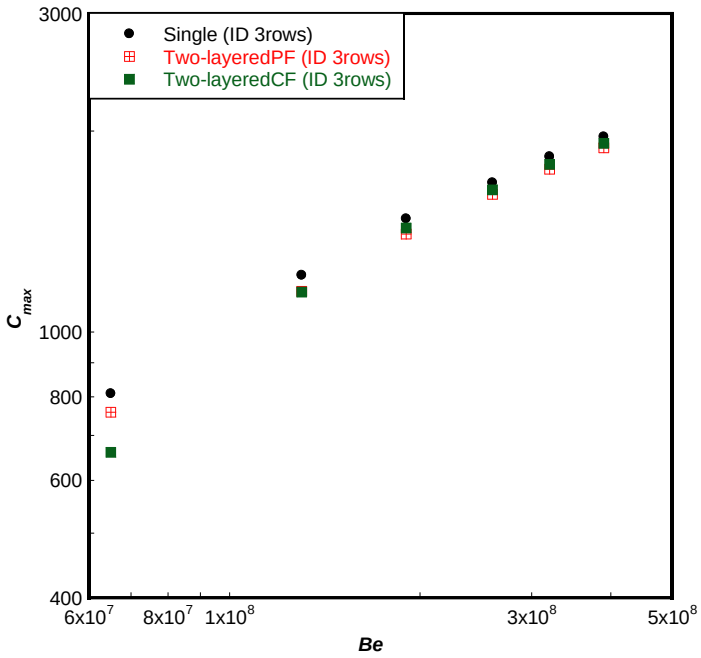

Figure 5.11: Comparison between maximised thermal conductance for combined single and two-layered microchannel with micro pin fins (fixed length)

5.3.3. Case Study 2: Optimisation results for reduced axial length with uniform heat flux

Figure 5.12 shows results of minimised peak temperature for the two-layered microchannel with reduced axial length of 6 mm, fixed total volume of 0.9 mm^3 and uniform heat flux applied to the heated base inserted with micro pin fins. From the results presented, there is an improvement of about 2% in the maximum thermal conductance of the two-layered microchannel with parallel flow of fluid when six rows of micro pin fins are inserted at a pressure drop of 10kPa but there is no improvement observed for pressure drops above 10kPa, as shown in Figure 5.12a. Figure 5.12b shows that there is an average improvement of about 2% in minimised

UNIVERSITEIT VAN PRETORIA
UNIVERSITY OF PRETORIA
YUNIBESITHI YA PRETORIA

peak temperature for the two-layered microchannel with counterflow of fluid inserted with micro pin fins for all the pressure drops except 10kPa.

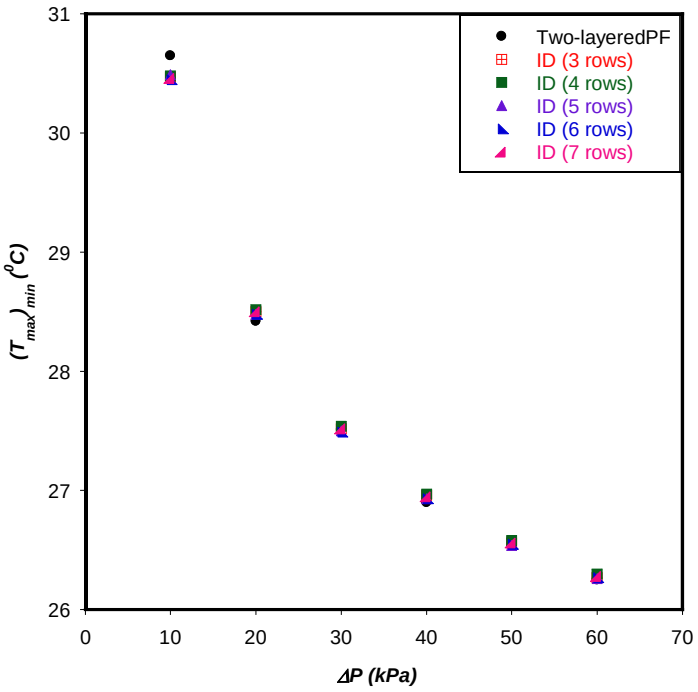

(a)

UNIVERSITEIT VAN PRETORIA
UNIVERSITY OF PRETORIA
YUNIBESITHI YA PRETORIA

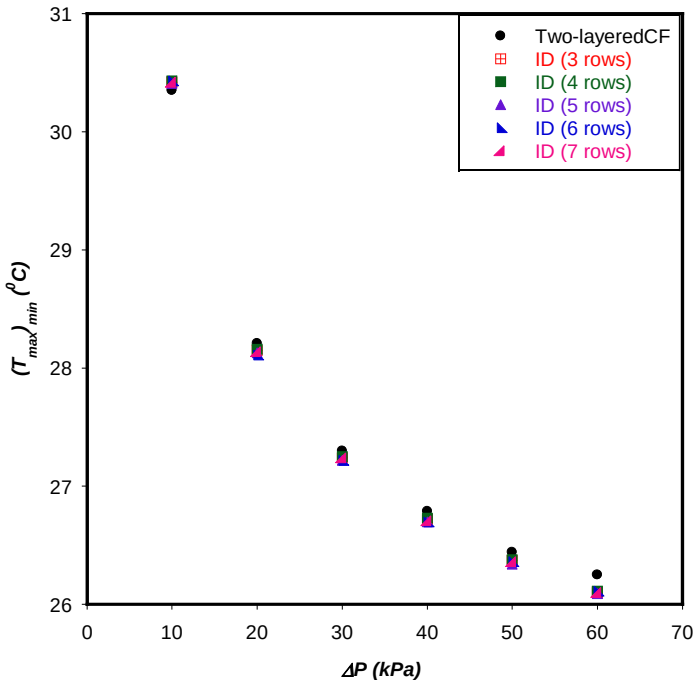

(b)

Figure 5.12: Effect of pressure drop on minimised peak temperature for the two-layered microchannel with micro pin-fin inserts *N* = 6mm (a) parallel flow (b) counterflow

5.3.3.1. Comparison between single and two-layered microchannels with micro pin-fin inserts and reduced axial length

Figure 5.13 shows the comparison between results of the thermal performance of the single and two-layered microchannels with micro pin-fin inserts and reduced axial length of 6 mm. In Figure 5.13a, when the results of minimised peak temperature of the combined single microchannel with five rows of micro pin-fin inserts are compared with those of the combined two-layered microchannels with five rows of micro pin-fin inserts, it can be observed that at pressure drops of 10 to 30kPa, the single microchannel with the micro pin-fin inserts performs best, while at higher

UNIVERSITEIT VAN PRETORIA
UNIVERSITY OF PRETORIA
YUNIBESITHI YA PRETORIA

pressure drops of 40 to 60kPa, the two-layered microchannel with counterflow of fluid has the best performance. The results of the maximised thermal conductance are shown in Figure 5.13b. This shows that at low pressure drops, the single microchannel with the micro pin fins is the best design, while at higher pressure drops, the combined two-layered microchannel and micro pin fins are the best design.

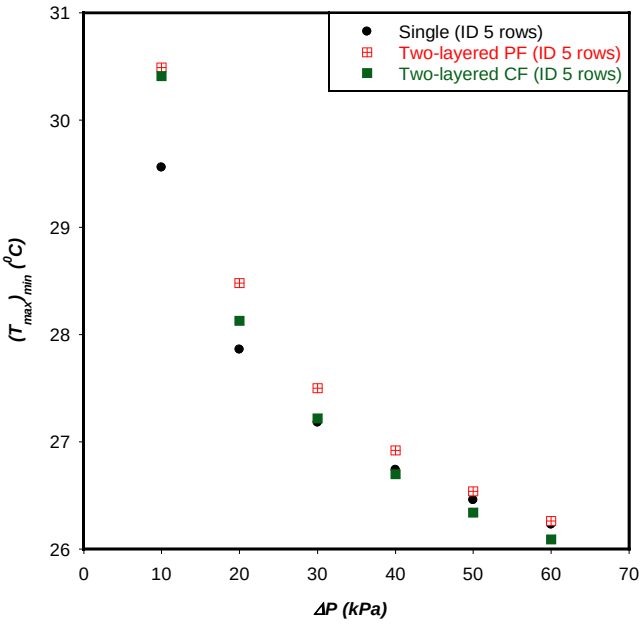

(a)

UNIVERSITEIT VAN PRETORIA
UNIVERSITY OF PRETORIA
YUNIBESITHI YA PRETORIA

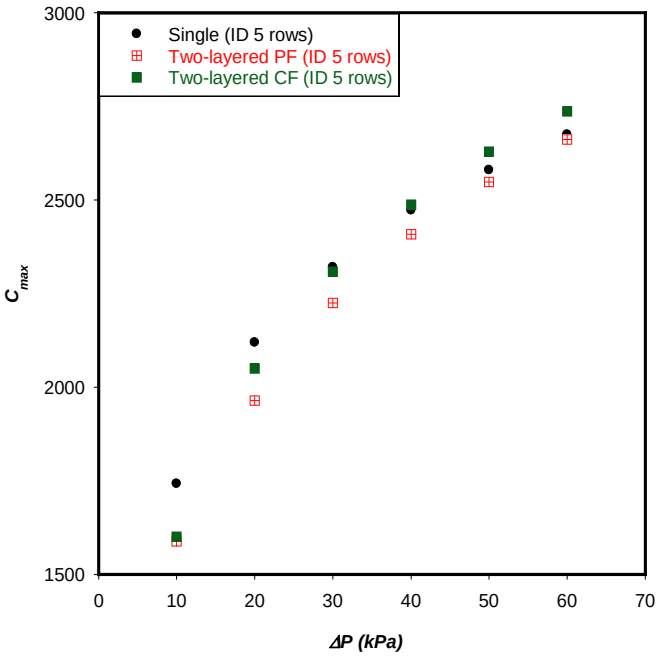

(b)

Figure 5.13: Comparison between the thermal performance of single and two-layered microchannels and micro pin fins N = 6 mm (a) minimised peak temperature (b) maximised thermal conductance

5.3.4. Case Study 3: Optimisation results for varying axial length with uniform heat load

In this section, the optimised two-layered microchannel obtained in Section 4.3.4 (when axial length is varied and uniform heat load of 100 W is applied to the bottom wall) is inserted with rows of circular micro pin fins. This is done to explore whether the thermal performance of this combined design will exceed that of the two-layered microchannel without the micro pin fins. The thermal performance is measured in terms of maximised thermal conductance defined by Equation (5.5) below:

UNIVERSITEIT VAN PRETORIA
UNIVERSITY OF PRETORIA
YUNIBESITHI YA PRETORIA

$$C_{\max} = \frac{Q}{(T_{\max})_{\min} - T_{in}} \tag{5.5}$$

Figure 5.14 shows the results of the combined two-layered microchannel with different flow arrangements inserted with three to six rows of micro pin fins. The results presented in Figure 5.14a show that inserting four rows of micro pin fins into the optimised two-layered PF when pressure drop is fixed at 10kPa improves the thermal performance by only 0.5%. For pressure drops of 20 kPa to 60 kPa, inserting micro pin fins into the two-layered microchannel decreases the thermal performance of the heat sink. This is not the case for the two-layered CF, as shown in Figure 5.14b. Inserting three to six rows of circular-shaped micro pin fins into the two-layered CF microchannel improves the thermal performance of the heat sink by about 2% for the range of pressure drop considered. Increasing the number of rows beyond four does not give better results; therefore, the optimal number of rows is four.

UNIVERSITEIT VAN PRETORIA
UNIVERSITY OF PRETORIA
YUNIBESITHI YA PRETORIA

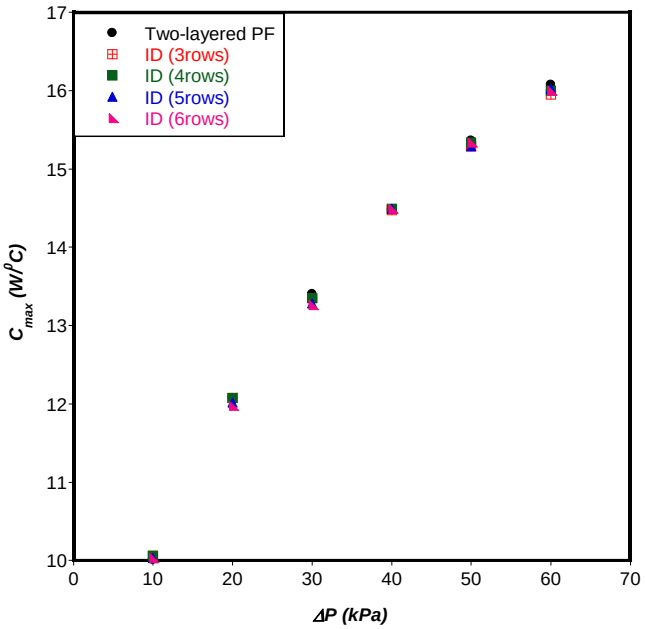

(a)

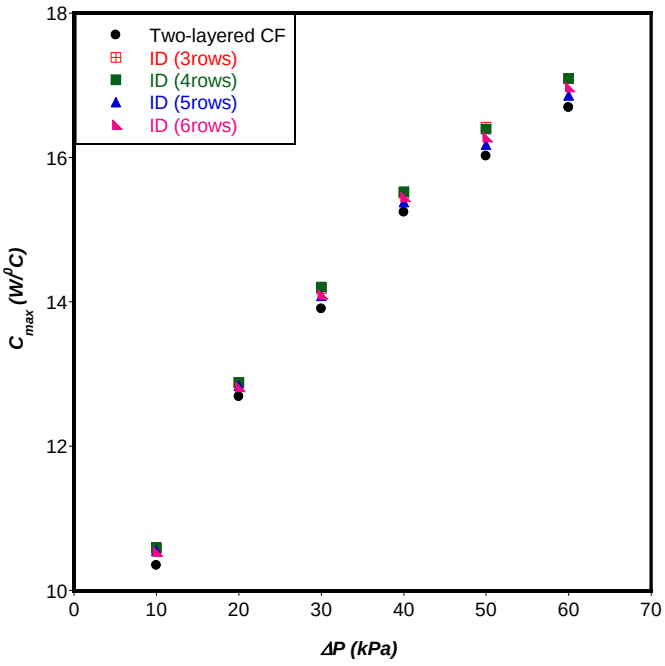

(b)

Figure 5.14: Maximised thermal conductance for combined two-layered microchannel and micro pin fins (a) parallel flow (b) counterflow

UNIVERSITEIT VAN PRETORIA
UNIVERSITY OF PRETORIA
YUNIBESITHI YA PRETORIA

Figure 5.15 shows the comparison between the single and two-layered microchannels with micro pin fins and without micro pin fins. Results show that the optimised single microchannel inserted with six rows of circular-shaped micro pin fins has the best thermal performance. The combined single microchannel and six rows of micro pin fins improve the maximised thermal conductance by about 9% when compared with the single microchannel, 14% when compared with the two-layered PF, 9% when compared with the two-layered CF, 14% when compared with the two-layered PF with micro pin fins and 7% when compared with the two-layered CF with micro pin fins.

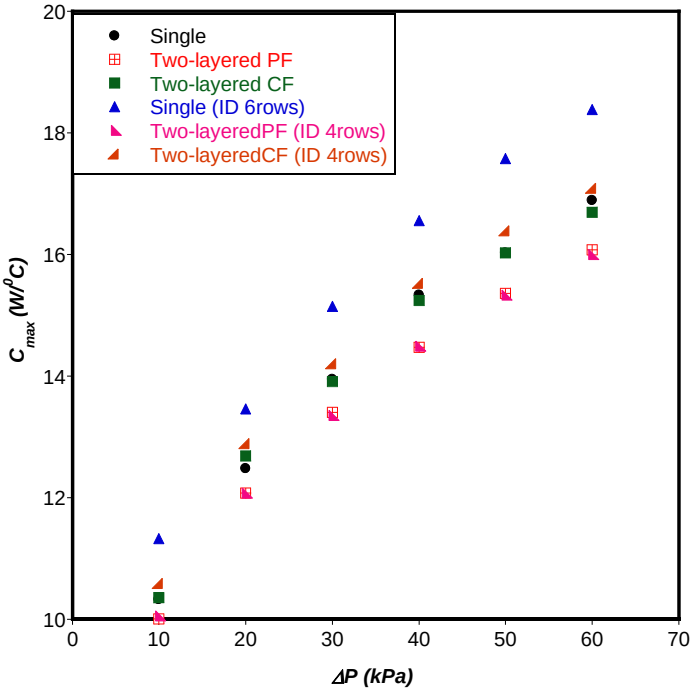

Figure 5.15: Comparison between the thermal performance of the single- and two-layered microchannels with and without micro pin fins for Q = 100 W

UNIVERSITEIT VAN PRETORIA
UNIVERSITY OF PRETORIA
YUNIBESITHI YA PRETORIA

5.3.5. Effect of increasing heat load on the thermal performance of the optimised single and two-layered microchannels with micro pin fins

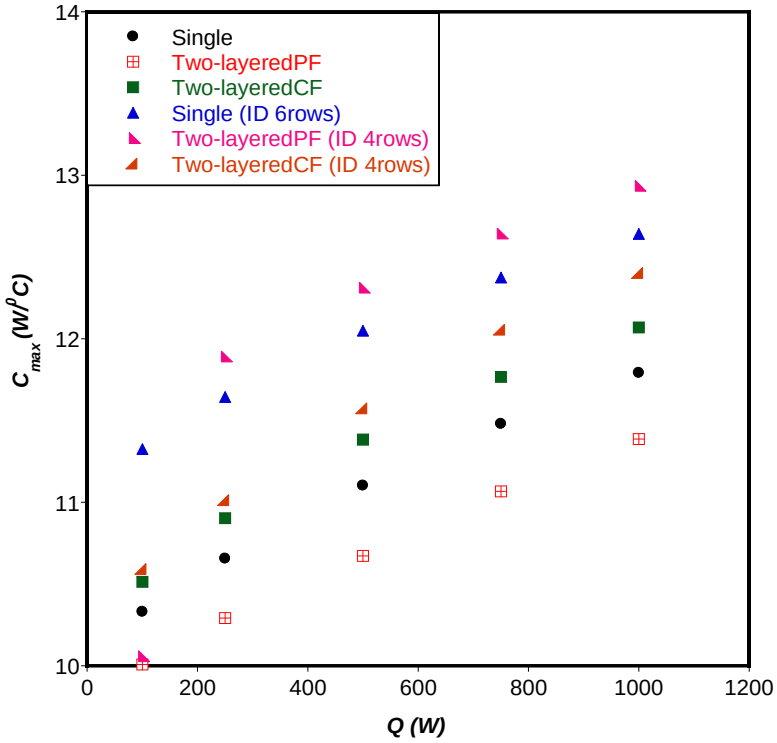

Figure 5.16: Effect of increasing heat load on the thermal performance of six different types of heat sinks at fixed ΔP = 10 kPa

The heat load on the bottom wall of the solid substrate is increased from 100 W to 1000 W and the effect of this increase on the thermal performance of the single and two-layered microchannels at their optimal axial lengths is investigated.

Results presented in Figure 5.16 show that when the heat load is fixed at 100W and the pressure drop is fixed at 10 kPa, the single microchannel has the best thermal performance, which is also shown in Figure 5.15. As *Q* is increased, the thermal performance of the two-layered microchannel with parallel flow of fluid and four rows of circular micro pin fins exceeds that of the single microchannel by an average

UNIVERSITEIT VAN PRETORIA
UNIVERSITY OF PRETORIA
YUNIBESITHI YA PRETORIA

of about 2%. It can also be observed that the two-layered microchannel with parallel-flow configuration without micro pin fins has the worst performance under increasing heat load. The microchannels with micro pin fins perform better than those without the micro pins under increasing heat load.

These results confirm that inserting micro pin fins into a microchannel enhances the thermal performance of heat sinks even under high heat load conditions.

5.4. COMBINED SINGLE MICROCHANNEL WITH DIFFERENT SHAPES OF MICRO PIN FINS

A numerical investigation into the thermal performance of a single microchannel with circular-, square- and hexagonal-shaped micro pin fins is presented in this section. It is shown that combining a single microchannel and circular-shaped micro pin-fins improves the thermal conductance of the heat sink. This section focuses on the comparison between the thermal performance of a single microchannel with three different shapes of micro pin-fin inserts with the aim of investigating which shape of micro pin fin gives the best thermal performance when inserted into a single microchannel. The microchannel has a fixed and finite volume, while the total volume of each shape of micro pin fin is also fixed. The cooling fluid is water assumed to be incompressible with homogeneous and temperature-dependent thermophysical properties. The objective is the maximisation of the thermal conductance, which is

UNIVERSITEIT VAN PRETORIA
UNIVERSITY OF PRETORIA
YUNIBESITHI YA PRETORIA

achieved by minimising the peak temperature of the solid substrate. A constant heat load Q is applied to the bottom of the solid substrate.

5.4.1. Physical model and design variables

Figure 5.17 shows the top view of a single microchannel with three different shapes of micro pin-fin inserts, namely square, hexagonal and circular shapes.

The total volume and manufacturing constraints are stated in Equations (4.3)-(4.7) and (4.13)-(4.15). In this section, the manufacturing constraints in Equations (5.1) and (5.2) are applied to the aspect ratio $\left(\frac{H_f}{L_f}\right)$ for the square- and $\left(\frac{H_f}{2L_f}\right)$ for the hexagonal-shaped micro pin fins, where L_f is the length of the each side of the square and hexagonal surface. A total fin volume constraint is applied to the different shapes of micro pin fins, as outlined in the equations below:

$$V_{f(circular)} = V_{f(square)} = V_{f(hexagonal)} \tag{5.5}$$

$$V_{f(circular)} = V_{f1} + V_{f2} + ... + V_{fn} = constant \tag{5.6}$$

$$V_{f(square)} = V_{f1} + V_{f2} + ... + V_{fn} = constant \tag{5.7}$$

$$V_{f(hexagonal)} = V_{f1} + V_{f2} + ... + V_{fn} = constant \tag{5.8}$$

Numerical simulations and optimisation are carried out for a fixed total volume V of 0.9 mm^3 with varied axial length N of 1 to10 mm. The temperature of water pumped

UNIVERSITEIT VAN PRETORIA
UNIVERSITY OF PRETORIA
YUNIBESITHI YA PRETORIA

across the microchannel is 20 °C at the inlet and total heat load applied to the bottom wall is 100W. The design space for the response surface for the fixed total volume is defined as $50 \leq W_c \leq 80$ µm, $50 \leq M - t_3 \leq 60$ µm, and $500 < H_c < 3000$ µm. The optimised design point chosen is required to meet the manufacturing constraints for pressure drops of 10 to 60kPa. In the GDO, the objective function is to minimise the peak temperature based on the design space. For the micro pin fins, the spacing between the pins (S_1 *to* S_n) is fixed as 50 µm and they are positioned centrally in the microchannel, while the design space for the response surface (taking into consideration the manufacturing constraints) is defined as $30 \leq H_f \leq 160$ µm and $40 \leq D_f \leq 60$ µm.

5.4.1.1. Grid refinement test

A grid refinement test is carried out for the combined microchannel with the different shapes of pin fins. Table 5.3 shows the dimensions of the combined microchannel and square-shaped micro pin fins geometry used for the grid refinement test, while Table 5.4 shows the grid refinement test results. For the combined design of the microchannel with hexagonal-shaped micro pin fins, Tables 5.5 and 5.6 show the dimensions of the geometry and the grid refinement test results respectively.

UNIVERSITEIT VAN PRETORIA
UNIVERSITY OF PRETORIA
YUNIBESITHI YA PRETORIA

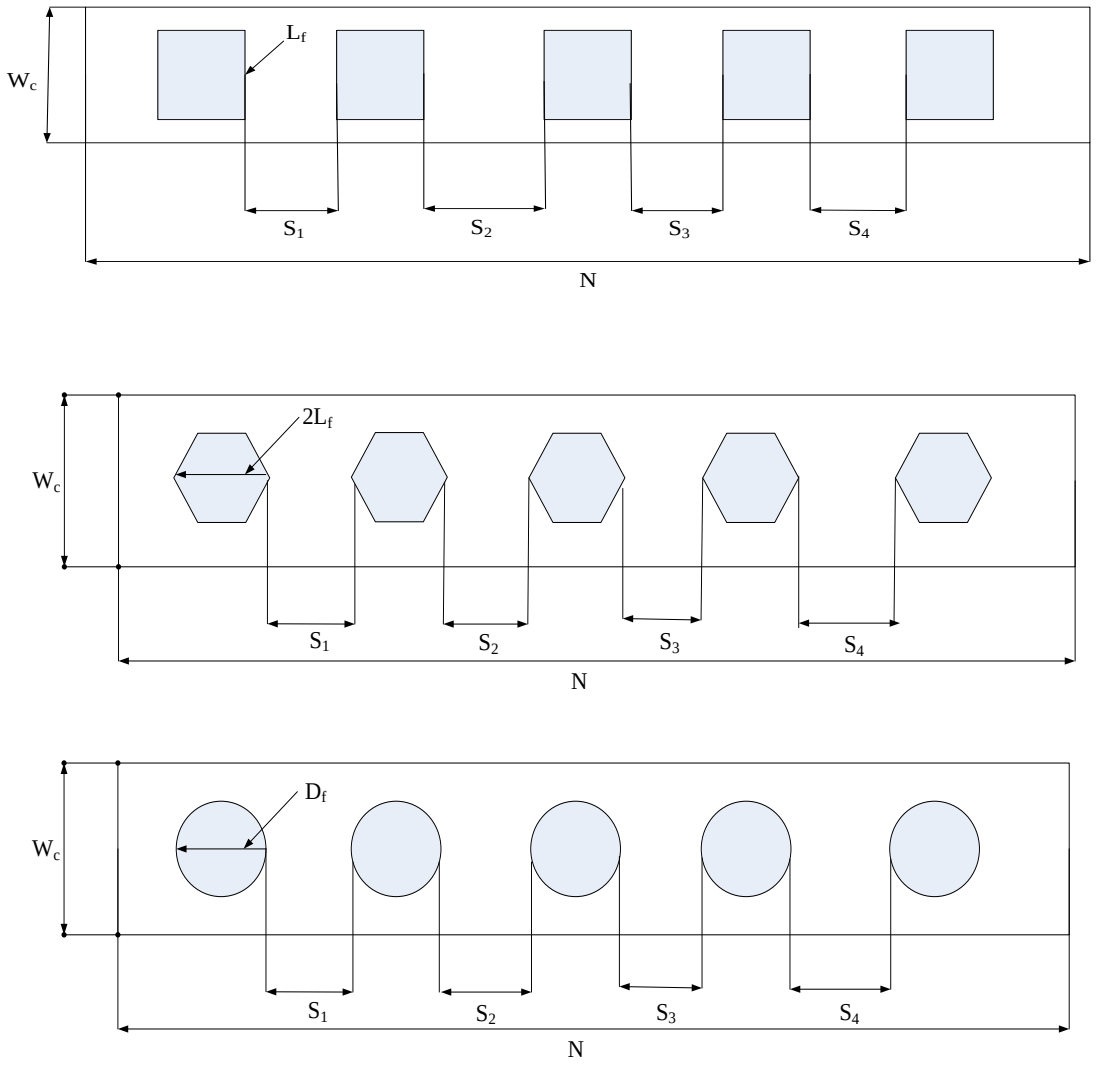

Figure 5.17: Top view of combined single microchannel and (a) square- (b) hexagonal- (c) circular-shaped micro pin fins

UNIVERSITEIT VAN PRETORIA
UNIVERSITY OF PRETORIA
YUNIBESITHI YA PRETORIA

Table 5.3: Dimensions of the microchannel and square-shaped micro pin-fin heat sink for grid refinement test

H_c (mm)	W_c (mm)	t_1 (mm)	$H-t_3$ (mm)	H_{f1} to H_{f6} (mm)	L_{f1} to L_{f6} (mm)	N (mm)
0.832	0.075	0.119	0.060	0.030	0.035	3.0

Table 5.4: Grid refinement test results for combined heat sink with square-shaped pin fins ($\Delta P = 10$ kPa)

Number of cells	$\Delta T(K)$	$\left\|\frac{(\Delta T)_i - (\Delta T)_{i-1}}{(\Delta T)_i}\right\|$
158 597	8.6459	-
238 368	8.8188	0.0196
373 895	8.8173	0.0002

Table 5.5: Dimensions of the microchannel and hexagonal-shaped micro pin-fin heat sink for grid refinement test

H_c (mm)	W_c (mm)	t_1 (mm)	$H-t_3$ (mm)	H_{f1} to H_{f6} (mm)	L_{f1} to L_{f6} (mm)	N (mm)
0.832	0.075	0.119	0.060	0.030	0.022	3.0

Table 5.6: Grid refinement test results for combined heat sink with hexagonal-shaped micro pin fins ($\Delta P = 10$ kPa)

Number of cells	$\Delta T(K)$	$\left\|\frac{(\Delta T)_i - (\Delta T)_{i-1}}{(\Delta T)_i}\right\|$
167 076	8.6607	-

UNIVERSITEIT VAN PRETORIA
UNIVERSITY OF PRETORIA
YUNIBESITHI YA PRETORIA

237 489	8.7982	0.0156
377 533	8.8237	0.0029

5.4.2. Comparison between the thermal performances of the combined single microchannel and different shapes of micro pin fins

The trend observed when the single microchannel is inserted with circular-shaped micro pin fins in Section 5.2.5 is also seen when square- and hexagonal-shaped micro pin fins are inserted into the optimised single microchannel. For the single microchannel with three to six rows of square-shaped micro pin-fin inserts, the aspect ratios $\left(\frac{H_f}{L_f}\right)$ of the square-shaped micro pin fins which meet the manufacturing constraints are 0.60, 0.69, 0.77 and 0.86 for three to six rows of micro pin fins respectively. The thermal performance of the combined design with square-shaped micro pin fins is also better than that of the single microchannel with a reduction of 2 to 3% in minimised peak temperature, which gives a corresponding 7 to 10% increase in

UNIVERSITEIT VAN PRETORIA
UNIVERSITY OF PRETORIA
YUNIBESITHI YA PRETORIA

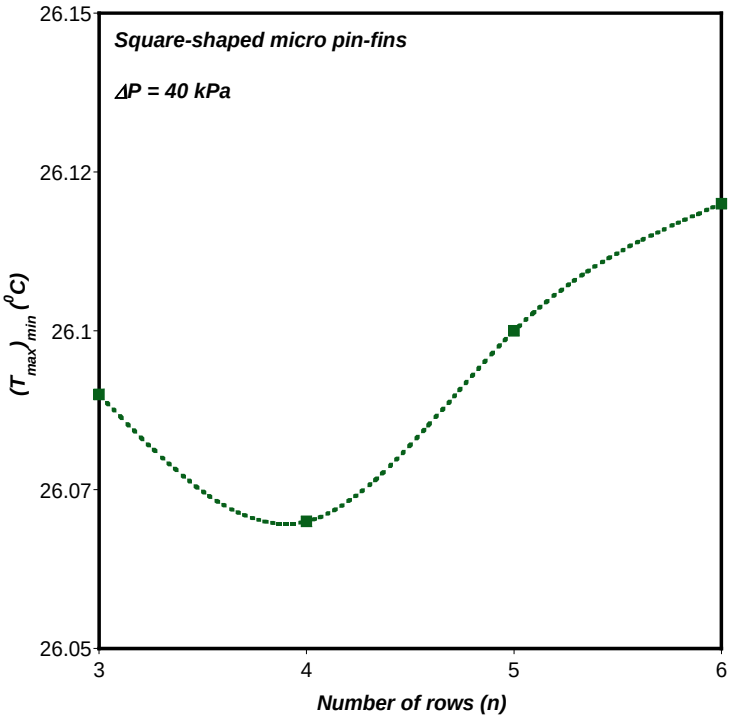

Figure 5.18a

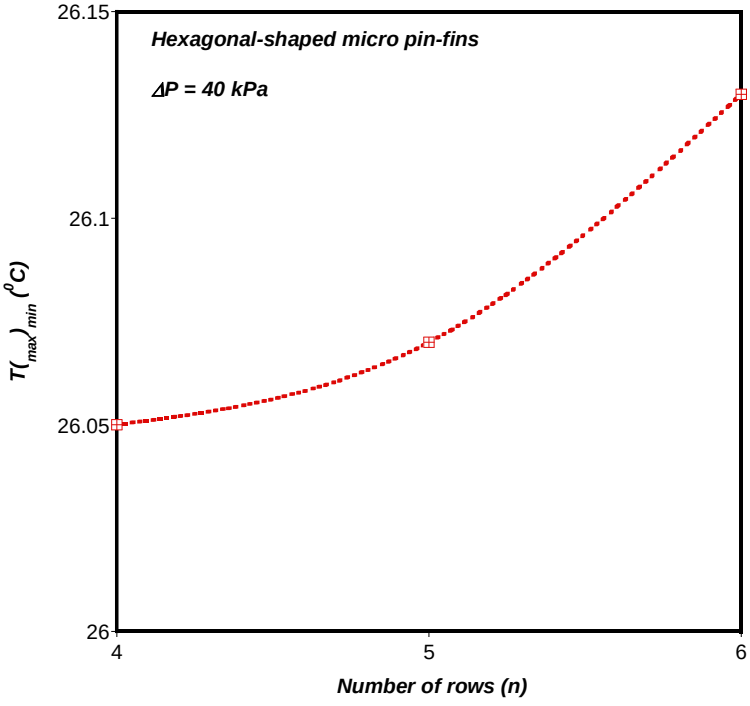

Figure 5.18b

Figure 5.18: Effect of number of rows on the minimised peak temperature for single microchannels with micro pin-fin inserts (a) square-shaped (b) hexagonal-shaped

UNIVERSITEIT VAN PRETORIA
UNIVERSITY OF PRETORIA
YUNIBESITHI YA PRETORIA

maximised thermal conductance for all the pressure drops considered in the study. The optimal number of rows for the square-shaped micro pin fins is four, as shown in Figure 5.18a.

Four to six rows of micro pin fins are used for the combined single microchannel and hexagonal-shaped micro pin fins because the manufacturing constraint for $\left(\frac{H_f}{2L_f}\right)$ is not met when the number of rows is less than four. The aspect ratios $\left(\frac{H_f}{2L_f}\right)$ of the hexagonal-shaped micro pin fins which meet the manufacturing constraints are 0.558, 0.624 and 0.683 for four to six rows of micro pin fins respectively. The thermal performance of the combined design with hexagonal-shaped micro pin fins is also better than that of the single microchannel with further decrease in minimised peak temperature of 2 to 3%, which also results in an 8 to 9% reduction in the minimised thermal resistance. The optimal number of rows of hexagonal micro pin fins is also four for all pressure drops considered in the study, as shown in Figure 5.18b. The optimised micro pin-fin size for all the different shapes gives a total fin volume V_f of 0.00023 mm^3. It can be concluded that an addition of 0.025% of micro pin-fin volume gives an increase in thermal performance of almost 10%.

Figure 5.19 shows results of the comparison between the thermal performance of the optimised combined heat sink design with the different shapes of micro pin fins. When the optimal designs are compared, the combined heat sink with six rows of circular-shaped micro pin fins has the best thermal performance but with an average decrease of 0.05% in minimised peak temperature and average increase of 0.2% in

UNIVERSITEIT VAN PRETORIA
UNIVERSITY OF PRETORIA
YUNIBESITHI YA PRETORIA

maximised thermal conductance when compared with the combined heat sink with square- and hexagonal-shaped micro pin fins. From these results, it can be concluded that considering the optimal number of rows, the shape of the micro pin fin does not have a significant effect on improving the thermal performance of the combined heat sink design.

Figure 5.20 shows the effect of the number of rows of micro pin fins on the thermal performance of the combined microchannel and different shapes of micro pin-fin inserts for a fixed pressure drop. It can be observed from the graph that the effect of the different shapes of micro pin fins inserted into the microchannel has different trends. For the circular-shaped micro pin fins, as the number of rows increases, the thermal conductance increases but beyond six rows, the thermal conductance begins to decrease. The square-shaped pin fins show an increase in thermal conductance up until the number of rows is four and thereafter, the thermal conductance begins to decrease. Increasing the number of rows of the hexagonal-shaped micro pin fins above four worsens the thermal conductance of the combined heat sink. The global optimal n_{opt} is clearly shown to be six rows of circular-shaped micro pin fins.

UNIVERSITEIT VAN PRETORIA
UNIVERSITY OF PRETORIA
YUNIBESITHI YA PRETORIA

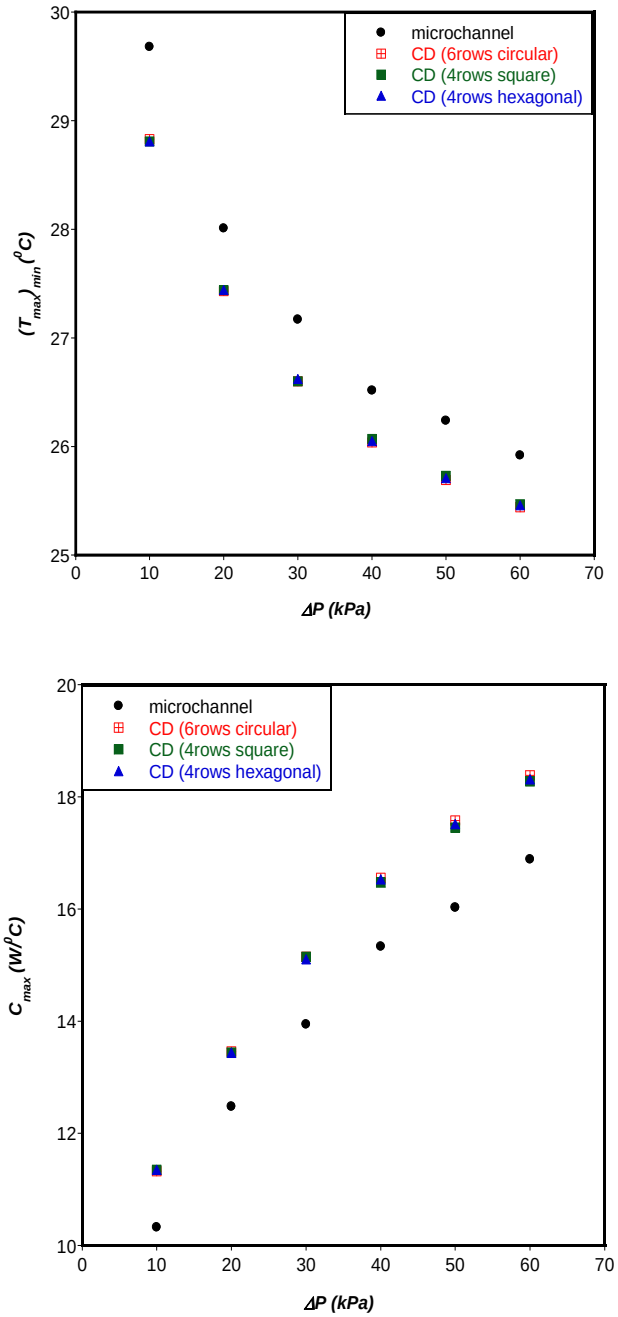

Figure 5.19: Comparison between the combined microchannel and different shapes of micro pin fins (a) minimised peak temperature (b) maximised thermal conductance

UNIVERSITEIT VAN PRETORIA
UNIVERSITY OF PRETORIA
YUNIBESITHI YA PRETORIA

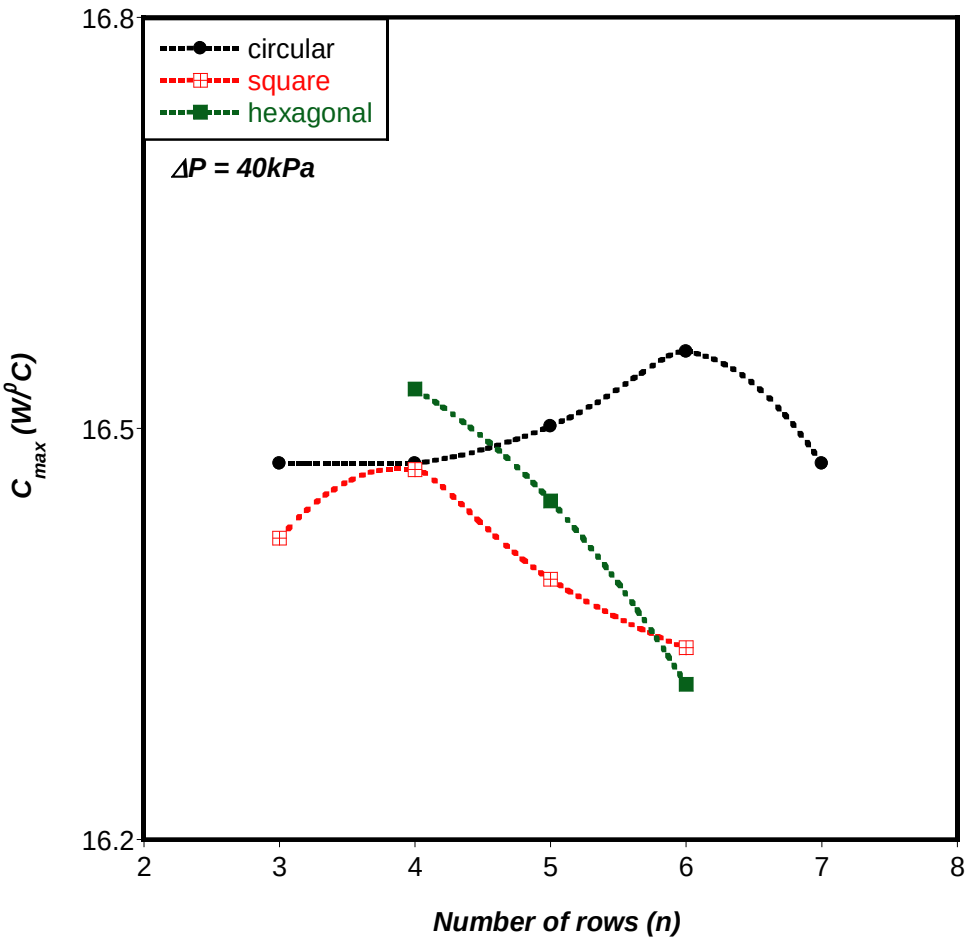

Figure 5.20: Effect of number of rows of micro pin fins on the thermal performance of combined heat sink

5.5. CONCLUSION

In this chapter, the three-dimensional numerical investigations carried out to optimise the geometric parameters of single- and two-layered microchannel heat sinks with micro pin-fin inserts using the constructal law technique for a fixed total volume was presented. Results from the combined design of the single microchannel and circular-shaped micro pin fins were compared with those obtained for the combined design of

UNIVERSITEIT VAN PRETORIA
UNIVERSITY OF PRETORIA
YUNIBESITHI YA PRETORIA

two-layer microchannel and circular-shaped micro pin fins for both fixed and varying axial lengths. Thereafter, investigations were carried out to study the thermal performance of combined design of the single microchannel with different shapes of micro pin-fin inserts and results obtained were also presented.

Inserting three to six rows of micro pin-fin inserts into the single microchannel with fixed axial length and uniform heat flux on its heated base further minimised the peak temperature of the solid substrate. The optimal number of rows was three, which resulted in a 4% improvement in the maximised thermal conductance at the lowest pressure drop considered in the study. When four to seven rows of micro pin fins were inserted into the single microchannel with reduced axial length and uniform heat flux, the optimal number of rows was six and there was a 5% improvement in the maximised thermal conductance at the lowest pressure drop considered in the study.

For the combined design of the two-layered microchannel with circular-shaped micro pin-fin inserts, there was no improvement in the thermal performance for both the parallel-flow and counterflow configurations with fixed axial length and uniform heat flux on the heated base of the solid substrate. When the axial length was reduced with the total volume fixed, there was about 2% increase in maximum thermal conductance for the combined design with parallel-flow configuration and pressure drop of 10kPa and also an average improvement of 2% for the combined design with counterflow arrangement when the pressure drop was between 20 kPa and 60 kPa. Comparing the results of maximised thermal conductance of the combined design of the single- and

UNIVERSITEIT VAN PRETORIA
UNIVERSITY OF PRETORIA
YUNIBESITHI YA PRETORIA

two-layered microchannel when the axial length was reduced to 6 mm, the single microchannel with micro pin-fin inserts had the best thermal performance at lower pressure drops. When the pressure drop was increased from 40kPa to 60kPa, the combined design of two-layered microchannel with counterflow arrangement and micro pin fins had the best thermal performance.

Results of the combined single and two-layered microchannels and pin fins for varying axial lengths and uniform heat loads showed that when the heat load was 100 W, the single microchannel with six rows of micro pin fins had the best thermal performance. When the heat load was increased from 250 W to 1 000 W, the combined two-layered microchannel with counterflow of fluid and four rows of micro pin fins had the best thermal performance.

When different shapes of micro pin fins were inserted into the single microchannel, the optimal number of rows of micro pin fins that gave the best thermal performance was three rows for the combined design with circular-shaped pin fins, five rows for that with triangular-shaped pin fins and three rows for the combined design with squared-shaped pin fins for fixed axial length and the range of pressure drop considered. This shows that the optimal number of rows depends on the shape of the micro pin fin. The combined design with the circular-shaped pin fins had the best thermal performance for all pressure drops used in the study.

When the axial length was relaxed, the optimal number of rows was five for the combined design with circular-shaped pin fins and three for both the triangular- and square-shaped pin fins and the combined design with the circular-shaped pin fins had

UNIVERSITEIT VAN PRETORIA
UNIVERSITY OF PRETORIA
YUNIBESITHI YA PRETORIA

the best thermal performance for pressure drop lower than 40 kPa, while the design with square-shaped pin fins had the best performance for pressure drop above 40 kPa. The effect of the pin-fin spacing on thermal performance of the combined design with circular-shaped pin fins was significant at pressure drops of 30 to 60 kPa but for the combined design with the other shapes of pin-fin inserts there was no significant effect.

UNIVERSITEIT VAN PRETORIA
UNIVERSITY OF PRETORIA
YUNIBESITHI YA PRETORIA

CHAPTER 6: TEMPERATURE NON-UNIFORMITY ON THE HEATED BASE OF A SOLID SUBSTRATE

6.1. INTRODUCTION

This chapter presents the numerical investigation of temperature variation on the heated base of the solid substrate which is being cooled using different heat sinks. The heat sinks considered are single microchannels, two-layered microchannels with parallel- and counterflow of fluid, single microchannels inserted with circular-shaped micro pin fins and two-layered microchannels inserted with circular-shaped pin fins. The thermal performance of the heat sinks based on the objective of minimised temperature gradient will be the focus of this chapter. The thermal performance of all the heat sinks based on maximised thermal conductance was considered in previous chapters but the heat sink that gives both maximised thermal conductance and minimised temperature gradient will be presented as the best option for the cooling of the solid substrate.

UNIVERSITEIT VAN PRETORIA
UNIVERSITY OF PRETORIA
YUNIBESITHI YA PRETORIA

6.2. TEMPERATURE VARIATION ALONG AXIAL LENGTH OF HEATED BASE

The tremendous effect of temperature non-uniformity on the reliability and performance of microelectronic devices stated by Wei [70] is the motivation for this section. The temperature variation along the axial length of the heated base of the silicon solid substrate being cooled gives a good knowledge of how temperature non-uniformity can be minimised and the best choice of heat sink design. The temperature rise on the heated wall is defined by

$$(\Delta T)_{base} = (T_{\max} - T_{\min})_{base} \tag{6.1}$$

6.2.1. Effect of single microchannel cooling on temperature variation

Figure 6.1 shows variations in temperature along the heated base of a solid substrate with uniform heat flux of 100 W/cm^2 applied to the base, which is cooled with a single microchannel with fixed axial length. The pressure drop range of 10 to 60 kPa corresponds to a fluid inlet velocity range of 0.329 m/s to 1.865 m/s. For a fixed axial length N of 10 mm for the single microchannel and fixed total volume V of 0.9 mm^3, the difference between the minimum and maximum temperature on the heated base is 16.02 ˚C when pressure drop is 10 kPa. When the pressure drop is increased to 20

UNIVERSITEIT VAN PRETORIA
UNIVERSITY OF PRETORIA
YUNIBESITHI YA PRETORIA

kPa, the temperature difference is reduced by 42% and a further increase in the pressure drop to 60 kPa further reduces the temperature difference by 51%.

The axial length of the solid substrate is also varied with a constant heat load of 100 W applied to the heated base to obtain an optimal axial length. This is discussed extensively in Section 4.2.5. For the optimal axial length of 3 mm when pressure drop is 10kPa, the temperature difference is 2.851 ˚C, which is a significant improvement of 82% when compared with that of the fixed axial length. When the pressure drop is increased to 60kPa, there is a 58% decrease in the temperature difference when the results for fixed axial length are compared with those of the optimal axial length. These results are presented graphically in Figure 6.2.

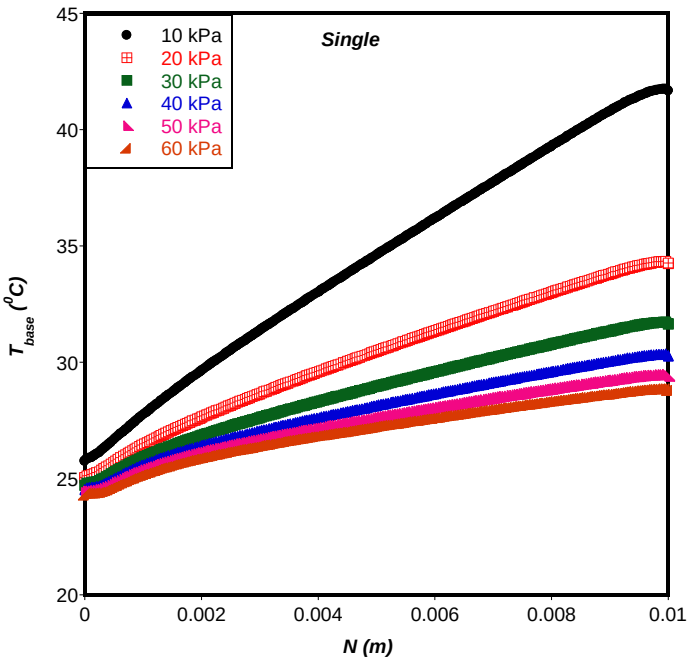

Figure 6.1: Temperature variation along the solid substrate heated base with uniform heat flux cooled by a single microchannel

UNIVERSITEIT VAN PRETORIA
UNIVERSITY OF PRETORIA
YUNIBESITHI YA PRETORIA

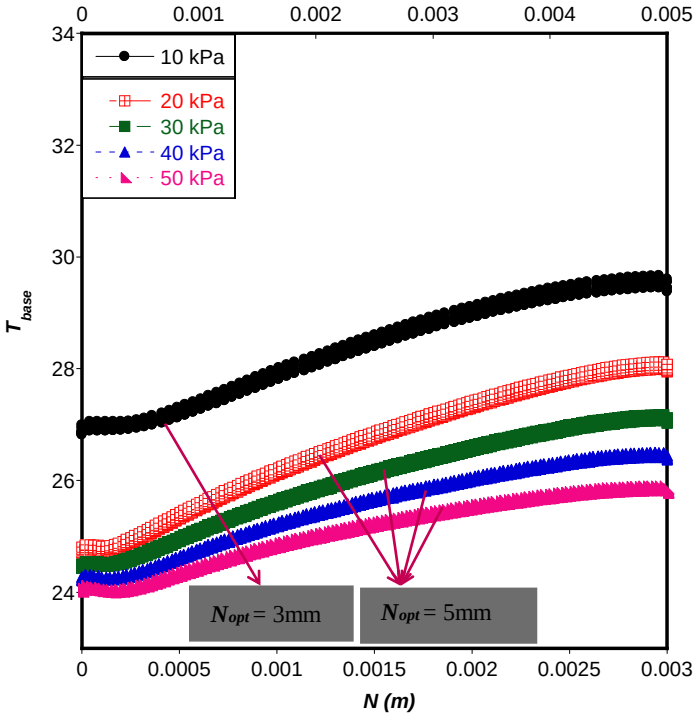

Figure 6.2: **Temperature variation along solid substrate heated base with uniform heat load cooled by a single microchannel**

6.2.2. Effect of combined single microchannel and circular-shaped pin-fin cooling on temperature variation

Figure 6.3 shows the temperature variation on the heated base of a solid substrate with uniform heat flux of 100 W/cm^2 cooled with combined single microchannel and three rows of circular-shaped micro pin-fin inserts. The total volume is still fixed at 0.9 mm^3 with a fixed axial length of 10 mm. The temperature difference on the heated base for pressure drop of 10kPa is 15.34 ˚C, which gives about 4% improvement over

UNIVERSITEIT VAN PRETORIA
UNIVERSITY OF PRETORIA
YUNIBESITHI YA PRETORIA

the single microchannel with fixed axial length. There is 70% reduction in the temperature difference when the pressure drop is increased to 60kPa.

When circular-shaped micro pin fins are inserted into the optimised microchannel heat sink with fixed total volume and uniform heat load of 100 W, it is discovered that the optimal number of rows of micro pin fins is six. This is discussed extensively in Section 5.4.3. The temperature variation on the heated base of the combined single microchannel and six rows of circular-shaped micro pin fins is shown in Figure 6.4. At the lowest pressure drop of 10 kPa, the temperature difference on the heated base is 2.657 ˚C. This gives about 86% reduction in temperature rise on the heated base when compared with the combined heat sink with fixed axial length. As the pressure drop is increased to 60 kPa, the temperature difference on the heated base decreases from 2.657 ˚C to 1.683 ˚C.

UNIVERSITEIT VAN PRETORIA
UNIVERSITY OF PRETORIA
YUNIBESITHI YA PRETORIA

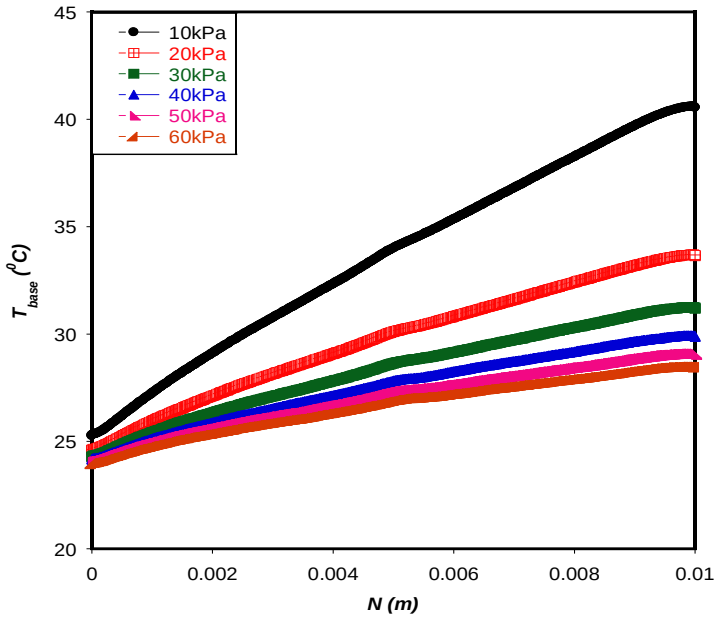

Figure 6.3: Temperature variation on the solid substrate heated base with uniform heat flux cooled with a combined single microchannel and micro pin-fin heat sink

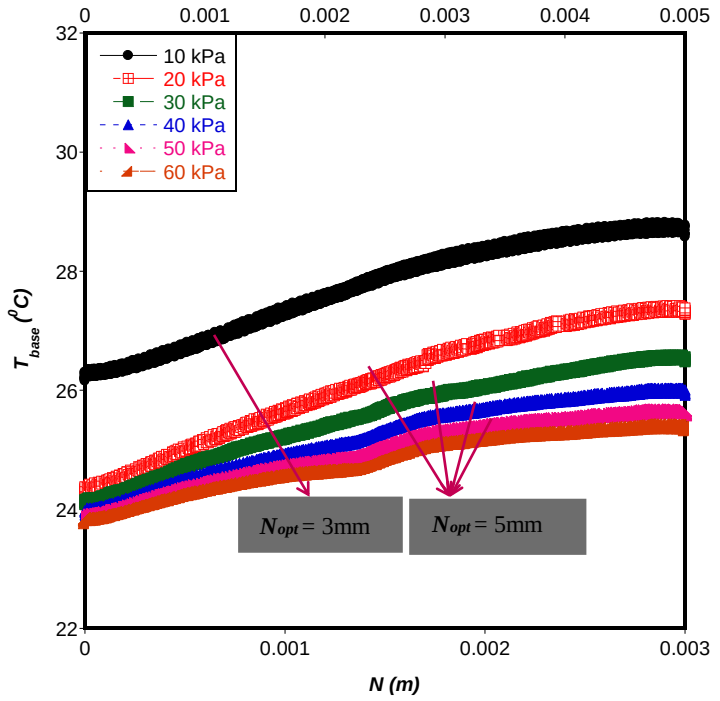

Figure 6.4: Temperature variation along the solid substrate heated base with uniform heat load cooled with a combined single microchannel and micro pin-fin heat sink

UNIVERSITEIT VAN PRETORIA
UNIVERSITY OF PRETORIA
YUNIBESITHI YA PRETORIA

6.2.3. Effect of two-layered microchannel cooling with parallel-flow configuration on temperature variation

Figure 6.5 shows the results of temperature variation on the heated base of a solid substrate when a two-layered microchannel with parallel flow of fluid is used to cool the solid substrate with fixed total volume V of 0.9 mm^3, fixed axial length N of 10 mm and uniform heat flux of 100 W/cm^2 applied to the heated base. The temperature difference on the heated base decreases by 67% (from 14.21 ˚C to 4.72 ˚C) when the pressure drop is increased from 10kPa to 60kPa.

When a uniform heat load is applied to the heated base, optimal axial lengths of the solid substrate and two-layered microchannels are obtained for the pressure drop range specified as discussed in Section 4.3.4. Results presented in Figure 6.6 show the temperature variation on the heated base with uniform heat load when the two-layered PF is employed for cooling. The temperature difference on the heated base decreases from 3.488 ˚C to 2.579 ˚C when pressure drop is increased from 10 kPa to 60 kPa. These results show 76% and 45% reduction in temperature difference for pressure drops of 10 kPa and 60 kPa respectively when two-layered PF with optimal axial length is compared with the one with fixed axial length.

UNIVERSITEIT VAN PRETORIA
UNIVERSITY OF PRETORIA
YUNIBESITHI YA PRETORIA

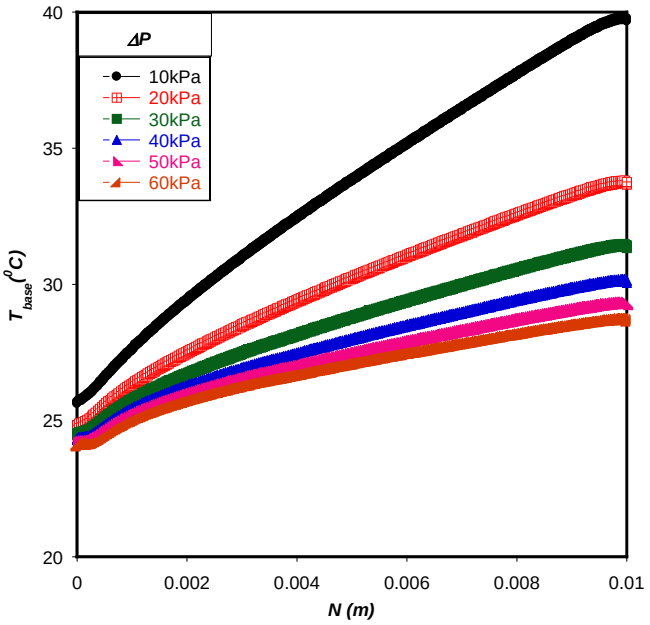

Figure 6.5: Temperature variation along the solid substrate heated base with uniform heat flux cooled by the two-layered microchannel PF

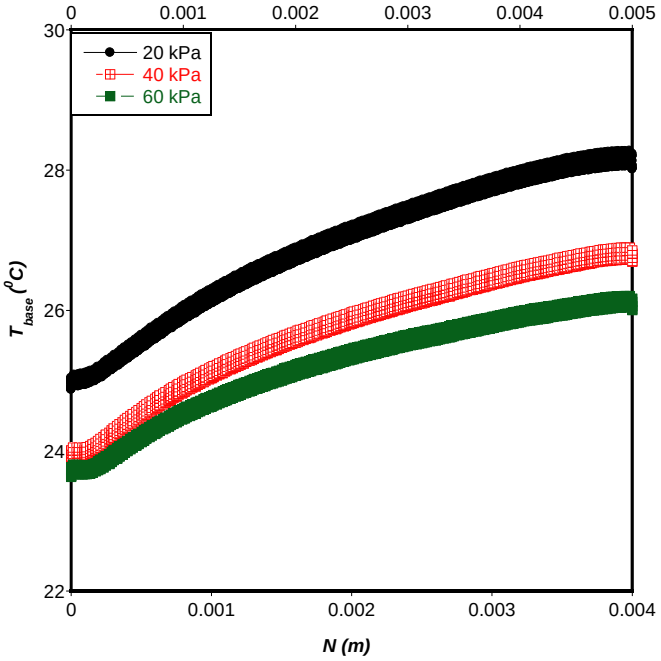

Figure 6.6: Temperature variation along the solid substrate heated base with uniform heat load cooled by the two-layered microchannel PF

UNIVERSITEIT VAN PRETORIA
UNIVERSITY OF PRETORIA
YUNIBESITHI YA PRETORIA

6.2.4. Effect of two-layered microchannel cooling with counterflow configuration on temperature variation

The effect of using a two-layered microchannel with counterflow of fluid to cool the heated base of a solid substrate with fixed total volume V of 0.9mm^3, fixed axial length N of 10mm and uniform heat flux on the heated base is also investigated and the results are presented in Figure 6.7. It can be observed that there is about 67% decrease in temperature difference from 13.38 ˚C to 4.46 ˚C when pressure drop is increased from 10kPa to 60kPa.

When the two-layered CF is used to cool the solid substrate with uniform heat load on the heated base and optimal axial length (as stated in Section 4.3.4), the temperature difference on the heated base decreases from 2.67 ˚C to 2.115 ˚C as the pressure drop is increased from 10kPa to 60kPa. This result is shown in Figure 6.8. When these results are compared with those of the fixed axial length, there is a decrease of 80% and 53% in temperature difference for pressure drops of 10 kPa and 60 kPa respectively.

UNIVERSITEIT VAN PRETORIA
UNIVERSITY OF PRETORIA
YUNIBESITHI YA PRETORIA

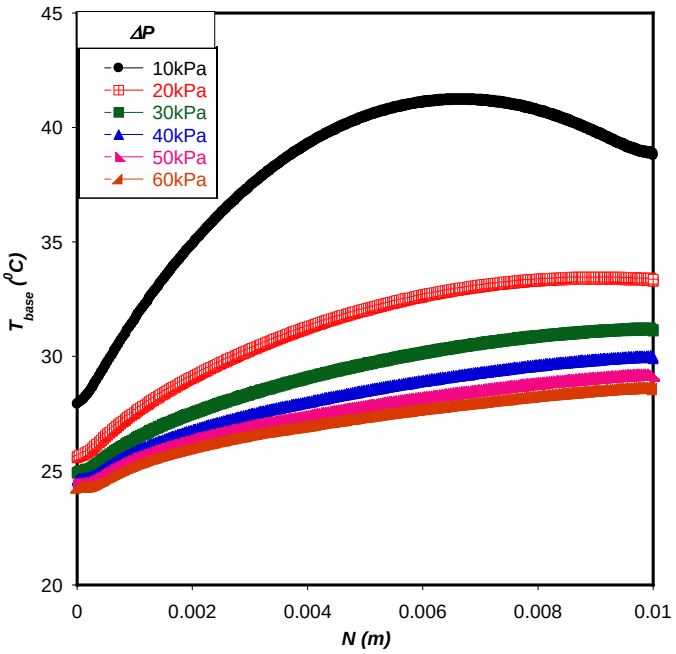

Figure 6.7: Temperature variation along the solid substrate heated base with uniform heat flux cooled by the two-layered CF

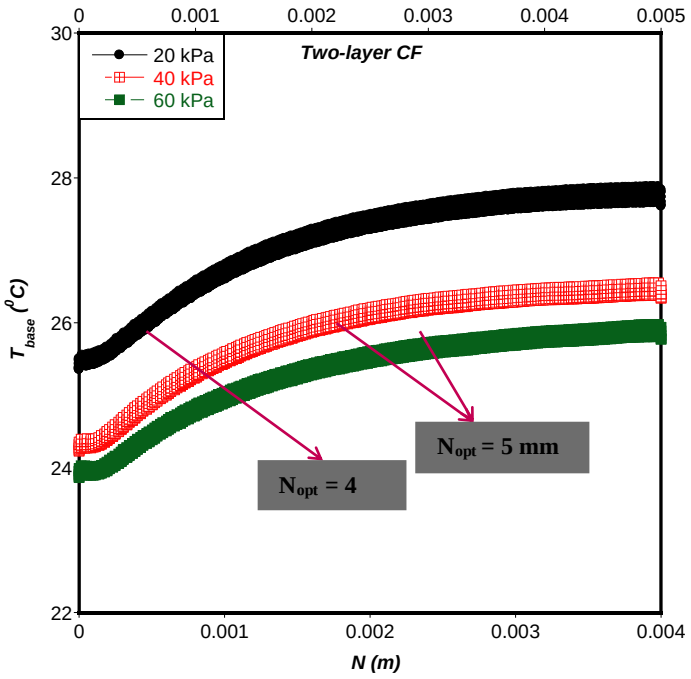

Figure 6.8: Temperature variation along the solid substrate heated base with uniform heat load cooled by the two-layered CF

UNIVERSITEIT VAN PRETORIA
UNIVERSITY OF PRETORIA
YUNIBESITHI YA PRETORIA

6.2.5. Effect of combined two-layered microchannel cooling with parallel-flow configuration and circular-shaped micro pin-fin inserts on temperature variation

Figure 6.9 shows the temperature variation on the heated base of the solid substrate when the two-layered microchannel PF inserted with three rows of micro pin fins is used in cooling the substrate. A uniform heat flux of 100 W/cm^2 is also applied to the heated base of the solid substrate with fixed axial length of 10 mm and fixed total volume of 0.9 mm^3. Results show that the temperature difference decreases from 16.57 ˚C to 5.34 ˚C when the pressure drop is increased from 10kPa to 60kPa. A 'dip' in temperature is also observed at the centre of the heated solid substrate as a result of the micro pin-fin inserts.

When the two-layered PF with micro pin-fin inserts is used to cool the solid substrate with uniform heat load on the heated base and optimal axial length (as stated in Section 5.3.4), the temperature difference on the heated base decreases from 3.516 ˚C to 2.871 ˚C as the pressure drop is increased from 10kPa to 60kPa. This result is shown in Figure 6.10. When these results are compared with those of the fixed axial length, there is a decrease of 79% and 46% in temperature difference for pressure drops of 10 kPa and 60 kPa respectively. The 'dip' observed for the fixed axial length of solid substrate with uniform heat flux is also observed in Figure 6.10. A 'zigzag' pattern of temperature distribution on the heated base of the solid substrate is also seen in Figure 6.10. This observation shows a temperature fluctuation on the heated

UNIVERSITEIT VAN PRETORIA
UNIVERSITY OF PRETORIA
YUNIBESITHI YA PRETORIA

base for shorter axial lengths of the solid substrate with uniform heat load cooled by the combined two-layered PF heat sink design.

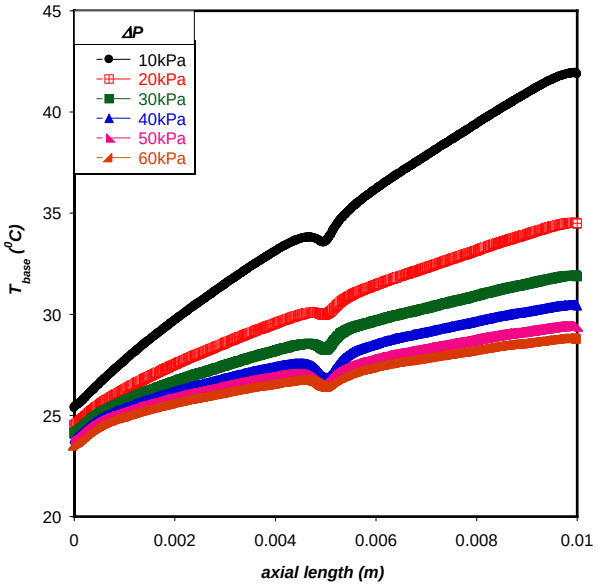

Figure 6.9: Temperature variation along the solid substrate heated base with uniform heat flux cooled by the two-layered PF with micro pin fins

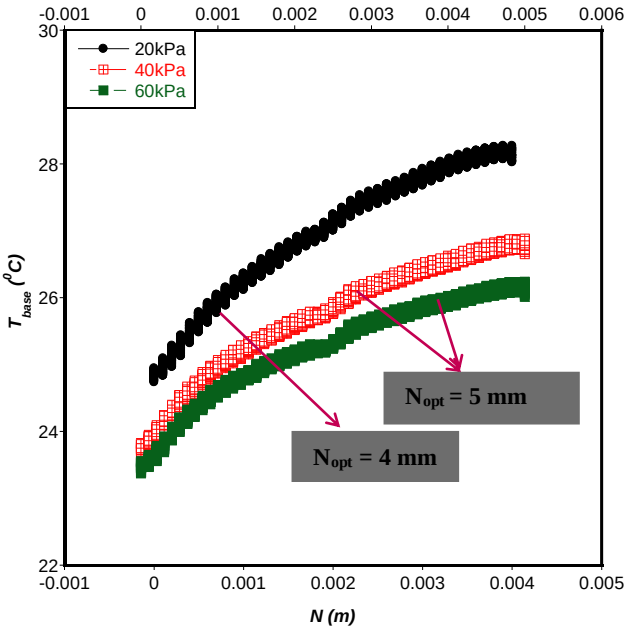

Figure 6.10: **Temperature variation along the solid substrate heated base with uniform heat load cooled by a two-layered PF microchannel with micro pin fins**

UNIVERSITEIT VAN PRETORIA
UNIVERSITY OF PRETORIA
YUNIBESITHI YA PRETORIA

6.2.6. Effect of combined two-layered microchannel cooling with counter flow configuration and circular-shaped micro pin-fin inserts on temperature variation

Results of temperature variation on the fixed axial length of the heated base of the solid substrate with uniform heat flux of 100 W/cm^2 cooled by a two-layered CF microchannel inserted with circular-shaped micro pin fins are presented in Figure 6.11. There is about 70% decrease in temperature difference on the heated base from 17.0 ˚C to 5.02 ˚C when the pressure drop is increased from 10kPa to 60kPa. A temperature 'dip' is also observed at the centre of the heated base where the micro pin fins are located.

When the two-layered CF with micro pin-fin inserts is used to cool the solid substrate with uniform heat load on the heated base and optimal axial length (as stated in Section 5.3.4), the temperature difference on the heated base decreases from 2.385 ˚C to 2.059 ˚C as the pressure drop is increased from 10kPa to 60kPa. This result is shown in Figure 6.12. When these results are compared with those of the fixed axial length, there are an 86% decrease and a 59% decrease in temperature difference for pressure drops of 10 kPa and 60 kPa respectively. The 'dip' and 'zigzag' temperature distribution patterns observed for the two-layered PF with micro pin fins are also observed for the two-layered CF with micro pin fins, as shown in Figure 6.12.

UNIVERSITEIT VAN PRETORIA
UNIVERSITY OF PRETORIA
YUNIBESITHI YA PRETORIA

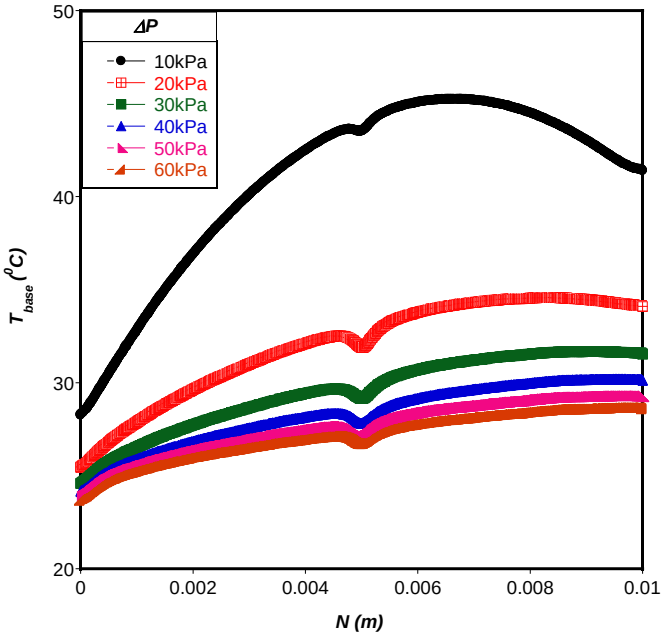

Figure 6.11: Temperature variation along the solid substrate heated base with uniform heat flux cooled by the two-layered CF with micro pin fins

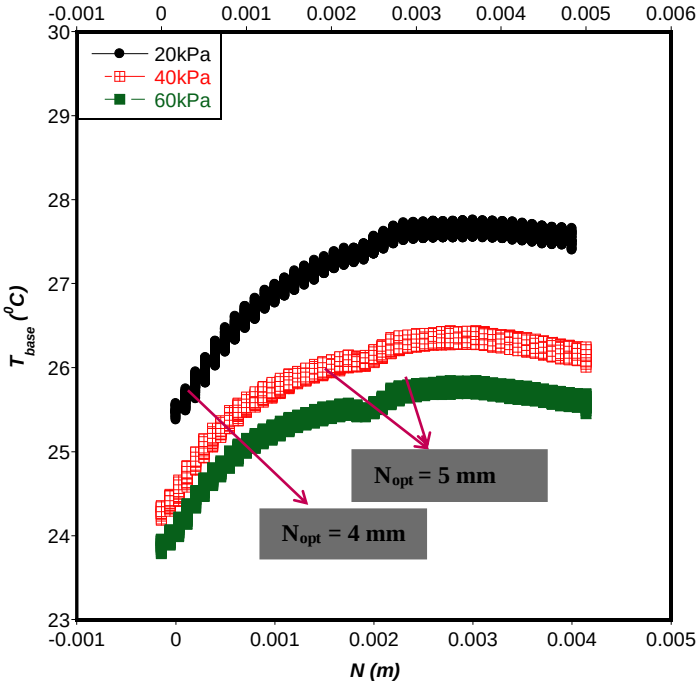

Figure 6.12: Temperature variation along the solid substrate heated base with uniform heat load cooled by a two-layered microchannel CF with micro pin fins

UNIVERSITEIT VAN PRETORIA
UNIVERSITY OF PRETORIA
YUNIBESITHI YA PRETORIA

6.2.7. Comparison between the temperature differences on the heated base of the solid substrate cooled by the different heat sinks

The results of temperature difference on the heated base of the solid substrate cooled using the different heat sinks with fixed axial length of 10 mm and uniform heat flux of 100 W/cm^2 are presented in Figure 6.13. It can be seen from these results that the two-layered CF heat sink performs best in minimising the temperature rise on the heated surface of a solid substrate for the pressure drop range considered. Results in Figure 6.14 show that for a solid substrate with reduced axial length and uniform heat load applied to the heated surface, the two-layered CF with four rows of micro pin-fin inserts performs best in minimising the temperature rise on the heated base for pressure drops of 10 kPa to 30kPa. When the pressure drop is increased from 40 kPa to 60 kPa, the single microchannel with six rows of micro pin-fin inserts performs the best in minimising the temperature rise.

When the results in this section are compared with those in Section 5.3, the single microchannel with six rows of circular-shaped micro pin-fin inserts has the best thermal performance based on maximised thermal conductance and minimised temperature rise for pressure drops of 40 kPa to 60 kPa. For lower pressure drops, no heat sink considered in the study could maximise thermal conductance and minimise temperature rise at the same time.

It is also observed that using a solid substrate with reduced axial length and uniform heat load gives the best results in maximising thermal conductance and minimising

UNIVERSITEIT VAN PRETORIA
UNIVERSITY OF PRETORIA
YUNIBESITHI YA PRETORIA

temperature rise to less than 3 ˚C for pressure drop of 10kPa and less than 2 ˚C for pressure drop of 60kPa.

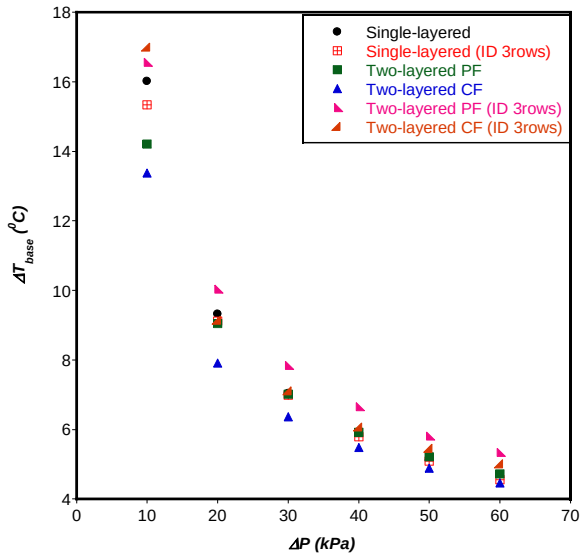

Figure 6.13: Comparison between temperature difference on the solid substrate heated base with fixed axial length and uniform heat flux

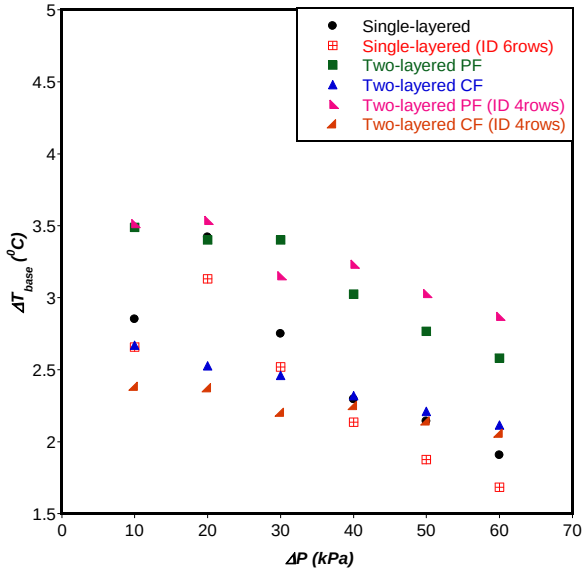

Figure 6.14: Comparison between temperature difference on the solid substrate heated base with reduced axial length and uniform heat load

UNIVERSITEIT VAN PRETORIA
UNIVERSITY OF PRETORIA
YUNIBESITHI YA PRETORIA

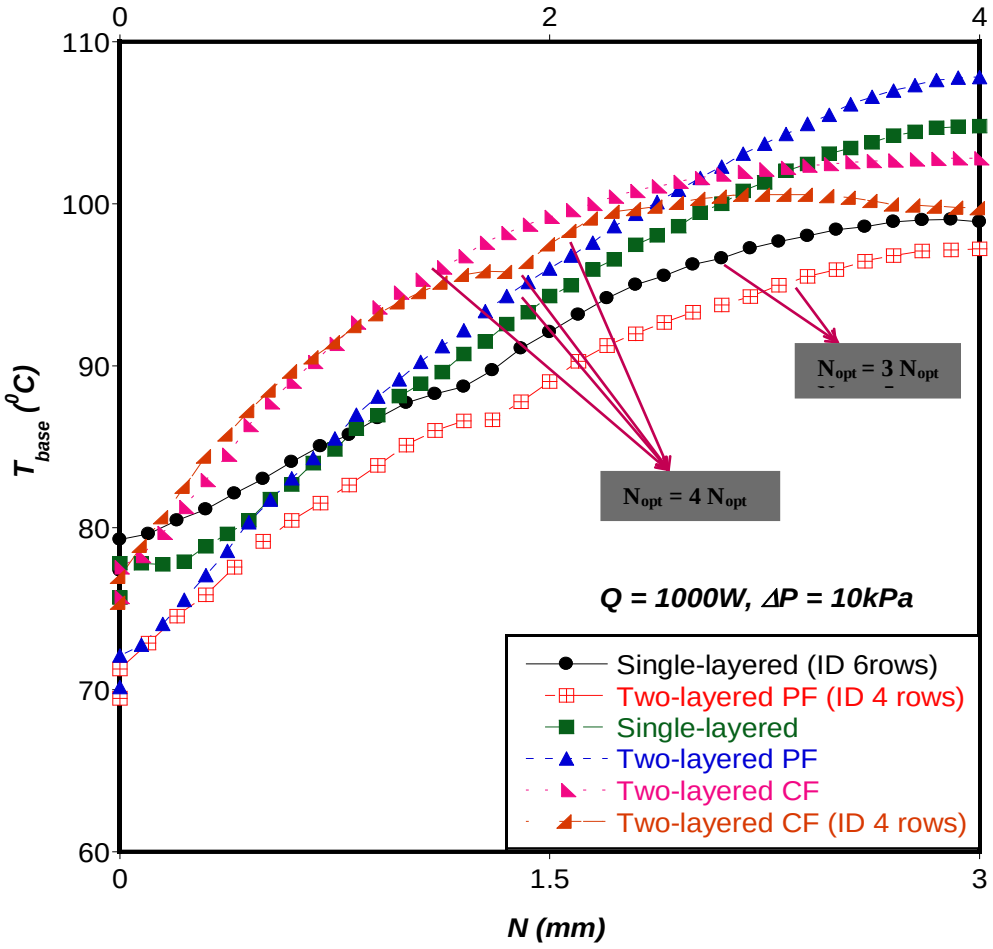

Figure 6.15: Temperature variation on the heated base of the solid substrate cooled with different heat sinks

The temperature variation on the heated base of the solid substrate with reduced axial length cooled using the different types of heat sinks is presented in Figure 6.15. For the heat load of 1000 W and fixed pressure drop of 10 kPa, the two-layered PF microchannel has the steepest temperature gradient, followed by the single microchannel, the two-layered PF with four rows of micro pin-fin inserts, the two-layered CF, the two-layered CF with four rows of micro pin-fin inserts and lastly, the single microchannel with six rows of micro pin-fin inserts with temperature rise

UNIVERSITEIT VAN PRETORIA
UNIVERSITY OF PRETORIA
YUNIBESITHI YA PRETORIA

$(\Delta T)_{base}$ of 37.64 ˚C, 29.09 ˚C, 27.75 ˚C, 27.11 ˚C, 25.20 ˚C and 21.65 ˚C respectively.

The results of the effect of increased pressure drop on $(\Delta T)_{base}$ are presented in Figure 6.16. It can be observed that for a heat load of 1 000 W, the single microchannel with six rows of micro pin-fin inserts performs best in minimising $(\Delta T)_{base}$ for the range of pressure drop considered in the study. The two-layered PF microchannel has the poorest performance in minimising $(\Delta T)_{base}$ as shown in Figure 6.16. As the pressure drop is increased, $(\Delta T)_{base}$ decreases and the lowest temperature difference on the heated base obtained is 10.21 ˚C at pressure drop of 60 kPa.

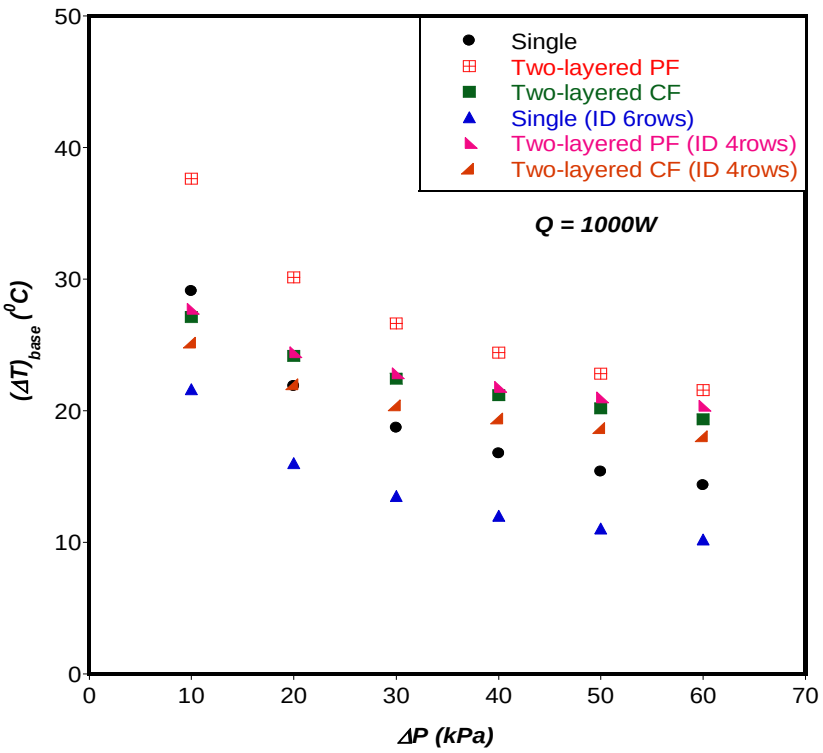

Figure 6.16: Effect of pressure drop on temperature rise on the heated solid substrate base cooled using different heat sinks

UNIVERSITEIT VAN PRETORIA
UNIVERSITY OF PRETORIA
YUNIBESITHI YA PRETORIA

6.3. CONCLUSION

In this chapter, results of temperature variation on the heated base of a silicon solid substrate with fixed axial length, uniform heat flux and optimal length as a result of varying axial length with uniform heat load cooled using different types of heat sinks were presented. The objective was to choose a heat sink design that maximised thermal conductance and minimised temperature difference on the heated base as the best design.

When the minimum temperature difference on the heated base of the solid was considered, results showed that for a fixed axial length of 10 mm, fixed total volume of 0.9 mm^3 and a uniform heat flux of 100 W/cm^2 applied to the heated base, the two-layered microchannel with counterflow of fluid had the best result in minimising the temperature rise on the heated solid substrate base for the range of pressure drop considered in the study.

The temperature variation on the solid substrate heated base with shorter axial length, fixed total volume of 0.9 mm^3 and uniform heat load of 100 W was also studied. It was observed that the two-layered microchannel with counterflow of fluid and four rows of micro pin-fin inserts performed best in minimising temperature rise on the heated base for pressure drops of 10 kPa to 30 kPa but the single microchannel with

UNIVERSITEIT VAN PRETORIA
UNIVERSITY OF PRETORIA
YUNIBESITHI YA PRETORIA

six rows of micro pin-fin inserts performed best when the pressure drop was increased.

The single microchannel with six rows of circular micro pin-fin inserts had the best thermal performance in maximising thermal conductance and minimising the temperature rise on the heated base of the solid substance for pressure drops of 40 kPa to 60 kPa. At lower pressure drops of 10 kPa to 30 kPa, no heat sink considered in the study could meet both objectives of maximising thermal resistance and minimising temperature rise on the solid substrate heated solid substrate at the same time.

UNIVERSITEIT VAN PRETORIA
UNIVERSITY OF PRETORIA
YUNIBESITHI YA PRETORIA

CHAPTER 7: CONCLUSIONS AND RECOMMENDATIONS

7.1. INTRODUCTION

This research study was based on constructal design and optimisation of different types of micro heat sinks with the objective of minimising the peak temperature of the solid substrate being cooled, thereby maximising the global thermal conductance. New designs of heat sinks which combine microchannels and micro pin fins were modelled and their performance compared with the existing ones. The micro heat sinks studied in this research work were single microchannels, combined design of single microchannels with circular-, square- and hexagonal-shaped micro pin-fin inserts, two-layered microchannels with parallel and counterflow of fluid, three-layered microchannels with parallel and counterflow of fluid, combined design of two-layered microchannel with parallel flow of fluid inserted with circular-shaped micro pin fins and the combined design of two-layered microchannel with counterflow of fluid inserted with circular-shaped micro pin fins.

The research was carried out by numerically investigating the heat transfer and fluid flow within the three-dimensional geometry to optimise the cooling structure. The

UNIVERSITEIT VAN PRETORIA
UNIVERSITY OF PRETORIA
YUNIBESITHI YA PRETORIA

numerical studies were carried out using computational fluid dynamics software (ANSYS 14.0), which has an optimisation algorithm. The detailed procedures on how the optimisation of the geometry of the cooling structure was carried out were discussed in this thesis. The numerical modelling and optimisation section discussed extensively the non-linear partial differential equations governing the transfer of heat and optimisation techniques employed.

The numerical and optimisation techniques presented in Chapter 3 were applied to the different heat sink designs in Chapters 4, 5 and 6. The computational fluid dynamics code was validated by comparing analytical and experimental results in open literature with the numerical results obtained, which were in good agreement.

7.2. CONCLUSIONS

The minimised peak temperature and maximised thermal conductance of all the heat sinks studied were dependent on pressure drop under uniform heat flux and uniform heat load boundary conditions on the base of the solid substrate. When the uniform heat flux boundary was considered, the optimal channel aspect ratio, solid volume fraction and hydraulic diameter did not change with increasing pressure drop but when the uniform heat load boundary condition was considered under varying axial length and fixed total volume, the optimal dimensions of the heat sink depended on the axial length. The peak temperature also decreased as pressure drop increased, while the thermal conductance increased. When comparing results between fixed and

UNIVERSITEIT VAN PRETORIA
UNIVERSITY OF PRETORIA
YUNIBESITHI YA PRETORIA

varying axial length of the cooling structure while keeping the total volume constant, there was significant improvement in the thermal conductance of all the heat sinks considered in the study for shorter axial lengths.

When the thermal performance of single and multi-layered microchannels with parallel- and counterflow configurations were compared for fixed total volume, fixed axial length for different fluid inlet velocities in Chapter 4, the single-layered microchannel performed best in maximising thermal conductance at low velocities but the three-layered microchannel with counterflow of fluid performed best at higher velocities. The two-layered microchannel had the least pressure drop and pumping power requirement. When the axial length was varied with the total volume kept constant and uniform heat load applied to the heated base, the single-layered microchannel performed best when minimised thermal resistance and pumping power requirements were considered at different pressure drops. Results of increasing heat load on the heated solid substrate base at fixed pressure drop showed that at the highest heat load considered in the study, the two-layered microchannel with counterflow of fluid had the best thermal performance.

Chapter 5 presented a new design of inserted micro pin fins into the single and two-layered microchannels and the results of their thermal performance were compared with those of the previous chapter. Results showed that inserting circular-shaped micro pin fins into the single microchannel improved the thermal performance for both fixed and reduced axial length. This was not the case for the two-layered

UNIVERSITEIT VAN PRETORIA
UNIVERSITY OF PRETORIA
YUNIBESITHI YA PRETORIA

microchannels when the axial length was fixed, but when the axial length was reduced for fixed total volume there was improvement in the thermal performance. The optimal number of rows of pin fins that gave the maximum thermal conductance was also stated for both fixed and reduced axial lengths.

When comparing the shapes of micro pin fins to use for the combined single microchannel and micro pin fins, results showed that out of the three different shapes considered in the study, the combined design with six rows of circular-shaped micro pin fins had the best thermal performance for a fixed total volume, reduced axial length and uniform heat load applied to the solid substrate heated base. Even though the combined design with six rows of circular-shaped micro pin fins had the best performance, the shape of the micro pin fin did not have a significant effect on the thermal performance.

In Chapter 6, the temperature variations along the heated base of the solid substrate cooled using six different heat sinks were examined because temperature non-uniformity on the heated base of a solid substrate has a large effect on the reliability and performance of microelectronic devices. It was shown that for fixed axial length and uniform heat flux on the solid substrate heated base, the two-layered microchannel with counterflow of fluid had the least temperature rise along the axial length of the heated base, but when the axial length was reduced with fixed total volume and uniform heat load applied to the heated base, the combined design of two-layered microchannel with four rows of circular-shaped micro pin fins had the least

UNIVERSITEIT VAN PRETORIA
UNIVERSITY OF PRETORIA
YUNIBESITHI YA PRETORIA

temperature difference at lower pressure drops, while the single microchannel with six rows of circular-shaped micro pin fins had the least temperature difference at higher pressure drops.

Therefore, when choosing a heat sink design for best thermal performance, the geometry of the structure, flow orientation and pressure drop are very important parameters to be taken into consideration. This agrees with what is expected by constructal law, i.e., there is no universal optimal design. The best configurations depend on the parameters and operating conditions.

7.3. RECOMMENDATIONS

In future, it is important that experimental investigations be carried out using the optimal parameters obtained in the study and results obtained can be compared with numerical results obtained in the study especially for the new design of combining microchannels and micro pin fins. The manufacturability of the new design can also be investigated.

Another area of extension of this work in future is comparing different optimisation techniques that have been used in optimising the geometry and thermal performance of heat sinks with the one used in this study and thereafter, comparing the numerical results obtained with experiments.

UNIVERSITEIT VAN PRETORIA
UNIVERSITY OF PRETORIA
YUNIBESITHI YA PRETORIA

Furthermore, an investigation into non-uniform heat flux applied to the base of the solid substrate can be carried out because of its practical importance. This can be done numerically and experimentally.

Water was the chosen cooling fluid in this research. In future research works, different cooling fluids used in microelectronic device applications should be used in the numerical and extended to experimental investigations.

UNIVERSITEIT VAN PRETORIA
UNIVERSITY OF PRETORIA
YUNIBESITHI YA PRETORIA

REFERENCES

[1] Celata, G.P., *Heat transfer and fluid flow in microchannels*, Begell House Inc., 2004.

[2] Bar-Cohen, A., in: *IEEE/CPMT Electron. Packag. Technol. Conf.*, 1997, pp. 29-33.

[3] Joshi, Y.K., Garimella, S.V., Thermal challenges in next generation electronic systems, *Microelectronics J.* 34 (3), 169, 2003.

[4] Joshi, Y., Baelmans, M., Copeland, D., Lasance, C.J., et al., Challenges in thermal modeling of electronics at the system level: summary of panel held at the Therminic 2000, *Microelectronics J.* 32 (10-11), 797-800, 2001.

[5] Bailey, C., in: *10th Electron. Packag. Technol. Conf.*, 2008, pp. 527-532.

[6] Wang, Y., Yuan, G., Yoon, Y., Member, S., Allen, M.G., Active cooling substrates for thermal management of microelectronics, *IEEE Trans. Components Packag. Technol.* 28 (3), 477-483, 2005.

[7] Tonapi, S.S., Fillion, R.A., Schattenmann, F.J., Cole, H.S., et al., in: *Adv. Semicond. Manuf. Conf. Work. 2003 IEEEI/SEMI*, 2003, pp. 250-254.

[8] Furlong, C., Pryputniewicz, R.J., Computational and experimental approach to thermal management in microelectronics and packaging, *Microelectron. Int.* 18 35-39, 2001.

UNIVERSITEIT VAN PRETORIA
UNIVERSITY OF PRETORIA
YUNIBESITHI YA PRETORIA

[9] Schmidt, R., Challenges in electronic cooling — opportunities for enhanced thermal management techniques — microprocessor liquid cooled minichannel heat sink, *Heat Transf. Eng.* 25 (3), 3-12, 2004.

[10] Yeh, L., Chu, R.C., *Thermal management of microelectronic equipment*, ASME Press Book Series on Electronic Packaging, ASME Press, New York 2002.

[11] Rodgers, P., Eveloy, V., in: *5th Int. Conf. Therm. Mech. Simul. Exp. Micro-Electronics Micro-Systems, EuroSimE2004*, 2004, pp. 527-529.

[12] Kandlikar, S.G., High flux heat removal with microchannels: a roadmap of challenges and opportunities, *Heat Transf. Eng.* 26 (8), 5-14, 2005.

[13] Li, J., Peterson, G.P., Geometric optimization of a micro heat sink with liquid flow, *IEEE Trans. Components Packag. Technol.* 29 (1), 145-154, 2006.

[14] Hassan, I., Phutthavong, P., Abdelgawad, M., Microchannel heat sinks: an overview of the state-of-the-art, *Microscale Thermophys. Eng.* 8 (3), 183-205, 2004.

[15] Garimella, S.V., Sobhan, C.B., Transport in microchannels: a critical review, *Annu. Rev. Heat Transf.* 13 1-50, 2003.

[16] Adham, A.M., Mohd-Ghazali, N., Ahmad, R., Thermal and hydrodynamic analysis of microchannel heat sinks: a review, *Renew. Sustain. Energy Rev.* 21 614-622, 2013.

[17] Ighalo, F.U., Optimisation of microchannels and micropin-fin heat sinks with computational fluid dynamics in combination with a mathematical optimisation algorithm. University of Pretoria, 2010.

UNIVERSITEIT VAN PRETORIA
UNIVERSITY OF PRETORIA
YUNIBESITHI YA PRETORIA

[18] Bejan, A., Lorente, S., The constructal law and the thermodynamics of flow systems with configuration, *Int. J. Heat Mass Transf.* 47 (14), 3203-3214, 2004.

[19] Bejan, A., Lorente, S., The constructal law and the evolution of design in nature, *Phys. Life Rev*. 8 209-240, 2011.

[20] Olakoyejo, O.T., Bello-Ochende, T., Meyer, J.P., Mathematical optimisation of laminar forced convection heat transfer through a vascularised solid with square channels, *Int. J. Heat Mass Transf.* 55 (9), 2402-2411, 2012.

[21] Bello-Ochende, T., Meyer, J.P., Ighalo, F.U., Combined numerical optimisation and constructal theory for the design of micro-channel heat sinks, *Numer. Heat Transf. Part A Appl.* 58 1-32, 2010.

[22] Bello-Ochende, T., Liebenberg, L., Malan, A.G., Bejan, A., Meyer, J.P., Constructal conjugate heat transfer in three-dimensional cooling channels, *J. Enhanc. Heat Transf.* 14 (4), 279-293, 2007.

[23] Bello-Ochende, T., Meyer, J.P., Bejan, A., Constructal multi-scale pin-fins, *Int. J. Heat Mass Transf.* 53 (13), 2773-2779, 2010.

[24] Bello-Ochende, T., Liebenberg, L., Meyer, J.P., Constructal design: geometric optimization of micro-channel heat sinks (December), 483-489, 2007.

[25] Muzychka, Y.S., Constructal design of forced convection cooled microchannel heat sinks and heat exchangers, *Int. J. Heat Mass Transf.* 48 (15), 3119-3127, 2005.

[26] Muzychka, Y.S., Constructal multi-scale design of compact micro-tube heat sinks and heat exchangers, *Int. J. Therm. Sci.* 46 (3), 245-252, 2007.

UNIVERSITEIT VAN PRETORIA
UNIVERSITY OF PRETORIA
YUNIBESITHI YA PRETORIA

[27] Olakoyejo, O.T., Bello-Ochende, T., Meyer, J.P., Constructal conjugate cooling channels with internal heat generation, *Int. J. Heat Mass Transf.* 55 4385-4396, 2012.

[28] Meyer, J.P., Olakoyejo, O.T., Bello-Ochende, T., Constructal optimisation of conjugate triangular cooling channels with internal heat generation, *Int. Commun. Heat Mass Transf.* 39 1093-1100, 2012.

[29] Bello-Ochende, T., Olakoyejo, O.T., Meyer, J.P., Bejan, A., Lorente, S., Constructal flow orientation in conjugate cooling channels with internal heat generation, *Int. J. Heat Mass Transf.* 57 241-249, 2013.

[30] Bejan, A., Lorente, S., *Design with constructal theory*, John Wiley & Sons, Inc., 2008.

[31] Rocha, L.A.O., Lorente, S., Bejan, A., *Constructal law and the unifying principle of design*, Springer New York, New York, NY 2013.

[32] Tuckerman, D.B., Pease, R.F.W., High-performance heat sinking for VLSI, *IEEE Electron Device Lett.* 2 (5), 126-129, 1981.

[33] Kandlikar, S.G., Grande, W.J., Evolution of microchannel flow passages: thermohydraulic performance and fabrication technology, *Heat Transf. Eng.* 24 3-17, 2003.

[34] Li, J., Peterson, G.P., 3-Dimensional numerical optimization of silicon-based high performance parallel microchannel heat sink with liquid flow, *Int. J. Heat Mass Transf.* 50 (15-16), 2895-2904, 2007.

UNIVERSITEIT VAN PRETORIA
UNIVERSITY OF PRETORIA
YUNIBESITHI YA PRETORIA

[35] Knight, R.W., Hall, D.J., Goodling, J.S., Jaeger, R.C., Heat sink optimization with application to microchannels, *IEEE Trans. Components, Hybrids, Manuf. Technol.* 15 (5), 832-842, 1992.

[36] Goldberg, N., Narrow channel forced air heat sink, *IEEE Trans. Components, Hybrids, Manuf. Technol.* 7 (1), 154-159, 1984.

[37] Perret, C., Boussey, J., Schaeffer, C., Coyaud, M., Analytic modeling, optimization, and realization of cooling devices in silicon technology, *IEEE Trans. Components Packag. Technol.* 23 (4), 665-672, 2000.

[38] Murakami, Y., Mikic, B.B., Parametric optimization of multichanneled heat sinks for VLSI cooling 24 (1), 2-9, 2001.

[39] Upadhye, H.R., Kandlikar, S.G., in: *ASME Conf. Micro-channels Mini-channels*, Rochester, New York, USA 2004.

[40] Khan, W.A., Yovanovich, M.M., Culham, J.R., in: *Twenty-Second Annu. IEEE Semicond. Therm. Meas. Manag. Symp.*, IEEE, 2006, pp. 78-86.

[41] Turkakar, G., Okutucu-Ozyurt, T., Dimensional optimization of microchannel heat sinks with multiple heat sources, *Int. J. Therm. Sci.* 62 85-92, 2012.

[42] Pence, D., Reduced pumping power and wall temperature in microchannel heat sinks with fractal-like branching channel networks, *Microscale Thermophys. Eng.* 6 319-330, 2002.

[43] Ryu, J.H., Choi, D.H., Kim, S.J., Numerical optimization of the thermal performance of a microchannel heat sink, *Int. J. Heat Mass Transf.* 45 (13), 2823-2827, 2002.

UNIVERSITEIT VAN PRETORIA
UNIVERSITY OF PRETORIA
YUNIBESITHI YA PRETORIA

[44] Ryu, J., Choi, D., Kim, S., Three-dimensional numerical optimization of a manifold microchannel heat sink, *Int. J. Heat Mass Transf.* 46 (9), 1553-1562, 2003.

[45] Muller, N., Fréchette, L., in: *Inter Soc. Conf. Therm. Phenom.*, 2002, pp. 449-456.

[46] Gawali, B.S., Kamble, D.A., Analysis of rectangular microchannel under forced convection heat transfer condition, *Int. J. Eng. Sci. Technol.* 3 2041-2043, 2011.

[47] Patel, V.U., Modi, A.J., Optimization of heat sink analysis for electronics cooling, *World J. Sci. Technol.* 2 64-69, 2012.

[48] Liu, D., Garimella, S.V., Analysis and optimization of the thermal performance of microchannel heat sinks, *Int. J. Numer. Methods Heat Fluid Flow* 15 (1), 7-26, 2005.

[49] Qu, W., Mudawar, I., Analysis of three-dimensional heat transfer in micro-channel heat sinks, *Int. J. Heat Mass Transf.* 45 (19), 3973-3985, 2002.

[50] Qu, W., Mudawar, I., Experimental and numerical study of pressure drop and heat transfer in a single phase microchannel heat sink, *Int. J. Heat Mass Transf.* 45 2549-2565, 2002.

[51] Chen, Y., Zhang, C., Shi, M., Wu, J., Three dimensional numerical simulation of heat and fluid flow in noncircular microchannel heat sinks, *Int. Commun. Heat Mass Transf.* 36 917-920, 2009.

UNIVERSITEIT VAN PRETORIA
UNIVERSITY OF PRETORIA
YUNIBESITHI YA PRETORIA

[52] Kou, H., Lee, J., Chen, C., Optimum thermal performance of microchannel heat sink by adjusting channel width and height, *Int. Commun. Heat Mass Transf.* 35 577-582, 2008.

[53] Husain, A., Kim, K.-Y., Optimization of a microchannel heat sink with temperature dependent fluid properties, *Appl. Therm. Eng.* 28 (8-9), 1101-1107, 2008.

[54] Husain, A., Kim, K.-Y., Shape optimization of micro-channel heat sink for micro-electronic cooling, *IEEE Trans. Components Packag. Technol.* 31 (2), 322-330, 2008.

[55] Toh, K.C., Chen, X.Y., Chai, J.C., Numerical computation of fluid flow and heat transfer in microchannels, *Int. J. Heat Mass Transf.* 45 5133-5141, 2002.

[56] Fedorov, A.G., Viskanta, R., Three dimensional conjugate heat transfer in the microchannel heat sink for electronic packaging, *Int. J. Heat Mass Transf.* 43 399-415, 2000.

[57] Ambatipudi, K.K., Rahman, M.M., Analysis of conjugate heat transfer in microchannel heat sinks, *Numer. Heat Transf. Part A Appl.* 37 711-731, 2000.

[58] Xia, G.D., Jiang, J., Wang, J., Zhai, Y.L., Ma, D.D., Effects of different geometric structures on fluid flow and heat transfer performance in microchannel heat sinks, *Int. J. Heat Mass Transf.* 80 439-447, 2015.

[59] Dehghan, M., Daneshipour, M., Valipour, M.S., Rafee, R., Saedodin, S., Enhancing heat transfer in microchannel heat sinks using converging flow passages, *Energy Convers. Manag.* 92 244-250, 2015.

UNIVERSITEIT VAN PRETORIA
UNIVERSITY OF PRETORIA
YUNIBESITHI YA PRETORIA

[60] Xie, G., Li, S., Sundén, B., Zhang, W., Li, H., A numerical study of the thermal performance of microchannel heat sinks with multiple length bifurcation in laminar liquid flow, *Numer. Heat Transf. Part A Appl.* 65 107-126, 2014.

[61] Qu, W., Mala, G.M., Li, D., Heat transfer for water flow in trapezoidal silicon microchannels, *Int. J. Heat Mass Transf.* 43 3925-3936, 2000.

[62] Lee, P., Garimella, S.V., Liu, D., Investigation of heat transfer in rectangular microchannels, *Int. J. Heat Mass Transf.* 48 1688-1704, 2005.

[63] Morini, G.L., Single-phase convective heat transfer in microchannels: a review of experimental results, *Int. J. Therm. Sci.* 43 631-651, 2004.

[64] Naphon, P., Khonseur, O., Study on the convective heat transfer and pressure drop in the micro-channel heat sink, *Int. Commun. Heat Mass Transf.* 36 (1), 39-44, 2009.

[65] Garimella, S.V., Singhal, V., Single-phase flow and heat transport and pumping considerations in microchannel heat sinks, *Heat Transf. Eng.* 25 15-25, 2004.

[66] Zhang, H.Y., Pinjala, D., Wong, T.N., Toh, K.C., Joshi, Y.K., Single-phase liquid cooled microchannel heat sink for electronic packages, *Appl. Therm. Eng.* 25 (10), 1472-1487, 2005.

[67] Peng, X.F., Peterson, G.P., The effect of thermofluid and geometrical parameters on convection of liquids through rectangular microchannels, *Int. J. Heat Mass Transf.* 38 755-758, 1995.

UNIVERSITEIT VAN PRETORIA
UNIVERSITY OF PRETORIA
YUNIBESITHI YA PRETORIA

[68] Hetsroni, G., Mosyak, A., Pogrebnyak, E., Yarin, L.P., Heat transfer in micro-channels: comparison of experiments with theory and numerical results, *Int. J. Heat Mass Transf.* 48 5580-5601, 2005.

[69] Rezania, A., Rosendahl, L.A., Andreasen, S.J., Experimental investigation of thermoelectric power generation versus coolant pumping power in microchannel heat sink, *Int. Commun. Heat Mass Transf.* 39 1054-1058, 2012.

[70] Wei, X., Stacked microchannel heat sinks for liquid cooling of microelectronics devices. Georgia Institute of Technology, 2004.

[71] Wei, X., Joshi, Y., Optimization study of stacked micro-channel heat sinks for micro-electronic cooling, *IEEE Trans. Components Packag. Technol.* 26 55-61, 2003.

[72] Wei, X., Joshi, Y., Stacked microchannel heat sinks for liquid cooling of microelectronic components, *J. Electron. Packag.* 126 (1), 60-66, 2004.

[73] Wei, X., Joshi, Y., Patterson, M.K., Experimental and numerical study of a stacked microchannel heat sink for liquid cooling of microelectronic devices, *J. Heat Transfer* 129 1432-1444, 2007.

[74] Patterson, M.K., Wei, X., Joshi, Y., Prasher, R., in: *Inter Soc. Conf. Therm. Phenom.*, 2004, pp. 372-380.

[75] Jeevan, K., Quadir, G.A., Seetharamu, K.N., Azid, I.A., Zainal, Z.A., Optimization of thermal resistance of stacked microchannel using genetic algorithms, *Int. J. Numer. Methods Heat Fluid Flow* 15 27-42, 2005.

[76] Jeevan, K., Azid, I.A., Seetharamu, K.N., Tehal, N., in: *Electron. Packag. Technol. Conf.*, 2004, pp. 553-558.

UNIVERSITEIT VAN PRETORIA
UNIVERSITY OF PRETORIA
YUNIBESITHI YA PRETORIA

[77] Cheng, Y.J., Numerical simulation of stacked microchannel heat sink with mixing-enhanced passive structure, *Int. Commun. Heat Mass Transf.* 34 (3), 295-303, 2007.

[78] Chong, S.H., Ooi, K.T., Wong, T.N., Optimisation of single and double layer counter flow microchannel heat sinks, *Appl. Therm. Eng.* 22 (14), 1569-1585, 2002.

[79] Hegde, P.G., Seetharamu, K.N., in: *33rd Int. Electron. Manuf. Technol. Conf. Penang, Malaysia*, 2008, pp. 1-6.

[80] Sharma, D., Singh, P.P., Garg, H., Numerical analysis of trapezoidal shape double layer microchannel heat sink, *Int. J. Mech. Ind. Eng.* 3 10-15, 2013.

[81] Vafai, K., Zhu, L., Analysis of two-layered microchannel heat sink concept in electronic cooling, *Int. J. Heat Mass Transf.* 42 2287-2297, 1999.

[82] Hung, T., Yan, W., Li, W., Analysis of heat transfer characteristics of double-layered microchannel heat sink, *Int. J. Heat Mass Transf.* 55 3090-3099, 2012.

[83] Lin, L., Chen, Y., Zhang, X., Wang, X., Optimization of geometry and flow rate distribution for double-layer microchannel heat sink, *Int. J. Therm. Sci.* 78 158-168, 2014.

[84] Hung, T., Yan, W., Wang, X., Huang, Y., Optimal design of geometric parameters of double-layered microchannel heat sinks, *Int. J. Heat Mass Transf.* 55 3262-3272, 2012.

[85] Leng, C., Wang, X., Wang, T., Yan, W., Multi-parameter optimization of flow and heat transfer for a novel double-layered microchannel heat sink, *Int. J. Heat Mass Transf.* 84 359-369, 2015.

UNIVERSITEIT VAN PRETORIA
UNIVERSITY OF PRETORIA
YUNIBESITHI YA PRETORIA

[86] Leng, C., Wang, X., Wang, T., An improved design of double-layered microchannel heat sink with truncated top channels, *Appl. Therm. Eng.* 79 54-62, 2015.

[87] Wu, J.M., Zhao, J.Y., Tseng, K.J., Parametric study on the performance of double-layered microchannels heat sink, *Energy Convers. Manag.* 80 550-560, 2014.

[88] Leng, C., Wang, X., Wang, T., Yan, W., Optimization of thermal resistance and bottom wall temperature uniformity for double-layered microchannel heat sink, *Energy Convers. Manag.* 93 141-150, 2015.

[89] Xie, G., Liu, Y., Sunden, B., Zhang, W., Computational study and optimization of laminar heat transfer and pressure loss of double-layer microchannels for chip liquid cooling, *ASME J. Therm. Sci. Eng. Appl.* 5 1-9, 2013.

[90] Kim, D., Kim, S.J., Ortega, A., Compact modeling of fluid flow and heat transfer in pin fin heat sinks, *J. Electron. Packag.* 126 (3), 342, 2004.

[91] Khan, W.A., Culham, J.R., Yovanovich, M.M., Modeling of cylindrical pin-fin heat sinks for electronic packaging, *IEEE Trans. Components Packag. Technol.* 31 (3), 536-545, 2008.

[92] Khan, W.A., Culham, J.R., Yovanovich, M.M., Performance of shrouded pin-fin heat sinks, *J. Thermophys. Heat Transf.* 20 408-414, 2006.

[93] Khan, W.A., Culham, J.R., Yovanovich, M.M., Optimization of pin-fin heat sinks using entropy generation minimization, *IEEE Trans. Components Packag. Technol.* 28 (2), 247-254, 2005.

UNIVERSITEIT VAN PRETORIA
UNIVERSITY OF PRETORIA
YUNIBESITHI YA PRETORIA

[94] Yeh, R.-H., An analytical study of the optimum dimensions of rectangular fins and cylindrical pin fins, *Int. J. Heat Mass Transf.* 40 (15), 3607-3615, 1997.

[95] Diez, L.I., Espatolero, S., Cortes, C., Campo, A., Thermal analysis of rough micro-fins of variable cross-section by the power series method, *Int. J. Therm. Sci.* 49 23-35, 2010.

[96] Park, K., Choi, D.H., Lee, K.-S., Numerical shape optimization for high performance of a heat sink with pin-fins, *Numer. Heat Transf. Part A Appl.* 46 909-927, 2004.

[97] John, T.J., Mathew, B., Hegab, H., Parametric study on the combined thermal and hydraulic performance of single phase micro pin-fin heat sinks - Part I: Square and circle geometries, *Int. J. Therm. Sci.* 49 (11), 2177-2190, 2010.

[98] Yang, Y.-T., Peng, H.-S., Numerical study of the heat sink with un-uniform fin width designs, *Int. J. Heat Mass Transf.* 52 (15-16), 3473-3480, 2009.

[99] Sahiti, N., Durst, F., Geremia, P., Selection and optimization of pin cross-sections for electronics cooling, *Appl. Therm. Eng.* 27 (1), 111-119, 2007.

[100] Galvis, E., Jubran, B.A., Behdinan, F.X.K., Fawaz, Z., Numerical modeling of pin–fin micro heat exchangers, *Heat Mass Transf.* 44 (6), 659-666, 2008.

[101] Rubio-Jimenez, C.A., Kandlikar, S.G., Hernandez-Guerrero, A., Numerical analysis of novel micro pin fin heat sink with variable fin density, *IEEE Trans. Components, Packag. Manuf. Technol.* 2 (5), 825-833, 2012.

[102] Tahat, M., Kodah, Z.H., Jarrah, B.A., Probert, S.D., Heat transfers from pin-fin arrays experiencing forced convection, *Appl. Energy* 67 419-442, 2000.

UNIVERSITEIT VAN PRETORIA
UNIVERSITY OF PRETORIA
YUNIBESITHI YA PRETORIA

[103] Peles, Y., Koşar, A., Mishra, C., Kuo, C.-J., Schneider, B., Forced convective heat transfer across a pin fin micro heat sink, *Int. J. Heat Mass Transf.* 48 (17), 3615-3627, 2005.

[104] Koşar, A., Mishra, C., Peles, Y., Laminar flow across a bank of low aspect ratio micro pin fins, *J. Fluids Eng.* 127 (3), 419, 2005.

[105] Koşar, A., Peles, Y., Thermal-hydraulic performance of MEMS-based pin fin heat sink, *J. Heat Transfer* 128 (2), 121, 2006.

[106] Kosar, A., Peles, Y., Micro scale pin fin heat sinks: parametric performance evaluation study, *IEEE Trans. Components Packag. Technol.* 30 855-865, 2007.

[107] Siu-Ho, A.M., Qu, W., Pfefferkorn, F., in: *ASME Int. Mech. Eng. Congr. Expo.*, Illinois, USA 2006, pp. 1-8.

[108] Siu-Ho, A., Qu, W., Pfefferkorn, F., Experimental study of pressure drop and heat transfer in a single-phase micropin-fin heat sink, *J. Electron. Packag.* 129 (4), 479, 2007.

[109] Qu, W., Siu-Ho, A., Measurement and prediction of pressure drop in a two-phase micro-pin-fin heat sink, *Int. J. Heat Mass Transf.* 52 5173-5184, 2009.

[110] Qu, W., Siu-Ho, A., Liquid single-phase flow in an array of micro-pin-fins — Part I: Heat transfer characteristics, *J. Heat Transfer* 130 (12), 124501-1-4, 2008.

[111] Naphon, P., Sookkasem, A., Investigation on heat transfer characteristics of tapered cylinder pin fin heat sinks, *Energy Convers. Manag.* 48 (10), 2671-2679, 2007.

UNIVERSITEIT VAN PRETORIA
UNIVERSITY OF PRETORIA
YUNIBESITHI YA PRETORIA

[112] Prasher, R.S., Dirner, J., Chang, J.-Y., Myers, A., et al., Nusselt number and friction factor of staggered arrays of low aspect ratio micropin-fins under cross flow for water as fluid, *J. Heat Transfer* 129 (2), 141, 2007.

[113] Wang, C., Yu, Y., Simon, T., Cui, T., North, M.T., in: *13th IEEE ITHERM Conf.*, 2012, pp. 944-950.

[114] Jasperson, B.A., Jeon, Y., Turner, K.T., Pfefferkorn, F.E., Qu, W., Microfabrication of short pin fins on heat sink surfaces to augment heat transfer performance, *IEEE Trans. Components Packag. Technol.* 33 148-160, 2010.

[115] Yang, Y., Peng, H., Numerical study of thermal and hydraulic performance of compound heat sink, *Numer. Heat Transf. Part A Appl.* 55 (5), 432-447, 2009.

[116] Ndao, S., Peles, Y., Jensen, M.K., Multi-objective thermal design optimization and comparative analysis of electronics cooling technologies, *Int. J. Heat Mass Transf.* 52 (19-20), 4317-4326, 2009.

[117] Bello-Ochende, T., Liebenberg, L., Meyer, J.P., Constructal cooling channels for micro-channel heat sinks, *Int. J. Heat Mass Transf.* 50 (21), 4141-4150, 2007.

[118] Almogbel, M., Bejan, A., Cylindrical trees of pin fins, *Int. J. Heat Mass Transf.* 43 4285-4297, 2000.

[119] Bello-Ochende, T., Maximum flow access in heat exchangers, heat generating bodies and inanimate flow systems: constructal law and the emergence of shapes and structures in thermo-fluid mechanics: comment on 'The emergence of design in pedestrian dynamics: locomotion, self-organisation, walking paths

UNIVERSITEIT VAN PRETORIA
UNIVERSITY OF PRETORIA
YUNIBESITHI YA PRETORIA

and constructal law" by Antonio F. Miguel , *Phys. Life Rev*. 10 (2), 191-2, 2013.

[120] Rocha, L.A.O., Lorenzini, E., Biserni, C., Geometric optimization of shapes on the basis of Bejan's constructal theory, *Int. Commun. Heat Mass Transf*. 32 1281-1288, 2005.

[121] Xie, G., Zhang, F., Sundén, B., Zhang, W., Constructal design and thermal analysis of microchannel heat sinks with multistage bifurcations in single-phase liquid flow, *Appl. Therm. Eng*. 62 791-802, 2014.

[122] Salimpour, M.R., Sharifhasan, M., Shirani, E., Constructal optimization of the geometry of an array of micro-channels, *Int. Commun. Heat Mass Transf*. 38 (1), 93-99, 2011.

[123] Salimpour, M.R., Sharifhasan, M., Shirani, E., Constructal optimization of microchannel heat sinks with noncircular cross sections, *Heat Transf. Eng*. 34 863-874, 2013.

[124] Li, Y., Zhang, F., Sunden, B., Xie, G., Laminar thermal performance of microchannel heat sinks with constructal vertical Y-shaped bifurcation plates, *Appl. Therm. Eng*. 73 185-195, 2014.

[125] Khuri, A.I., Mukhopadhyay, S., Response surface methodology, *Wiley Interdiscip. Rev. Comput. Stat*. 2 (2), 128-149, 2010.

[126] Box, G.E.P., Wilson, K.B., On the experimental attainment of optimum conditions, *J. R. Stat. Soc. B* 13 1-45, 1951.

UNIVERSITEIT VAN PRETORIA
UNIVERSITY OF PRETORIA
YUNIBESITHI YA PRETORIA

[127] Kalil, S.J., Maugeri, F., Rodrigues, M.I., Response surface analysis and simulation as a tool for bioprocess design and optimization, *Process Biochem*. 35 (6), 539-550, 2000.

[128] Shang, J.S., Li, S., Tadikamalla, P., Operational design of a supply chain system using the Taguchi method, response surface methodology, simulation, and optimization, *Int. J. Prod. Res.* 42 3823-3849, 2004.

[129] Myers, R.H., Montgomery, D.C., Anderson-Cook, C.M., *Response surface methodology: process and product optimization using designed experiments*, John Wiley & Sons, 2009.

[130] Barton, R.R., in: *Proc. Winter Simul. Conf.*, 1992, pp. 289-299.

[131] Barton, R.R., in: *Proc. Winter Simul. Conf.*, 1998, pp. 167-174.

[132] Donohue, J.M., in: *Proc. Winter Simul. Conf.*, 1994, pp. 200-206.

[133] Simpson, T.W., Peplinski, J.D., Koch, P.N., Allen, J.K., in: *ASME Des. Eng. Tech. Conf.*, Sacramento, California 1997, pp. 1-14.

[134] Barton, R.R., in: Proc. Winter Proceedings of the 2010 Winter Simulation Conference B. Johansson, S. Jain, J. Montoya-Torres, J. Hugan, and E. Yücesan, eds. (2009), 75-86, 2010.

[135] Cheng, Y., Xu, G., Zhu, D., Zhu, W., Luo, L., Thermal analysis for indirect liquid cooled multichip module using computational fluid dynamic simulation and response surface methodology, *IEEE Trans. Components Packag. Technol.* 29 39-46, 2006.

UNIVERSITEIT VAN PRETORIA
UNIVERSITY OF PRETORIA
YUNIBESITHI YA PRETORIA

[136] Chiang, K.-T., Modeling and optimization of designing parameters for a parallel-plain fin heat sink with confined impinging jet using the response surface methodology, *Appl. Therm. Eng.* 27 2473-2482, 2007.

[137] Chiang, K.-T., Chang, F.-P., Application of response surface methodology in the parametric optimization of a pin-fin type heat sink, *Int. Commun. Heat Mass Transf.* 33 (7), 836-845, 2006.

[138] Chiang, K.-T., Chou, C.-C., Liu, N.-M., Application of response surface methodology in describing the thermal performances of a pin-fin heat sink, *Int. J. Therm. Sci.* 48 (6), 1196-1205, 2009.

[139] Park, K., Moon, S., Optimal design of heat exchangers using the progressive quadratic response surface model, *Int. J. Heat Mass Transf.* 48 (11), 2126-2139, 2005.

[140] Srisomporn, S., Bureerat, S., Geometrical design of plate-fin heat sinks using hybridization of MOEA and RSM, *IEEE Trans. Components Packag. Technol.* 31 (2), 351-360, 2008.

[141] Li, P., Kim, K.-Y., Multiobjective optimization of staggered elliptical pin-fin arrays, *Numer. Heat Transf. Part A Appl.* 53 (4), 418-431, 2008.

[142] Park, K., Oh, P.-K., Lim, H.-J., The application of the CFD and Kriging method to an optimization of heat sink, *Int. J. Heat Mass Transf.* 49 (19-20), 3439-3447, 2006.

[143] Yu, S.-H., Lee, K.-S., Yook, S.-J., Optimum design of a radial heat sink under natural convection, *Int. J. Heat Mass Transf.* 54 (11-12), 2499-2505, 2011.

UNIVERSITEIT VAN PRETORIA
UNIVERSITY OF PRETORIA
YUNIBESITHI YA PRETORIA

[144] Versteeg, H.K., Malalasekera, W., *An introduction to computational fluid dynamics: the finite volume method*, Prentice Hall, England, 2007.

[145] *ANSYS FLUENT 14.0 User's Guide*, ANSYS, Inc., Southpointe 2011.

[146] Pantakar, S.V., *Numerical heat transfer and fluid flow*, Hemisphere Publishing Corp., New York, USA 1980.

[147] White, F.M., *Viscous fluid flow*, McGraw-Hill, 1991.

[148] Chen, V.C.P., Tsui, K., Barton, R.R., Meckesheimer, M., A review on design, modeling and applications of computer experiments, *IIE Trans.* 38 273-291, 2006.

[149] Giunta, A.A., Wojtkiewicz Jr., S.F., Eldred, M.S., Overview of modern design of experiments methods for computational simulations, *Am. Inst. Aeronaut. Astronaut.* (2003-0649), 1-17, 2003.

[150] Bhattacharjee, S., Grosshandler, W.L., The formation of a wall jet near a high temperature wall under microgravity environment, *ASME 1988 Natl. Heat Transf. Conf. Vol. 1* 1 711-716, 1988.

[151] Petrescu, S., Comments on the optimal spacing of parallel plates cooled by forced convection, *Int. J. Heat Mass Transf.* 37 1283, 1994.

[152] Laermer, F., Urban, A., Challenges, developments and applications of silicon deep reactive ion etching, *Microelectron. Eng.* 68 349-355, 2003.

[153] Madou, M.J., in: Gad-el-Hak, M. (Ed.), *MEMS Handb.*, CRC Press, Taylor & Francis Group, 2002, p. 1368.